Faculty of Engineering and Science

Department of Chemical Engineering

Aptameric Formulation for Enhanced Biopharmaceutical Delivery

Tan Kei Xian

This thesis is presented for the Degree of

Doctor of Philosophy

of

Curtin University

January 2018

DECLARATION

To the best of my knowledge and belief this thesis contains no material previously published by any other person except where due acknowledgment has been made.

This thesis contains no material which has been accepted for the award of any other degree or diploma in any university.

Signature: 

Date: 17th January 2018

ABSTRACT

Targeted delivery of drug molecules to specific cells in mammalian systems demonstrates a great potential to enhance the efficacy of current pharmaceutical therapies. Conventional strategies for pharmaceutical delivery are often associated with poor therapeutic indices and high systemic cytotoxicity, and this results in poor disease suppression, low surviving rates, and potential contraindication of drug formulation. The emergence of aptamers has elicited new research interests into enhanced targeted drug delivery due to their unique characteristics as targeting elements. Aptamers can be engineered to bind to their cognate cellular targets with high affinity and specificity, and this is important to navigate active drug molecules and deliver sufficient dosage to targeted malignant cells. However, the targeting performance of aptamers can be impacted by several factors including endonuclease-mediated degradation, rapid renal filtration, biochemical complexation, and cell membrane electrostatic repulsion. This has subsequently led to research interests in the development of smart aptamer-immobilised biopolymer systems as delivery vehicles for controlled and sustained drug release to specific cells with minimal systemic cytotoxicity.

This research work reports the synthesis and *in vitro* characterization of a novel multi-layer co-polymeric drug delivery system using a water-in-oil-in-water (w/o/w) double emulsion integrated with ultra-sonication technique. A drug-loaded PLGA-Aptamer-PEI (DPAP) formulation was generated using a thrombin-specific DNA aptamer as the targeting ligand while Bovine Serum Albumin (BSA) was used as a biopharmaceutical drug to investigate the drug delivery characteristics. Biophysical characterization of the DPAP system showed a spherical shaped particulate system with a unimodal particle size distribution with an average D[4,3] hydrodynamic size of ~0.685 µm and a zeta potential of +0.82 mV. The zeta potential and D[4,3] average size of the DPAP layered compartments demonstrated pH dependence. The DPAP formulation showed a high encapsulation efficiency of 89.4±3.6%, a loading capacity of 17.89±0.72 mg BSA protein/100 mg PLGA polymeric particles, low cytotoxicity and a controlled drug release characteristics in 43 days. It was also demonstrated that the release rate of DPAP formulation is accelerated under acidic endosomal conditions of ~pH 5.5 due to increased

polymer degradation rate, enhancing intracellular accumulation of drug molecules. The ionic strength of the binding medium affected the degradation and drug release rates of DPAP micro-particles. A strong binding and shielding effect of DPAP towards encapsulated BSA molecules was observed under increasing ionic strength. The binding characteristics, targeting capability, biophysical properties, encapsulation efficiency, and drug release characteristics of the DPAP system were investigated under varying conditions of ionic strength, polymer composition and molecular weight, and degree of PEGylation of the synthetic core. DPAP formulation using PLGA (65:35) and PEI with a molecular weight of ~800 MW demonstrated an encapsulation efficiency of 78.93% and a loading capacity of 0.1605 mg BSA per mg PLGA. DPAP (PLGA 65:35, PEI MW~25,000) formulation showed enhanced drug release rate with a biphasic release profile. The release characterisation data indicated a lower targeting power and reduced drug release rate for PEGylated DPAP formulations. The DPAP formulation demonstrated a strong targeting performance towards its targeted protein receptors, indicating the capability of the formulation to enhance current drug delivery strategies for specific aptamer-target systems. To demonstrate this, MgO nanoparticles was encapsulated within the DPAP formulation as insulin resistance reversal candidates in diabetes treatment. *In vitro* experimental work using diabetic 3T3-L1 cells demonstrated the efficacy of DPAP in introducing a significant dosage of MgO drug molecules to the targeted cells with a remarkable reduction in the oxidation of reducing sugars due to insulin resistance reversal ability. The results generated from this work show promise and provide a basis to optimise the performance of DPAP system as an effective drug carrier for enhanced *in vivo* cell targeting in drug delivery.

ACKNOWLEDGEMENT

First and foremost, I thank God for His guidance and grace in providing me the opportunity and capability to proceed in this PhD programme.

I would like to express my most sincere gratitude and special appreciation to my supervisor Professor Michael Kobina Danquah for being a tremendous mentor in this journey. I would like to thank him for his guidance, insightful advice and immense knowledge in guiding the direction of my research project. His quick responses and prompt replies to my emails have been priceless to my progress. I sincerely thank him for all his positive encouragements and vibes which continuously kept me moving forward to achieve my goal. I am very much thankful to my supervisor, Dr. John Lau Sie Yon for his valuable guidance, encouragement, and keen interest in my PhD journey. I express my deep sense of gratitude for always supporting my ideas and decisions. Sincerely appreciate your physical presence and help in solving encountered hardships during this journey, especially for your generous financial support (SCI grant) which gave me a golden opportunity to attend an international conference. I would also like to thank my committee members particularly Prof. Michael Danquah, Dr. John Lau and Dr. Amandeep Sidhu for their continuous enlightenment, insightful feedback, support and motivation. I want to thank Dr. Hani Al-Salami, Curtin University, Australia for joining my thesis committee as my co-supervisor. It is such an honour to work with an expert in the area of drug delivery.

A special thanks to the Ministry of Higher Education (Malaysia) for providing the funding for this project and the HDR scholarship through the Fundamental Research Grant Scheme (FRGS). I wish to thank the laboratory technicians, mainly Ms. Magdalene Joing and Ms. Michelle Martin, for giving me kind assistance whenever I faced challenges such as instrument breakdown or lack of essential materials in the laboratory. My sincere thanks also go to my colleagues for their valuable suggestions and encouragement.

Last but not the least, I would like to express my special appreciation to my beloved family especially my husband, Tang Chin Chiong who have been supporting me emotionally

since the beginning of my PhD journey. Thank you for having faith in my decision to pursue PhD and strive towards my career goal.

LIST OF PUBLICATIONS FROM THESIS

ISI-Indexed Journals:

1. **Tan, Kei X.**, Danquah, M. K., Lau, S. Y., Sidhu, A. S., & Ongkudon, C. M. (2016). Aptamer-mediated polymeric vehicles for enhanced cell-targeted drug delivery. *Current Drug Targets*, *17*(16), 1-11. doi: 10.2174/1389450117666160617120926 (ISI-indexed, IF = 3.029)

2. **Tan, Kei X.**, Danquah, M. K., Lau, S. Y., Sidhu, A. S., & Ongkudon, C. M. (2016). Towards targeted cancer therapy: Aptamer or oncolytic virus? *European Journal of Pharmaceutical Science, 96*, 8-19. doi: 10.1016/j.ejps.2016.08.061 (ISI-indexed, IF = 3.773)

3. **Tan, Kei X.**, Danquah, M. K., Lau, S. Y., Sidhu, A. S., & Ongkudon, C. M. (2017). Biophysical characterization of layer-by-layer synthesis of aptamer-drug microparticles for enhanced cell targeting. *Biotechnology Progress*. doi: 10.1002/btpr.2524 (ISI-indexed, IF = 2.167)

4. **Kei X. Tan**, Michael K. Danquah, Lau Sie Yon, Amandeep Sidhu. (2018). Process evaluation and *in vitro* selectivity analysis of aptamer-drug polymeric formulation for targeted pharmaceutical delivery. *Biomedicine & Pharmacotherapy*. https://doi.org/10.1016/j.biopha.2018.03.052 (ISI-indexed, IF = 2.759).

5. Dominic Agyei, Caleb Acquah, **Kei Xian Tan**, Hii Hieng Kok, Michael K. Danquah. (2018). Prospects in the use of aptamers for characterizing the structure and stability of bioactive proteins and peptides in food. *Analytical and Bioanalytical Chemistry*. doi: 10.1007/s00216-017-0599-9. (ISI-indexed, IF = 3.431).

6. **Kei X. Tan**, Safina Ujan, Michael K. Danquah, Lau Sie Yon, Amandeep Sidhu. (2017). Stage-wise probing of a multi-layered aptameric formulation for targeted delivery. *The Canadian Journal of Chemical Engineering.* (ISI-indexed, IF = 1.356) (Submitted; under review).

7. **Kei X. Tan**, Michael K. Danquah, Lau Sie Yon, Amandeep Sidhu. (2017). Binding characterization of aptamer-drug layered microformulations and *in vitro* release assessment. *Pharmaceutical Development and Technology*. (ISI-indexed, IF = 1.860) (Submitted; under review).

8. **Kei X. Tan**, Jaison Jeevanandam, Lau Sie Yon, Michael K. Danquah. (2017). Aptamer-navigated copolymeric drug carrier system for *in vitro* delivery of MgO nanoparticles as type 2 diabetes insulin resistance reversal drug candidate. *Journal of Pharmacy and Pharmacology*. (ISI-indexed, IF = 2.405) (Submitted; under review).

9. Caleb Acquah, **Kei Xian Tan**, Eugene Obeng Marfo, Dominic Agyei, Michael Kobina Danquah (2017). Affinity monitoring of structural and functional

characteristics of bioactive peptides via aptameric ligand sensing. *Analytical and Bioanalytical Chemistry*. (ISI-indexed, IF = 3.431) (Submitted; under review).

Book Chapters

10. **Kei X. Tan**, Ahmed. Barhoum, Michael K. Danquah. (2017). Risks and toxicity of nanoparticles nanostructured materilas. In *Emerging applications of nanoparticles and architecture nanostructures*. Elsevier.
11. Dominic Agyei, **Kei X. Tan**, Sharad, Chibuike, Michael (2017). Peptides for biopharmaceutical applications. In *Peptide applications in biomedicine, biotechnology and bioengineering.* Elsevier.
12. **Tan, Kei X.**, Ujan, S., & Danquah, M. K. (2017). Colloidal formulation of aptamers for advanced therapeutic delivery. In *Composites in biomedical engineering*. Elsevier. (Submitted; abstract accepted).

Conference Paper

13. **Kei X. Tan**, Safina Ujan, Michael K. Danquah, Sie Yon Lau. (2017). Engineered Aptamer-Based Micro-Formulation for Targeted Delivery, presented at The 6th International Conference on Biomedical Engineering and Biotechnology (ICBEB 2017), GuangZhou, China, 2017.
14. **Kei X. Tan**, Safina Ujan, Michael K. Danquah, Sie Yon Lau. (2017). Synthesis and Characterization of Aptamer-Navigated Drug Loaded Polymeric Micro-particles for Enhanced Targeted Delivery, presented at The 9th Annual Congress on Drug Design & Drug Formulation, Seoul, South Korea. DOI: 10.4172/2169-0138-C1-020

Table of Contents

List of Figures

List of Tables

Abbreviations

(3-(4,5-dimethylthiazol-2-yl)-5-(3-carboxymethoxyphenyl)-2-(4-sulfophenyl)-2H-tetrazolium) assay	MTS
1-ethyl-3-(3-dimethylaminopropyl) carbodiimide	EDC
3,5-Dinitrosalicyclic acid assay	DNS
Bovine serum albumin	BSA
Drug-loaded PLGA Aptamer-conjugated PEI formulation	DPAP
Drug-PLGA formulation	DP
Drug-PLGA-Aptamer formulation	DPA
Dynamic light scattering	DLS
Fourier transform infrared spectroscopy	FTIR
Magnesium Oxide	MgO
N-hydroxysuccinimide	NHS
Phosphate buffered saline	PBS
Poly (ortho esters)	POE
Poly(beta-amino ester)	PBAE
Poly(ethylene imine)	PEI
Poly(lactic-*co*-glycolic acid)	PLGA
Poly(vinyl alcohol)	PVA
Polyethylene glycol	PEG
Scanning electron microscopy	SEM
Systematic evolution of ligands by exponential enrichment	SELEX
Thermogravimetric analysis	TGA
Transmission electron microscopy	TEM
Ultra-violet	UV
Water-in-oil-in-water	w/o/w

CHAPTER 1

INTRODUCTION

1.1 BACKGROUND

Conventional therapeutic delivery systems for pharmaceutical applications and therapeutic treatments are challenged with inefficient therapeutic effects associated with poor pharmacokinetics and pharmacodynamics, resulting from non-specific targeting of active drug molecules towards both healthy and malignant cells. As a result, patients often experience serious adverse side effects from various treatments including chemotherapy, radiotherapy and immunotherapy. This has eventually raised research interests into the search for new, smart and advanced therapeutic delivery designs that can address the limitations of current pharmaceutical drug delivery systems for better therapeutic indices.

Targeted drug delivery is one of the most advanced form of pharmaceutical delivery. It is a viable approach for enhanced *in vivo* cell targeting to enable a sustained and controlled delivery of drug molecules with sufficient dosage to elicit maximum therapeutic efficacy at malignant sites over a desired timeframe. Targeted drug delivery makes use of targeting elements such as aptamers to navigate and direct active drug ingredients specifically towards targeted cells in order to reduce the amount of drug loss during delivery, and minimize systemic cytotoxicity. Therefore, the search for an efficient cell-targeting agents and synthetic delivery vectors to specifically target cancerous, viral and bacterial infections has become a major research endeavour. Aptamers serve as great cell-targeting agents as they can be generated and molecularly engineered to bind specifically to a wide range of cellular and biomolecular targets.

In this research study, a thrombin-specific DNA aptamer is used as the targeting element for the design of a novel co-polymeric drug delivery vector and navigation system through a stage-wise multi-layered complexation of poly(lactic-*co*-glycolic acid) (PLGA) and poly(ethylene imine) (PEI) to improve *in vivo* targeting of specific mammalian cells.

Aptamers represent a new era of binding ligands in biomedicine, biotechnology, pharmaceutical delivery, clinical diagnostics and therapeutic applications due to their high binding affinities, specificity and selectivity towards their cognate targets (McKeague & DeRosa, 2012). They are short oligonucleotides (~20-50 nucleotides) of either single-stranded ribonucleic acid (ssRNA) molecules or deoxyribonucleic acid (ssDNA) (Sun et al., 2014). Their unique features of folding into specific 3-D conformation with up to pico-molar range of dissociation constants (Song et al., 2012; Sun et al., 2014; Ye et al., 2012) make them recognize and bind to their targets with very high affinities via Van der Waal interactions, hydrophobic interactions, hydrogen bonding, or hydrophobic interactions (Upadhyay, 2013; Witt et al., 2015). By the use of Systematic Evolution of Ligands by Exponential Enrichment (SELEX) technology, aptamers can be generated *in vitro* to bind to a wide range of targets including ions, proteins, tissues, cells, peptides, bacteria, viruses and toxins (Radom et al., 2013; Santosh & Yadava, 2014). SELEX is an iterative selection process involving sequential target incubation, selection, amplification and enrichment steps to generate molecular libraries with a specific target clone to extract desired sequences known as aptamers (M. Alibolandi et al., 2015; Orava, Cicmil, & Gariépy, 2010; Radom et al., 2013).

Aptamers possess a great therapeutic potential as a new generation of targeting agents due to their advantageous biological and physiochemical characteristics. These characteristics include biocompatibility, low immunogenicity, ease of synthesis and biochemical labelling, scalable production, small hydrodynamic size for effective membrane penetrations, and high thermal and chemical stability (Baird, 2010; Gedi & Kim, 2014; P.-H. Kim et al., 2011). Aptamers can be effectively employed either as standalone biological drugs or drug carriers for mediated and targeted drug delivery strategies.

The first approved aptamer-based drug, named Pegatanib, by the U.S Food and Drug Administration (FDA) in 2004 has become the landmark in the drug development of aptamers and incited high research interests on the clinical potentials of aptamers (Song et al., 2012). Pegatanib is a therapeutic agent for treating neovacular age-related macular degeneration which greatly affects visual performances of the aged population. Pegatanib aptamer works by targeting and antagonising the vascular endothelial growth factor

(VEGF)-165 which controls angiogenesis, vascular permeability and ocular neovascularization (Song et al., 2012). There are a number of aptamer based biological drugs undergoing clinical trials. These include REG1 aptamer targeting human coagulation factor IXa to treat coronary artery disease; AS 1411 aptamer targeting nucleolin protein receptors to cure renal cancer and acute myeloid leukemia; and NOX-E36 aptamer to treat type 2 diabetes mellitus by binding onto monocyte chemoattractant protein-1 (Song et al., 2012; Sun et al., 2014). This demonstrates that aptamers are potential agents for drugs and vaccines delivery to allow specific target binding in the human body system for successful disease or tumour therapy while reducing negative impacts to normal cells

Notwithstanding the aforementioned therapeutic potentials of aptamers, the efficacy of aptamer-mediated drug delivery systems is challenged by several factors including rapid renal elimination and bio-distribution, electrostatic repulsion between aptamer and targeted cells, endonuclease attack, and unwanted biochemical immobilization of aptamer molecules (Lakhin et al., 2013). This has driven research interest into the application of bio-polymers as delivery vectors to minimise the limitations of aptamer-mediated delivery.

Biopolymeric delivery carriers are more favourable for medical and pharmaceutical applications compared to bacteria and viruses due to their safety, low immunogenicity, biocompatibility and biodegradability. Their tunable biophysical characteristics, and ease of surface modifications and coupling offer opportunities to engineer their functional attributes to provide a sustained, prolonged and controlled drug release profile (Saranya & Radha, 2014; Stevanovic & Uskokovic, 2009). An ideal biocompatible polymer encapsulates the active molecules without affecting their biochemical properties and activities; offers a stage-wise release of the molecules while minimizing initial burst; and provides a controlled release for optimal dosage over a period of time (Stevanovic & Uskokovic, 2009; M. Tan & Danquah, 2012). Compared to polymeric nanoparticles, microparticles have a more favorable size that is better phagocytized by cells (Balashanmugam et al., 2014) though nanoparticles present an enhanced surface area to facilitate cell adsorption. Aptamers can be encapsulated, complexed or conjugated with polymeric systems to protect them from the physiological environment and enable them

to traverse the membrane of target cells to reach targeted intracellular sites (Orava, Cicmil, & Gariépy, 2010). Though there are numerous studies on the application of polymeric micro/nano-particles in drug, gene and vaccine delivery, the emergence of aptamers has created the opportunity to further improve target specific delivery with the use of tuneable biodegradable polymeric particles. Hence, the use of biopolymers in targeted drug delivery as carriers to encapsulate targeting ligands such as drug-conjugated aptamers holds a great promise to optimize the performance of aptamer mediated targeted delivery. A number of research reports have discussed the potential of targeted drug delivery using aptamer-conjugated polymeric particles to treat leukemia (Aravind, Jeyamohan, et al., 2012; Jianwei Guo et al., 2011), colon cancer (Sayari et al., 2014), breast cancer (M. Alibolandi et al., 2015; L. Li et al., 2014), and prostate cancer (Min et al., 2011).

Biopolymers such as PLGA and PEI are ideal candidates for pharmaceutical applications. They are approved by FDA for clinical and medical applications due to their safety and competency. Their tunable properties such as surface charge, particle size and distribution, pH-based degradation mechanism, and low cytotoxic effects, make them effective for the encapsulation of both targeting elements and drugs at high payloads for specific and controlled drug release at target sites over a desired period. PLGA polymeric particles have been demonstrated to encapsulate DNA molecules with high encapsulation efficiencies and biological drugs with high loading capacities as well as providing a sustained drug release with minimal systemic cytotoxicity (Balashanmugam et al., 2014). PEI is a cationic biopolymer with the ability to form a polyplex with negatively charged oligonucleotides such as aptamers via condensation and electrostatic interactions to improve drug cellular uptake into target cells. Also, PEI provides effective cell transfection with minimal systemic cytotoxicity at moderate concentrations (Kurosaki et al., 2012; Subramanian et al., 2015). PEI allows high endosomal release of encapsulated active drug molecules to the nucleus for enhanced therapeutic effects via its proton sponge mechanism (Gong et al., 2012). PEI biopolymer has been reported by various researcher as a competent vector for targeted delivery system (Kurosaki et al., 2012; Subramanian et al., 2015). Hence, targeted drug delivery using polymeric particles encapsulating the targeting aptamer ligand conjugated with the drug to target specific sites, such as tumour

cells, is a promising development that can enhance the specificity, selectivity and drug dosage essential to improve effective therapeutic indices for various applications.

This project focuses on the synthesis and characterization of a layer-by-layer aptamer mediated PLGA/PEI copolymeric delivery system for enhanced targeted delivery. In particular, this thesis covers the design concept, synthesis and characterizations of a novel multifunctional co-polymeric aptamer-mediated drug carrier called DPAP. The DPAP formulation is made up of different compartments (a) BSA protein, acting as a drug model, |D|, (b) hydrophobic PLGA polymeric core encapsulating BSA, |P|, (c) thrombin-specific DNA aptamer coupled onto the surface of PLGA, |A|, (d) hydrophilic PEI polymer outermost layer surrounding the BSA-PLGA-Aptamer core, |P|. To date, no research study has reported on aptamer conjugated-drug loaded-PLGA-PEI co-polymeric system with this DPAP formulation design. The biophysical characteristics of the DPAP formulation in terms of hydrodynamic size and zeta potential, morphological analyses, and targeted drug delivery efficacy measurements under different molecular compositions and physicochemical conditions based on *in vitro* encapsulation efficiency, loading capacity, drug release kinetics and profile, systemic cytotoxicity, targeting capability, binding characteristics, and transfection efficiency are discussed herein.

1.2 PROBLEM STATEMENTS/ RESEARCH GAPS

Aptamer-mediated pharmaceutical delivery systems have gained a significant research attention due to the unique biophysical and specific binding properties of aptamers, making them ideal targeting elements for targeted therapeutic delivery (J. Guo et al., 2011; Vavalle & Cohen, 2012). Biodegradable polymeric particles with tuneable biophysical properties have also demonstrated to be effective carriers for controlled and sustained drug delivery. Thus, a targeted drug delivery system using engineered biodegradable polymeric particles encapsulating drug-conjugated aptamer to specific cell sites has the potential to enhance specificity, drug dosages, therapeutic indices, and controlled release profile for various clinical applications. However, to date, no single formulation has been reported to adequately address the challenges of aptamer-mediated drug delivery systems. Current reported formulations have limitations resulting from aptamer polarity, negatively

charged cell surface, poor targeting capability, cell membrane impermeability, low transfection efficiency, rapid nuclease-mediated degradation and renal excretion (Lakhin et al., 2013; Santosh & Yadava, 2014; Sun et al., 2014; Sundaram et al., 2013; Wu, 2011; J. Zhu et al., 2014). These contribute to low targeting and therapeutic performances of aptamer mediated systems. This project seeks to design a novel DPAP system that can overcome the aforementioned drawbacks of conventional aptameric formulations to provide a controlled release profile with improved pharmacokinetics, specificity and therapeutic indices. Key research questions to be answered in this project relate to understanding the effects of synthesis conditions and physiocochemical parameters on the biophysical characteristics and drug delivery efficacy of the formulation.

1.3 RESEARCH QUESTIONS

1. Can a suitable targeted delivery formulation be generated with desired biophysical characteristics to improve drug efficiency and therapeutic index?

2. Can such an aptamer-navigated co-polymeric particulate system provides a better targeting capability and more controlled drug release kinetics?

3. Can DPAP formulation enhance the transfection efficiency and drug dosage at the targeted site?

1.4 OBJECTIVES

The main objective of this research project is to synthesise and characterise a novel aptamer-drug biopolymeric formulation with improved encapsulation efficiency and biophysical characteristics for sustained and controlled drug delivery. The main objective is subdivided into the following specific objectives.

1. To develop a pH-sensitive, biodegradable and cationic polymer particulate system with defined biophysical properties for efficient encapsulation of aptamer and drug molecules.

2. To investigate the degradation kinetics of the aptamer formulation under varying physicochemical conditions in order to determine drug release profile and aptamer binding characteristics.

3. To determine the performance of the drug-aptamer-biopolymer formulation for enhanced *in vitro* cell transfection.

1.5 NOVELTY

Figure 1.1 shows a novel product design of aptamer-drug formulation aimed at maintaining the structural and biochemical integrity of the active drug as well as the biophysical binding characteristics of the aptamer for enhanced targeted delivery. The design presents a multifunctional formulation based on the use of biodegradable polymers as the drug carrier, aptamer cargo and transport vehicle. In this design, the outer layer of the drug-encapsulated particles is functionalized with the aptamer before the drug-polymer-aptamer complex is further encapsulated within an outer polymeric layer. The inner and outer polymeric particulates are both cationic in nature with the latter being more cationic in order to promote cell membrane binding and internalization. The DPAP design framework provides a more effective protection to the encapsulated drug and aptamer to prevent drug leakages and ensure controlled and sustained drug release at the targeted sites with increased therapeutic index and minimal side effects. The positively charged outermost particulate layer electrostatically interacts with negatively charged target cell membrane to facilitate the transportation of the negatively-charged aptamer to the target cell membrane. As a result, the encapsulated aptamer is released to bind onto the target surface receptors, biomarkers or proteins in order to trigger a receptor-mediated internalization, also referred to as endocytosis. The receptor-mediated internalization increases the cellular uptake of the drug encapsulated DPAP microparticles into the target cells. The acidic environment of the endosome induces hydrolytic bonding cleavage between the aptamer and the conjugated particles, and also inner polymer degradation via

hydrolysis. Consequently, the encapsulated drug is released from the particles. The aptamer is removed in the later stage where the endosome fuses with lysosome containing endonucleases that degrade nucleotide linkages. The released drug diffuses out from the endosomal membrane into the cytosol and enters the nucleus to trigger therapeutic effects.

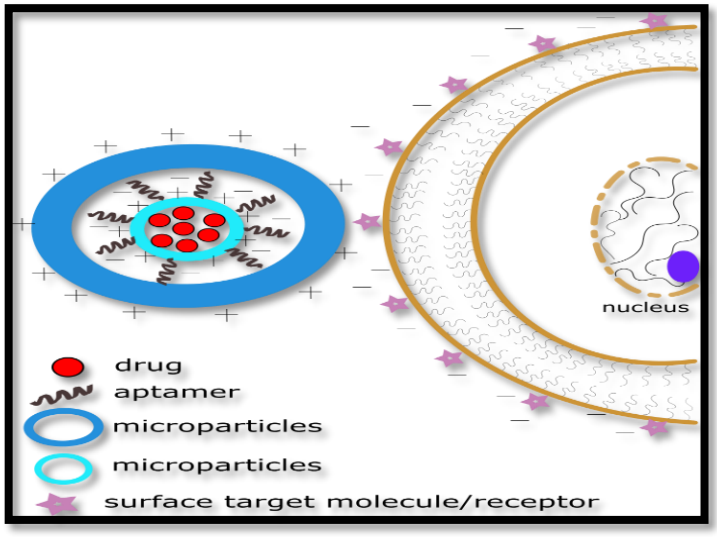

Figure 1.1: Novel DPAP aptamer-drug design formulation for enhanced cell targeting

1.6 SCIENTIFIC MERITS AND SIGNIFICANCE OF RESEARCH

This research project will promote significant research contributions and scientific merits to the medical field, biotechnology, biomedical science, and pharmaceutical delivery and therapy. The research findings from this project would constitute new and insightful knowledge on the structural formulation and characteristics of aptamer-biopolymeric conjugates as well as its modifiable features to optimize targeting capability, drug delivery and drug uptake into desired cells. In addition, this research project will provide an in-depth understanding of the degradation mechanism of the novel formulation and how effective molecular engineering can regulate the stimuli-responsiveness of the polymeric system for controlled and sustained drug release characteristics.

The emergence of aptamers as targeting elements has created an opportunity to improve conventional pharmaceutical delivery systems by directing and delivering active drug

ingredients specifically to targeted malignant sites in order to optimize therapeutic effects with improved therapeutic indices and minimal systemic cytotoxicity (M. Alibolandi et al., 2015; Aravind, Jeyamohan, et al., 2012). The use of biodegradable polymeric particles as delivery vectors can protect encapsulated molecules such as aptamers and drugs from harsh physiological environments without altering their molecular functions and biochemical features.

The major limitations associated with current cancer therapeutic treatments (radiotherapy, chemotherapy and immunotherapy) are due to the lack of specific targeting ability, and effective delivery mechanisms (Balashanmugam et al., 2014). The proposed multi-layer aptamer-polymeric particulate formulation holds a great promise in improving the specificity, performance and therapeutic indices of pharmaceutical delivery systems. The DPAP formulation possesses a significant potential in addressing the drawbacks of current drug delivery mechanisms for disease treatments.

1.7 THESIS LAYOUT

- Chapter 1, which covers the Introduction, presents an overview of conventional pharmaceutical delivery systems and the concept of DPAP formulation.
- Chapter 2 covers a critical literature review of various drug delivery carriers, methods for formulation, clinical potential of aptamers and challenges faced by aptamers as new targeting elements, as well as efficacy of aptamer-mediated targeted drug delivery systems for clinical therapies.
- Chapter 3 discusses experimental work carried out on the synthesis, biophysical characterization, thermal stability, binding characteristics, drug release profiles, PEGylation effects, targeting capability, effects of synthesis conditions, and *in vitro* transfection efficiency of DPAP formulation under various physiochemical conditions.
- Results and discussions are presented in Chapter 4 which include the following in-depth discussions:

- Stage-wise probing of the multi-layered DPAP formulation for targeted delivery.
- The binding characteristics of DPAP micro-particles as well as the effect of PEGylation on the biophysical properties and functionalities of DPAP particulate system as a targeted delivery system.
- The targeting capability and drug release pattern of DPAP formulation in the presence of both targeted and non-specific proteins are well-discussed.
- The effects of varying synthesis parameters and incubation conditions on the performance of DPAP particulate system.
- The in-depth discussion on the potentials and capabilities of DPAP formulation in carrying and delivering sufficient therapeutic dosage of active drug molecules towards specific mammalian cells to elicit desired cytotoxic effects in an *in vitro* experimental setup.

- Chapter 5 covers the conclusion which presents a summary of the key findings from this research in addition to reflections on the thesis objectives. Suggestions for future work towards further development of the DPAP systems are also provided.

CHAPTER 2

LITERATURE REVIEW

2.1 OVERVIEW

The search for smart delivery systems is an important research endeavour to develop new and improved alternatives to conventional pharmaceutical delivery systems for better clinical success. This has increased research interests in the use of aptamers as specific and robust binding ligands for targeted pharmaceutical delivery. Notwithstanding, aptamer-mediated targeted delivery is challenged by several biophysical and biochemical factors. Therefore, the application of biopolymers as delivery carriers holds a great promise to enhance the efficacy of aptamer-based targeted delivery. This chapter critically reviews existing work in the literature on aptamer based drug formulations, gives an account on the potential and drawbacks of the use aptamers as targeting elements in comparison to other targeting ligands, as well as reviewing biopolymer formulations for targeted pharmaceutical delivery.

2.2 GENERATION OF APTAMERS

As mentioned earlier, aptamers are generated *in vitro* by an iterative process called SELEX. As seen in Figure 2.1, SELEX begins with a chemically synthesized pool of randomized oligonucleotides as the initial library. The library consists of single-stranded oligonucleotides containing random sequence regions of around 30 to 40-mers flanked by constant sequences at the primer binding site for PCR amplification (Radom et al., 2013). For instance, a library pool consisting of 30-mer DNA or RNA sequences will generate 4^{30} randomized DNA or RNA oligonucleotides (McKeague & DeRosa, 2012). This large pool provides a credible diversity that consists of various affinity-binding oligonucleotides for a given target (Baird, 2010; Radom et al., 2013; Ye et al., 2012). The concept of SELEX is to simulate evolution by introducing iterative selection rounds, usually about 10 to 15, rounds [3], followed by exponential PCR amplification (Radom et

al., 2013). SELEX commonly begins with a random pool of 10^{13}-10^{16} ssDNA or RNA library that undergo iterative selection rounds to produce an oligonucleotide with high binding affinity to the target (Radom et al., 2013; Ye et al., 2012). The ssDNA or RNA library is incubated with an immobilized target, and the target-bound sequences are separated from the unbounded using various washing steps. The bound sequences are then eluted from the target using heat or chaotropic agents (such as urea) (McKeague & DeRosa, 2012). The process proceeds with the amplification of eluted target-bound oligonucleotides via PCR to synthesize new enriched oligonucleotide library for the next round of SELEX with a more stringent binding condition (McKeague & DeRosa, 2012). The enriched library from SELEX are cloned and sequenced for comparative analysis in order to detect aptamers with desired properties or consensus sites responsible for target recognition (Radom et al., 2013). Subsequently, a solid-phase chemical synthesis is employed to generate desired aptamers in a large scale (McKeague & DeRosa, 2012). There have been various modifications to conventional SELEX. These include modifications with alterations in target immobilization, library, PCR amplification and selection stringency to either simplify the SELEX process or select improved aptamers (McKeague & DeRosa, 2012). For instance, cell-SELEX enables aptamer generation from whole living cells. The negative control step is significant to eliminate aptamers that bind to non-specific and common cell surface proteins. Although cell-SELEX is a complicated process, the identify aptamers are effective molecular probes for cell-targeted drug delivery, and cell-specific diagnosis and therapy. Other SELEX modifications include mirror-image SELEX that utilizes enantiomers of natural compounds for selection (Vater & Klussmann, 2015); genomic SELEX which is based on the genomic sequence of an organism to target proteins of the same organism (Zimmermann et al., 2010); conditional SELEX which is used to select aptamers under specific assay conditions using regulator molecules (Mendonsa & Bowser, 2004); and toggle SELEX which is used to change target in alternating rounds of the selection process (Derbyshire et al., 2012).

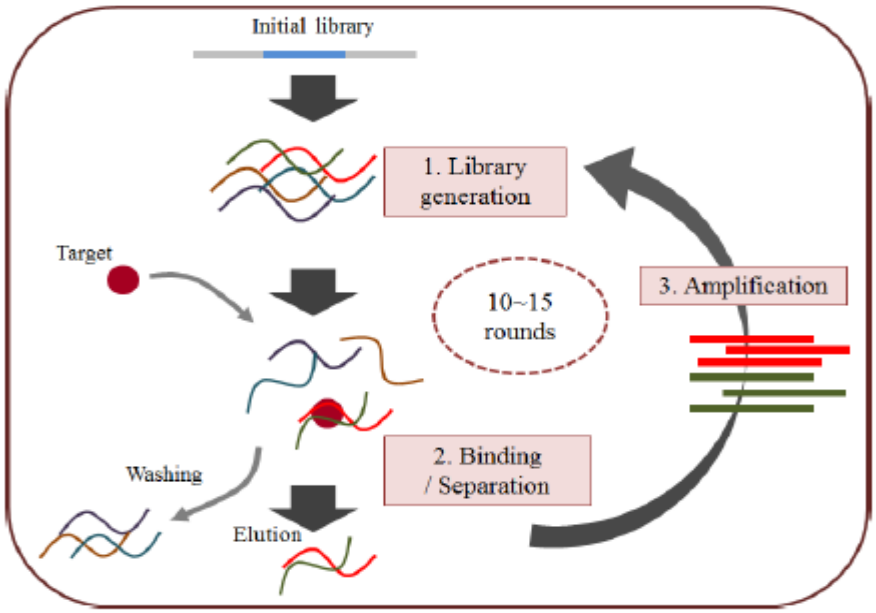

Figure 2.1: The general procedures of SELEX (Song et al., 2012)

2.3 APTAMERS AS TARGETING ELEMENTS

Aptamers are used as targeting molecules to direct chemotherapeutic drugs effectively to specific cellular sites, to increase cellular uptake via internalization, and to minimize cytotoxic effects (Y. F. Huang, Shangguan, Liu, Philips, et al., 2009; Radom et al., 2013; J. Zhu et al., 2014). The interaction between an aptamer and its target is based on their nature and 3-D structures. Aptamers interact with their targets via hydrophobic interaction, hydrogen bonding, electrostatic interaction, and Van der Waals interactions (McKeague & DeRosa, 2012; Upadhyay, 2013; Witt et al., 2015), and are capable of spontaneously undergoing structural re-conformation to enable binding to their targeted receptors (J. Zhu et al., 2014). The mechanism of aptameric targeting is based on drug-conjugated aptamers offering improved recognition and binding to specific cell surface receptors or internalized surface markers such as PTK7, PSMA, and nucleolin (Orava, Cicmil, & Gariepy, 2010). This consequently results in endocytosis, a receptor-mediated internalization process via endosome to enhance cellular uptake of drugs into the target cells (M. Alibolandi et al., 2015; Y. F. Huang, Shangguan, Liu, Philips, et al., 2009; Radom et al., 2013). The internalization of receptors occurs either via clathrin-dependent or clathrin-independent

vesiculation (Erdmann et al., 2014). For instance, the chemotherapeutic drug doxorubicin (Dox) is conjugated to an aptamer via a hydrazine linker to form a covalent bond between them. The drug can also be intercalated into the folded structure of the aptamer to form a physical drug-aptamer complex (Orava, Cicmil, & Gariepy, 2010). The binding properties of the aptamer and the cytotoxic effect of Dox are maintained even after conjugation (Y. F. Huang, Shangguan, Liu, Philips, et al., 2009; Radom et al., 2013). After internalization, hydrolysis of the covalent bond between the aptamer and the drug occurs in the acidic environment of the endosome. In the case of encapsulated aptamers, the aptamer has to diffuse out from the endosome into the cytosol before the endosome fuses with lysosomes which contain hydrolytic enzymes that can degrade the aptamer. Hence, linkers that are labile to acid can be hydrolysed in the endosomal acidic environment and linkers that are susceptible to hydrolytic and proteolytic enzymes can be broken down in the lysosomal acidic environment (G. Vilar, Tulla-Puche, J., Alericio, F. , 2012). After hydrolysis, the drug is released to diffuse through the endosomal membrane into the cytosol for nuclei entry and intercalation into the gDNA to produce cytotoxic effects (Y. F. Huang, Shangguan, Liu, Philips, et al., 2009; Radom et al., 2013). In brief, the critical steps involved in aptamer targeting and cellular uptake mechanism are targeting, internalization and cytotoxicity effects. Aptamer-mediated target delivery is highly dependent on the abundance of target cell surface receptors, possibility of inducing a receptor-mediated internalization upon aptamer binding, nature and size of the conjugated cargo, and the endocytic pathway of the target cell (Orava, Cicmil, & Gariepy, 2010).

Aptamer-mediated drug delivery system holds a great promise as aptamers can be artificially synthesized and evolved to specifically recognize large as well as very small structural differences within a desired target, generating a more efficient delivery system with high targeting power and desired features shown in Table 2.1 (Radom et al., 2013; Sun et al., 2014). With their flexible structures, aptamers can interact with hidden epitopes which could not be recognized by antibodies. As compared to other delivery agents such as antibodies, aptamers have a favorable size of approximately 25-fold smaller than monoclonal antibodies, resulting in higher tumor penetration. One significant advantage of aptamers is that they are non- or low-immunogenic and do not induce human immune responses (Santosh & Yadava, 2014). However, aptamers are shown to have some

shortcomings as compared to other delivery systems, including their cross-reactivity or negative effects on secondary targets due to the unknown targeting mechanism in normal cells, leading to undesirable side effects (Lakhin et al., 2013). There are also researchers reported that the affinity (Kd) of monoclonal antibodies is approximately 1000 times greater than that of aptamers, in a study comparing the anti-cancer efficacy and targeting specificity of both antibodies and aptamers (J. Zhu et al., 2014). Despite of countless promising results shown by aptamers in preclinical studies, there are many aptamers failed in clinical trials and thus, hinder their practical applications due to factors such as tumor heterogeneity and chemoresistance (J. Zhu et al., 2014).

Table 2.1: The desired features of aptamers as targeting elements for pre-clinical and clinical therapeutic applications

Aptamers	
Characteristics	**Advantages**
Stable in a board range of temperature, pH & ionic strengths	Biological activity is not affected
Small size with low molecular weight	Rapid blood circulation and effective cell penetration
Diverse targets	Recognize non-antibodies specific targets
Thermally and chemically stable	Robust under various conditions
Natural biological product	Non-toxic and non-immunogenic
Chemically synthesized	Highly scalable and economical

2.4 BIOPHYSICAL CHALLENGES TO APTAMER-BASED DELIVERY

Aptamers typically bind to the surface proteins of the target cells in the blood or interstitial fluids, and this requires biochemical stability in these compartments for a longer time. Consequently, factors such as induced negatively charged surface gradients, nuclease-mediated degradation, rapid bio-distribution from the bloodstream into tissues, and rapid renal filtration affect the stability of the aptamer (Sundaram et al., 2013). As a result, aptamers have short *in vivo* half-lives (Orava, Cicmil, & Gariepy, 2010). Nuclease-mediated degradation is a significant problem challenging preclinical and clinical

therapeutic applications of aptamers. Typically, the degradation time of aptamers in the blood stream is between several minutes to over 10 min depending on their concentration and conformational structure (Lakhin et al., 2013). However, strategies to circumvent this problem by chemical modifications to produce nuclease-resistant aptamers exist (Santosh & Yadava, 2014; Sun et al., 2014; J. Zhu et al., 2014). Also, aptamers are rapidly removed from the bloodstream by renal filtration due to their small molecular weight of 5-15 kDa whilst the kidney filters and excretes substances with 30-50 kDa molecular weight (Lakhin et al., 2013; Wengerter, 2014). Nevertheless, the lifespan of aptamers in the bloodstream can be prolonged via conjugation with molecules of 20 or 40 kDa molecular weight, such as polyethylene glycol (PEG), without losing their binding characteristics. The 2'-hydroxyl group of aptamers can be modified with 2'-fluoro or 2'-O-methoxyethyl to increase resistance against hydrolysis (Erdmann et al., 2014). Furthermore, aptamers are small and hydrophilic negatively-charged nucleic acid molecules that are incapable of crossing biological barriers such as cell membranes passively as they are impermeable to cell membrane, and this affects intracellular target-specific recognition (Wu, 2011). Another issue associated with the use of aptamers as target-specific mediators for drug delivery is the difficulty in controlling the pharmacokinetics and pharmacodynamics. The binding kinetics of the aptamer to the surface protein target can influence or dictate the rate of drug biosorption. Also, over-expression of the therapeutic action of aptamers can greatly impact the human body system. This drawback can be improved by adding antidotes or polycationic biopolymers to control the duration within the bloodstream. Aptamers are also capable of fusing into the human gDNA, and this can result in a non-target normal cell evolving to become cancerous through the alteration of normal protein expression by the foreign aptamer sequence (Khan, 2013).

2.5 BIODEGRADABLE POLYMERS FOR APTAMER-DRUG DELIVERY SYSTEMS

Polymeric delivery systems rely on biodegradable polymers for the formulation of particulate systems as delivery carriers in pharmaceutical drug delivery and *in vivo* therapy. Biodegradable polymers can be engineered to be safer and more efficient than other

delivery systems such as bacterial or viral system due to their tunable biophysical characteristics, stability and biocompatibility (Balashanmugam et al., 2014; Wu, 2011). An ideal polymer encapsulates active molecules without affecting their biochemical properties and activities, and should offer a stage-wise release of the molecules while minimizing initial burst and providing a controlled release for optimal dosage over a period of time (Stevanovic & Uskokovic, 2009; M. Tan & Danquah, 2012). Compared to polymeric nanoparticles, microparticles have a more favorable size that is better phagocytized by cells (Balashanmugam et al., 2014) though nanoparticles present an effective surface area for cell adsorption. Aptamers can be encapsulated, complexed or conjugated with polymeric systems to protect them from the physiological environment and enable them to traverse the membrane of target cells to reach targeted intracellular sites (Orava, Cicmil, & Gariepy, 2010). Some biodegradable polymers that can be used to generate aptamer-polymer formulations are discussed as follow.

2.5.1 Poly(lactic-co-glycolic acid) (PLGA)

PLGA is a synthetic and resorbable polyester polymer approved by FDA and World Health Organization (WHO) and used as a delivery carrier of targeting and/or therapeutic agents for drug delivery and medical applications (Stevanovic & Uskokovic, 2009; G. Vilar, Tulla-Puche, J., Alericio, F. , 2012). PLGA is a copolymer of Polylactic acid (PLA) and Polyglycolic acid (PGA), and can protect encapsulated aptamers from nuclease and proteolytic degradation as well as maintaining the binding efficiency and specificity of the aptamers. PLGA can be synthesized in any size and shape to harbour molecules of various sizes and functionalities (Makadia & Siegel, 2011). Also, PLGA is cost-effective to synthesize and can be adapted for different *in vivo* applications due to its high biocompatibility and low toxicity. Hydrolyzed PLGA produces lactic acid and glycolic acid as the monomers of PLGA, and these are actually the byproducts of many cellular metabolic pathways (Davaran et al., 2014; Nikitczuk et al., 2013; Stevanovic & Uskokovic, 2009; G. Vilar, Tulla-Puche, J., Alericio, F. , 2012). PLGA particles have positively charged surfaces, making them suitable to bind electrostatically with negatively charged aptamers (L. Li et al., 2014). PLGA has been demonstrated as an effective carrier for vaccine delivery because it can be phagocytosed by antigen presenting cells (APCs) and

macrophages in *vivo* to facilitate adaptive immunity development (Nikitczuk et al., 2013; Wengerter, 2014). Thus, PLGA can be used effectively if the encapsulated drug targets phagocytic cells that are infected with pathogens (G. Vilar, Tulla-Puche, J., Alericio, F. , 2012). PLGA possesses a high encapsulation capacity to carry heavy DNA payload, making it a highly efficient DNA delivery vector (Balashanmugam et al., 2014). PLGA-based aptamer mediated drug delivery systems show promising results such as high encapsulation efficiency, low cytotoxicity, enhanced cellular uptake, high therapeutic index, sustained drug release and retention, and enhanced stability as demonstrated by the following studies: AS1411 DNA aptamer-labeled paclitaxel (PTX)–loaded PLGA-lecithin-PEG nanoparticles in targeting the nucleolin of chronic lymphocytic leukemia and MCF-7 cells (Aravind, Jeyamohan, et al., 2012); epithelial cell adhesion molecule (EpCAM) aptamer conjugated doxorubicin (DOX)-PEG-PLGA nanopolymersomes to treat human breast adenocarcinoma cells (M. Alibolandi et al., 2015); AS1411 aptamer conjugated PTX-loaded PEG-PLGA nanoparticles in targeting the nucleolin on glioma cells (Jianwei Guo et al., 2011); EpCAM aptamer functionalized curcumin-loaded PLGA-Lecithin-PEG in targeted drug delivery to colon cancer cells (L. Li et al., 2014); drug-encapsulated prostate-specific membrane antigen (PSMA) aptamer-PLGA-*b*-PEG nanoparticles (Dhar et al., 2008; Farokhzad et al., 2006); PSMA targeted A10 RNA aptamer-drug-PLGA-*b*-PEG nanoparticles in treating prostate cancer (Cheng et al., 2007b), and AS1411 aptamer-functionalized PTX-loaded PLGA nanoparticles in targeting glial cancer cells (Aravind, Varghese, et al., 2012). PLGA is an ideal polymeric aptamer-mediated delivery due to its high encapsulation capacity (Balashanmugam et al., 2014), pH and temperature-driven adjustable degradation rate (Aravind et al., 2013; G. Vilar, Tulla-Puche, J., Alericio, F. , 2012), tunable physicochemical and mechanical properties (Makadia & Siegel, 2011), well established clinical safety with FDA approval and extensive application in therapeutic delivery (Aravind, Varghese, et al., 2012), and diffusion-based controlled release (Aravind et al., 2013; Makadia & Siegel, 2011).

2.5.2 Poly(ethylene imine) (PEI)

PEI is a widely researched and used polymer for gene delivery due to its high transfection efficiency. It is a well-characterized polycationic polymer and transfection agent (Nguyen

et al., 2008; Stevanovic & Uskokovic, 2009), and encapsulates DNA via electrostatic interactions (Nguyen et al., 2008). It is capable of condensing negatively charged DNA into positively charged molecules to enable interactions with cell membrane surface for enhanced uptake via endocytosis. PEI is also a pH-sensitive polymer with a buffering effect, and this is suitable for maintaining the acidic environment of phagosome in order to release encapsulated DNA (Nguyen et al., 2008). PEI has also been demonstrated to increase transfection efficiency (Nguyen et al., 2008). However, at high dosages PEI can demonstrate significant cytotoxic effects and this is a major drawback to its application (Balashanmugam et al., 2014). Some studies have demonstrated the use of PEI in enhancing aptamer mediated delivery systems by improving the loading capacity, release rate, and transfection efficiency. Kurosaki et al. (2012)reported the application of mucin 1 (MUC1) aptamer coated-pDNA-PEI nanoparticles for effective tumor targeting and increased gene expression (Kurosaki et al., 2012). Another study on EpCAM aptamer-PEI-siRNA nanocomplex showed targeted delivery of siRNA to inhibit tumor cell proliferation (Subramanian et al., 2015).PEI is a powerful non-viral transfection agent under both *in vitro* and *in vivo* conditions and can increase the performance of aptamer-mediated delivery by controlling the release rate and improving the transfection efficiency to a greater extent without any notable cytotoxic effect at low concentrations (Kurosaki et al., 2012). Additionally, the cationic property of PEI enables the stable encapsulation of aptamer via electrostatic interaction with aptamer to form polyplexes (Nguyen et al., 2008). Characteristics of PEI including high encapsulation payload, non-mutagenicity, ability to increasing endosomal release via proton sponge mechanism and the capacity to facilitate active transport of aptameric formulations into the nucleus, protecting the aptamer from nuclease degradation without affecting binding specificity over extended period (Chen et al., 2013), make it a suitable carrier for aptamer-mediated drug delivery.

2.5.3 Chitosan as a modified natural polysaccharide

Polysaccharide polymers are made up of monomers with various configuration of o-glycoside bond (Kumari et al., 2010). Chitosan is a modified natural polysaccharide which is widely employed in pharmaceutical formulations due to its biocompatibility, biodegradability and low toxicity (Saranya & Radha, 2014). It is synthesized from

partially N-deacetylated crustacean, derived from the natural chitin biopolymer, using methods such as micro emulsion, ionotropic gelatin and emulsification solvent diffusion (Kumari et al., 2010; Saranya & Radha, 2014). It is cationic, making it suitable as an aptamer-mediate or gene delivery vehicle. The encapsulation mechanism of chitosan is largely a self-assembly process due to the spontaneous electrostatic interaction between cationic chitosan and anionic biomolecules such as DNA (G. Vilar, Tulla-Puche, J., Alericio, F. , 2012). Chitosan is also mucoadhesive, and this makes it a potential drug delivery vehicle for pulmonary application (G. Vilar, Tulla-Puche, J., Alericio, F. , 2012). Many studies have reported the use of chitosan as a drug and/or aptamer carrier to provide high encapsulation efficiency, low burst release, and continuous and sustained release of bioactives. A chitosan-based S58 aptamer nanoparticulate complex (CS(S58)-NP) preserved the efficacy of S58 aptamer to antagonize the action of TGF-β in human Tenon's capsule fibroblasts in order to restrain fibroblast cell proliferation (Chen et al., 2013). The recent study by X. Zhu et al. (2015) also demonstrated the antifibrotic effects of CS(S58)-NP in drug therapy. Chitosan has also been reported as a promising carrier for the delivery of SN38 drug to MUC1 overexpressing colon cancer cells by using MUC1-DNA aptamer as the recognition element (Sayari et al., 2014). Chitosan has demonstrated to improve the pharmacokinetics, solubility, targeted delivery and efficacy of SN38 in chemotherapeutics (Sayari et al., 2014). It is an ideal polymeric carrier for aptamer-mediated delivery due to its favorable characteristics such as cationic nature for encapsulating negatively charged molecules such as aptamers (G. Vilar, Tulla-Puche, J., Alericio, F. , 2012), stable and sustained release (Chen et al., 2013), high aptamer protection (Chen et al., 2013), and mucoadhesive property that favors delivery of bioactives for improved intestinal absorption (Kumari et al., 2010).

2.5.4 Poly(beta-amino ester) (PBAE)

PBAE is a novel micro-polymer and has successfully been used to formulate and deliver plasmid molecules due to its pH sensitiveness and effectiveness for acidic endosomal delivery (Balashanmugam et al., 2014). Its biodegradation results in products that are non-toxic and safe to cells. It is also capable of condensing and protecting DNA molecules to improve endocytosis. However, PBAE particulate formulations are challenged with

reduced cell transfection efficiency under high PBAE concentrations, and this is as a result of the strong binding between PBAE and DNA molecules (Balashanmugam et al., 2014). Also cell cytotoxicity increases with increasing PBAE concentration hence, optimal dosage evaluation to minimize cytotoxicity is essential to achieve effective cell transfection. J. Zhang et al. (2014) demonstrated enhanced efficacy of a modified pH-sensitive AS1411 aptameric copolymer [D-α –tocopheryl polyethylene glycol 1000-block-PBAE] (Apt-TPGS-b-PBAE) in targeted drug delivery of PTX with improved nucleolin-target recognition, pH-responsive drug release and high cytotoxicity. The copolymer TPGS-b-PBAE was produced via Michael-type step growth polymerization of a diacrylate and amine prior to free radical crosslinking (J. Zhang et al., 2014). Though this material has not been widely employed for aptamer mediated drug delivery, it has been utilized effectively as a transport vehicle for various drug and gene delivery systems with reduced burst, increased tumor accumulation and prolonged release (Balashanmugam et al., 2014; Fields et al., 2012; Fisher et al., 2014; Vlerken, 2008). The cationic PBAE polymers are capable of encapsulating aptamers, trigger specific cellular uptake and buffer the endosomal acidic environment for aptamer release (Fields et al., 2012). Vlerken (2008) reported the use of PBAE polymer to increase the retention time of higher concentrations of PTX at tumor site with minimal systemic clearance. These characteristics demonstrate potentials for use as a carrier for aptamer mediated targeted delivery.

2.5.5 Polyethylene glycol (PEG)

PEG has widely been employed to enhance the therapeutic efficiency of various proteins in term of pharmacodynamics and pharmacokinetics (Liechty et al., 2010), and has been approved by FDA for pharmaceutical delivery in rectal, nasal and injectable formulations (Liechty et al., 2010). PEG is a polyether diol produced from aqueous anionic polymerization of ethylene oxide. It is a hydrophilic polymer, non-toxic, non-immunogenic, and can be removed via hepatic and renal clearances. PEG micro formulations have demonstrated to improve the solubility of sparingly soluble therapeutic agents for enhanced drug delivery (Dhar et al., 2008). In addition, its hydrophilic nature protects proteins from the immune system, and can also be conjugated covalently with

proteins or peptides without crosslinking (Liechty et al., 2010). Although PEG conjugation can improve the activity of proteins, it can be compensated with increased circulation time to release effective therapeutic dosage (Liechty et al., 2010). Many studies have been reported on the use of PEG copolymer as a delivery carrier for aptamer mediated pharmaceutical delivery. PEG particles are often bio-conjugated with other polymers for enhanced targeted delivery. Some PEG bio-conjugated polymers for aptamer mediated delivery include AS1411 DNA aptamer-labeled PTX–loaded PLGA-lecithin-PEG nanoparticles (Athulya Aravind & Yutaka Nagaoka, 2012), EpCAM aptamer conjugated DOX-PEG-PLGA nanopolymersomes (M. Alibolandi et al., 2015), EpCAM aptamer functionalized curcumin-loaded PLGA-Lecithin-PEG (L. Li et al., 2014), and drug-encapsulated PSMA aptamer-PLGA-*b*-PEG (Dhar et al., 2008; Farokhzad et al., 2006). PEG particles possess desirable biophysical characteristics that improve aptamer mediated delivery. These include systemic clearance reduction of encapsulated bioactives (Jianwei Guo et al., 2011; L. Li et al., 2014), and enhancement of pharmacokinetic and pharmacodynamics (Farokhzad et al., 2006; Liechty et al., 2010). It can used for PEGylation of other particles to give stronger protective effect and improve the formulation stability by acting as a barrier to the external environment (Makadia & Siegel, 2011), as well as prolonging circulation time for optimal therapeutic effects (Dhar et al., 2008). Several FDA approved drugs such as PEG-L-asparaginase, PEG-interferon-α, and PEG-adenosine deaminase are formulated with PEG to enhance pharmaceutical properties (Dhar et al., 2008; Liechty et al., 2010).

2.5.6 Poly (ortho esters) (POE)

POE represents a class of pH-sensitive polymers classified as POE I, POE II, POE III and POE IV with varying physico-chemical properties and drug release profiles based on their monomer make up and synthesis approach (Nguyen et al., 2008). POE I is challenged with acidic degradation products and this causes autocatalytic polymer degradation. POE II is a modified version of POE I to resolve the issue of acidic autocatalytic degradation. However, it offers a low degradation rate due to its hydrophobicity. POE III is not widely used as it is difficult to synthesise at a specific molecular weight. POE IV is hydrophobic with incorporated latent acid monomers in its backbone to contain acid-labile ester

linkages for rapid hydrolytic degradation. Its pH-sensitive characteristics favor gene delivery to phagocytic molecules like dendritic cells and macrophages. POE IV is highly reproducible with straightforward synthesis process, and its hydrophobic nature can be tuned to control the polymer degradation rate and thus drug release rate (G. Vilar et al., 2012). Some studies have demonstrated the successful use of POE for plasmid DNA delivery applications (Nguyen et al., 2008; Wang et al., 2004). Plasmid DNA encoding for a specific antigen diffused into the cells after phagocytosis of polymer-DNA complex resulting in the release of encapsulated DNA in the acidic environment of late phagosome. As a result, adaptive immunity is activated from the expression of the foreign antigens (Nguyen et al., 2008; G. Vilar et al., 2012). Past studies have demonstrated the success of POE particles in encapsulating pDNA for efficient vaccine delivery (Nguyen et al., 2008; Wang et al., 2004). POE particles were molecularly engineered to possess high payload and improved DNA vaccine efficacy by preventing DNA degradation, enhancing uptakes by APCs, and allowing pH-responsive rapid DNA release in the phagosome (Wang et al., 2004). These promising outcomes show the potential of POE polymers as transport vehicles for DNA aptamer formulations for targeted release applications. POE IV possesses attractive characteristics that are crucial to enhance aptamer-mediated delivery. These include pH-dependent degradation for aptamer release at specific sites (Nguyen et al., 2008), the presence of latent acid enabling control over polymeric erosion rate, great mechanical and thermal properties that regulate both degradation and release rate (G. Vilar et al., 2012), and modifiable physicochemical properties such as hydrophobicity, morphology and molecular weight to obtain desirable *in vivo* biodegradation to alter the release rate of encapsulated biomolecules (Deng et al., 2003; G. Vilar et al., 2012).

2.6 COPOLYMERSOME-APTAMER CONJUGATION CHEMISTRY

Aptameric linkage to polymeric formulation involves a self-assembly technique that allows functional carboxyl and amine groups to form structural arrangements between the aptamer and polymer through localised interactions. The self-assembly characteristics of the aptameric conjugation limit the ability to regulate the ligand binding transpiring at the molecular level (Si-shen et al., 2014). The copolymer blend ratios are often adjusted to

vary the functional groups available for targeting ligands and this effectively controls the surface density of the aptamer (Gu et al., 2008). Two studies have been conducted on ligand variation technique to control the surface density of linker molecules on the particulate formulation. The technique involves controlling the partial chains of the copolymer to regulate the conjugation of targeting ligands (Si-shen et al., 2014). Cheng et al. (2007a) devised a pre-conjugation process that involves alteration of targeted and non-targeted copolymer blend ratios before the formation of colloidal polymeric suspension. The susceptibility of aptamer ligands in organic solvents to potentially diminish bioactive functionality limits further studies on this technique. Alternatively, Y. Liu et al. (2010) developed a post-conjugation process which utilised co-polymeric moieties to conjugate the targeting ligand onto the surface of the formulation. The surface density of the targeting ligand on the polymeric formulation is controlled by varying the ligand concentration in the conjugation stage.

The chemical stability of aptamers and their available reactive sites enables distinct conjugation chemistry routes to implant targeting ligands into the copolymer matrix (Grumezescu, 2016a). Co-polymeric formulations are generally developed by either self-assembled monolayers of aptamers on polymeric surface or conjugation to the polymeric structure via carbodiimide chemical route. The self-assembly method or conjugation technique ensures that the characteristics of the aptamer including binding affinity, sensitivity, bioactivity, and specificity are not compromised in the process (Oh et al., 2014). The process must maintain the upper limit of the aptamer surface density which allows targeting ligands to detect the target cell in the absence of steric hindrance or secondary electrostatic interactions that could hamper the functionality of the ligand (Tiwari & Tiwari, 2013). The technique for aptameric linkage to copolymers must ensure appropriate spatial orientation of the ligand within the copolymer matrix for high specificity and binding affinity (Rinker et al., 2008). Aptameric functionality is often diminished by heterogeneous orientation of the targeting ligands and this impacts *in vivo* performance efficiency, resilience, and the pharmacokinetic response of the formulation (Rege & Medintz, 2009).

Non-specific adsorption of targeting ligands onto the polymeric surface through weak localised electrostatic interactions is a convenient and simple technique but with limited applications since the aptameric layer could easily be washed off (Yang et al., 2011). The non-covalent linkage strategy in Figure 2.2 is facilitated through affinity interactions strengthened by the presence of linkers in streptavidin-biotin complex. The site-specific conjugation method of forming aptameric linkages to polymeric surfaces utilises succinimidyl ester-amine or maleimide-thiol linkers as chemical routes (Oh et al., 2014). The aptamer is freely suspended in the covalent conjugation to pertinent functional groups, functionalised linkers or spacers on the polymer surface. The suspension enables targeting ligands to tailor or adapt to various structural arrangements to suit the target site (Grumezescu, 2016b). The site-specific covalent conjugation of the aptamer on the polymeric surface results in strong and resolute linkages with the capacity to resist extreme physiological and pathological environments (Rege & Medintz, 2009). Cerruti et al. (2009) devised a PEGM or poly(ethyl-ene-co-glycidyl methacrylate) matrix covalently conjugated to TNT aptamer through free primary amines linked to epoxy groups of the glycidyl methacrylate group to form a non-hydrolysable covalent bond without affecting the targeting affinity of the ligand. The chemical schemes for site-specific covalent conjugation involve amine, thiol and biotin termini groups on targeting ligands which limits the available chemical routes for the formation of aptamer-polymersome conjugates (Balamurugan et al., 2008). A common aptamer-polymersome covalent coupling involves the use of 1-ethyl-3-(3-dimethylaminopropyl) carbodiimide (EDC) and N-hydroxysuccinimide (NHS) as shown in Figure 2.3.

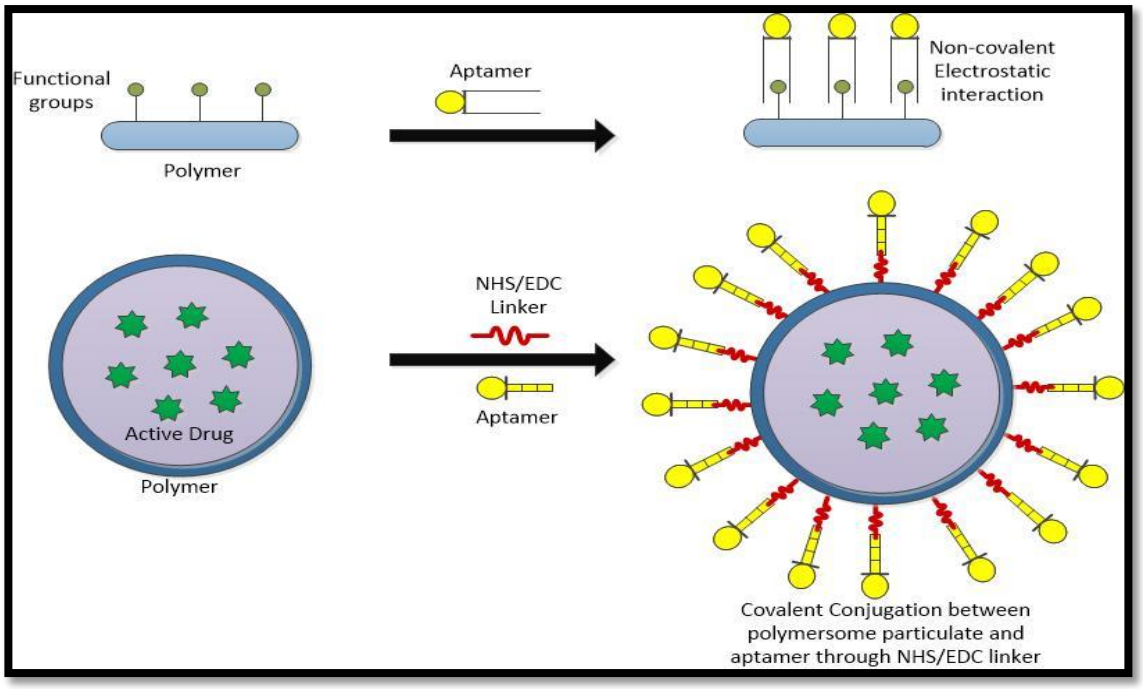

Figure 2.2: Conjugation chemistry using covalent and non-covalent bonding

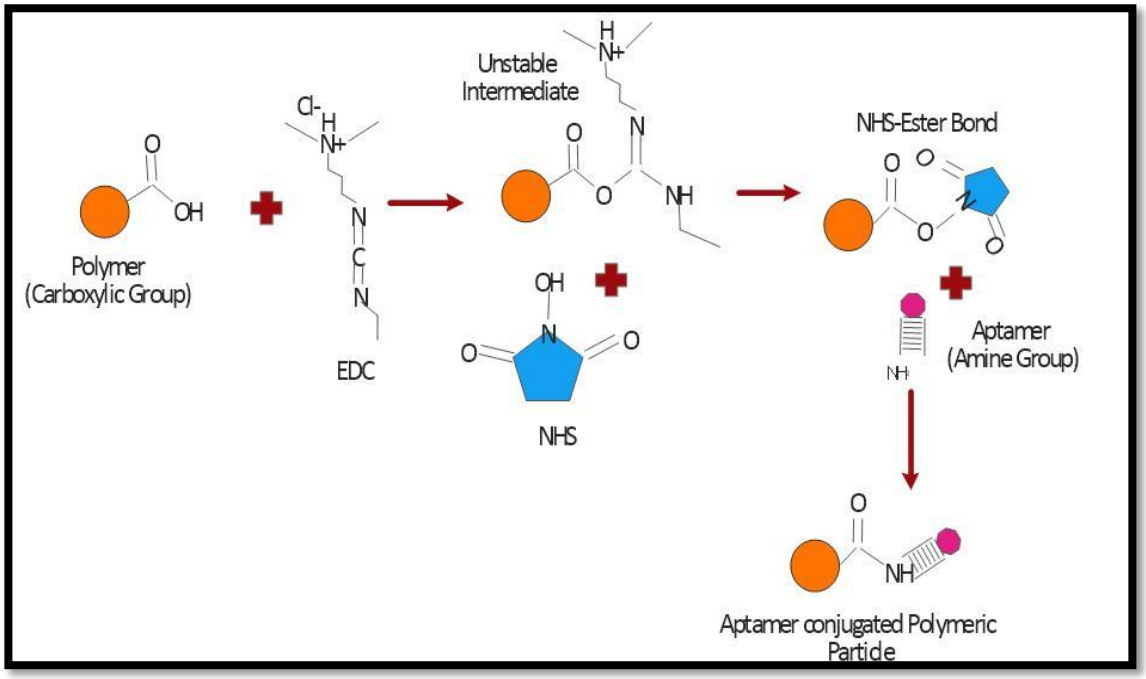

Figure 2.3: NHS/EDC coupling mechanism

2.7 CURRENT RESEARCH ON APTAMER-MEDIATED FORMULATIONS FOR TARGETED DELIVERY

Effective targeted delivery can enhance the performance indices of drug therapies, and aptamers demonstrate suitable and specific binding characteristics to promote targeted delivery and inhibit pathogen expression systems. Aptamers have been used as active drugs to inhibit specific targets with high affinity. REG1 aptamer has been demonstrated a factor IXa inhibitor in REG1 anticoagulation to treat acute coronary syndrome (Vavalle & Cohen, 2012). A recent study by Gao et al. (2014)elucidated the use of NS2-specific DNA aptamer as a NS2 viral protein inhibitor to block RNA replication thus, preventing virus production of hepatitis C virus (HCV) *in vitro*. This promising result demonstrates NS2 aptamer as a potential drug for treating HCV (Gao et al., 2014). Aptamers are also exploited in drug delivery as targeting elements due to their high specificity for internalized cell surface protein receptors or extracellular ligands (Jianwei Guo et al., 2011). For example, the prostate-specific membrane antigen (PSMA) is the internalized prostate cancer surface marker used in the diagnosis of prostate cancer (Cheng et al., 2007b), and Min et al. (2011) developed a dual aptamer complex which includes an A10 RNA aptamer that targets PSMA (+) prostate cancer cells, and a DUP-1 peptide aptamer that targets PSMA(-) prostate cancer cells (Min et al., 2011). The dual aptamer complex was loaded with DOX, an anticancer drug, on the A10 aptamer oligonucleotide strand for targeted delivery, DOX was successfully delivered to the prostate cancer cells via cell internalization induced by the binding of aptamers to PSMA, causing apoptosis in both PSMA (+) and (-) cells (Min et al., 2011). Y. F. Huang, Shangguan, Liu, Phillips, et al. (2009) reported the efficiency of the DNA aptamer, sgc8c, as a target-recognition factor for drug delivery. The sgc8c aptamer, which was conjugated with DOX, directed DOX to the target T-cell acute lymphoblastic leukemia CCRF-CEM cells by binding to tyrosine kinase 7(PTK7) protein receptors on the cells. As a result, cytotoxicity effect to the tumor cells increased whilst toxicity to surrounding normal cells was minimal (Y. F. Huang, Shangguan, Liu, Phillips, et al., 2009). The use of small interfering RNAs (siRNAs) are highlighted as therapeutic tools for various diseases due to the significant role it plays in triggering a RNA interference (RNAi) pathway to regulates specific gene expression. A siRNA-aptamer conjugate was introduced by Chu et al. (2006) to mitigate prostate cancer

cell proliferation. The results showed successful inhibition of gene expression by siRNA delivered under aptamer mediation to the cancer cells that express PSMA antigen (Chu et al., 2006). They also reported that the gene expression inhibition was rapid within 30 min, indicating that the protection of aptamers and siRNAs from nucleases is not necessary since internalization is rapid (Chu et al., 2006). Other clinical studies showed that the AS1411 aptamer is able to bind and target an over-expressed protein known as nucleolin in various tumor cells, leading to a potential therapeutic tool for acute myeloid and leukemia (Sun et al., 2014). The binding of nucleolin with aptamers induces endocytosis or macropinocytosis that increases the intracellular delivery of drug into targeted cell (Jianwei Guo et al., 2011).

Jianwei Guo et al. (2011) investigated the efficiency of AS1411 DNA aptamer conjugated with PEG-PLGA nanoparticles for targeted delivery of PTX to nucleolin, which are highly expressed on the plasma membrane of tumour cells and endothelial cells of angiogenic blood vessels, to cure infiltrative brain tumors-gliomas with significant increased tumor inhibition and prolonged survival (Jianwei Guo et al., 2011). The work of Aravind, Jeyamohan, et al. (2012) showed that AS1411 anti-nucleolin aptamer-PLGA-lecithin-PEG nanoparticles were more effective in targeted drug delivery as they offered high encapsulation efficiency, sustained drug release and enhanced cancer killing effect at specific target sites compared to non-aptamer-targeted nanoparticles and PLGA nanoparticles alone (Aravind, Jeyamohan, et al., 2012). The effectiveness of the AS1411 aptamer was evidenced by enhanced uptake of PTX-loaded nanoparticles into the tumor cells overexpressing nucleolin receptors on the plasma membrane. M. Alibolandi et al. (2015) studied the effectiveness of EpCAM-targeted RNA aptamer conjugated PEG-PLGA nano-polymersomes in targeted delivery of doxorubicin to human breast adenocarcinoma cell line *in vitro* with improved doxorubicin therapeutic index in EpCAM cancer cells (M. Alibolandi et al., 2015). L. Li et al. (2014) also reported the application of RNA aptamers in targeting EpCAM on the surface of colorectal adenocarcinoma cells for efficient targeted delivery of curcumin to colon cancer cells by using EpCAM aptamer-functionalized curcumin-encapsulated PLGA-lecithin-PEG nanoparticles (L. Li et al., 2014). Table 2.2, 2.3 and 2.4 presents a summary of some reported research work on aptamer-mediated pharmaceutical delivery.

Table 2.2: Summary of some reported work on aptameric nano/micro formulations for targeted delivery

Aptamer	Carrier - Micro/nano particles (MPs / NPs)	Target	Active component	Disease	Reference
A10 RNA aptamer	PLGA-*block*-PEG-COOH NPs, superparamagnetic iron oxide NPs, PLGA-PEG NPs	PSMA (+)	Doxorubicin, Platinum (IV) compound of cisplatin, and docetaxel	Prostate cancer	(Cheng et al., 2007b; Dhar et al., 2008; Farokhzad et al., 2006; Min et al., 2011)
DUP-1 peptide aptamer	Superparamagnetic iron oxide NPs	PSMA (-)	Doxorubicin	Prostate cancer	(Min et al., 2011)
sgc8c DNA aptamer	Aptamer-drug conjugate	Protein tyrosine kinase 7 on CCRF-CEM cells	Doxorubicin	Acute lymphoblastic Leukemia	(Y. F. Huang, Shangguan, Liu, Phillips, et al., 2009)
siRNA aptamer	Aptamer-drug conjugate	PSMA	siRNA-therapeutic drug	Prostate cancer	(Chu et al., 2006)

AS1411 DNA aptamer	PEG-PLGA NPs, PLGA-lecithin-PEG NPs, magnetic fluid-PLGA NPs, and TPGS-b-PBAE	Nucleolin protein	Paclitaxel	Acute myeloid leukemia, chronic lymphocytic leukemia, breast cancer, gliomas, and renal cancer	(Aravind, Jeyamohan, et al., 2012; Aravind et al., 2013; Aravind, Varghese, et al., 2012; Jianwei Guo et al., 2011; J. Zhang et al., 2014)
RNA aptamer	PEG-PLGA NPs, and PLGA-lecithin-PEG NPs	EpCAM on human breast adenocarcinoma cells-MCF-7 cells, and colorectal adenocarcinoma cells	Doxorubicin, and Curcumin	Breast cancer, and colon cancer	(M. Alibolandi et al., 2015; L. Li et al., 2014)
MUC1 aptamer	PEI NPs, and Chitosan NPs	MUC1 cell surface glycoprotein on lung epithelial cells, and	pDNA, and SN38 drug	Lung cancer, and colon cancer	(Kurosaki et al., 2012; Sayari et al., 2014)

		colon cancer cells			
EpCAM aptamer	PEI NPs	EpCAM transmembrane glycoprotein	siRNA	Breast cancer, and retinoblastoma	(Subramanian et al., 2015)
S58 aptamer	Chitosan NPs	TGF- β receptor	S58 aptamer	Tenon's capsule fibroblasts	(Chen et al., 2013)

Table 2.3: Comparison of some aptamer-polymeric formulations as pharmaceutical targeted delivery agents

Targeted Polymeric formulation for cell-specific delivery	**Synthesis technique**	**Target Site**	**Encapsulation efficiency %**	**Loading capacity for active drug %**	**Ref.**
PTX loaded PEG-PLGA encapsulation with AS1411 Aptamer	**Solvent evaporation method** which formed a colloidal suspension after evaporating solvent from polymeric emulsion	Gliomas (Infiltrative brain tumors)	44.7	1.0	(J. Guo et al., 2011)

PTX loaded PLGA-Lecithin-PEG encapsulation with AS1411 Aptamer	**Nanoprecipitation** involving spontaneous emulsification of the organic phase when added to the aqueous phase to form nanoparticle dispersion	B-cell chronic lymphocytic leukemia (CLL)	60.8	-	(Athulya Aravind & Yutaka Nagaoka , 2012)
Gemzar (GEM) loaded PEG-PLGA nanopolymersomes conjugated to AS1411 aptamer	**pH gradient method** involving the addition of active drug solution at specific pH to form a transmembrane pH gradient at the desired drug to lipid ratio prior to the formation of colloidal suspension	Large cell neuroendocrine carcinoma NSCLC (Non-small cell lung cancer)	95.3	8.6	(Mona Alibolandi et al., 2016)
Vinorelbine loaded PLGA/PEG conjugated to S2.2 aptamer	**Self-assembly method** dependent on the local interactions between the functional groups of the aptamer and the polymer to form structural arrangements	Stage IV Advanced Breast cancer (Metastatic breast cancer)	50.7	6.6	(Z. Liu et al., 2015)
Ursolic acid (UA) loaded PLGA-b-PEG copolymer conjugated to	Conjugation of aptamer through **carbodiimide crosslinker chemistry** which allowed	EpCAM expression in gastric and breast cancer cells	80.1	4.0	(J. Liu et al., 2016)

SYL3C Aptamer	EDC to couple NHS with carboxyls. Aptamers can easily conjugated to the EDC/NHS crosslinked carboxyl group.				

Table 2.4: Some aptamer-polymersome formulations in clinical trials

Aptamer-polymersome formulations	**Targeting site**	**Disease**	**Clinical trial Phase**	**Identifier ID**	**Ref.**
Targeted polymeric nanoparticle BIND-014 (PEG matrix embedded with targeting ligand and loaded with drug docetaxel)	PSMA (prostate-specific membrane antigen) over expressed transmembrane protein present on prostate cancer cells	Metastatic castration-resistant Prostrate carcinoma (CRPC)	Trial Phase II	NCT01812746	(BIND Therapeutics, 2013)
REG1 loaded with Bivalirudin and linked to 34-nucleotide PEGylated RNA aptamer, pegnivacogin	Specific binding affinity to factor VIIa/IXa. Inhibits catalytic activities of the factor.	Unstable angina or myocardial infarction of acute coronary artery disease (CAD)	Trial Phase III	NCT01848106	(Lincoff et al. 2016)

Polymeric nanoparticle BIND-014 (PEG matrix embedded with targeting ligand and loaded with drug docetaxel)	HER2 (Human epidermal growth factor receptor 2) over expressed on breast cancer cells	KRAS mutation positive or squamous cell non-small lung cancer (NSCLC)	Trial Phase II	NCT02283320	(Therapeutics, 2014)
PEG linked to anti-VEGF specific RNA aptamer and loaded with Macugen (Pegaptanib Sodium)	Specifically binds to angiogenic factor known as vascular endothelial growth factor (VEGF) over expressed on cancers that can metasize	Proliferative diabetic retinopathy (PDR) with or without macular involvement	Trial Phase I	NCT01487070	(Retina Institute of Hawaii, 2011)
PEG polymersome formulation loaded with the drug E10030 and conjugated with anti-PDGF aptamer	Platelet-derived growth factor (PDGF) located on mesenchymal cells	Neovascular age-related Macular Degeneration	Trial Phase I	(NCT00569140)	Jo et al. 2006; Sundaram et al. 2013b)

2.8 COLLAGEN IN DRUG-CONJUGATED APTAMER

Cancer invasion is characterized as the degradation of fibrillar collagens and remodeling of extracellular matrix. Collagen is defined as the major protein component of connective tissues. The quantity of type I and type III collagen degradation products in serum is reported to be associated with the cancer survival rate, reflecting tumor metastasis (Nurmenniemi et al., 2012). Aptamer has been demonstrated as an efficient therapeutic

agent in treating oral cancer by acting as an anti-heparanase aptamer that inhibits the degradation of type III collagen. Heparanase is an enzyme responsible for carcinoma cell invasion and tumor metastasis. Consequently, the aptamer-mediated inhibition of collagen degradation decreases the amount of collagen degradation products, indicating the tissue invasion is blocked effectively (Simmons et al., 2014). Kaida et al. (2013) illustrated the therapeutic application of DNA aptamer in treating diabetic nephropathy by reducing the gene expression of advanced glycation end products and their receptors as well as the type IV collagen in diabetic kidney (Kaida et al., 2013). Another study by Xiaoyan Zhu et al. (2012) indicated a novel aptamer, S58 in recognizing and interacting with TGF-β receptor II in order to prevent the human Tenon's fibroblasts in transdifferentiating into myofibroblast. The experimental results showed that S58 is capable of suppressing the TGF-β2-induced collagen contraction (Xiaoyan Zhu et al., 2012).

2.9 TARGETED CANCER THERAPY: THE USE OF APTAMER OR ONCOLYTIC VIRUS?

2.9.1 Global cancer scenario

Cancer is a major global health problem causing about one in every seven deaths worldwide (Society, 2015). The high mortality rate of cancer persists regardless of the significant developments in cancer therapies over the past few decades (P. K. Singh et al., 2012). It has been reported that over 60% of cancer deaths happen in low-medium resource economies due to poverty, ignorance, environmental pollution, and poor medical and health systems (Siegel et al., 2015). Notwithstanding the advancements in modern medicine, the global cancer 'epidemic' is increasing significantly. The American Cancer Society predicts that there will be approximately 21.7 million of new cancer cases with 13 million deaths in 2030 (Society, 2015). According to GLOBOCAN, about 15 million new cancer cases and 8.8 million cancer mortality cases, excluding non-melanoma skin cancer, are expected globally in 2015 (J. Ferlay, Soerjomataram, I., Ervik, M., Dikshit, R., Eser, S., Mathers, C., Rebelo, M., Parkin, D.M., Forman, D., Bray, F. , 2013). It has been reported that about one-third of cancer cases in developed nations are due to unhealthy

behaviors including poor nutrition, obesity, and physical inactivity (Society, 2015). Cancers that are common in men are lung and bronchus, colorectal, prostate, pancreas and liver cancers whilst women are mostly diagnosed with breast, colorectum, pancrease, ovary, and lung and bronchus cancers (J. Ferlay et al., 2015; Siegel et al., 2015). According to American Cancer Society, the top five cancers in both men and women are breast, prostate, cervix uteri, lung and colorectal cancers (Saranath, 2014; Siegel et al., 2015). Globally, most of the cancer related deaths are caused by lung, stomach and liver cancers (J. D. Sharma, Kalit, M., Nirmolia, T., Saikia, S. P., Sharma, A., Barman, D. , 2014) and a summary is displayed clearly in Table 2.5 below.

Table 2.5: A summary of different types of cancers with causes, mortality, region effects and treatment

Cancer type	Common causes	Estimated number of cancer deaths in 2015	Region	Treatment	References
Lung	Tobacco intake and consumption, infectious agents such as hepatitis B virus (HBV), radon gas exposure, asbestos, secondhand smoke, some metals and organic chemicals, air pollution, radiation, tuberculosis (medical history), and genetic susceptibility	1,732,185	Central and Eastern Europe, Eastern Asia, Northern America, Northern Europe, and South East Asia	Cessation or tobacco avoidance, appropriate vaccination, surgery, chemotherapy, targeted therapies, and radiation therapy	(J. Ferlay et al., 2015; Society, 2015)
Breast	First birth at older age, high	560,407	Northern America,	Surgical removal of	(J. Ferlay et al., 2015;

	usage of menopausal hormone therapy, poor medical treatment, obesity, long-term heavy smoking, genetic susceptibility (family history), and oral contraceptives consumption		Northern and Southern Europe, Australia, New Zealand, Europe, Oceania, and the Americas	cancerous cells, mastectomy, radiation therapy, hormone therapy, and chemotherapy,	Society, 2015)
Liver	Poor prognosis, tobacco consumption, alcohol consumption, infectious agents such as HBV and/or hepatitis C virus (HCV), alcoholic liver disease, diabetes, and overweight	806,873	Eastern and South-Eastern Asia, Southern Europe, Northern America, and Western Africa	Alcohol avoidance, vaccination, surgical removal of part of the liver, liver transplantation, embolization, ablation, and targeted drugs	(J. Ferlay et al., 2015; Siegel et al., 2015; Society, 2015)
Stomach	Poor hygiene, high salt intake, poor food preservation methods, poor nutrition, infectious agents, and high prevalence of *Helicobacter pylori*	785,558	Eastern Asia, Central and Eastern Europe, Central and South America	Surgery (gastrectomy), chemotherapy, radiation therapy, and targeted therapy	(J. Ferlay et al., 2015; Siegel et al., 2015)
Colorectal	Poor prognosis,	752,731	Australia, New	Surgery, colostomy,	(J. Ferlay et al., 2015;

	obesity, moderate to heavy alcohol intake, high intake of red meat, long-term smoking, poor nutrition, low calcium consumption, chronic inflammatory bowel disease, and family history		Zealand, Central and Eastern Europe	chemotherapy, radiation therapy, and targeted therapy	Society, 2015)
Prostate	Family history, age, inherited genetic susceptibility, obesity, and high consumption of dairy foods and/or processed meats	335,643	Australia, New Zealand, Northern America, South America, Southern Africa, Caribbean, Western and Northern Europe, and Oceania	Active surveillance, surgery, brachy therapy, external beam radiation, hormonal therapy, radiation therapy, and vaccination (sipuleucel-T)	(J. Ferlay et al., 2015; Society, 2015)
Cervical	Infectious agents such as human papillomavirus (HPV), sexual activity at early age, multiple sexual partners, suppressed human immune system, consumption of oral	284,923	Eastern Africa, Melanesia, Southern and Middle Africa	Prophylactic vaccination against HPV16/18, surgery, radiation therapy, chemotherapy, loop electrosurgical excision procedure, laser ablation, cryotherapy,	(J. Ferlay et al., 2015; Saranath, 2014; Siegel et al., 2015; Society, 2015)

	contraceptives, and tobacco intake.			and targeted drug therapy	
Pancreatic	Tobacco intake, family history, poor prognosis, heavy alcohol consumption, overweight, diabetes, and genetic syndromes	359,354	Asia, Eastern Asia, Europe	Surgery, chemotherapy, radiation therapy, and targeted drugs	(J. Ferlay et al., 2015; Society, 2015)
Leukaemia	Poor prognosis, genetic susceptibility (family history), ionizing radiation exposure (eg: medical radiation), down syndrome, genetic abnormalities, obesity, parental smoking, and chemical exposure (eg: benzene, formaldehyde)	283,373	Northern America, Australia, and New Zealand	Chemotherapy, and stem cell transplantation	(J. Ferlay et al., 2015; Siegel et al., 2015; Society, 2015)
Ovarian	Family history of ovarian or breast cancer, pelvic inflammatory disease, Lynch syndrome, menopausal hormone therapy,	163,765	Asia, Europe, and the Americas	Surgery (salpingo-oophorectomy, hysterectomy, omentum), and chemotherapy	(J. Ferlay et al., 2015; Society, 2015)

	obesity, and tobacco intake				

Cancer cases are expected to increase, and the challenge is to develop effective medical interventions to address this top public health concern. Cancer therapies such as chemotherapy and radiotherapy provide immediate pathways to treat cancerous cells, and have been partially or completely successful in many cases. However, these therapies are challenged with low therapeutic index due to their infectiveness to completely block cancer growth and metastasis; significant adverse effects to normal cells; and the potential evolution of cancer cells with higher drug resistance (P. K. Singh et al., 2012). Unfortunately, for many recovered cancer patients after treatment with chemotherapy, surgery, immunotherapy, and targeted agents, the malignant cells recur after months or years later (Cripe, 2009). There are several possible factors responsible for such recurrence. These include the low targeting efficacy of chemotherapy and radiotherapy to desired tumor cells, the difficulty in developing tailored treatment regimen for specific cancer scenarios, and the resistance to therapeutic agents by some cancerous cells (Cripe, 2009). Multifunctional targeted therapy presents the opportunity to design new targeting agents with high specificity and minimal or no systemic cytotoxicity, directing high drug dosage to desired tumor site, and thus creating enhanced therapeutic index (P. K. Singh et al., 2012). Today, there are several molecular targeting agents for cancer available for clinical applications whilst many more are being developed with the aim of revolutionizing the range and efficacy of cancer therapies (Shaikh, 2012).

2.9.2 Oncolytic viruses: Conventional cancer targeting agents

Chemotherapy targets and kills both normal and tumor cells that divide rapidly. In contrast, targeted cancer therapies are intended to target desired tumor cells without affecting the growth of other normal cells (Aravind, Jeyamohan, et al., 2012). It employs targeting agents to interact with specific targeted molecules in order to inhibit the growth and spread of desired cancer cells (M. Alibolandi et al., 2015; Aravind, Jeyamohan, et al., 2012; Balashanmugam et al., 2014). With advanced knowledge and capabilities in medical bioscience, biotechnology and molecular biology, it has become possible to molecularly

engineer viruses as targeting agents with enhanced selectivity and oncolysis for cancer treatments and gene therapy (Cripe, 2009; P. K. Singh et al., 2012). Oncolytic virotherapy is a new cancer treatment that enhances the specificity of conventional tumor cell inactivation mechanisms by employing tumor-selective OVs that infect, replicate and lyse tumor cells specifically within cancerous tissues without affecting normal cells and tissue counterparts, thus providing an improved therapeutic index with minimal effects on normal cells (Bartlett, 2013; Cripe, 2009; Guo et al., 2008; P. K. Singh et al., 2012). Also, cancer cells lack many natural protection mechanisms against viruses and thus, are susceptible to virus infection (Svyatchenko, 2012). OVs possess various targeting mechanisms including pro-apoptotic, transductional, transcriptional, and translational (Russell & Peng, 2007). Figure 2.4 showed that OVs work by infecting tumor cells and replicating within them. After replication, cytolysis occurs to trigger cancer cell death and release their progeny for further infection to surrounding tumor cells (Guo et al., 2008; T. T. Smith, Roth, J. C., Friedman, G. K., & Gillespie, G. Y. , 2013). Other specific anti-tumoral mechanisms include direct cytotoxicity, transgene expression, triggering anticancer immunity, and sensitization to radiotherapy and chemotherapy (Vähä-Koskela, 2007). Examples of OVs are adenovirus, adeno-associated virus, gammaretrovirus, parvovirus, lentivirus, herpes simplex virus, newcastle disease virus, measles virus, reovirus, and chicken anaemia virus (Cripe, 2009; Guo et al., 2008; P. K. Singh et al., 2012; T. T. Smith et al., 2014). An ideal viral vector is capable of substituting most of its viral genome with the desired therapeutic gene for expression at the tumor site (Giacca & Zacchigna, 2012). OVs possess desirable characteristics when they are the wild-type with non-pathogenic animal viral components, and cause cytotoxicity to tumor cells without infecting other normal cells (Chiocca, 2014). OVs are convenient and easy to genetically manipulate (Svyatchenko, 2012) to form attenuated viral mutants with deleted or mutated genes that are essential for replication (Cripe, 2009). OVs are promising agents to target cancer stem cells (CSCs) which are responsible for initiating tumor sites, self-renewing and differentiating for tumor growth as well as inducing metastasis (T. T. Smith, Roth, J. C., Friedman, G. K., & Gillespie, G. Y. , 2013). As summarized in Table 2.6, extensive research works have been carried out on the application of OVs to target the cell surface markers of CSCs such as prominin-1 and CD133, in order to inhibit the spread of cancer

cells. The evolution of cancer is seeded from a small number of active CSCs. In comparison with normal cancer cells, CSCs are more resistant to conventional chemo/radio-therapy, and can lead to the recurrence of a more resilient and metastatic cancer. Hence, OVs provides the opportunity to not only inactivate normal cancer cells but also targeting CSCs to improve survival rate and reduce the possibility of cancer recurrence (T. T. Smith, Roth, J. C., Friedman, G. K., & Gillespie, G. Y. , 2013).

Numerous clinical studies have demonstrated the efficacy of OVs in killing cancer cells that are resistant to radiotherapy or chemotherapy (Eager, 2011). One research study reported that oncolytic adenovirus conjugated with actively targeting Arg-Gly-Asp(RGD)-poly(cystaminebisacrylamide-diaminohexane) (poly(CBA-DAH)) biopolymer can be delivered safely to specific cancer cells for inducing apoptosis and suppressing both IL-8 and VEGF expression by expressing the short hairpin RNA. The observed therapeutic effects included anti-angiogenesis, inhibition of tumor migration, invasion and growth, high gene transfection efficiency, and low cytotoxicity (J. Kim et al., 2011). Adenoviruses can selectively and actively kill tumor cells via cell lysis with amplified transgene expression, conditional replication and progeny production, and diffusion into neighbored cancer cells. The concerns associated with potential metathesis of oncolytic viruses is dependent on the transformations in the viral surface protein in terms of structural reorganisation and epitope mapping which are critical for specific and targeted tumour attack. Hence since intracapsular nucleic acid replication and translations during metathesis could result in surface transformations that can potentially affect the nature of the recognition proteins of progenies then the specificity of the signalling pathway would be affected. For instance, Ayala-Breton et al. (2014) genetically engineered the vesicular stomatitis virus by replacing its G glycoprotein with fusion (F) and hemagglutinin (H) envelope glycoproteins. This resulted in a higher recognition of virus towards CD46-overexpressing cancer cells, rapid viral replication and stronger cytopathic effect. The viral surface proteins of some virus have been modified to target surface receptors of specific cancer cells with high affinity. This modification is usually inherent to the viral genome and it is inherited upon subsequent duplications (Verheije & Rottier, 2012).

Another study byP.-H. Kim et al. (2011) demonstrated the hepatoma-specific adenovirus (YKL-1001) conjugated with arginine-grafted bioreducible polymer (ABP) as an effective tumor targeting and therapeutic agent to inactivate liver cancer cells such as HepG2 and Huh 7 cells via systemic administration. This bioconjugate is more resistant to neutralizing antibodies, resulting in longer circulatory half-life, increased gene transduction efficiency and lytic potency, and limited cytotoxic effects for a more efficient and safe therapeutic delivery (P.-H. Kim et al., 2011). The result also illustrated the efficacy of adenovirus-ABP complex in killing coxsackie-adenovirus receptor (CAR)-deficient tumor cells via CAR-independent routes (P.-H. Kim et al., 2011). Additionally, a gibbon ape leukemia virus (GALV)-based replicating retrovirus vector (RRV) armed with a yeast cytosine deaminase (CD) suicide gene was indicated to provide high cancer cell inactivation and inhibit *in vivo* cancer growth to treat hepatocellular carcinoma with enhanced gene delivery and transduction efficiency (Lu, 2012). This study showed significantly suppressed cancer growth due to the production of high suicide gene toxicity by GALV-RRV with no cytotoxicity to surrounding normal tissues (Lu, 2012). The suicide genes encoded enzymes that intracellularly converted the non-toxic prodrug into toxic metabolites, leading to cancer cell deaths via suicide gene therapy (Lu, 2012). X. Zhang et al. (2007) engineered a recombinant adeno-associated virus (rAAV) vector to deliver thrombospondin-1 type 1 repeats (3TSR) and endostatin for anti-angiogenic gene therapy with significant anti-angiogenic and anticancer effects *in vivo* (X. Zhang et al., 2007). The experimental results illustrated the transgene expression of 3TSR and endostatin that caused efficient suppression of the vascular endothelial growth factor (VEGF)-induced angiogenesis at both local and distant sites in mice with pancreatic cancer cells (X. Zhang et al., 2007). Bhutia et al. (2013) investigated the efficacy of adenovirus in delivering melanoma differentiation-associated gene-7 (*mda-7)* to targeted tumor cells for blocking the proliferation of breast cancer stem cells via the suppression of Wnt/β-catenin signaling pathway, endoplasmic reticulum stress and apoptosis without harming normal stem cells (Bhutia et al., 2013). The result also showed the enhancement of chemotherapy and antibody-elicited killing due to the expression of *mda-7*/interleukin-24 within the breast tumor cells after the adenovirus.*mda*-7 infection (Bhutia et al., 2013).

OVs possess positive traits that make them effective as targeting and delivery agents. For instance, adenovirus provides large foreign DNA capacity; efficient intracellular delivery of therapeutic genes; cancer-selective killing; low mutagenesis rate and genotoxicity; non-integration into genome or chromosomes of host; and high titers concentration (J. Kim et al., 2011; P.-H. Kim et al., 2011). One of the favorable characteristics of OVs is their viral persistence whereby infected cancer cells turn into a source of constant viral production to help in spreading the viral vector to metastatic tumor cells (Chiocca, 2014; Lu, 2012). Most genes that encode for viral proteins are knocked off or removed from the viral genome hence, OVs do not infect human whilst killing cancer cells. Also, the microenvironment of cancer cells is optimal for viral replication (T. T. Smith, Roth, J. C., Friedman, G. K., & Gillespie, G. Y. , 2013). Many research studies have demonstrated the effectiveness of OVs in combating a wide range of human cancer cells in both preclinical and clinical trials (Cripe, 2009). Safety concerns such as sensitivity towards immune system and drug can be armed in Ovs (Chiocca, 2014). Likewise, larger OVs can be equipped to express immune-stimulating transgenes to enhance their therapeutic effects by attracting more immune effector cells (T. T. Smith, Roth, J. C., Friedman, G. K., & Gillespie, G. Y. , 2013). Therefore, OVs are able to undergo genetic manipulations to provide enhanced gene therapies that target specific receptors as well as various activated cellular pathways (J. Kim et al., 2011; T. T. Smith, Roth, J. C., Friedman, G. K., & Gillespie, G. Y. , 2013). Additionally, OVs with various tropisms are capable of combating multiple tumor types. They are capable on acting on distant metastasis besides primary tumors (Chiocca, 2014).

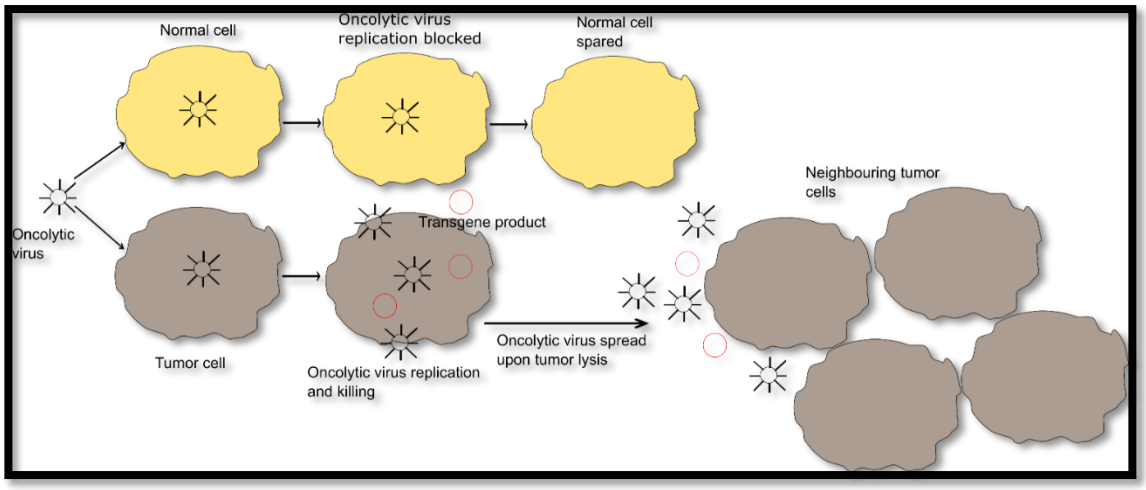

Figure 2.4: Mechanism of OVs in killing tumor cells

Table 2.6: Summary of some oncolytic viruses for targeted delivery

Oncolytic virus (OV)	**Target**	**Cancer**	**Positive effects**	**Reference**
Adenovirus, reovirus, herpes simplex virus-1, vaccinia virus, measles virus	Prominin-1 and CD133 of CSCs	Cancer stem cells (CSCs)	Inhibited the spread of tumor cells; minimized cancer relapse; and increased survival rate	(T. T. Smith, Roth, J. C., Friedman, G. K., & Gillespie, G. Y. , 2013)
Adenovirus conjugated with Arg-Gly-Asp(RGD)-poly(cystaminebisacrylamide-diaminohexane) (poly(CBA-DAH)) biopolymer	Interleukin-8 and vascular endothelial growth factor	Human cancer cells (A549 lung carcinoma, MCF7 breast adenocarcinoma, HT1080 fibrosarcoma)	Induced apoptosis; suppressed expression of IL-8 and VEGF; and anti-angiogensis	(J. Kim et al., 2011)

Adenovirus (YKL-1001) conjugated with arginine-grafted bio-reducible polymer (ABP)	A-fetoprotein expressing HepG2 and Huh 7 liver cancer cells, and CAR-deficient tumor cells	Hepatocellular carcinoma	Increased the gene transduction efficiency; enhanced the lytic potency, prolonged the circulatory half-life; and minimized cytotoxicity	(P.-H. Kim et al., 2011)
Gibbon ape leukemia virus (GALV)-based replicating retrovirus vector (RRV)	Prodrug 5-fluorocytosine (5-FC)	Hepatocellular carcinoma	Enhanced gene delivery; improved transduction efficiency; and increased cancer killing effect	(Lu, 2012)
Recombinant adeno-associated virus (rAAV) vector	Vascular endothelial growth factor	Pancreatic cancer cells	Successfully delivery of thrombospondin-1 type 1 repeats (3TSR) and endostatin; and anti-angiogenesis	(X. Zhang et al., 2007)
rAAV serotypes 6	NEU antigen in NEU-expressing breast cancer cells	Breast cancer	Expressed neu oncogene; and triggered cell-mediated and humoral immune responses	(Steel, 2013)
Adenovirus. melanoma differentiation-associated gene-7 (*mda-7)*	Wnt/β-catenin signaling pathway	Breast cancer stem cells	Expression of *mda-7;* suppression of Wnt/β-catenin signaling pathway; endoplasmic reticulum stress; and apoptosis	(Bhutia et al., 2013)

2.9.3 Challenges of OVs as targeting elements

Undoubtedly, more research efforts are needed to fully exploit the therapeutic potential of oncolytic virotherapy. In 1999, a healthy teenager was killed as a result of toxic shock in a clinical trial involving the use of adenovirus to treat inherited Ornithine

Transcarbamylase Deficiency (Svyatchenko, 2012)). Another incident happened in 2002 when 2 volunteers developed leukemia after receiving a trial gene therapy to treat X-linked severe combined immunodeficiency (Svyatchenko, 2012). These cases, amongst other recently reported serious side-effects and cancer resurgence cases, demonstrate the limitations of OVs in gene therapy particularly in relation to the triggering of immune responses against the viral vectors and transgenes, and also inducing mutations as a result of inappropriate insertion of transgenes (Svyatchenko, 2012). OVs possess several other shortcomings which limit their therapeutic applications. These shortcomings include high immunogenicity, low capacity for gene insertion, short-term gene expression, limited viral vector delivery as a result of poor viral transduction, and the propensity of eliciting insertional mutagenesis and tumorigenicity (J. Luo, Luo, Y., Sun, J., Zhou, Y., Zhang, Y., Yang, X. , 2015). Some OVs can only be therapeutically effective to cancer cells that contain specific oncogenic profiles such as the activated Ras pathway in the case of reovirus (T. T. Smith, Roth, J. C., Friedman, G. K., & Gillespie, G. Y. , 2013). Therapeutic efficiency of certain OVs including adenovirus and vaccinia virus is limited by pre-existing immunity. In such cases, OVs are eradicated by phagocytic cells and neutralizing antibodies before they kill the tumor cells (Ferguson et al., 2012; J. Kim et al., 2011; Russell & Peng, 2007; T. T. Smith, Roth, J. C., Friedman, G. K., & Gillespie, G. Y. , 2013). OVs such as adenovirus tend to accumulate in the liver, causing liver toxicity, short half-life and adverse side effects within the host, and be excreted rapidly by neutralizing antibodies *in vivo (J. Kim et al., 2011; P.-H. Kim et al., 2011).* OVs also face challenges such as non-specific uptake and clearance by the liver, lung and spleen to hinder their systemic availability (Ferguson et al., 2012).

OVs administered intravenously are removed from blood circulation rapidly and the increasing antiviral immunity speeds up this elimination process for subsequent exposures (Russell & Peng, 2007). This limits the systemic administration and delivery of therapeutic drugs which are essential for targeting both primary and metastatic tumors (P.-H. Kim et al., 2011). It has been reported that interactions between adenovirus and red blood cells and platelets result in toxicity, reduced therapeutic availability, and undesirable side effects (Ferguson et al., 2012; P.-H. Kim et al., 2011). In addition, the expression of coxsackie-adenovirus receptor (CAR) was observed to be low on cancer

cells, leading to low CAR-mediated viral transduction efficiency (P.-H. Kim et al., 2011). Viral vectors like retrovirus have various disadvantages in term of flexibility, storage, production and safety issues including activating latent disease (Nie et al., 2011). Gammaretrovirus, which used to be the most utilized gene vehicle, has been reported to be inefficient in transducing non-replicating cells and possesses the propensity to induce insertional mutagenesis (Giacca & Zacchigna, 2012). Also, there is a possibility that OVs can evolve into a pathogen and evade the host immune system, and might result in person-to-person transmission of the original or pathogenic derivative (Russell & Peng, 2007). Although adenoviruses are effective and safe to be involved in cancer therapy based on various clinical trials (Phase I and II), they are incapable of being used as a monotherapy due to their low efficacy in tumor-killing (Svyatchenko, 2012).

2.9.4 Aptamers as a new class of targeting agents for cancer therapy

Aptamers have gained significant interests in biomedical science and pharmaceutical delivery as ideal targeting agents for drug delivery. Aptamers have the potential to recognize and bind specifically to targeted cells *in vivo* for successful therapeutic outcomes with minimal cytotoxic effects to surrounding normal cells (Balashanmugam et al., 2014). Aptamers fold into specific 3-D structures to interact with their targets under affinity binding conditions with dissociation constants ranging from pico- to nano- molar (Sun et al., 2014). The strong and specific binding characteristics of aptamers make them effective targeting elements. Aptamers are chemically and thermally stable due to their strong phosphodiester bonds, and those with small molecular weights are able to diffuse through blood circulation more rapidly with high cellular penetration. Aptamers are mostly non-immunogenic, and their production technique is scalable and inexpensive (Gedi & Kim, 2014; Santosh & Yadava, 2014; Sun et al., 2014). With great targeting mechanisms, aptamers are able to specifically recognize minor structural differences within the target molecule of interest. For example, aptamers can identify and bind to hidden epitopes, a characteristic feature which is not easily achieved with conventional targeting ligands (Radom et al., 2013; Sun et al., 2014).

Aptamer can be used either alone or as the aptamer-drug conjugate whereby it is used alone when it acts as a medical drug. For example, pegatanib aptamer is a FDA-approved

aptamer-based drug to target, bind and antagonize vascular endothelial growth factor (VEGF) with high affinity via its unique 3-D conformation. This inhibits the binding of VEGF to its receptors in order to prevent angiogenesis and reduce vascular permeability (Song et al., 2012). Vavalle and Cohen (2012) demonstrated that REG1 aptamer (clinical trial Phase II) is capable of treating acute coronary syndrome by selectively inhibiting factor IXa in the REG1 anticoagulation system. Another research study by Gao et al. (2014) demonstrated the efficiency of NS2-specific aptamer as an inhibitor that impedes the binding of NS2 towards NS5A protein to prevent viral RNA replication, which then leads to anti-Hepatitis C virus infection. Aptamers can also be used as ideal drug carriers to act as a navigator and guide the medical drug to targeted cancerous site without causing cytotoxic effect to surrounding healthy cells. This is predominantly due to the high affinity and selectivity of aptamers as targeting element towards extracellular receptors or surface biomarkers of cancer cells as shown in Table 2.7. Aptamer-mediated targeted drug delivery system is highly specific and significantly increases the dosage of delivered drug to targeted tumor cells as well as improving the therapeutic index (Radom et al., 2013; J. Zhu et al., 2014). There are many research conducted on the efficiency of different type of aptamer-drug conjugates and the details are well documented in this review. It has been scientifically proven that the use of aptamers as targeting agents in targeted pharmaceutical delivery can enhance the therapeutic action of antitumor agents on a variety of cancers including brain cancer (Jianwei Guo et al., 2011), breast cancer (M. Alibolandi et al., 2015; Aravind, Jeyamohan, et al., 2012), pancreatic cancer (Sun et al., 2014), colorectal cancer (L. Li et al., 2014), lymphoblastic leukemia (Aravind, Jeyamohan, et al., 2012; Y. F. Huang, Shangguan, Liu, Philips, et al., 2009), hepatic cancer (M. Alibolandi et al., 2015) and prostate cancer (Min et al., 2011).

Aptamers act as navigators to direct therapeutic payloads to desired targeted sites while minimizing systemic cytotoxicity to other normal cells and effectively triggering receptor-mediated internalization, called endocytosis, to increase the cellular uptake of therapeutic molecules into targeted tumor cells (Y. F. Huang, Shangguan, Liu, Philips, et al., 2009; Radom et al., 2013; J. Zhu et al., 2014). In order to enhance interaction with their desired targets, aptamers spontaneously re-conform their molecular binding structures to maximum binding at their active sites via hydrogen bonding, and electrostatic,

hydrophobic and Van der Waal interactions (Upadhyay, 2013; J. Zhu et al., 2014). Aptamer-mediated targeted drug delivery is a promising approach for cancer therapy as aptamers can be generated and engineered to possess high binding affinities towards specific internalized cell surface receptors or biomarkers such as nucleolin for breast cancer cells, protein tyrosine kinase (PTK7) for acute lymphoblastic leukemia, and prostate-specific membrane antigen (PSMA) for prostate cancer cells as shown in Table 2.7 (Orava, Cicmil, & Gariépy, 2010). The mechanism of aptamer targeting and cellular uptake comprises of three steps including targeting, endocytosis and cytotoxic effects (Orava, Cicmil, & Gariépy, 2010). The targeting mechanism of aptamers as shown in Figure 2.5 begins when the aptamer binds to its desired biomarker to trigger a receptor-mediated internalization. The aptamer-receptor complex is then internalized via either clathrin-independent or clathrin-dependent vesiculation into the endosome of the targeted tumor cells (Erdmann et al., 2014). This internalization process leads to increased drug uptake into the target cells (M. Alibolandi et al., 2015; Radom et al., 2013; Tuerk, 1990). Y. F. Huang, Shangguan, Liu, Philips, et al. (2009) conjugated doxorubicin (Dox) anticancer drug to sgc8c aptamer via a hydrazone linker or covalent bond to form the Dox-aptamer complex with no effect on the bioactivity of Dox and aptameric binding properties (Y. F. Huang, Shangguan, Liu, Philips, et al., 2009; Radom et al., 2013). After internalization, the acidic environment of the endosome triggers hydrolytic bonding cleavage that hydrolyzes the covalent bond between the conjugated chemotherapeutic drug and the aptamer. Consequently, the released drug passively diffuses through the endosomal membrane into the cytosol and finally enter the nucleus and intercalate into the gDNA of the targeted cancer cells to induce therapeutic effects (Y. F. Huang, Shangguan, Liu, Philips, et al., 2009; Radom et al., 2013). The aptamer is eliminated later during the fusion of endosome and lysosomes containing endonucleases that degrade the aptamers. Briefly, the endosomic acidic environment induces hydrolysis of acid-susceptible linkers whereas the acidic environment of the lysosome degrades linkers that are labile to proteolytic, hydrolytic or digestive enzymes (G. Vilar, Tulla-Puche, J., Albericio, F. , 2012). The effectiveness of aptamer-mediated targeted therapeutic delivery can be affected by several factors such as the size, charge and nature of the conjugated

chemotherapeutic drugs, amplitude of target cell surface biomarkers, and the endocytic nature of the targeted cell (Orava, Cicmil, & Gariépy, 2010).

Table 2.7: A list of surface biomarkers expressed onto different tumor cells

Surface biomarker	**Surface biomarker-expressing tumor cells**
Nucleolin	Melanomas, gastric, breast, leukemia, lung tumor cells (Aravind, Jeyamohan, et al., 2012).
Protein tyrosine kinase 7 (PTK 7)	Lung, gastric, colon tumor cells (L. Li et al., 2014; Min et al., 2011).
Epithelial cell adhesion molecule (EpCAM)	Bladder, ovarian, breast, pancreas, hepatocellular tumor cells (M. Alibolandi et al., 2015).
Prostate specific membrane antigen (PSMA)	Prostate, kidney tumor cells (Sun et al., 2014).

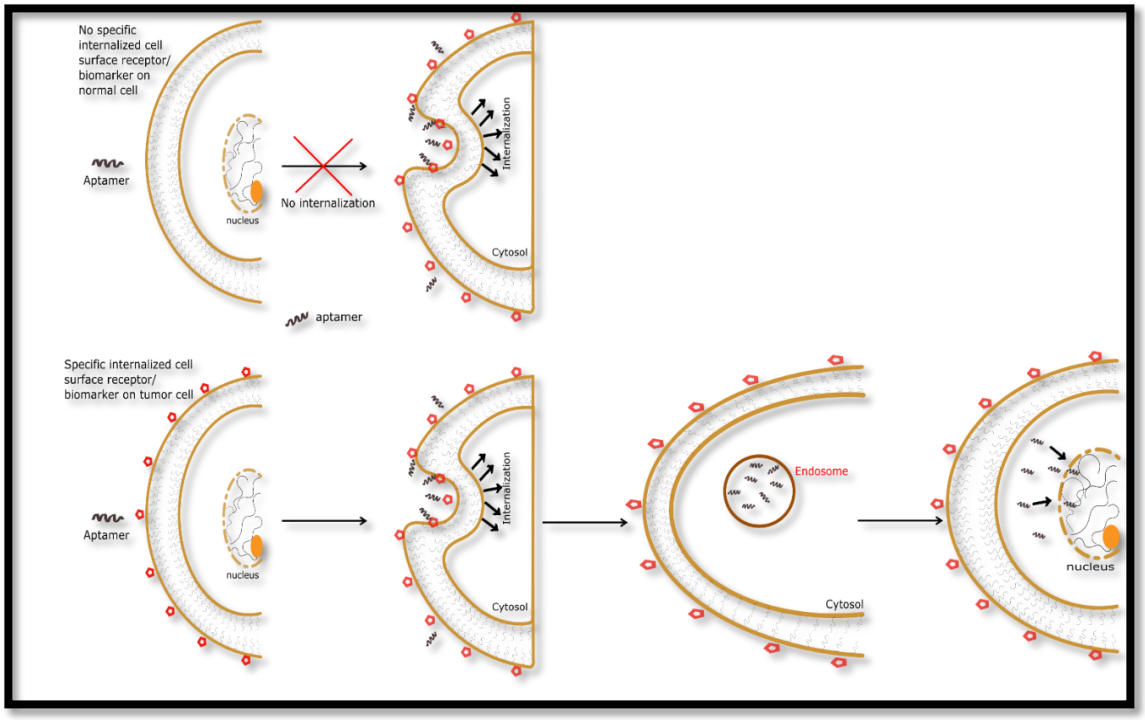

Figure 2.5: The killing mechanism of aptamer-mediated formulations towards tumor cells

2.9.5 Biophysical limitations of aptamer-mediated targeted delivery

Although numerous reported pre-clinical targeted delivery studies using aptamers have reported promising results, there are only several commercialized aptamer-based drugs on the market as most aptamer-mediated targeted delivery technologies fail at various phases of clinical trials (Liechty et al., 2010; J. Zhu et al., 2014). For example, AS1411 DNA aptamer clinical study failed at phase II clinical trial for the treatment of renal cell carcinoma notwithstanding the numerous pre-clinical validations (J. Zhu et al., 2014). Also, BAX499 aptamer clinical study for the treatment of hemophilia was terminated at phase I due to low therapeutic index (Peyvandi, 2013). This demonstrates that major biochemical and biophysical challenges that impede effective aptamer-mediated *in vivo* targeted delivery still remain to be addressed. Aptameric targets are often internalized surface protein receptors or biomarkers of the target cells residing in interstitial fluids or blood plasma. It is therefore essential that the aptamers are biochemically stable in these extracellular fluid compartments for a period of time. However, the stability of aptamers in these compartments is challenged by negatively charged cell membrane electrostatic repulsion, endonuclease degradation, rapid renal clearance, and rapid bio-distribution of aptamers from the blood plasma into tissues (Lakhin et al., 2013; Sundaram et al., 2013; Wengerter, 2014). Consequently, aptamers have a short circulating half-life and this affects their performance as biological drugs, drug carriers and/or targeting agents (Liechty et al., 2010; Orava, Cicmil, & Gariépy, 2010; Sun et al., 2014).

Aptamers are oligonucleotides with a low molecular weight of 8-25kDa, making them labile to rapid renal excretion. The kidney filters and removes molecules from the bloodstream within the molecular weight range of 30-50 kDA (Sundaram et al., 2013). The delivery of sufficient drug dosage to targeted sites is therefore significantly impeded by rapid renal excretion, leading to ineffective *in vivo* therapies (Lakhin et al., 2013; Wengerter, 2014). Additionally, nuclease-mediated degradation is one of the major drawbacks limiting the application of aptamers for effective pre-clinical and clinical therapeutic delivery. Aptamers are generally degraded in the bloodstream within minutes based on their conformation and concentration. Consequently, the amount of aptamers remaining in the bloodstream is inadequate for an effective therapeutic event to take place

(Lakhin et al., 2013; Sundaram et al., 2013). Also, aptamers are hydrophilic negatively-charged molecules that are impermeable to biological barriers such as the cell membrane. Electrostatic repulsive forces exist between the aptamer and the target cell membrane surface, and this significantly obstructs effective aptamer-receptor binding, cell membrane permeation, receptor-mediated internalization, intracellular target-specific binding, and the desired cytotoxic effect (Orava, Cicmil, & Gariépy, 2010; Wu, 2011). Furthermore, the simple structures of aptamers result in a small drug loading capacity, and this consequently decreases the drug dosage delivered to the targeted site (Sun et al., 2014). Aptameric binding mechanism can also affect the effective application of aptamers as targeting elements. Aptamers target cell surface protein receptors and this can potentially alter the drug bisorption rate to eventually affect the pharmacokinetic and pharmacodynamic properties. There is the possibility of aptamers fusing into the human genome to express foreign proteins which can lead to the evolution of non-specific normal cells into cancerous cells (Du et al., 2006).

2.9.6 Molecular mechanism of action: OVs vs Aptamers

OVs are highly selective to cancerous site and this allows them to only duplicate and spread within the cancerous cell zone without killing surrounding healthy cells. For instance, OVs such as Measles virus and Coxsackie virus have been reported to possess a natural preference towards cancer cells due to the presence of unique surface protein markers that induce specific binding affinities to corresponding cancer cells ("Thorne D, Dalrymple A, Dillon D, Duke M, Meredith C. A comparative assessment of cigarette smoke aerosols using an in vitro air-liquid interface cytotoxicity test. Inhal Toxicol. 2015:1-12. doi:10.3109/08958378.2015.1080773,"). As a result of the protein attachment, OVs latch onto the cancer cells for penetration followed by replication inside the cancer cells using the replication machinery of the host cells. OV particles then leave the host cells via cell lysis or budding after completing viral replication in order to target other surrounding cancer cells. Other OVs, including adenovirus, can be genetically engineered to knock off specific enzymes that are available only in tumor cells, and this leads to competition between the OV and tumor cells for the same mechanism of survival. The tumor antigens produced by tumor cells are usually undetected by the human immune

system for destruction. However, in the presence of OVs that engage in tumor cells destruction, intracellular tumor antigens are released to activate the immune system. Thus, there is a synergetic effect between OVs and the body immune system (Ledford, 2015).

Aptamers can be engineered to kill cancer cells by interacting specifically with a wide range of surface biomarkers expressed onto various cancer cells as shown in Table 2.7. The mode of action begins when the aptamer selectively binds onto the surface receptors or internalized surface biomarkers of targeted cancer cells to stimulate endocytosis (M. Alibolandi et al., 2015; Y. F. Huang, Shangguan, Liu, Philips, et al., 2009; Radom et al., 2013). The mechanism of action for aptamer can be found in above section as follows:

The mechanism of aptamer targeting and cellular uptake comprises of three steps including targeting, endocytosis and cytotoxic effects (Orava, Cicmil, & Gariépy, 2010). The targeting mechanism of aptamers begins when the aptamer binds to its desired biomarker to trigger a receptor-mediated internalization. The aptamer-receptor complex is then internalized via either clathrin-independent or clathrin-dependent vesiculation into the endosome of the targeted tumor cells (Erdmann et al., 2014). This internalization process leads to increased drug uptake into the target cells (M. Alibolandi et al., 2015; Radom et al., 2013; Tuerk, 1990). Y. F. Huang, Shangguan, Liu, Philips, et al. (2009) conjugated doxorubicin (Dox) anticancer drug to sgc8c aptamer via a hydrazone linker or covalent bond to form the Dox-aptamer complex with no effect on the bioactivity of Dox and aptameric binding properties (Y. F. Huang, Shangguan, Liu, Philips, et al., 2009; Radom et al., 2013). After internalization, the acidic environment of the endosome triggers hydrolytic bonding cleavage that hydrolyzes the covalent bond between the conjugated chemotherapeutic drug and the aptamer. Consequently, the released drug passively diffuses through the endosomal membrane into the cytosol and finally enter the nucleus and intercalate into the gDNA of the targeted cancer cells to induce therapeutic effects (Y. F. Huang, Shangguan, Liu, Philips, et al., 2009; Radom et al., 2013). The aptamer is eliminated later during the fusion of endosome and lysosomes containing endonucleases degrade the aptamers.

2.9.7 Aptamer-conjugated polymeric particulates as targeted delivery systems

Aptamers serve as great cell-targeting elements with much potential in advancing conventional targeted drug delivery systems with increased therapeutic index and minimal systemic cytotoxicity. Notwithstanding, unresolved challenges associated with aptamer-mediated *in vivo* delivery have highly impacted practical applications of aptamers for effective clinical therapies. These challenges have triggered significant interests into the use of synthetic delivery systems as drug carriers. Biomedical research into effective synthetic therapeutic delivery carriers to overcome the drawbacks of aptamers has become a significant research endeavor. The emergence of biocompatible and biodegradable polymers that can be molecularly engineered to tune their biophysical and biochemical properties such as particulate size and distribution, surface area and morphology, chemical compositions, and toxicity has created opportunities to optimize the capacity of aptamers as targeting elements for sustained and controlled release of drug at effective dosages.

Polymeric particles have gained recognition as efficient and safe delivery vehicles in pharmaceutical drug delivery and *in vivo* therapeutic treatment as compared to other delivery systems such as bacterial and viral delivery systems. This is due to their unique properties including biocompatibility, low or non-immunogenicity, biodegradability, and bioavailability in addition to their tunable physicochemical features to generate a controlled drug release profile (Saranya & Radha, 2014). The use of polymeric particles as synthetic delivery carriers for aptamers conjugated with drug to target desired cells in pharmaceutical delivery is a promising approach to improve the specificity, selectivity and therapeutic efficacy whilst enhancing transfection efficiency (M. Alibolandi et al., 2015). There are various reported studies on aptamer-conjugated polymeric micro/nano-particles as therapeutic delivery carriers. These aptamer-polymer formulations have demonstrated promising results to improve the specificity of drug delivery systems by targeting various biomarkers including epithelial cell adhesion protein molecule (EpCAM) on breast and colon cancerous cell surfaces (M. Alibolandi et al., 2015; Subramanian et al., 2015), nucleolin on acute myeloid leukemia, gliomas and renal tumor cells (Aravind, Jeyamohan, et al., 2012; Jianwei Guo et al., 2011), PSMA on prostate tumor cell surfaces (Baird, 2010), and mucin-1 (MUC-1) on lung epithelial cancer cells (Lu, 2012; X. Zhang

et al., 2007). An ideal polymeric carrier is capable of protecting the encapsulated drug and aptamer molecules from the physiological environment without compromising their bioactivity and biophysical properties whilst providing a controlled release of the active agents in optimal dosages with the appropriate release kinetics (M. Tan & Danquah, 2012). Consequently, a reproducible and predictable drug release profile for a sustained period of time can be achieved; the therapeutic effects of drugs with short half-lives can be prolonged for enhanced therapy; side effects, drug waste and frequent drug dosing can be significantly reduced for a better patient compliance (G. Vilar, Tulla-Puche, J., Alericio, F. , 2012). There are many reported efficient aptamer-polymeric formulations using polymers such as poly(lactic-co-glycolic acid) (PLGA), poly(ethylene imine) (PEI), polyethylene glycol (PEG), poly(β-amino ester) (PBAE), chitosan, and poly (ortho esters) (POE). PLGA is one of the widely used biopolymer for pharmaceutical delivery. It is an approved synthetic biopolymer by the Food and Drug Administration (FDA) and World Health Organization (WHO) as a safe delivery carrier of active therapeutic molecules (Stevanovic & Uskokovic, 2009; G. Vilar, Tulla-Puche, J., Alericio, F. , 2012). In addition, PLGA has positive biochemical and biophysical properties for enhanced drug delivery. These include high DNA cargo capacity (Balashanmugam et al., 2014), ease of formulation into different shapes and sizes (Makadia & Siegel, 2011), provision of prolonged and controlled release profile, and modifiable temperature and pH sensitive degradation rates (Aravind et al., 2013; G. Vilar, Tulla-Puche, J., Alericio, F. , 2012). Table 2.8 summarized the pros and cons of both aptamers and OVs whilst Table 2.9 demonstrated the FDA-approved as well as those aptamers and OVs undergoing clinical trials.

Table 2.8: Comparison between OVs and aptamers as targeting elements

Parameters	**OVs**	**Aptamer**	**Reference**
Size	Nano-sized, and bigger than aptamers	8-25 kDA	(Giacca & Zacchigna, 2012; Lakhin et al., 2013; Sun et al., 2014)

Charge	Neutral, negative or positive depending on the total charge of its genes and coated protein	Negatively charged due to phosphate backbone	(Ahmad et al., 2014; Radom et al., 2013)
Therapeutic effect	Can be engineered for improved high therapeutic efficiency	Can be engineered for improved high therapeutic efficiency	(M. Alibolandi et al., 2015; Balashanmugam et al., 2014; Giacca & Zacchigna, 2012; Jianwei Guo et al., 2011; Russell & Peng, 2007; T. T. Smith, Roth, J. C., Friedman, G. K., & Gillespie, G. Y. , 2013)
Mechanism of action	Transcriptional, translational, pro-apoptotic, transductional	Receptor-dependent internalization via hydrogen bonding, electrostatic and Van der Waals interaction	(Y. F. Huang, Shangguan, Liu, Philips, et al., 2009; Russell & Peng, 2007)
Versatility of application	Vaccination, targeted cancer therapy, and gene therapy	Biosensing, diagnostic and therapeutic applications, *in vivo* imaging, targeted therapy, food inspection, targeted drug delivery, new drug and biomarker discovery	(P.-H. Kim et al., 2011; Song et al., 2012; Woller, 2014)
Stability	Thermally stable	Thermally and more chemically stable	(Song et al., 2012; Sun et al., 2014)
Ease of formulation	Can be engineered to improve formulation	Easily formulated	(Baird, 2010; Russell & Peng, 2007; Santosh & Yadava, 2014)

Table 2.9: A list of FDA-approved oncolytic viruses and aptamers and those undergoing clinical trials

Oncolytic virus		
Oncolytic Virus	**Developmental Stage**	**Medical Application**
Imlygic (oncolytic herpes simplex virus type 1)	FDA-approved	A genetically modified virus to cure melanoma skin cancer found in lymph glands or on skin. It is administered by injections targeting melanoma lesions (FDA, 2015). Retrieved from http://www.fda.gov/NewsEvents/Newsroom/PressAnnouncements/ucm469571.htm on 1st August 2016.
MG1MA3 maraba virus and AdMA3 adenovirus	Clinical Trial Phase I	To target MAGE-A3 protein-expressing cancer cells in order to trigger immune responses (Ottawa Hospital Research Institute, 2015). Retrieved from http://www.ohri.ca/newsroom/newsstory.asp?ID=649 on 1st August 2016.
LOAd703 adenovirus	Clinical Trial Phase I/IIa	To treat pancreatic cancer by stimulate the immune system in addition to the killing effect of adenovirus towards cancer cells (U.S. National Institutes of Health, 2016). Retrieved from https://clinicaltrials.gov/ct2/show/NCT02705196?term=oncolytic+virus&rank=3 on 1st August 2016.
CG0070 adenovirus	Clinical Trial Phase III	To cure bladder cancer using granulocyte macrophage-colony stimulating factor (GM-CSF)-encoded adenovirus to trigger systemic immune response (U.S. National Institutes of Health, 2016). Retrieved from https://clinicaltrials.gov/ct2/show/NCT02705196?term=oncolytic+virus&rank=3 on 1st August 2016.
Aptamer		
Aptamer	**Developmental Stage**	**Medical Application**

Pegatanib aptamer (Macugen)	FDA-approved	To inhibit angiogenesis and medicate neovascular age-related macular degeneration (Song et al., 2012).
Nuclein-specific AS 1411	Clinical Trial Phase II completed	To cure acute myeloid leukemia (Sun et al., 2014).
REG1 aptamer-based anticoagulant	Clinical Trial Phase III recruiting	To inhibit factor IXa in treating acute coronary syndrome (Vavalle & Cohen, 2012).
E10030 DNA aptamer	Clinical Trial Phase III recruiting	To target platelet-derived growth factor in treating age-related macular degeneration (Ni et al., 2011).

2.9.8 Current research on aptamer-mediated polymeric formulations for targeted cancer therapy

Aptamer mediated-targeted delivery using tunable polymeric systems is undoubtedly a promising development to improve conventional pharmaceutical delivery. There are various research studies reporting drug-aptamer conjugated polymeric formulations with positive outcomes. Min et al. (2011) developed a dual PSMA aptamer conjugated with the anticancer drug, Dox, to target and treat both PSMA (+) and PSMA (-) highly expressed prostate tumor cells. The study demonstrated efficient delivery of Dox to targeted prostate tumor cells with enhanced selective cell uptake and successful induction of apoptosis in desired target cells. Guo and his team (Jianwei Guo et al., 2011) reported the therapeutic efficacy of nucleolin specific AS1411 DNA aptamer-functionalized PEG-PLGA formulation in targeted delivery of paclitaxel, a drug to treat gliomas and brain tumor cells, by targeting internalized cell surface receptors called nucleolin. Blood circulation and retention of paclitaxel at the targeted site was prolonged. As a result, the drug dosage administration and cytotoxicity on the targeted tumors was improved significantly with prolonged survival of experimental animals. Aravind, Varghese, et al. (2012) designed an

aptamer-labeled paclitaxel-conjugated PLGA polymeric system with accurate tumor cell targeting, and it induced significant endocytosis and intracellular accumulation of the drug-conjugated polymeric particles to trigger apoptosis (Liechty et al., 2010). Another clinical research conducted by Aravind, Jeyamohan, et al. (2012) demonstrated that drug-encapsulated AS1411 aptamer conjugated PLGA-lecithin-PEG polymeric particles are effective in improving specific cell targeting with greater tumor killing effects for chronic leukemia and MCF-7 breast cancer cells as well as sustained drug release at the target site for enhanced therapeutic performance. A clinical study reported that targeted drug delivery using aptamer conjugated PEG-PLGA particles can offer a better therapeutic index as compared to non-targeted polymeric formulations. The study demonstrated a greater drug encapsulation efficiency using polymeric formulations and enhanced drug cellular uptake with stronger killing effects on human breast adenocarcinoma cells and minimal systemic cytotoxicity to surrounding normal cells using epithelial cell adhesion molecule (EpCAM) targeted RNA aptamer (M. Alibolandi et al., 2015). The work of Li and his team (L. Li et al., 2014) further supported that EpCAM aptamer functionalized polymeric particles result in efficient targeted drug delivery. Their work showed that EpCAM aptamer-PLGA-lecithin-curcumin-PEG formulation can improve *in vivo* therapy significantly with enhanced drug bioavailability, increased binding to targeted colon tumor cells, greater cellular uptake as well as high cytotoxicity specifically to colorectal cancer cells.

PEG biopolymer is an FDA approved polymer for nasal, injectable and rectal formulations. It is one of the biopolymers of interest for pharmaceutical delivery due to its favorable characteristics such as enhancing the dissolution rate of partially soluble drugs (Dhar et al., 2008); hydrophilic sheltering proteins and peptides from the immune system; prolonging the circulation time of encapsulated molecules to reduce systemic removal (Jianwei Guo et al., 2011; L. Li et al., 2014); and enhancing the formulation stability to protect encapsulated bioactives from the physiological environment (Makadia & Siegel, 2011). Numerous studies have been reported on the use of PEI biopolymer as a powerful non-viral transfection agent to boost aptamer-mediated delivery for high transfection efficiency, improved release rate, and enhanced cargo capability. A study using mucin 1(MUC1) aptamer-labelled pDNA conjugated PEI complex in treating human lung tumor

cells has demonstrated an efficient targeted gene delivery with improved gene expression, greater transfection efficiency and controlled release rate (Kurosaki et al., 2012). A recent study by Subramanian *et al*. 2015 also illustrated the use of PEI nanocomplex in targeted delivery of siRNA using EpCAM aptamer to selectively inhibit tumor cell proliferation (Subramanian et al., 2015). Chitosan is a modified natural polysaccharide, and has been widely used as a therapeutic delivery carrier. Sayari et al. (2014) have demonstrated the use of chitosan polymeric particles for specific delivery of the anticancer drug, SN38, to cure colon cancer using MUC1 DNA aptamer to increase the targeting ability and cellular uptake of targeted tumors (Sayari et al., 2014). Another research study also reported the use of chitosan particles in encapsulating S58 aptamer that targets human Tenon's capsule fibrolasts to treat myofibroblast trans-differentiation by antagonizing TGF-β receptor II. The results showed chitosan as a potential drug carrier with good encapsulation efficiency, low systemic cytotoxic effect, and sustained release profile (Chen et al., 2013). Poly(beta-amino ester) (PBAE) is a novel pH sensitive biopolymer, and has been utilized for endosomal delivery of various drugs and genes. For instance, Zhang and his team designed a dual-functional pH sensitive nucleolin-specific AS1411 aptamer conjugated D-α – tocopheryl polyethylene glycol 1000-block-PBAE copolymer (Apt-TPGS-b-PBAE) with improved synergistic effect of target recognition and pH-sensitive release of drug in the endosomal acidic environment. As a result, the retention of drug at the targeted site was prolonged with significant inhibition of tumor proliferation due to enhanced cytotoxicity as compared to individual drug therapies (J. Zhang et al., 2014). pH-responsive PBAE has also been conjugated with PLGA as a single formulation to deliver drugs in the research study of van Vlerken (2008). This study demonstrated an extended circulation time and a high drug accumulation at the target site to enhance breast cancer treatment.

2.9.9 Future outlook

The diversity of cancer cells and intra-tumor genetic heterogeneity continue to be the most significant challenge to the development of effective cancer therapies. It is improbable that a single therapy will be effective to completely destroy tumors cells in all cancer patients. More research efforts are essential to develop robust and tunable therapies capable of providing specific and tailored treatment to different cancer scenarios. This can

be achieved by developing multimeric formulated aptamers with high specificity, binding affinity and sensitivity to boost the discovery of malignant cells as well as providing a sustained therapeutic effect. Multimodal tumor treatments that combine several therapies such as chemotherapy and gene therapy along with multiple agents including aptamers and OVs for specific therapeutic activity, will be a great promise with huge potency in killing tumor cells and increasing the survival rate of patients.

2.10 NOVEL POLYMERIC APTAMER-DRUG FORMULATION FOR TARGETED DELIVERY

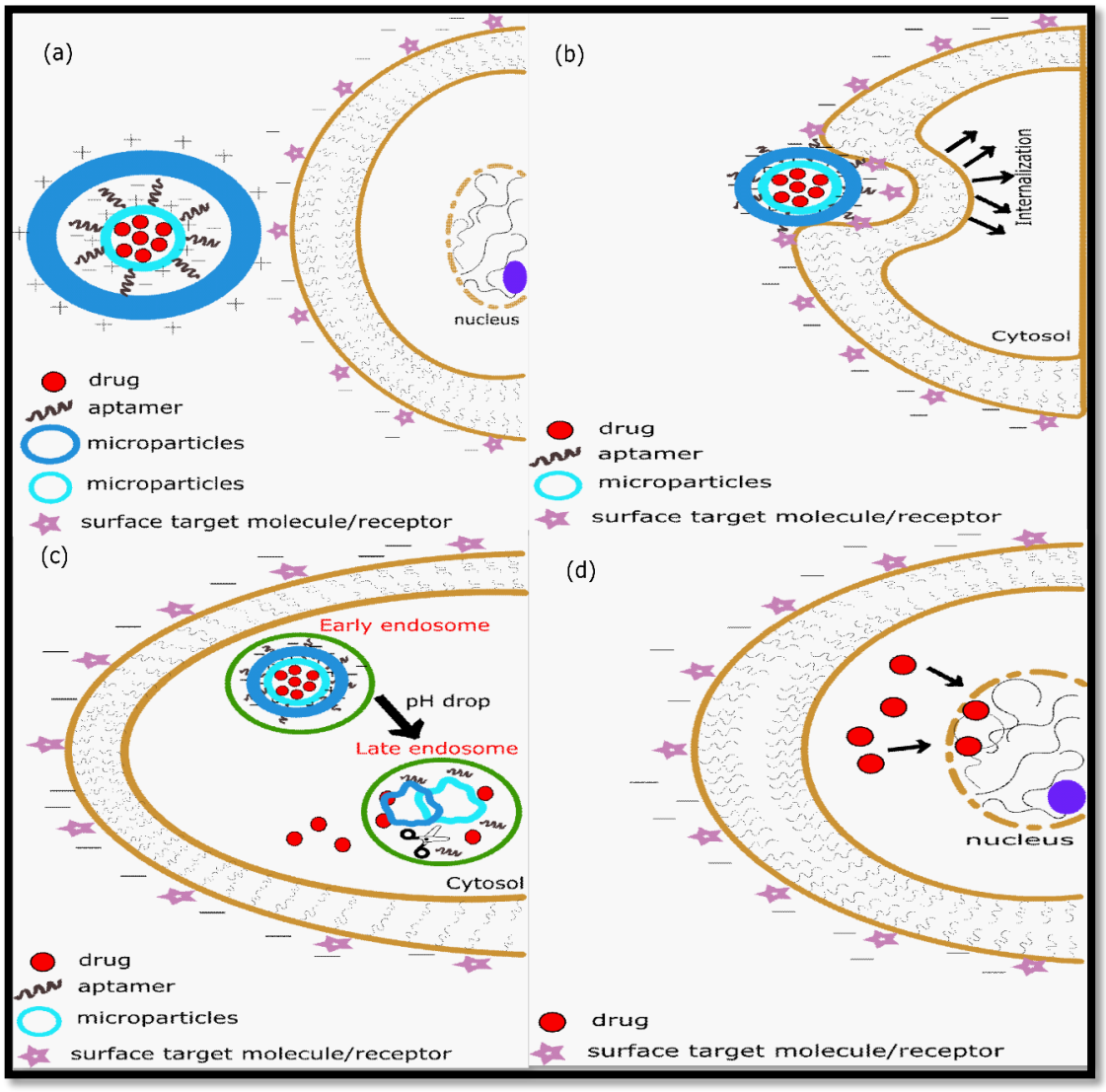

Figure 2.6: Novel DPAP aptamer-drug design formulation and stepwise delivery mechanism for enhanced cell targeting. (a) Electrostatics interactions between positively charged polymeric particles and negatively charged cell membrane. (b) The binding of aptamers to target cell receptors to induce internalization process. (c) The degradation of microparticles and DNA aptamers in the endosomal acidic environment to release of encapsulated drugs. (d) The diffusion of drugs into the nucleus to cause cytotoxic effects

Figure 2.6 shows a novel product design of aptamer-drug formulation aimed at maintaining the structural and biochemical integrity of the active drug as well as the biophysical binding characteristics of the aptamer for enhanced targeted delivery. The design presents a multifunctional formulation based on the use of biodegradable polymers as the drug carrier, aptamer cargo and transport vehicle. In this design, the outer layer of the drug-encapsulated particles is functionalized with the aptamer before the drug-polymer-aptamer complex is further encapsulated within an outer particulate layer. The inner and outer polymeric particulates are both cationic in nature with the latter being more cationic in order to promote cell membrane binding and internalization. The DPAP design framework provides a more effective protection to the encapsulated drug and aptamer to prevent drug leakages and ensure controlled and sustained drug release at the target sites with increased therapeutic index and minimal side effects.

Firstly, the positively charged outermost particulate layer electrostatically interacts with negatively charged target cell membrane as shown in Figure 2.6 (a). This interaction facilitates the transportation of negatively-charged aptamers to the target cell membrane. As a result, the encapsulated aptamer is released to bind onto the target surface receptors, biomarkers or proteins in order to trigger a receptor-mediated internalization, also referred to as endocytosis as shown in Figure 2.6 (b). The receptor-mediated internalization via endosome increases the cellular uptake of drug encapsulated particles into the target cells as displayed in Figure 2.6 (c) (M. Alibolandi et al., 2015; Y. F. Huang, Shangguan, Liu, Philips, et al., 2009; Radom et al., 2013). The acidic environment of the endosome induces hydrolytic bonding cleavage between the aptamer and the conjugated particles, and also polymeric degradation via hydrolysis. Polymeric particles such as PLGA are hydrolytically unstable and degrade into water-soluble and non-toxic monomers due to the hydrolysis of its ester bonds within the polymer chain, following gradual hydration

and swelling via water uptake from the surrounding aqueous media (Liechty et al., 2010; Stevanovic & Uskokovic, 2009). (Figure 2.6 (c)). For polymers such as PLGA, the accumulation of lactic acid and glycolic acid monomers reduces the local pH and induces autocatalytic ester hydrolysis due to increased production of carboxylic end groups (Stevanovic & Uskokovic, 2009). Consequently, the encapsulated drugs are released from the particles. The aptamers are removed in the later stage where the endosome fuses with lysosome containing hydrolytic and proteolytic enzymes that degrade nucleotide linkages (G. Vilar, Tulla-Puche, J., Alericio, F. , 2012). Hydrolytic cleavage can degrade bonding such as ester bonds, ester derivatives, poly(orthoesters), poly(anhydrides), poly(cyanoacrylate) and poly(phosphoesters) derivatives (Liechty et al., 2010). The released drug diffuses out from the endosomal membrane into the cytosol, enters the nucleus and intercalate into the genomic DNA to trigger cytotoxic effects as illustrated in Figure 2.6 (d) (Y. F. Huang, Shangguan, Liu, Philips, et al., 2009; Radom et al., 2013).

CHAPTER 3

RESEARCH METHODOLOGY

3.1 LIST OF MATERIALS, CHEMICALS, REAGENTS, AND CELL LINES

Material	**Description**	**Supplier**
Poly(lactic-*co*-glycolic acid) acid (PLGA)	Molecular weight 30,000-60,000 Da; 50:50 ratio of lactide:glycolide	Sigma Aldrich**,** Malaysia
Poly(lactic-*co*-glycolic acid) acid (PLGA)	Molecular weight 40,000-75,000 Da; 65:35 ratio of lactide:glycolide	Sigma Aldrich**,** Malaysia
Branched poly(ethylene imine) (PEI)	Molecular weight 25,000 Da	Sigma Aldrich**,** Malaysia
		Sigma Aldrich**,** Malaysia
Branched poly(ethylene imine) (PEI)	Molecular weight 800 Da	Sigma Aldrich**,** Malaysia
Poly(vinyl alcohol) (PVA)	Molecular weight 31,000-50,000 Da (98-99% hydrolysed)	Sigma Aldrich**,** Malaysia
1-ethyl-3-(3-dimethylaminopropyl)-carbodiimide (EDC)	Molecular weight 191,70 g/mol (commercial grade, premium quality level)	Sigma Aldrich**,** Malaysia
N-hydroxysuccinimide (NHS)	Molecular weight 217,13 g/mol (≥98% (HPLC)	Sigma Aldrich**,** Malaysia
Acetone	Molecular weight 58.08 g/mol (Laboratory Reagent, ≥99.5%)	Sigma Aldrich**,** Malaysia
Thrombin (lyophilized powder)	From human plasma	Sigma Aldrich**,** Malaysia

Lysozyme human recombinant	Expressed in rice (≥100,000 units/mg protein)	Sigma Aldrich**,** Malaysia
Silica gel bead	3.5 mm bead size, Type II	Sigma Aldrich**,** Malaysia
Phosphate buffered saline (PBS) tablets	One tablet dissolved in 200 mL deionized water at 25ºC yields 0.01 M phosphate buffer, 0.0027 M potassium chloride, 0.137 M sodium chloride, and pH 7.4	Sigma Aldrich**,** Malaysia
Bovine serum albumin (BSA)	Molecular weight ~66,000 Da (≥98% by agarose electrophoresis)	Santa Cruz, USA
15-mer thrombin specific-DNA aptamer	5'-GGT TGG TGT GGT TGG-3' (5.0 μmole scale, PCR Grade, 225 OD)	1st BASE, Malaysia
Tris EDTA	Ready-to-use buffer (DNases, RNases and Protease)	Acros Organics, Malaysia
Citric acid	99.9% purity	Fisher Scientic, Singapore
Magnesium nitrate hexahydrate	98%	Alfa Aesar, USA
Magnesium acetate tetrahydrate	98%	Alfa Aesar, USA
Fresh *Amaranthus tricolor* (red spinach), *Amaranthus blitum* (green spinach) and *Andrographis paniculata*		Sarawak, Malaysia
3t3-L1 adipose cell lines		National Cell Culture Society (NCCS), Pune, India

3.2 SYNTHESIS OF DPAP PARTICULATE FORMULATION

The DPAP formulation was synthesized using a water-in-oil-in-water (w/o/w) double emulsion technique with sonication. 2% w/v BSA solution was prepared by mixing BSA with de-ionized water and 6.7% w/v PLGA was prepared by mixing PLGA with acetone to form a polymeric stock matrix. The BSA solution was transferred into the polymer stock and mixed thoroughly using an ultrasonic homogenizer (Labsonic^{R} M, Sartorius Group, Germany.) at 70% amplitude, 0.7 s pulse cycle for 2 min to form the DP system. 2% w/v PVA solution was added to the DP mixture as a hardening agent to emulsify and produce DP emulsion droplets via sonication under the mentioned conditions. Subsequently, the organic solvent accompanying the emulsion was evaporated at room temperature by shaking gently for 2 h at 200 rpm. The mixture was centrifuged at 4000 rpm and 4ºC for 20 min using a refrigerated centrifuge (Universal 320R, Hettich, UK) to remove residual organic solvent prior to freeze-drying in order to produce solidified BSA-loaded PLGA particles (DP particles).

3.2.1 Formulation of different DPAP micro-particulate system with various molecular compositions

The multifunctional co-polymeric DPAP layered formulation (drug-PLGA-aptamer-PEI) was produced by water-in-oil-in-water (w/o/w) double emulsion. Three different DPAP formulations were synthesised: 1) DPAP made of drug-PLGA (50:50 of lactide:glycolide)-aptamer-PEI (molecular weight of 800 Da); 2) DPAP made of drug-PLGA (65:35 of lactide:glycolide)-aptamer-PEI (molecular weight of 25,000 Da); and 3) DPAP made of drug-PLGA (65:35 of lactide:glycolide)-aptamer-PEI (molecular weight of 800 Da). 6.7% w/v PLGA was prepared in acetone to produce a polymeric stock. 2% w/v BSA solution was prepared with de-ionized water. The BSA solution was then mixed with the PLGA polymeric stock using a magnetic stirrer at 500 rpm for 5 min to create the DP segment. Magnetic stirrer was utilized for homogenization. 2% w/v PVA hardening agent was added to the DP solution to form emulsified DP droplets before organic solvent evaporation via gentle shaking at 200 rpm for 2 h. The mixture was further centrifuged

(Universal 320R, Hettich, UK) at 4ºC and 4000 rpm to remove residual organic solvent. The resulting DP pellet was freeze-dried for 48 h.

3.2.2 Synthesis of PEGylated micro-particles

The DPAP formulation was PEGylated by introducing a PEG layer into different sections of the DPAP framework based on the following combinations: 1) BSA-PLGA-PEI-PEG (DP-PEI-PEG) 2) BSA-PLGA-PEI-PEG-APT (DP-PEI-PEG-Apt) 3) BSA-PLGA-PEG-APT (DP-PEG-Apt). DPAP was PEGylated to evaluate its impact on DPAP matrix as a drug delivery vehicle. PEGylation has been reported to enhance drug encapsulation and delivery in different polymeric formulations (Aravind, Jeyamohan, et al., 2012; Cheng et al., 2007b; L. Li et al., 2014). DP formulation was produced as described in Section 3.2. 12% w/v PEI and 6.7% w/v PEG stock solutions were prepared separately in acetone. The DP mixture was added to both the PEI and PEG stocks at ratios of 1:6 and 1:1 respectively and mixed gently for 5 min to create DP-PEI and DP-PEG formulations. 2% w/v PVA solution was added for emulsification followed by solvent evaporation and centrifugation to remove residual liquid as described under Section 3.2. 6.7% w/v PEG solution was added to the DP-PEI system to form DP-PEI-PEG micro-particles. The aptamer molecules were conjugated via EDC and NHS coupling reaction to synthesis DP-PEI-PEG-Apt and DP-PEG-Apt formulations prior to freeze-drying.

3.2.3 Synthesis of aptamer-conjugated PLGA micro-particles

1% w/v PLGA polymeric mixture was prepared in deionized water and coupled with aptamer molecules via EDC and NHS activation chemistry to produce aptamer-conjugated PLGA (PA) formulation.

3.2.4 Synthesis of thrombin-conjugated silica capsules

Thrombin molecules were first immobilized onto the surface of silica capsular to mimic cell membrane surface proteins for *in vitro* drug release. Silica gel beads were used to produce thrombin-conjugated silica capsules via a simple adsorption method. 10 mg thrombin was mixed with 500 mg silica beads in PBS buffer solution for 5 min at 200 rpm.

Absorbance reading at 280 nm was used to evaluate thrombin immobilization. The mixture was centrifuged for 10 min at 4000 rpm and 4ºC to collect thrombin-conjugated silica capsules (pellets).

3.2.5 Synthesis of MgO nanoparticles

Two synthesis approaches were used to generated MgO nanoparticles; chemical and green biosynthesis approaches. MgO nanoparticles were synthesized by chemical approach using sol-gel method as described by (Jeevanandam et al., 2017b). Equimolar ratio of magnesium precursor and gelling agent were dissolved in ethanol separately and then mixed to form a gel of magnesium network at pH 5. The gel was then subjected to aging for 12 h and drying for 24 h at 100°C to form a sol-gel powder. The obtained sol-gel powders were calcined in a box furnace (Carbolite 1200°C heavy duty box furnace) at 650°C for 2 h at a heating rate of 5°C/min to form pure hexagonal shaped MgO nanoparticles. Green synthesized MgO nanoparticles were generated using *A.tricolor* plant leaf extracts as described previously by (Jeevanandam et al., 2017a). Briefly, fresh leaves were extracted using distilled water in a w/v ratio of 1:10. The mixtures were shaken for 20 min at 350 rpm and heated at 100°C before filtration. The magnesium precursors were then mixed with the aqueous leaf extracts with constant stirring and heating at 60°C for 10 min. MgO_1 is used to designate MgO nanoparticles chemically synthesized whilst MgO_2 is used for MgO nanoparticles generated via green synthesis. Both MgO nanoparticles were used to investigate and compare their effects on biophysical properties, encapsulation efficiency, cellular uptake, and cytotoxicity of DPAP-MgO formulations. Dynamic Light Scattering (DLS) technique using Malvern Zetasizer Nano ZS was conducted to determine the average D[4,3] hydrodynamic size, particle size distribution, and zeta potential of different MgO nanoparticles and DPAP carrying MgO nanoparticles. The morphological characterization of these formulations was carried out using Transmission Electron Micrograph (TEM).

3.2.6 *In vitro* generation of DPAP formulation carrying MgO drug nanoparticles

DPAP formulation was generated using a double emulsion water-in-oil-in-water (w/o/w) method integrated with ultra-sonication as previously reported by K. X. Tan et al. (2017).

MgO nanoparticles were encapsulated within the inner core of DPAP micro-particles as drug molecules. Two DPAP-MgO micro-particulate systems were generated: 1) DPAP formulation encapsulating chemically synthesised MgO nanoparticles (DPAP-MgO_1); and 2) DPAP formulation carrying green synthesised MgO nanoparticles (DPAP-MgO_2). Basically, 0.001 M each of MgO_1 and MgO_2 nanoparticles were sonicated for 15 min before encapsulation into PLGA polymeric particles. 10 w/v% PLGA was prepared by dissolving PLGA into acetone to produce a polymeric matrix. Each MgO nanoparticle solution was added to the PLGA polymeric matrix and sonicated for 2 min at 70% amplitude, and 0.7 s pulse cycle using Labsonic^R M ultra-sonicator. 2% w/v PVA emulsifying agent was added to the mixture to solidify the DP (MgO-P) emulsion droplets under constant ultrasonication. Next, the DP mixture was shaken gently at 200 rpm for 2 h at ambient temperature to evaporate the organic solvent from the emulsion. The DP mixture was further centrifuged at 4ºC and 4000 rpm for 20 min using Universal 320R centrifuge to remove residual organic solvent and PVA followed by freeze-drying for 48 h to generate solid MgO-entrapped PLGA (DP) particles. Aptamer conjugation was conducted via EDC and NHS coupling chemistry to produce DPA formulation as described in section 3.3 below. The DPA particulates were added to 12% w/v PEI polymeric stock to produce both MgO_1- and MgO_2-loaded PLGA-Aptamer-PEI (DPAP-MgO_1 and DPAP-MgO_2) formulations.

3.3 EDC AND NHS ACTIVATION CHEMISTRY

The thrombin-specific DNA aptamer was conjugated onto the outer layer of the DP particles by EDC and NHS activation chemistry. The DP particles were incubated in PBS buffer containing 400 mM EDC and 100 mM NHS for an hour with gentle shaking at 200 rpm followed by centrifugation at 4000 rpm and 4ºC for 20 min. EDC enabled the coupling of carboxyl groups followed by NHS activation which replaced EDC with hydroxyl groups. This chemical coupling process is necessary to enhance electrophilicity in order to catalyse the formation of covalent amide linkages between the amine groups of DNA aptamer and the carboxyl groups of DP particles. The resulting NHS-activated DP-COOH complex was incubated with 20µl of 100 µM aptamer for an hour at 200 rpm

followed by centrifugation to enable aptamer conjugation for the generation of aptamer-DP particles (DPA). The DPA system was wash with de-ionised water and centrifuged for 20 min at 4000 rpm and 4ºC repeatedly to eliminate unbound aptamer molecules. The resulting DPA conjugates particles were used to produce the DPAP formulation using PEI polymer as the outermost polymeric layer that encapsulating DPA particles. 12% w/v PEI stock was prepared by mixing PEI with acetone, and 1% w/v DPA was added, and mixed thoroughly using ultrasonic homogenizer for 2 min. 2% w/v PVA solution was added to produce DPAP emulsion droplets prior to solvent evaporation and the system was incubated at room temperature for 2 h under 200 rpm. The mixture was then centrifuged for 20 min before freeze-drying to produce BSA-loaded PLGA-Aptamer-PEI particles (DPAP particles).

3.4 BIOPHYSICAL CHARACTERISATION OF DPAP FORMULATION

Dynamic light scattering (DLS) analysis using Malvern Zetasizer Nano ZS, Model ZEN3600 (UK) was used to study the D[4,3] average particle size, particle size distribution and zeta potential of each surface layer configuration during the synthesis of DPAP particles as well as PEGylated formulations, DPAP carrying MgO, and different formulations made up of various molecular compositions. DLS analysis was also used to determine the size and charge of DPA, PA, and aptamer after thrombin binding. The morphology and shape of the DPAP particles were examined using scanning electron microscopy (SEM) and transmission electron microscopy (TEM).

3.5 CHEMICAL ANALYSIS OF DPAP PARTICLES

Fourier transform infrared spectroscopy (FTIR) was used to identify various functional groups and chemical bonds in DPAP particles in order to identify any potential modifications in the initial compositional structures during the synthesis process. The principle of FTIR is based on relative spectral vibration of molecules in a sample on exposure to infra-red (IR) within a specific range of wave number or frequency. The IR spectra of DPAP was obtained in the frequency range 500 to 3900 cm^{-1}.

3.6 DETERMINATON OF BSA AND APTAMER ENCAPSULATION EFFICIENCIES

The amounts of encapsulated BSA and aptamer within the DPAP particulate formulation were quantified as the difference between the initial amounts of BSA and aptamer applied during formulation and the amount of free BSA and aptamer detected in the PVA hardening agent after DP and DPAP composites formation. After the formation of DP composite, the DP suspension was centrifuged at 4000 rpm and 4ºC for 20 min using a refrigerated centrifuge (Universal 320R, Hettich), and the free BSA in the supernatant was measured using a UV-Visible spectrophotometer (Lambda 25 UV/Vis Double Beam, Perkin Elmer) at 260 nm. The free aptamer concentration in the supernatant was measured at 280 nm after centrifuging the DPAP suspension at 4000 rpm and 4ºC for 20 min. All the measurements were repeated three times and averaged. The encapsulation efficiency and loading capacity were calculated using following equations:

$$\text{Encapsulation efficiency (\%)} = \frac{Amount\ of\ encapsulated\ BSA\ or\ aptamer}{Amount\ of\ BSA\ or\ aptamer\ applied}\ x\ 100$$

$$\text{Loading capacity} = \frac{Amount\ of\ encapsulated\ BSA\ (mg)}{Total\ PLGA\ added\ (mg)}$$

3.6.1 Encapsulation efficiency and loading capacity of DPAP formulated with MgO nanoparticles

The concentration of encapsulated MgO_1 and MgO_2 drug nanoparticles was measured using UV-visible spectrophotometry (Perkin Elmer, Lambda 25 UV/Vis Double Beam) at 320 – 330 nm for MgO_1 and 320 nm for MgO_2 nanoparticles respectively. The concentration of encapsulated MgO nanoparticles within DPAP formulation was calculated as the difference between the initial concentration of MgO and the amount of free MgO molecules in the supernatant after the formation of DP. The concentrations of free MgO_1 and MgO_2 nanoparticles were determined after centrifuging DP at 4000 rpm and 4ºC for 20 min and analysing the supernatant. The loading capacities and encapsulation efficiencies of DPAP-MgO_1 and DPAP-MgO_2 formulations were estimated using the following equations:

Loading capacity = $\frac{Amount\ of\ entrapped\ MgO1/MgO2\ (mg)}{Original\ amount\ of\ PLGA\ \ added\ (mg)}$

Encapsulation efficiency (%) =

$$\frac{Amount\ of\ loaded\ Mgo1\ or\ MgO2\ or\ aptamer}{Total\ amount\ of\ initially\ added\ MgO1\ or\ MgO2\ or\ aptamer\ applied}\ x\ 100$$

3.7 *IN VITRO* RELEASE PROFILE

The release profile of BSA protein from the DPAP particulate formulation was investigated in a physiological PBS buffer system using an incubator shaker. 2 % w/v concentration of DPAP particles in PBS buffer was incubated at pH 7.4, temperature 37ºC and speed 120 rpm. At designated time intervals (24 h intervals from day 1 to day 8; 72 h interval from day 9 to day 38; and 120 h interval from day 38 to day 43), the DPAP/buffer mixture was centrifuged for 10 min at 4000 rpm and 4ºC to form DPAP pellet, and the 5 mL supernatant was decanted for UV spectrophotometric analysis at 260 nm to determine the concentration of released BSA. The removed 5 mL supernatant was replenished fresh PBS buffer to re-suspend the DPAP pellet for continuous incubation.

3.7.1 *In vitro drug release characterisation of different DPAP formulations*

The *in vitro* release profiles of DPAP formulations [1) DP(50:50)AP(~800 Da), 2) DP(65:35)DP(~25,000 Da), and 3) DP(65:35)AP(~800 Da)] and the PEGylated DPAP formulations [1) DP-PEI-PEG, 2) DP-PEI-PEG-Apt, and 3) DP-PEG-Apt] were investigated in a physiological PBS buffer at pH 7.4 with variable ionic strengths of a) 100 mM b) 500 mM c) 1 M sodium chloride (NaCl). Incubation was performed at 120 rpm and 37ºC. UV-visible spectrophotometry was used to determine drug release concentration over time. The incubation systems are sampled and centrifuged at 4000 rpm and 4ºC for 10 min. 5 mL supernatant is collected and analysed at 260 nm and 280 nm. An equal volume of fresh PBS buffer is added to maintain a constant volume for continuous incubation.

3.7.2 *In vitro* drug release profile of DPAP formulation under various temperature and pH levels

The BSA release profile of DPAP formulation was studied *in vitro* at 150 rpm under variation conditions of temperature and physiological buffer pH. 2% w/v DPAP suspensions were incubated at 3 different temperature levels: 1) 25ºC, room temperature for 12 days; 2) 37ºC, temperature of human body system for 12 days; and 3) 41ºC, elevated feverish temperature condition for 4 h. This experiment is essential to acquire a better understanding of the initial drug release characteristics of DPAP at extremely high temperature, 41°C. At designated time intervals (4.5 h intervals for Day 1; and 24 h intervals from Day 2-12), the DPAP suspension was centrifuged at 4ºC and 4000 rpm for 10 min in order to collect 5 mL supernatant aliquot for UV 280 nm BSA release analysis. Fresh PBS buffer was used to replenish the mixture volume for continuous incubation. For drug release studies at 41ºC, samples were aliquoted at every 10 min over a shorter incubation duration of 4 h. BSA drug release profile of DPAP formulation under varying pH levels of 5, 6, and 7 was also investigated at 37°C using the same conditions and analyses described earlier.

3.8 MTS CYTOTOXICITY ASSAY

MTS cytotoxicity assay is a type of proliferation assay that uses a colorimetric method to quantify viable cells. Chinese hamster wild-type cell line V79B cells were cultured in a 96-well microtitre plate to obtain 5 x 10^3 cells/well using a 10% fetal bovine serum supplemented DMEM media in a humidified CO_2 incubator at 37±2ºC and 5±1% CO_2 for 24±2 h to allow cell attachment. The V79B cells were incubated with the DPAP particles at 6 different concentrations: 0.15625, 0.3125, 0.625, 1.25, 2.5, and 5 µl/ml to a final volume of 6 ml of each. 200 µl of each treatment was pipetted into selected wells and DPAP sample solution without cells was used as the blank. The plate was then incubated for 24 h±30 min at 37±2ºC and 5±1% CO_2 in the CO_2 incubator. After 24 h±30 min incubation, 40 µl of MTS reagent was added into each well. Subsequently, the plate was incubated for an hour in the CO_2 incubator. After the 1 hour incubation, the plate was

analysed with ELISA plate reader at 492 nm. With this assay, a sample is considered cytotoxic if the cell viability is equal or less than 50% (Bakand, 2009).

3.9 LAYER-BY-LAYER BIOPHYSICAL ANALYSIS OF DP, DPA, DPAP FORMULATIONS

Layer-by-layer surface analysis of the different compartments of DPAP particulates was performed via dynamic light scattering (DLS) measurements to investigate the surface charge and hydrodynamic size distribution under varying conditions of pH, ionic strength and temperature. In brief, 0.1% w/v DP, DPA, and DPAP suspensions were prepared using PBS buffer, and 0.1 M HCl and 0.1 M NaOH were used to vary the pH of the suspensions from 3 to 11. To study the effect of temperature on the hydrodynamic size, 0.2% w/v DP, DPA, and DPAP suspensions were synthesized and exposed to water baths set at different temperatures: 25°C, 30°C, 37°C, and 42°C. The effect of temperature is critical to understand the extent of surface molecular kinetics on the charge and size of the particulates.

3.10 EFFECTS OF IONIC STRENGTH ON THE STRUCTURAL AND BINDING STABILITY OF DPAP FORMULATION

The effect of ionic strength on the hydrodynamic size, surface charge and binding stability of DPAP particles was investigated using a monovalent cation (Na^+). This is intended to study potential changes in the characteristics features of DPAP under high salinity serum conditions. Different concentrations of Na^+ were prepared (20 mM, 50 mM, 100 mM, and 1 M), and 0.5 mL of each was added to 0.36% w/v DPAP suspensions and incubated for 30 min. Subsequently, the DPAP/Na^+ suspensions were centrifuged at 4000 rpm and 4°C for 10 min and aliquots of the supernatants were collected for UV absorbance measurements at 260 nm and 280 nm. The remaining DPAP/Na^+ solutions were used for hydrodynamic size and zeta potential measurements.

3.11 THERMOGRAVIMETRIC ANALYSIS OF DP AND DPAP PARTICULATE SYSTEMS

The thermal stability of lyophilised DP and DPAP micro-particles was investigated using thermogravimetric analysis with differential scanning calorimetry (Novotny et al.) to simultaneously determine the change in mass and enthalpy of the formulations respectively at a constant heating rate in an inert environment. This study is important to understand the thermal stability of the bio-polymer complexation and monitor potential molecular rearrangements in the form of exotherm within the particulate matrices of DP and DPAP formulations. The TGA system was purged with nitrogen at 20°C per min before use. ~ 9 mg each of DP and DPAP particles were placed on aluminium pans and analysed from 30°C to 800°C at a constant heating rate of 10°C per min and 25.0 mL/min nitrogen gas as the inert medium. STARe evaluation software was used to analyse the TGA results of DP and DPAP particles.

3.12 INVESTIGATION OF BSA AND APTAMER CONJUGATIONS TO DPAP FORMULATION

The binding characteristics of BSA and aptamer molecules within the polymeric layers of DPAP formulation were investigated via UV-spectrophotometric analysis in order to investigate the kinetics of drug encapsulation. 2% w/v BSA solution was added to 10% w/v PLGA and incubated for 30 min 5 min at 500 rpm. The incubation mixture is sampled at regular time intervals and centrifuged at 4000 rpm, 4°C for 5 min. Supernatant is collected and analysed at UV 280 for drug concentration. For aptamer affinity binding to DP particles, 1% w/v DP solution was activated via EDC and NHS chemistry and incubated with 20µl of aptamer (100 µM) for 1 h at 200 rpm. Similarly, the incubation mixture is sampled at regular time intervals and centrifuged at 4000 rpm, 4°C for 5 min. The supernatant is collected and analysed at UV 260 nm for aptamer concentration.

3.13 BINDING CHARACTERISTICS OF DPAP POLYMERIC FORMULATIONS

The binding characteristics of 1) PA formulation; 2) aptamer molecules; 3) PLGA-PEI-PEG formulation; 4) PLGA-PEI-PEG-Apt; 5) PLGA-PEG-Apt towards thrombin were investigated by incubating 0.1% w/v of each of formulation with 0.05% w/v thrombin in PBS buffer for 20 min at 200 rpm. After incubation, the mixtures were centrifuged at 4000 rpm and 4ºC for 10 min. The supernatants were collected and analysed for thrombin concentration.

3.13.1 The selective binding of thrombin and release of encapsulated BSA in the presence of different proteins

0.1% w/v DPAP solution was prepared by mixing DPAP particles in PBS buffer. 0.1% w/v DPAP solution was then examined *in vitro* under 3 different conditions: 1) 0.1% w/v DPAP incubation with 0.1% w/v thrombin molecules; 2) 0.1% w/v DPAP incubation with 0.1% w/v lysozyme and 0.1% w/v lactalbumin molecules; 3) 0.1% w/v DPAP incubated with 0.05% w/v thrombin, 0.05% w/v lysozyme and 0.05% w/v lactalbumin molecules, for 30 min at 200 rpm. At regular time intervals during incubation, the mixtures were centrifuged for 10 min at 4000 rpm, 4ºC and a 2-5mL aliquot of the supernatant analysed at UV absorption 280 nm. Released BSA drug concentration was analysed relative to protein concentrations in the original stock solutions.

3.13.2 The *in vitro* release of encapsulated BSA in the presence of immobilized thrombin

The rate of BSA release was investigated under 3 different conditions: 1) 0.1% w/v DPAP incubation with 0.1% w/v silica capsules; 2) 0.1% w/v DPAP incubation with 0.1% w/v thrombin-conjugated silica capsules; 3) 0.1% w/v DPAP incubation with 0.1% w/v silica capsules in the presence of free thrombin molecules, for 30 min at 200 rpm. At regular time intervals during incubation, the mixtures were centrifuged for 10 min at 4000 rpm, 4ºC and a 2-5mL aliquot of the supernatant analysed at UV absorption 280 nm. Released BSA drug concentration was analysed relative to protein concentrations in the original stock solutions.

3.14 3,5-DINITROSALICYLIC ACID (DNS) ASSAY

DNS assay was carried out by incubating DPAP-MgO_1 and DPAP-MgO_2 sample with 3T3 L1 cells over a 25 h incubation duration. 3T3 L1 cells were kept in DMEM-thrombin medium with penicillin (100 U/ml), 10% FBS, and streptomycin (100 µg/ml) in a humidified environment of 50 µg/ml carbon dioxide at 37ºC. 5 mL of the pretreated 3T3 L1 cell was added to a 6-well plate before the addition of 1 mL DPAP-MgO_1 and DPAP-MgO_2 samples at different dosages. Optical densities and concentrations were determined at various time intervals. The DMEM medium with glucose was tested with DNS assay after every 5 h to determine the insulin resistance reversal ability of DPAP-MgO_1 and DPAP-MgO_2 formulations. The color intensities of the tested samples were also monitored.

3.15 STATISTICAL ANALYSIS

All experimental studies were conducted for at least 3 times and averages were reported as final results. Experimental data is reported as average ± standard error and/or standard deviation.

CHAPTER 4

RESULTS AND DISCUSSION

4.1 DPAP DESIGN CONCEPT AND DEGRADATION MECHANISM

To synthesis DPAP particles for targeted drug delivery, an integrated water-in-oil-in-water (w/o/w) double emulsion and sonication method was used. Compositionally, the DPAP particulate formulation was made up of a hydrophobic PLGA polymeric core entrapping BSA as a protein drug. Thrombin-specific DNA aptamer molecules were conjugated onto the surface of the PLGA polymeric core, and the outermost layer was glazed with a cationic polymer (PEI) particles surrounding the inner aptamer-conjugated BSA-loaded PLGA particles via electrostatic interactions with the aptamer layer to produce the DPAP system as shown by the schematic drawing in Figure 4.1. The DPAP particulate is designed to present multifunctional characteristics where both PLGA and PEI biopolymers act as delivering vectors and carrier for the drug and aptamer. Figure 4.1 shows the design and synthesis of the DPAP particulate system starting from BSA encapsulation within PLGA particles to protect its functional and structural integrity, then the conjugation of aptamer onto the PLGA surface, and finally the entrapment of DPA particles within the PEI outermost layer to maintain the binding properties of the aptamer for enhanced target cell recognition, interaction and delivery efficiency. The outer polymeric particulates, made up of cationic PEI, promote a positively charged DPAP polymeric surface in order to improve the binding of receptors onto target cells and endocytosis. This design concept is capable of shielding the entrapped protein drug and aptamer more effectively from premature release, degradation and undesirable biochemical complexation with bio-actives from physiological environment. Thus, problems associated with low drug dosage, poor drug biochemical integrity, protease and/or endonuclease degradation, as well as reduced targeting and binding affinity of the aptamer can be significantly reduced. Consequently, a more sustained and controlled drug release characteristics with enhanced pharmacokinetics and therapeutic index can be achieved.

Figure 4.2 demonstrates the *in vivo* degradation mechanism of the DPAP particulate system in targeted drug delivery. The cationic PEI outermost layer tends to bind any negatively charged cell membranes due to electrostatic attractions. However, with the presence of intercalated aptamers within the PEI particles as the targeting elements, the binding activity of the PEI is site-directed, making the DPAP binding specific to target cell surface receptors or protein markers on target cells. The outer layer PEI and aptamer complex acts synergistically via condensation of the aptamer by cationic PEI particles with high transfection efficiency and the reduction of electrostatic repulsion to facilitate the migration of electronegative aptamer molecules to negatively charged target cell membrane thus, triggering internalization. Internalization, also called receptor-mediated endocytosis, promotes enhanced target cell uptake (M. Alibolandi et al., 2015; Radom et al., 2013). Within the target cell, amine moieties associated with PEI are protonated and this results in counter-ion influxion and reduced osmotic potential. The PEI polymeric layer, as a result of osmotic imbalance, swells and bursts to release the encapsulated aptamer and the drug-loaded PLGA (DP) particles. The low pH environment of the endosome induces PLGA hydrolysis through the cleavage of ester bonding within its chain. This leads to gradual water uptake into the PLGA particulate matrix, resulting in swelling followed by degradation of PLGA to release the encapsulated drug molecule (Liechty et al., 2010; Stevanovic & Uskokovic, 2009). The accumulation of PLGA monomers (lactic and glycolid acids) continues to lower the local pH, leading to autocatalyic ester hydrolysis for more drug release (Stevanovic & Uskokovic, 2009). The released drug molecules diffuse into the cytosol and move towards the nucleus to induce therapeutic effects as highlighted in Figure 4.2 (Radom et al., 2013).

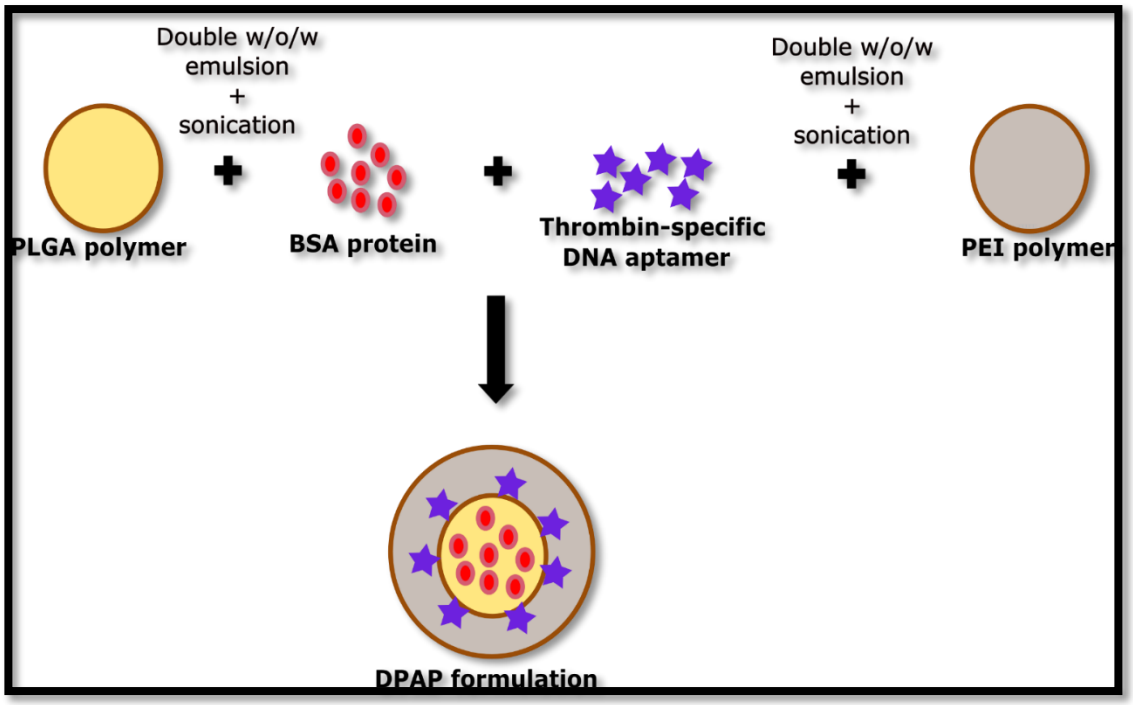

Figure 4.1: Schematics of the synthesis of DPAP particulate system by integrated w/o/w double emulsion and sonication technology

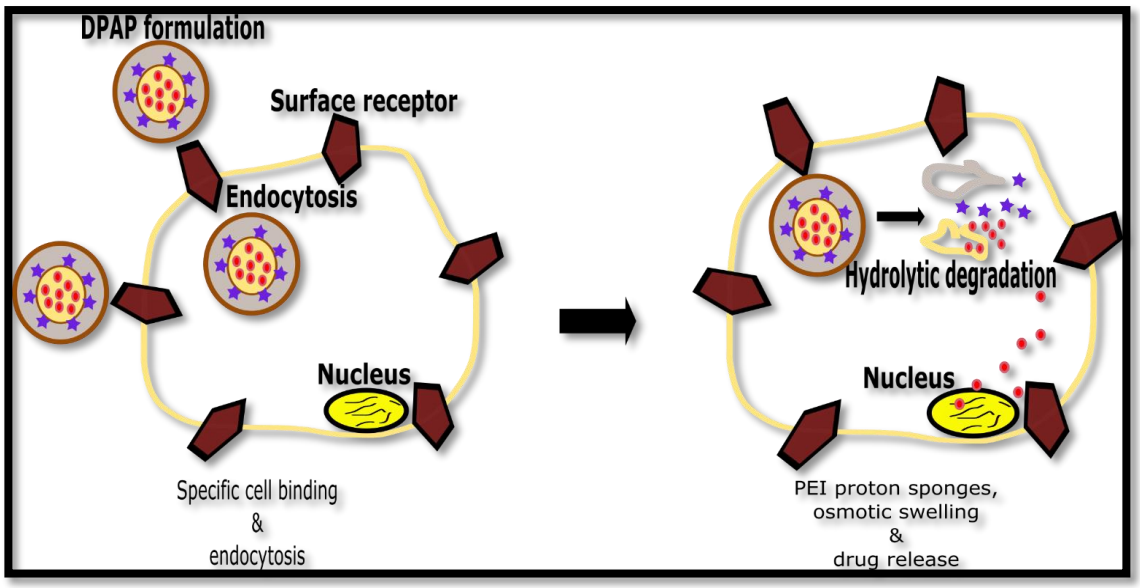

Figure 4.2: Site-directed in vivo degradation mechanism of multi-functional DPAP particulate formulation in target cells for enhanced drug delivery

4.1.1 *In vitro* generation of DPAP particulate system using magnetic homogenization

DPAP particulate system was generated using a layer-by-layer synthesis technique and water-in-water (w/o/w) double emulsion method. The effect of different homogenisation technologies on the biophysical characteristics of the formulation was investigated. Magnetic stirring and ultra-sonication were used in this work to investigate potential differences in terms of hydrodynamic size, surface charge, size distribution, and encapsulation efficiency, resulting from different mixing energies driving particulate dispersion. The working principle of magnetic stirring is based on magnetic field triggering an immersed flea or magnetic bar to rotate rapidly in a volume of liquid (De Bruyker et al., 2011). Probe-mediated ultrasonic homogenization works by generating electrical energy which is converted into mechanical energy with high-frequency using a transducer. The high mechanical energy induces the probe to vibrate rapidly in a longitudinal direction to create ultrasonic forces that impinges the sample volume. As a result, bubbles are produced and collapsed rapidly due to the formed vacuum during probe retraction (Majid et al., 2015).

The layer-by-layer schematic design of DPAP formulation is shown in Figure 4.3. The DPAP layer-by-layer architectural design commences with the innermost PLGA polymeric core which encapsulates the BSA protein drug molecules. The next layer comprises of thrombin-targeting DNA aptamer molecules coupled onto the outer surface of PLGA polymeric layer via EDC/NHS chemistry. The final outermost layer of DPAP is formulated by intercalation of PEI polymeric particles within the aptamer layer via strong electrostatic forces between electronegative aptamer molecules and cationic PEI particles. DPAP outer layer is engineered to hold a positive zeta potential in order to facilitate cellular interactions with target cells; induce cellular uptakes; and improve transfection efficiency of drug molecules. The co-polymeric PLGA and PEI layers act as delivery vehicles to carry both active pharmaceutical ingredients and targeting element whilst the DNA aptamer acts as a navigator to target and direct drug molecules to the desired cellular site in a controlled release fashion.

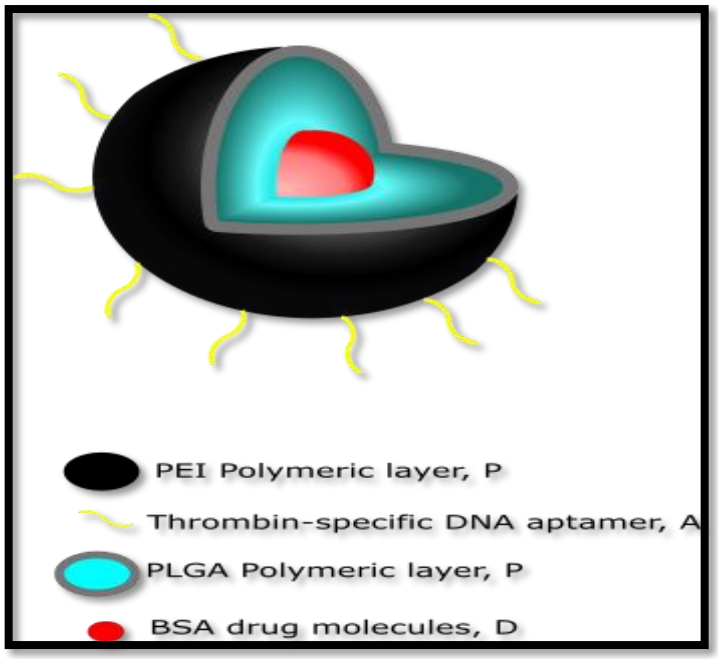

Figure 4.3: The structural architecture of the novel DPAP formulation based on the concept design of an aptamer-navigated, drug-loaded, co-polymeric delivery carrier system

4.1.2 DPAP formulation carrying MgO nanoparticles and degradation mechanism

DPAP targeted delivery system was developed *in vitro* via w/o/w double emulsion technique in conjunction with ultra-sonication. Figure 4.4 illustrates the schematics of DPAP formulation encapsulated with MgO nanoparticles as the drug payloads within the inner hydrophobic PLGA core. The thrombin-targeting DNA aptamer molecules acting as the targeting element were coupled via EDC/NHS chemistry onto the outer surface of PLGA particles. The aptamer molecules are vital in navigating the DPAP system towards target cells through specific surface protein recognition. This reduces non-specific interactions between DPAP and non-targeted cells. Hence a sufficient concentration of the functional drug molecules may be delivered to the target sites to trigger optimal remedial responses. The outer layer of the DPAP is created from molecular intercalation between the aptamer molecules and positively charged hydrophilic PEI particles.

DPAP design concept is based on improving cell-targeting using aptamers as the targeting ligand in order to deliver drug molecules to desired sites. The slightly electropositive characteristic of DPAP reduces cellular barriers and electrostatic repulsion that could

hinder effective DPAP-cell membrane interactions. The multi-layer design of DPAP using a co-polymeric assembly is deliberated to give extra protection to its bioactive components, such as drug molecules and targeting elements. The copolymeric assembly provides shielding from challenging physiological environments including initial drug burst, short circulating half-lives, endonuclease-mediated degradation, and non-specific systemic clearance. Also, the co-polymeric feature facilitates a pH-dependent degradation mechanism, allowing the control of DPAP degradation under the right intracellular event (such as the endosome) to release encapsulated drug molecules. The effective transfection efficiency and proton sponge effect of PEI particles offer high internalization and endosomal escape of entrapped drug molecules towards the nucleus to enhance therapeutic outcomes. The hydrolytic degradation of polymeric particles can offer a controlled and sustained drug release over a desired time period. Hence, DPAP design concepts have the potential to address some of the limitations associated with conventional drug delivery system.

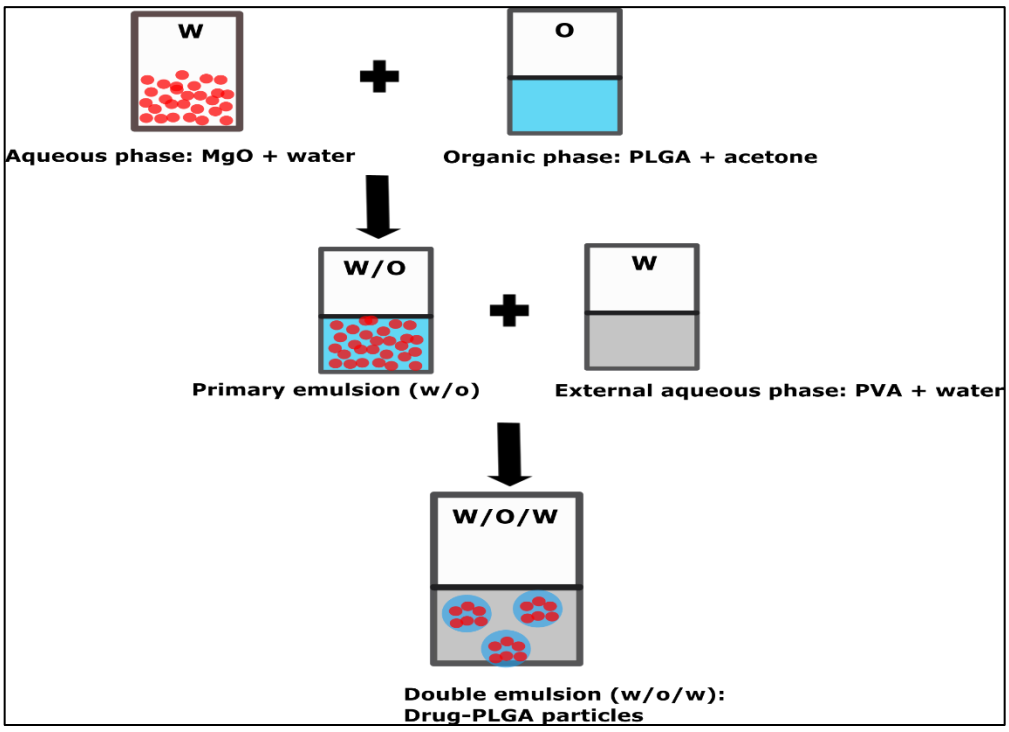

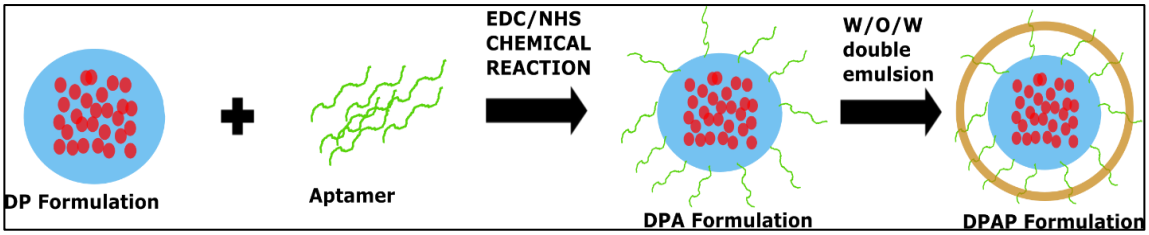

Figure 4.4: Schematic drawing of DPAP formulation process encapsulating MgO nano-drug particles and aptamer navigating molecules.

4.2 EFFECT OF pH ON THE HYDRODYNAMIC SIZE AND SURFACE CHARGE OF BSA

Figure 4.5 shows that the average D[4,3] hydrodynamic size of BSA molecule under varying pH conditions of pH 3 to 11 generally ranged from ~8.6 to 14.60 nm with a polydispersity index (PdI) of ~0.3, except pH conditions 4 and 7 which showed an average hydrodynamic size of 58.2 nm and 229.5 nm respectively. The pH effect on hydrodynamic size distribution is the result of surface electrical charge accumulation and stability in response to protonation and deprotonation of the protein molecule. At the isoelectric point (IEP) of BSA, both the inter-chain electrostatic repulsive forces and excess charge density of the molecule are reduced to zero, and this results in a higher inter-chain aggregation. The results showed BSA IEP of 4.31 under the experimental conditions. At the IEP, the protein possesses a net charge of zero with minimal intermolecular repulsive forces, and this causes the structure of the protein to be less stable and more hydrophobic. As a result, the protein molecules tend to aggregate and precipitate with minimum solubility(Salgin, 2012). Charge accumulation and neutralization can also result in changes in the 3D structure of the protein and affects the spatial orientation in solution and the degree of thermal entropy required to achieve molecular stability (Tripathi, 2015; Watt, 2007). The IEP of BSA in aqueous solutions have previously been reported to vary (Barbosa, 2010; Y. Li et al., 2008), mostly from ~4.2 to 5.7. The variation in the IEP values is due to potential interference with native ionic groups associated with the buffer environment, the use of different measurement techniques, and physicochemical conditions of the buffer/protein system in terms of purity, temperature and ionic conductivity (Salgin, 2012). At pH 4, the average hydrodynamic size of BSA molecules peaked at 58.2 nm due to the

close proximity to the IEP of BSA, resulting in increased protein-surface interactions, reduced repulsive interaction between protein molecules and increased hydrodynamic size (Barbosa, 2010; Jun, 2011; Y. Li et al., 2008). Under this condition, the protein conforms to a characteristic slow migration nature with a higher protein maximum dimension and asymmetry (Barbosa, 2010; Cao, 2013). BSA has been reported to have various pH-dependent conformations and its normal form is in the pH range 4.5 to 7.0 (Barbosa, 2010). At pH 7, BSA showed a maximum size of 229.5 nm. This protein size enlargement of more than 25% is due to the introduction of large surface charge density of the protein molecule with increased hydrophobic interactions and intra-molecular repulsion, resulting in unfolding of the protein tertiary structure and irreversible protein aggregation (Barbosa, 2010; Jun, 2011). Further increase in pH showed basic conformational transition of BSA molecules that normally occurs between pH 8 to 9. Consequently, the protein loses rigidity and affects the amino-terminal and ligand binding regions (Barbosa, 2010; Cao, 2013). Around pH 10, BSA will gradually transit into aged forms with reduced tertiary contacts, and then become cleaved at pH > 10.5 (Cao, 2013). The average hydrodynamic size of BSA increased slightly as pH increased. This is expected as at low pH, BSA biomolecules are coil-like and are slowly converted into hard spheres as pH increases (Y. Li et al., 2008). Zeta potential measurements indicate biomolecular stability facilitated by the degree of repulsion between adjacent molecules in a dispersion (Salgin, 2012). The surface charge and stability of protein molecules are influenced by pH due to amino acid dissociation balance (Y. Li et al., 2008). The results showed that BSA demonstrated positive zeta potential at low pH, and decrease from +12.90 mV to -22.80 mV with increasing pH from 3 to 11. This decrease in zeta potential is due to charge deprotonation with increasing hydroxide ion concentration. Zeta potential of proteins is generally affected by molecular denaturation, aggregation, conformational structural changes, and surface modifications (Barbosa, 2010).

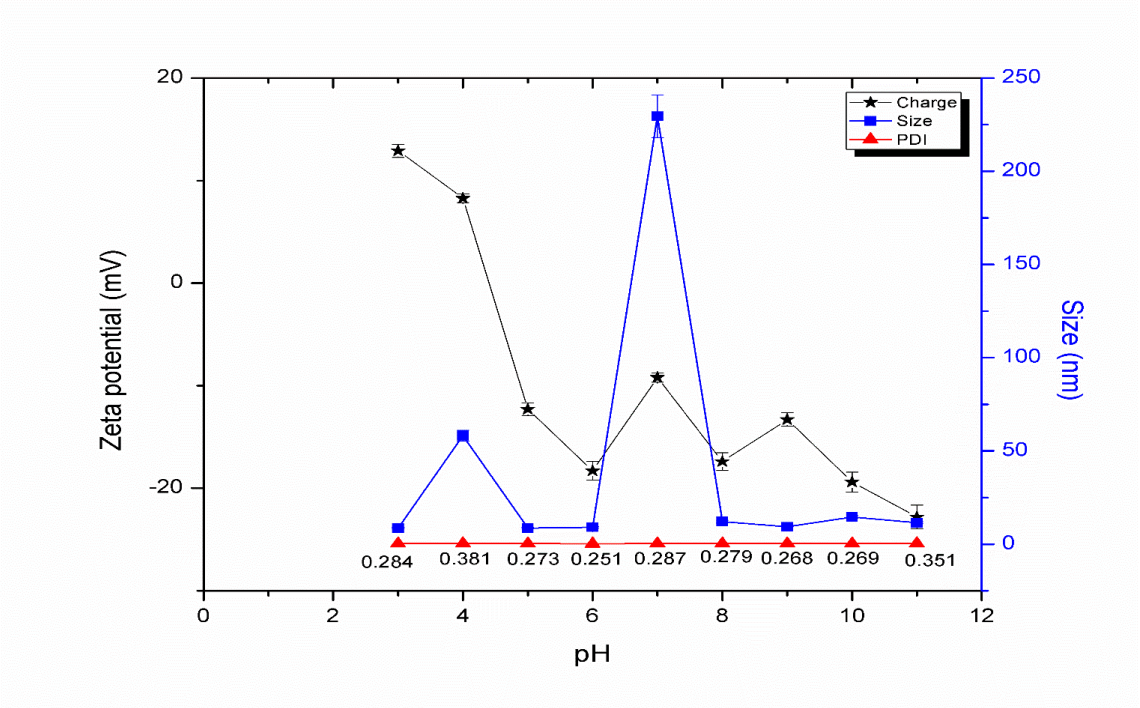

Figure 4.5: The average D[4,3] hydrodynamic size and zeta potential of BSA under varying pH conditions.

4.3 EFFECT OF pH ON THE HYDRODYNAMIC SIZE AND SURFACE CHARGE OF THROMBIN-SPECIFIC DNA APTAMER

As shown in Figure 4.6, changing the medium pH from 3 to 9 steadily increased the electronegativity of the thrombin-binding aptamer from -5.97 mV to -12.5 mV with a significant increase to -20.8 mV at pH 10 and -38.5 mV at pH 11. The average D[4,3] hydrodynamic size of the aptamer was lowest at pH 3 (239.8 nm) and pH 11 (291.0 nm), potentially due to denaturation of DNA. The isoelectric point (IEP) of the aptamer was determined as 2.41. Hence, for *in vivo* applications and drug delivery, the net surface charge of the aptamer is negative. The thrombin-specific binding aptamer used in this work is a short DNA oligonucleotide, and demonstrates fairly stable surface charge and average hydrodynamic size characteristics over a broad pH range from ~4 to 9 according to Figure 4.6. DNA aptamer is made up of hydrophobic purines and pyrimidines which are water-insoluble at around pH 7. However, under moderate acidic or alkaline medium conditions, the surface charge of the purines and pyrimidines groups are altered to enhance

solubility in aqueous systems through hydrolysis of DNA phosphodiester bonds. The degree of hydrolysis and the potential effect on DNA solubilization is minimal around pH ~7. Under extreme alkaline pH conditions, high concentrations of hydroxide ions are present in the media, resulting in a nucleophilic attack of the aptamer phosphorus moieties and eventual hydrolytic cleavage of phosphodiester bonds. Consequently, the DNA oligonucleotide is degraded or denatured into smaller DNA fragments and this explains the reduced hydrodynamic size of the aptamer at pH 11. The size of the aptamer was also small under extreme acidic pH of 3. Strong acidic conditions can lead to purine protonation as well as cleavage of DNA β-glycosidic bonds between purine bases and phosphodiester bonds into nucleotides and nucleosides (Gates, 2009). The variation in polydispersity index with pH change is due to the relationship between electronegativity, surface charge stability and overall impact on homogeneous molecular aggregation. Polydispersity indices under alkaline conditions were generally higher than those of acidic conditions. This is due to increasing electronegativity of the aptamer molecules and associated intermolecular repulsion, resulting in the generation of more stable and uniform individualized molecules with reduced tendency to form aggregates having a non-uniform size distribution.

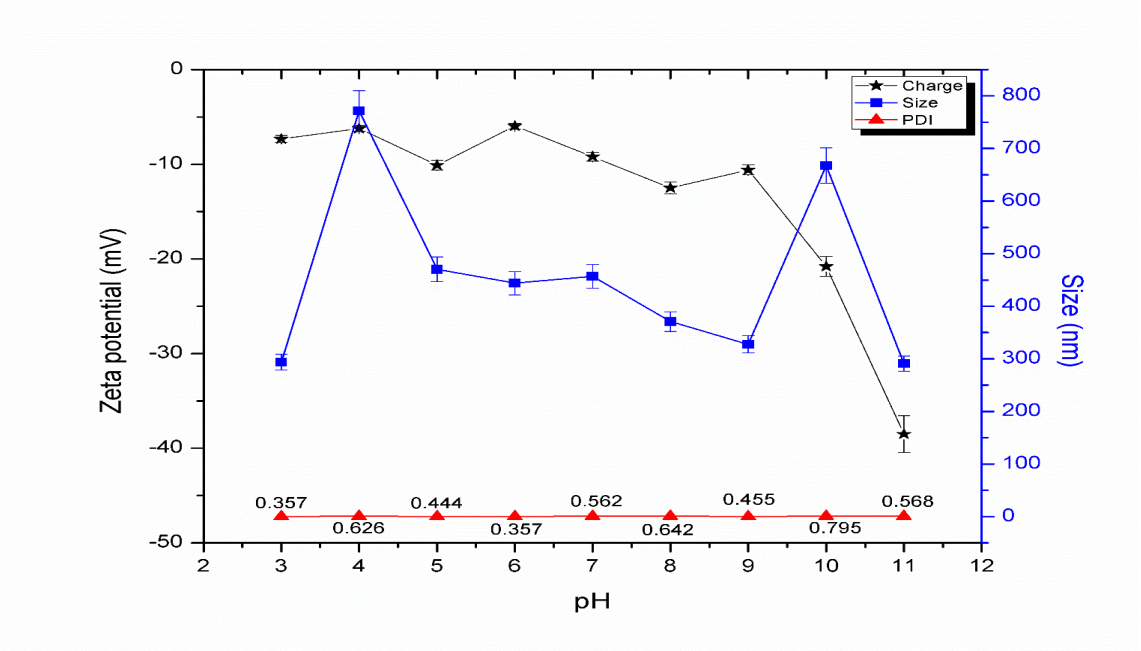

Figure 4.6: The average D[4,3] hydrodynamic size and zeta potential of thrombin-specific DNA aptamer under varying pH conditions.

4.4 LAYER-BY-LAYER DLS ANALYSIS OF DPAP PARTICULATE SYSTEM

4.4.1 Layer-by-layer hydrodynamic size analysis of DPAP formulation

Dynamic light scattering (DLS) analysis using Malvern Zeta-sizer Nano was conducted to investigate the zeta potential, hydrodynamic size distribution and the colloidal stability of the different layered compartments of the DPAP system as well as cumulative effects on the biophysical properties on the final DPAP formulation at pH 7. The DLS data is important to probe the unique biophysical characteristics of each layered compartment and how that changes during synthesis and contributes to the overall characteristics features of DPAP micro-particles. The D[4,3] average hydrodynamic diameter of the inner DP particulate layer was 1059 nm, representing an increase from 229.5 nm for naked BSA upon successful encapsulation of BSA by PLGA polymeric particles. In w/o/w double emulsion with ultrasonication method, the dissolved water-soluble BSA in aqueous phase is mixed and dispersed in the organic phase containing PLGA solution in acetone (polymeric matrix). And, followed by the emulsification and solvent evaporation process under appropriate stress mixing parameters to produce solidified DP complex via phase separation (Makadia & Siegel, 2011). Hence, electronegative BSA molecules were confined successfully within a positively charged PLGA polymeric shell core via absorption and intermolecular electrostatic interactions amongst them, corresponding with the increase in hydrodynamic size of DP formulation. The size of these emulsified particle droplets can be altered by different stirring rate and temperature. The average hydrodynamic size of DP increased to 1318 nm after EDC/NHS coupling and surface modification reaction, with the slight increase resulting from the addition of carboxylic functional groups onto the DP particle surface. After EDC/NHS coupling reaction, the pH of the DP solution was adjusted to ~2.7 in order to activate the surface charge of DP particles for enhanced electrostatic conjugation of the aptamer molecules onto the DP-EDC/NHS layer. DLS results in Table 4.1 indicated that both EDC/NHS coupling and pH adjustment did not significantly alter the hydrodynamic size of DP particles. The hydrodynamic size of the formulation reduced to 1217 nm after successful conjugation of aptamer molecules onto the surface of DP particles to form DPA particulate system. This

hydrodynamic size reduction is due to electrostatic interactions between negatively charged aptamer molecules and positively charged DP particles, resulting in partial condensation of the particulate system. DLS analysis of the final DPAP formulation supported successful intercalation of PEI on the outer aptameric membrane of the DPA micro-environment to form DPAP formulation. This is due to the significant reduction in size of the DPAP formulation; from 1217 nm for DPA to 685.6 nm for DPAP. This demonstrates that the outmost cationic PEI polymeric layer electrostatically interacted with and the condensed negatively charged DNA aptamer, resulting in the formation of stable intercalated polyplexes. Furthermore, the negatively charged DNA aptamer facilitated the stabilization of the PEI polymeric layer by creating a surface network configuration with reduced positive charges to generate particulate formulation with improved size homogeneity.

Table 4.1: The D[4,3] hydrodynamic size of individual layers of DPAP formulation

Individual Layer of DPAP	**Average of Z-Ave (d.nm)**	**Average of PdI**	**Average of Zeta Potential (mV)**
D	230 ±35SD	0.287±0.039SD	-11.000
DP	1059±134SD	0.601±0.009SD	-10.200
DP after EDC/NHS coupling	1318±57SD	0.624±0.023SD	-9.350
DP at pH 2.7	1488±106SD	0.429±0.026SD	+4.210
DPA	1217±285SD	0.683±0.088SD	-8.390
DPAP	686±375SD	0.489±0.092SD	+0.820

4.4.2 Layer-by-layer zeta potential characterization of DPAP particulate system

Zeta potential is an important parameter to investigate the stability of a colloidal particulate formulation. Based on the data obtained from DLS analysis in Figure 4.7, the naked BSA protein was highly electronegative with a zeta potential of -11 mV. After encapsulation with PLGA, the zeta potential of DP particles charged to -10.2 mV, demonstrating that PLGA electro-potential activity is largely neutral, hence, conferred no significant alteration to the electronegativity of BSA. The zeta potential of DP increased

to +4.21 mV after surface charge modification with EDC/NHS at pH 2.7. This surface modification strategy enabled effective conjugation of aptamer molecules onto the DP particles by neutralizing additional negatively charged surface moieties resulting from the conjugation of carboxylic groups to the terminal end of PLGA (L. Li et al., 2014). This pH adjustment through protonation was essential to reinstate positively charged surface characteristics for aptameric binding. With the introduction of the aptamer, the zeta potential decreased from +4.21 mV to -8.39 mV, indicating effective conjugation of the aptamer onto the surface of DP particles to form a negatively charge DPA system. The surface charge of the final DPAP formulation became positively charged with a zeta potential of +0.82 mV after complexation with the outer most layer made of hydrophilic PEI intercalated into the aptamer anchors. With the aptamer intercalated within the outer PEI molecular complex, electrostatic repulsive forces between the aptamer and the target cell membrane surface can be reduced significantly to facilitate improved target cell interactions, membrane permeation and endocytosis. DPAP formulation represents a molecularly engineered multifunctional particulate system consisting of a targeting element (an aptamer), active protein drug molecules, and a positively charged outer layer to enhance electrostatic interactions with negatively charged target cells and thus, improve targeted drug delivery.

DPAP formulation is a co-polymeric (PLGA and PEI) system harboring DNA aptamer and BSA molecules in different compartments. The co-polymeric nature and layered conjugation assembly of the drug and ligand molecules of DPAP endows it with multifunctional features for enhanced drug encapsulation, site targeting, and controlled drug release kinetics of active molecules. This makes it superior to other existing single polymer formulations in term of size, zeta potential colloidal particulate size and charge stability, cell transfection, drug and DNA aptamer payload capacity, and drug release profile. PLGA is highly recommended as pharmaceutical delivery carrier due to its high drug encapsulation efficiency; modifiable particle size to harbor molecules of different sizes and shapes; FDA-approved clinical safety; and pH-sensitive endosomal degradation. Polycationic PEI is a well-known non-viral transfection agent that entraps and condenses negatively charged aptamer in order to reduce target cell membrane electrostatic repulsions, leading to enhanced drug uptake into target cells and transfection efficiency

for better therapeutic indices. The proton sponge effect of PEI facilitates endosomal release of entrapped content into cytosol and delivers drugs towards nucleus via active transport (Benjaminsen, 2013). The presence of PEI polymeric layer helps to overcome initial burst release of BSA-encapsulated PLGA for prolonged drug release. Subramanian et al. (2015) reported the use of PEI as an efficient gene carrier to reduce tumor cell proliferation due to its capability in DNA condensation, non-mutagenic feature, low systemic cytotoxicity and good transfection efficiency at low concentrations.

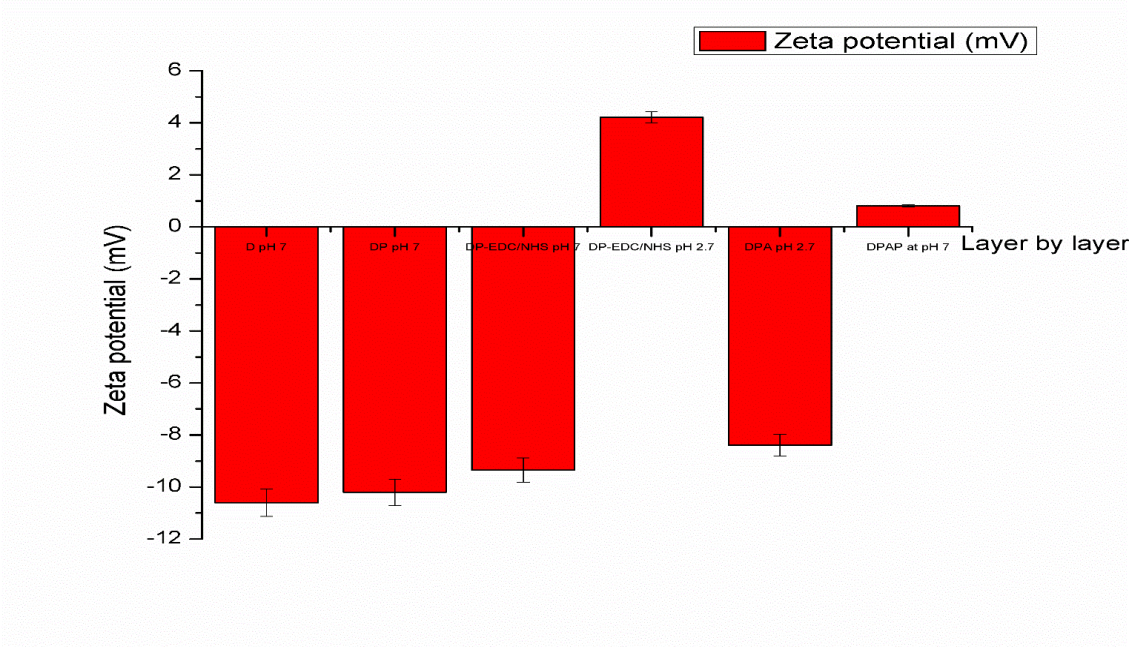

Figure 4.7: Zeta potential data of individual layers in DPAP formulation. The different layers are DP, DP-EDC/NHS, DPA and DPAP.

4.4.3 Effect of pH on the hydrodynamic size of DP, DPA and DPAP formulation

Figure 4.8 shows increasing average D[4,3] hydrodynamic size of DP from 959.5 nm to 1220 nm over the pH range 3 – 7, and decreased sharply to 671.6 nm at pH 8, and remained in this region from pH 9 to 11. The result demonstrates that DP particles maintain the highest average hydrodynamic size at pH close to neutrality. The hydrodynamic size is low under high acidity and alkalinity when excess OH^- and H^+ ions interfere with the structural stability or the electrostatic binding equilibrium of BSA within the PLGA matrix. Figure 4.9 shows DP formulation is positively charged under acidic pH conditions of 3 and 4. Under these conditions, the degree of inter-particulate electrostatic repulsion

between DP particles is maximal due to high electropositivity from protonation ($DP^+ < // > H^+$), resulting in reduced surface charge compatibility for agglomeration. On the other hand, extreme alkali conditions produce excess OH^- ions which endow DP particles with a net electronegative charge through deprotonation, facilitating inter-particulate repulsion between negatively charged DP particles ($DP^- < // > OH^-$). DP particles possess reduced average hydrodynamic size under high alkaline conditions, and this is as a result of hindered agglomeration by electrostatic repulsion. At extremely high pH of 11, DP displayed a positive charge with reduced hydrodynamic size, potentially due to structural degradation under extreme alkaline conditions.

The average hydrodynamic size of DPA particles was consistent within the narrow range 976.7-1197 nm at pH 3 and 6-10 as there was no charge accumulation to alter the conformation and bonding structures within DPA formulation (Tripathi, 2015). The significant charge stability of the outer aptameric layer of DPA enables conformational rigidity over a wide pH range. From the zeta analysis, the IEP of DPA was determined as pH 4.75. Accordingly, the average hydrodynamic size of DPA peaked at pH 4 and 5 (1670 nm and 755.6 nm respectively) due to the close proximity to the IEP, resulting in reduced intermolecular repulsion, and increased hydrophobicity and aggregation of particles (Jun, 2011; Salgin, 2012). The highest hydrodynamic size of DPA obtained was 2204 nm at pH 11, and this can be attributed to the presence of high surface charge density under extreme alkaline environment, causing strong repulsive forces and hydrophobic attractions, affecting the DPA structures and resulting in coalescence of new conformants from DPA structural deformation.

Figure 4.8 shows that under extreme acidic and alkaline conditions, DPAP formulation displayed low average hydrodynamic sizes of 519.2 nm, 324.2 nm, 559.1 nm at pH 3, 10 and 11 respectively. This is due to the presence of excess OH^- and H^+ ions which alter the surface charge of DPAP formulation, leading to hydrolytic cleavage of DPAP particulate bonding structures including hydrogen bonding, electrostatic interaction, covalent bonding, and Van der Waals interactions. The average size of DPAP micro-particles was constant within the range 685.6-780.8 nm over pH 5 to 8, representing a significant

biophysical stability of DPAP particulate system at pH close to neutral, and this is certainly advantageous to *in vivo* clinical applications.

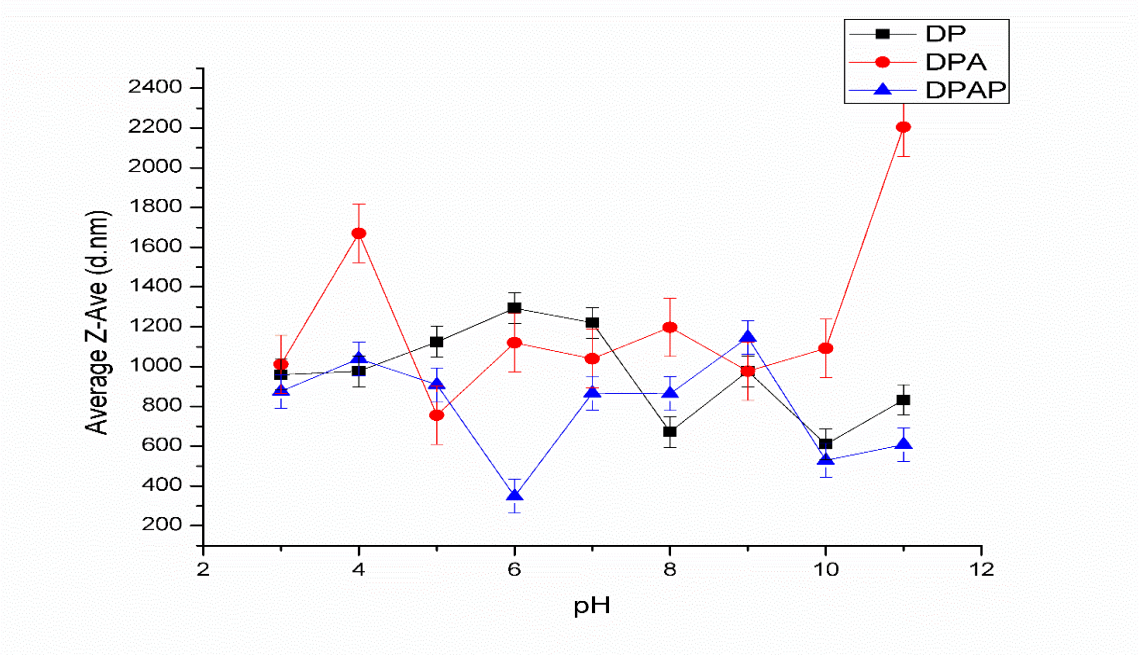

Figure 4.8: D[4,3] average hydrodynamic size of DP, DPA, and DPAP formulation over the range of pH 3-11.

4.4.4 Effect of pH on the zeta potential of DP, DPA and DPAP formulations

The effect of pH on the surface polarity and size distribution of a colloidal formulation can be attributed to the degree of charge stabilization in response to protonation and deprotonation. DLS analysis data in Figure 4.10 shows that the electronegativity of DP increased gradually with increasing pH from pH 3 to 11, except at pH 7 and pH 11 with zeta potentials +0.0181 mV and +0.0391 mV respectively. DLS analysis showed the isoelectric point (IEP) of DP formulation as pH 3.63. IEP addresses the pH condition where excess electrical charge density and intermolecular electrostatic repulsions of the molecules are lowered to zero, leading to stronger inter-chain aggregation amongst molecules. DP formulation showed increasing electronegativity with increasing pH gradient due to charge deprotonation phenomenon under high OH^- conditions. Excess OH^- ions bound and interact with DP particle surface to form an electronegative layer. At neutral pH 7, DP showed a positive zeta potential close to zero. This is due to the lack of

extra OH- or H+ ions to cause deprotonation or protonation. Under this condition, surface charge activation for solubilisation and hydrolysis is minimal.

Zeta potential measurements for DPA showed increasing electronegativity +5.67 mV to -11 mV over the pH range 3 to 11. The IEP of DPA was determined as 4.75. As the medium increases in alkalinity, DPA particles lose H^+ ions due to deprotonation, resulting in increasing electronegativity of the DPA system. DPA possessed a positive surface charge at pH 3 as a result of protonation of the electronegative aptameric exterior. DPA particles showed an electronegative surface charges at pH 7 due to the anionic characteristics of the conjugated aptamer molecules onto the DP outer layer. The alternating degree of electronegativity with increasing pH could be due to surface redistribution of ionic species to maintain biophysical stability of the complex.

Figure 4.10 shows the average zeta potential of DPAP reduced steadily from +4.72 mV to -5.94 mV over the pH range 3-11. This can be explained by deprotonation of PEI cationic groups on the DPAP surface layer thus increasing the electronegativity of the DPAP particles. The converse phenomenon explains why DPAP microspheres were positively charged at pH 3 and 4. The low pH conditions enabled protonation of DPAP system, creating a shielding effect with increased positive charge. DPAP was positive at pH 7 with a surface charge of +0.82 mV due to the absence of excess OH^- ions to trigger deprotonation. Positively surface charge of DPAP at pH 7 is important to improve target cell interactions and intracellular uptake of drug ingredients into desired cells. In addition, the IEP of DPAP was determined as 5.59, indicating that the structural conformations and functionality of DPAP can be modified via surface molecular engineering to provide a controlled drug release pattern using a pH-sensitive degradation mechanism under physiological conditions. DPAP system demonstrates desirable features as a potential multifunctional transport vehicle for targeted pharmaceutical delivery.

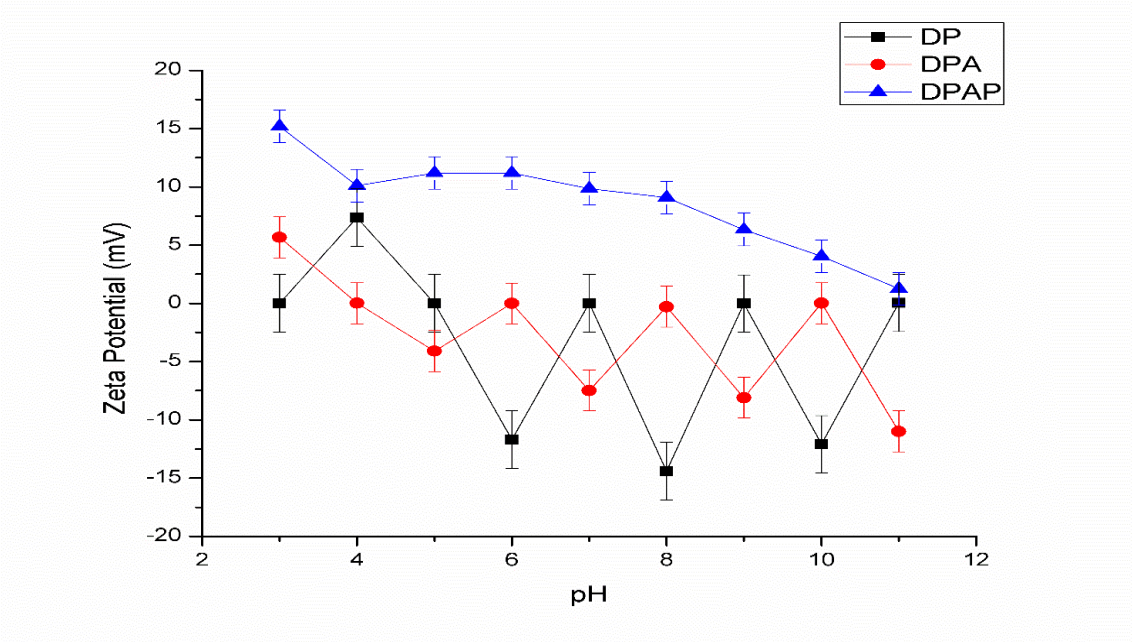

Figure 4.9: Surface charge distribution of DP, DPA, and DPAP formulation over the range of pH 3-11.

4.4.5 Effect of temperature on the hydrodynamic size of DP, DPA and DPAP formulations

Figure 4.10 shows the average D[4,3] hydrodynamic size of DP formulation remained largely the same at 25°C, 30°C, and 42°C with 1129 nm, 1033 nm, and 1048 nm respectively. However, the size of DP increased significantly to 1406 nm at 37°C. High temperature variations can significantly affect the strength of inter-particulate interactions amongst polymeric formulations. It can be inferred that intact polymer chain dynamics and structural bonding of DP micro-particles were not significantly perturbed under ambient temperature conditions between 25°C and 30°C. When the temperature was elevated to 37°C, the average hydrodynamic size of DP particles increased. This can be explained by the increased intra-molecular mobility of DP particles under high thermal flux conditions, boosting their kinetic energy and causing polymer chain stretching in all directions and expansion per unit volume of space. This results in weak intra-particulate attractive forces, forming DP particles with larger diameters (Kim, 2011). It may be deduced that induced diffusion of drug molecules from DP can be triggered under elevated temperature conditions due to hydrolytic phase transition at 37ºC. Notably, a further

temperature increase to 42ºC did not result in average size increase due to complete thermo-molecular hydrolysis of PLGA structures beyond the phase transition temperature. De and Robinson (2004) reported that temperature and particulate size affect the stability of PLGA nano/micro-formulations. Their work is in keeping with our research findings as they established that PLGA micro-particles are more resistant to temperature than PLGA nanoparticles in terms of degree of aggregation. DP micro-particles did not aggregate under high temperatures.

Figure 4.10 shows the influence of DPA average hydrodynamic size on temperature. DPA particles subjected to increasing temperature conditions showed a narrow fluctuating trend in average hydrodynamic size. The narrow fluctuating trend is potentially a reflection of the randomness in the particle surface molecular movements of the conjugated aptamer layer and polymer subunits under high temperature conditions. DPA micro-particles were larger in size than DP micro-particles due to aptamer conjugation, and they demonstrated a lesser degree of sensitivity to temperature variations. DPA formulation showed a higher thermal stability with limited potential for aggregation than DP over the same temperature range, and this is partly due to inter-particle repulsion existing between electronegative DPA aptamer outer layers. Also, DNA aptamer molecules on DPA exterior possess strong phosphodiester backbones that enhance its thermal stability and thus, enabling it to un-anneal/re-anneal repeatedly with increasing temperature.

DPAP formulation maintained a fairly constant average hydrodynamic size in the range of 834.7 – 888.9 nm for 25°C, 37°C, and 42°C, except at 30°C which showed an increment to 1333 nm. The polymeric chain dynamics, particle mobility, hydrophilic and hydrophobic chains, and adhesion strength of DPAP micro-particles were less susceptible to temperature changes. This also supports that DPAP formulation holds a high lower critical solution temperature (LCST) with less dehydration. Hence, DPAP particulate system demonstrated a higher degree of resistance to temperature compared to the others. Figure 4.10 shows the average hydrodynamic size of both DPA and DPAP formulation peaked at 30ºC. This demonstrates that 30ºC is the optimal temperature point which induces polymer aggregation and swelling due increased internal energy, entropy, and energetic interactions as well as higher solution diffused into the formulations (D. Ahmed

& Saeed, 2013; Mondal & Mukherjee, 2008). The significant decrease in the average hydrodynamic size of DPA and DPAP were observed beyond 30ºC, indicating the initiation of polymer hydrolysis which is corresponding with the gradual transition from the bulk polymer swelling phase. Pre and post swelling DPAP particles demonstrated a more consistent average hydrodynamic sizes, allowing DPAP carry and release drug molecules effectively over a wide temperature range in mammalian system.

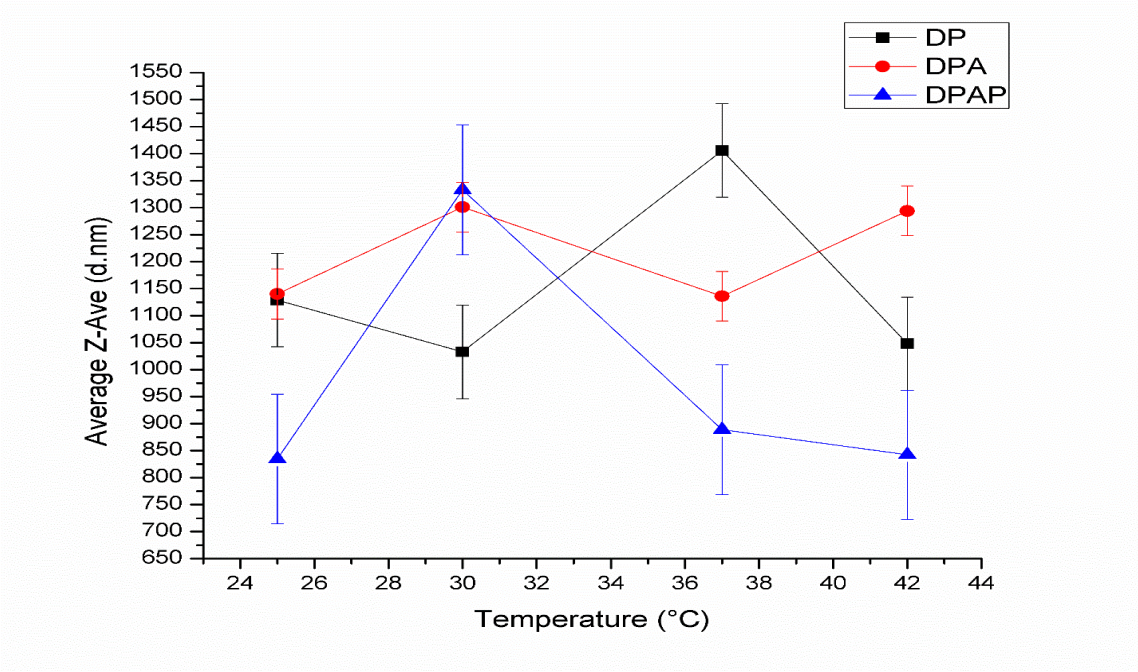

Figure 4.10: Average D[4,3] hydrodynamic size of DP, DPA, and DPAP particulate system under varying temperature conditions of 25ºC, 30ºC, 37ºC, and 42ºC.

4.4.6 Effect of temperature on the zeta potential of DP, DPA and DPAP formulations

Temperature is a critical parameter in examining the stability of polymeric drug formulations. It is also important to understand potential changes in drug release kinetics under varying temperature conditions in response to variations in body temperatures from patient to patient. DLS analysis was used to study the effect of varying temperatures on the surface charge and stability of DP, DPA, and DPAP formulations at a constant pH of 7. Figure 4.11 shows DP remained electronegative at temperatures 25°C, 30°C, 37°C, and 42°C with zeta potentials of -6.15 mV, -6.93 mV, -9.48 mV, and -8.61 mV respectively. This indicates that the surface electrical charge density and ionization of DP micro-

particles at pH 7 are not influenced by temperature. Minor differences in the zeta potential values could be attributed to induce stretching of surface molecules and/or molecular re-arrangements in response to increasing thermal flux. DPA micro-particles possess similar zeta potential values at temperatures 25°C, 30°C, 37ºC and 42°C with surface charges -7.01 mV, -7.76 mV, -9.27 mV, -9.21 mV respectively. This indicates that the electronegativity of the aptameric outer surface offered sufficient stability over the temperature range investigated. DPAP particulate system maintained a positive charge over the range of temperature investigated with +4.95 mV for 25°C, +4.34 mV for 30°C, +6.88 mV for 37°C, and +5.11 mV for 42°C. The data generally indicates DP, DPA and DPAP are stable under temperature conditions within the range 25-42°C. The electropositive nature of DPAP was preserved under elevated temperature conditions, demonstrating its capacity to maintain surface charge characteristics for effective transfection efficiency and cellular uptake for patients with slightly higher or lower body temperatures.

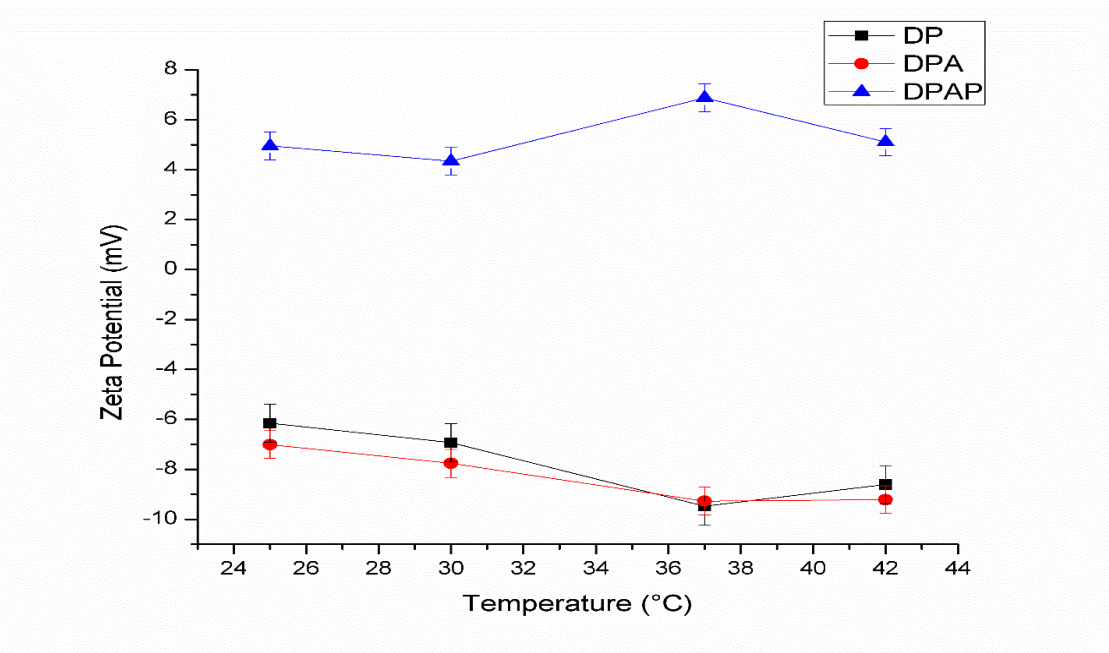

Figure 4.11: Surface charge stability of DP, DPA, and DPAP particulate systems under varying temperature conditions of 25ºC, 30ºC, 37ºC, and 42ºC.

4.5 BIOPHYSICAL CHARACTERIZATION OF DPAP PARTICULATE SYSTEM

The BSA loaded PLGA-Aptamer-PEI particulate system was formulated by water-in-oil-in-water (w/o/w) double emulsion method integrated with sonication. The D[4,3] average diameter of the DPAP particles was 0.686 µm with a zeta potential was +0.82 mV. The average particle size of the formulation is essential to promote effective DPAP-cell membrane surface interaction and intracellular trafficking. The measured average particulate size of the DPAP formulation is within the range effective to increase *in vivo* half-life of both drug and aptamer (Aravind, Jeyamohan, et al., 2012) and also prevent aptamers and drug-loaded polymeric particles from systemic clearance and rapid renal filtration, which is typically challenging for small size biomaterials with molecular weights within the range of 30 – 50 kDa (Lakhin et al., 2013; Wengerter, 2014). Compared to nanoparticles, microparticles are easier to be phagocytized by human phagocytic immune cells in vaccine delivery applications (Nguyen et al., 2008; Putnam, 2006). The low electropositive potential of the DPAP formulation is result of the intercalation between the aptamer and the PEI system and this is necessary to enhance cell membrane interactions whilst simultaneously enabling specific targeting of disease cells for endocytosis.

Figure 4.12 shows the particle size distribution of the DPAP formulation with a z-average of 685.5 nm. The distribution shows two different peaks: peak 1 with 593.4 nm size, 92.7% intensity and 265.6 nm standard deviation; and peak 2 with 5368 nm size, 7.3% intensity and 329.6 nm standard deviation. The high peak 1 intensity of 92.7% demonstrates that the size distribution of DPAP is largely unimodal. The emergence of peak is highly due to agglomeration of DPAP particles facilitated by inter-particulate collision of DPAP droplets during solvent evaporation. The distribution also showed a polydispersity index of 0.49, indicating a narrow size distribution of the formulation. The polydispersity index also shows desired levels for improving drug delivery efficiency in term of tissue distribution and blood circulation duration (M. Alibolandi et al., 2015).

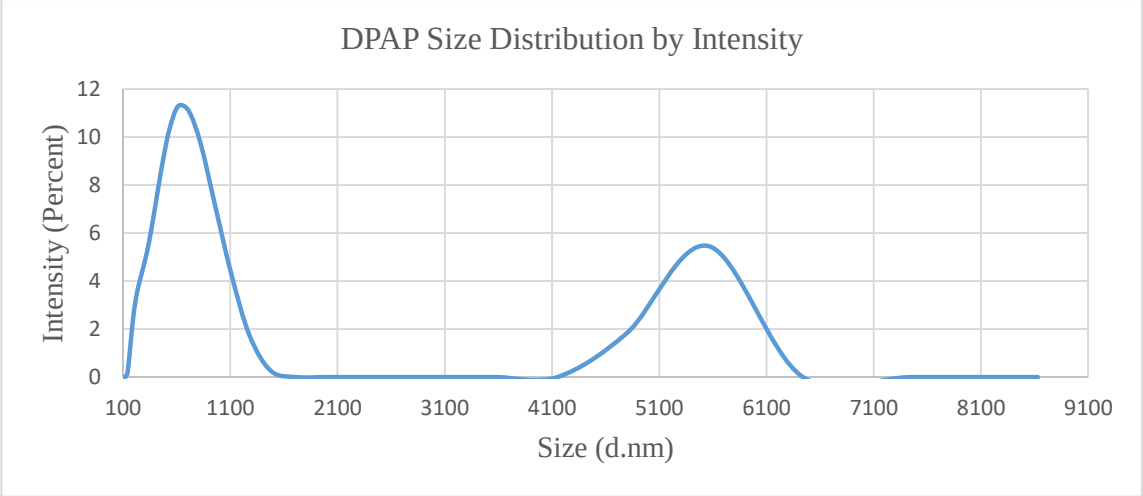

Figure 4.12: Particle size distribution data for DPAP formulation at pH 7

The morphological characteristics of DP and DPAP micro-particles were investigated via SEM and TEM analyses. The micrographs showed the shape of both DP (Figure 4.13 and 4.15(a)) and DPAP (Figure 4.14 and 4.15(b)) micro-particles were spherical with moderately rough surface features and small particles pore to improve cell-particle interactions. DP and DPAP particulate systems showed uniform dispersion. The average particle size of DP ranged from 279 nm to 1200 nm whilst DPAP was between 860 nm and 1300 nm based on TEM and DLS analysis. The microsphere morphologies of DP and DPAP formulation were similar, and this demonstrates that the incorporation of PEI did not significantly change the surface properties of DP particles. TEM images in Figure 4.15 reveals that the particle size and volume of DPAP were significantly larger than DP, indicating successful conjugation of DNA aptamer onto DP surface and PEI intercalation on the outermost layer. The average particle size of DPAP, which is < 2 µm, would facilitate a significant number of internalized DPAP particles into target cells to improve drug delivery due to its effective surface area for phagocytosis and endocytosis (Pacheco, 2013). Particle size and shape play a significant role in formulating and delivering drugs to target cells for improved transfection and enhancing therapeutic efficiency. Microparticle formulations have been reported to protect DNA aptamers from endonuclease-mediated degradation, kidney filtration, and also provide an efficient delivery of aptamers to target cells (M. Alibolandi et al., 2015; Balashanmugam et al., 2014). The rough surface morphology of DPAP is important for effective surface

modifications, making it easy for conjugation with other targeting elements and biomarkers to enhance transfection (Balashanmugam et al., 2014).

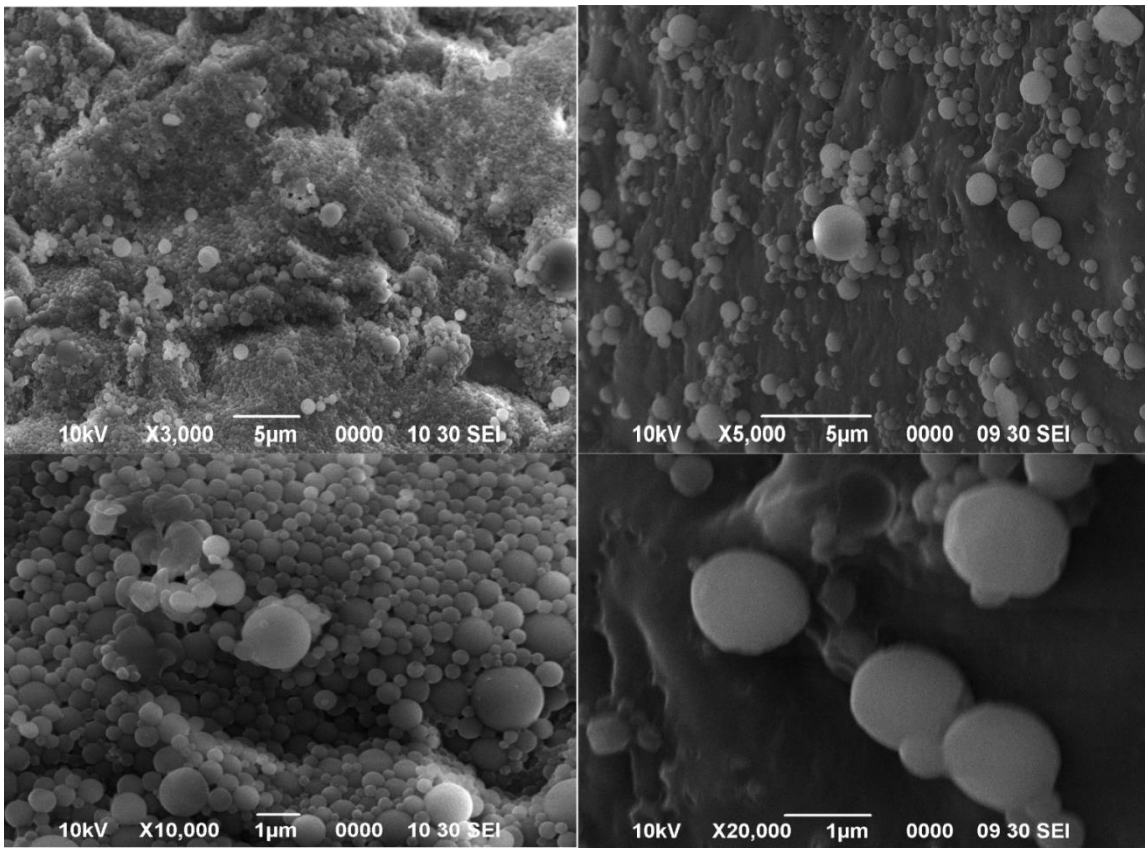

Figure 4.13: SEM analysis of BSA-encapsulated PLGA (DP) formulation showing moderately rough surface features. SEM analysis was performed at 10 kV over a magnification of x3000 to x20000

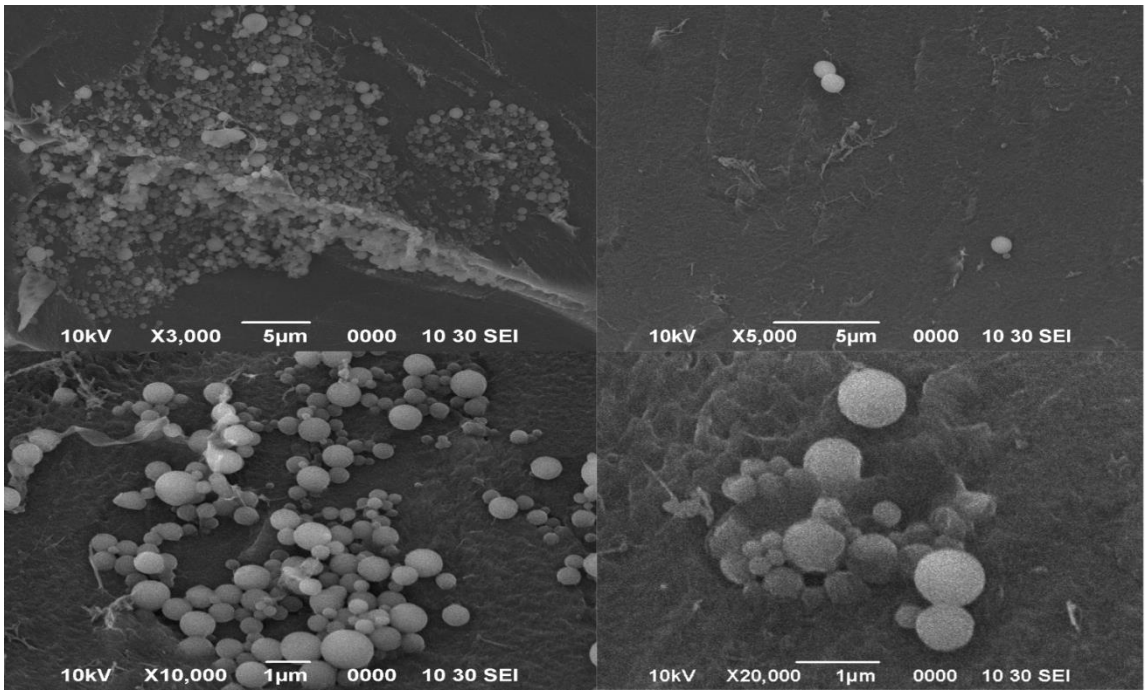

Figure 4.14: SEM analysis of BSA-encapsulated PLGA-Aptamer-PEI (DPAP) formulation showing moderately rough surface features. SEM analysis was performed at 10 kV over a magnification of x3000 to x20000

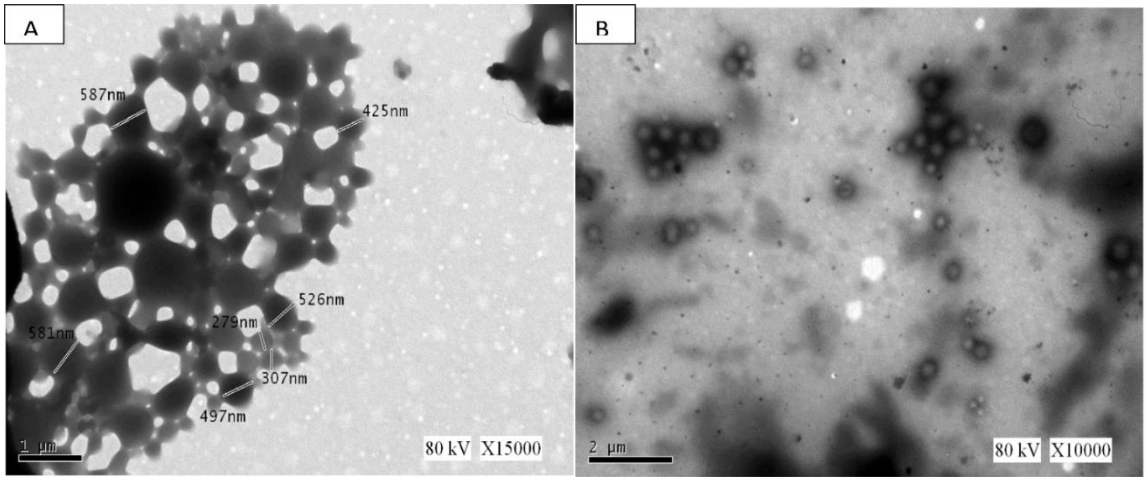

Figure 4.15: TEM analysis of (a) DP and (b) DPAP particulate formulation showing microparticle size of < 2 µm which is suitable for improved internalization of particles into target cells. TEM analysis was performed at 80 kV with magnifications of (a) x15000 and (b) x10000

4.6 FUNCTIONAL GROUP CHARACTERISATION OF DPAP PARTICULATE SYSTEM

FTIR analysis was used to investigate the structural characteristics, chemical composition and functional groups present in the DPAP formulation. This analysis was important to identify potential in-process molecular derivatization of active moieties associated with the biopolymers during formulation. The FTIR transmittance spectra in Figure 4.16 identifies functional groups within the wave number range 3900 to 500 cm^{-1}. The spectra indicates the presence of carbonate esters, pyroles, hydrocarbons and alcohols. The peaks at 2940.17 cm^{-1}, 1419.62cm^{-1}, 1663.09cm^{-1}, 3278.17cm^{-1} and 1237.31cm^{-1} wave numbers correspond to the presence of N-H (stretching), N-H (bending), NH-C=O (amide), O-H, and O=C=O carboxylate groups. The presence of primary aliphatic alcohol functional group originated from PLGA segments which consist of methene, methyl and methane proton (Stevanovic et al., 2008). Alphatic carbonate ester groups also originated from PLGA through the formation of ester linkages between PLGA monomers that resulted in the generation of aliphatic polyester (Lanao, 2013).(Lanao, 2013) The aliphatic hydrocarbons demonstrate repeated units of PEI polymer, indicating the presence of PEI polymeric particulate within the DPAP system (Ma, 2016).

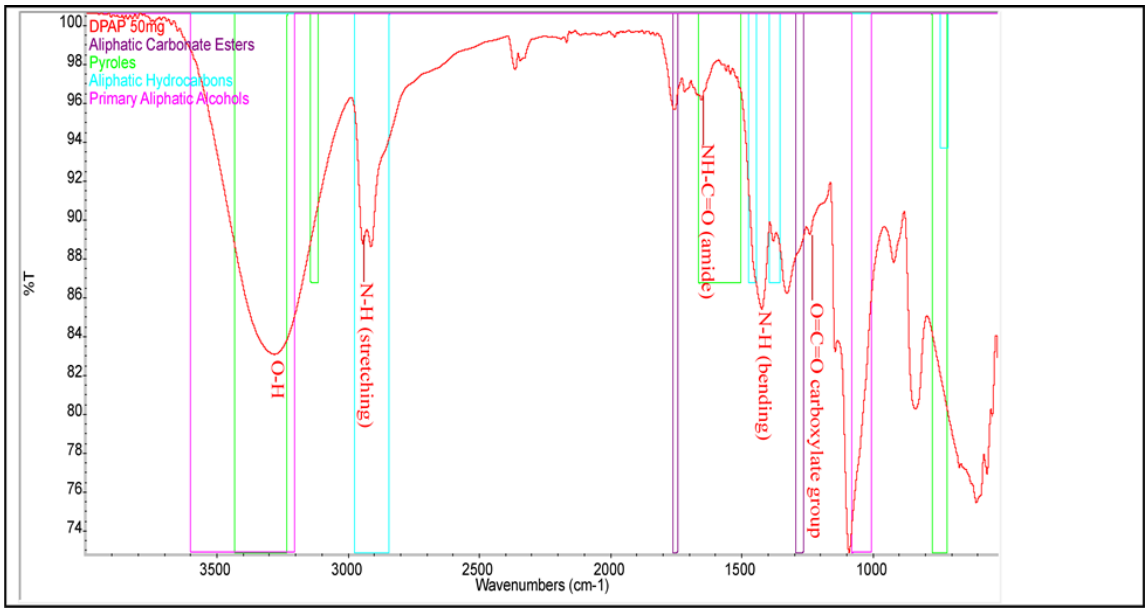

Figure 4.16: FTIR transmittance spectra of DPAP particulate system showing the presence of aliphatic carbonate ester groups, pyroles, aliphatic hydrocarbons and primary aliphatic alcohols

4.7 EFFECT OF pH ON THE BIOPHYSICAL CHARACTERISTICS OF DPAP FORMULATION

The isoelectric point (pI) of the DPAP particulate formulation, determined using DLS analysis, was pH 5.59, indicating that both the structure and functionality of DPAP formulation can easily be engineered for controlled drug release applications via pH-induced degradation under *in vivo* physiological conditions in mammalian systems. Thus, the DPAP formulation shows potential as a multifunctional particulate vehicle for controlled release of drug molecules to targeted sites. Figure 4.17 generally shows decreasing zeta potential of DPAP from +4.72 to -5.94 mV with increasing pH. However, at pH 7, the DPAP particles demonstrated a positive surface charge with a zeta potential of +0.82 mV. The positive zeta potential is necessary to facilitate targeted cell adhesion and intracellular uptake for delivering sufficient drug dosage to relevant sites under *in vivo* conditions. The study further demonstrated that higher pH conditions significantly reduce the surface charge of DPAP, making it more electronegative. The presence of OH^- ions enables interactions with H^+ ions of DPAP particles in a neutralization process called deprotonation. The loss of H^+ ions increases the electronegativity of DPAP particulate formulation. At pH 7, the surface charge of DPAP particles remained unchanged since no excess OH^- ions were present to trigger deprotonation. The converse phenomenon explains why DPAP formulation demonstrated a positive surface charged at pH 3 and 4. The presence of excess H^+ ions under low pH conditions enables interactions with OH^- ions of DPAP in a protonation process, resulting in the formation of positively charged DPAP particulate system. Figure 4.17 also shows that under extreme acidic and alkaline conditions, the average hydrodynamic size of DPAP particulate formulation displayed the lowest values of 519.2 nm, 324.2 nm, 559.1 nm at pH 3, 10 and 11 respectively. The presence of excess H^+ ions and OH^- ions could induce surface charge alterations of DPAP particles, facilitating the cleavage of DPAP particulate bonding structure including covalent bonding, hydrogen bonding, electrostatic interaction, and Van der Waals interaction. The average hydrodynamic size of DPAP particles formulation was largely constant (685.6 - 780.8 nm) over a pH range of 5-8, indicating the stability of DPAP formulation at neutral and near neutral pH conditions and this is particularly advantageous

for *in vivo* applications. Table 4.2 summarizes the influence of pH on the D[4,3] hydrodynamic size and zeta potential of encapsulated molecules and DPAP formulation.

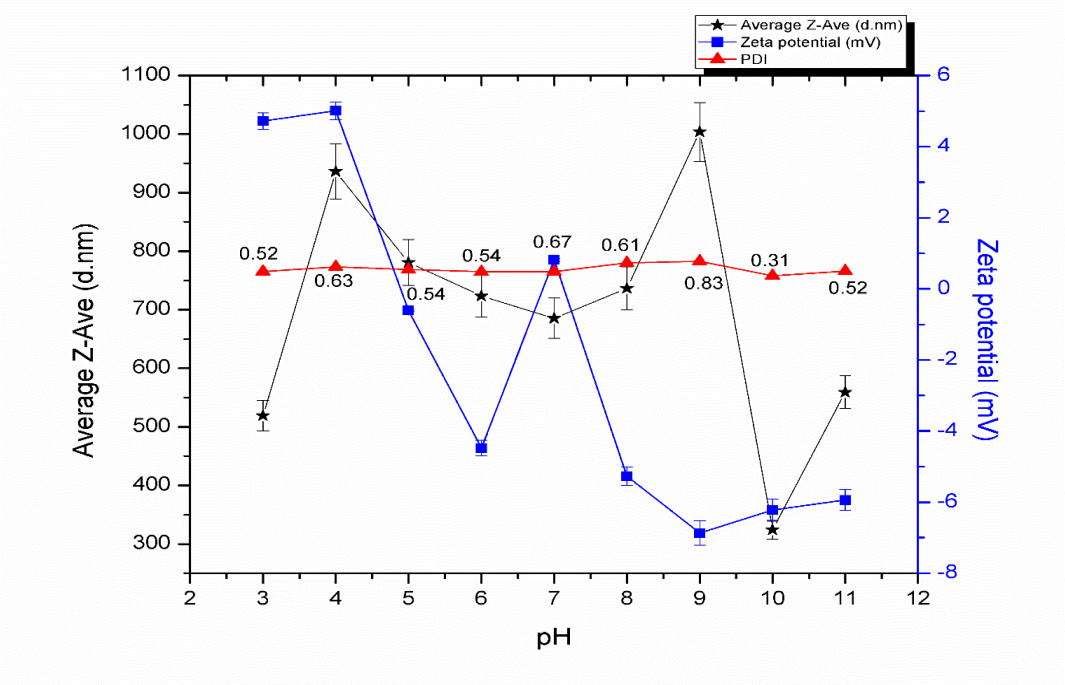

Figure 4.17: Effect of pH on the D[4,3] hydrodynamic size and surface charge of DPAP formulation. Conditions of pH investigated ranged from 3 to 11

Table 4.2: DLS analytical data of BSA protein, DNA aptamer, and DPAP formulation under varying pH

pH	Sample	Average of Z-Ave (d.nm)	Average of PdI	Average of Zeta Potential (mV)
3	BSA protein	8.65	0.28	+12.90
	DNA aptamer	293.80	0.36	-7.33
	DPAP formulation	519.20	0.49	+4.72
4	BSA protein	58.20	0.38	+9.27
	DNA aptamer	771.70	0.63	-6.22

	DPAP formulation	936.20	0.62	+5.01
5	BSA protein	8.61	0.27	-12.30
	DNA aptamer	470.20	0.44	-10.10
	DPAP formulation	780.80	0.54	-0.61
6	BSA protein	9.12	0.25	-18.30
	DNA aptamer	443.80	0.36	-5.97
	DPAP formulation	723.70	0.48	-4.48
7	BSA protein	229.50	0.29	-9.20
	DNA aptamer	457.00	0.56	-9.20
	DPAP formulation	685.60	0.76	+0.82
8	BSA protein	12.19	0.28	-17.40
	DNA aptamer	370.80	0.64	-12.50
	DPAP formulation	736.60	0.73	-5.27
9	BSA protein	9.32	0.27	-13.30
	DNA aptamer	327.70	0.46	-10.60
	DPAP formulation	1004.00	0.78	-6.87
10	BSA protein	14.58	0.27	-19.40
	DNA aptamer	667.40	0.80	-20.80
	DPAP formulation	324.20	0.37	-6.22

11	BSA protein	11.48	0.35	-22.80
	DNA aptamer	291.00	0.57	-38.50
	DPAP formulation	559.10	0.50	-5.94

4.8 EFFECT OF IONIC STRENGTH

4.8.1 Effect of ionic strength on the size and surface charge stability of DPAP particulate system

Ionic strength measures the total concentration or conductivity of ionic species in a solution. In this work, varying concentrations of NaCl solution were added to DPAP suspensions to increase ionic strength and provide counter-cations and –anions to interact with cationic DPAP. Consequently, the added Cl^- ions interacted electrostatically with positively charged DPAP micro-particles, lowering its hydrophilicity. Figure 4.18 shows that the average D[4,3] hydrodynamic size of DPAP particles increased significantly with increasing ionic strength from 20 mM to 1 M NaCl. With increasing ionic strength, high concentrations of highly electronegative chloride ions bind onto DPAP particle surface, making it more hydrophobic DPAP with a reduced electrical charge for repulsion. This subsequently induces aggregation between neighboring particles, eventually causing more DPAP to coalesce. Na^+ ions provide an electrostatic shielding mechanism to DPAP particles and control cell membrane interactions with DPAP particles. The higher conductivity of the Na^+ medium facilitates stewarded diffusion of drug molecules from the DPAP matrix. Work by Sang et al. (2015) demonstrates that addition of NaCl can enhance the structural stability of polymeric compound and polyplex with large particle sizes for improved transfection efficiency.

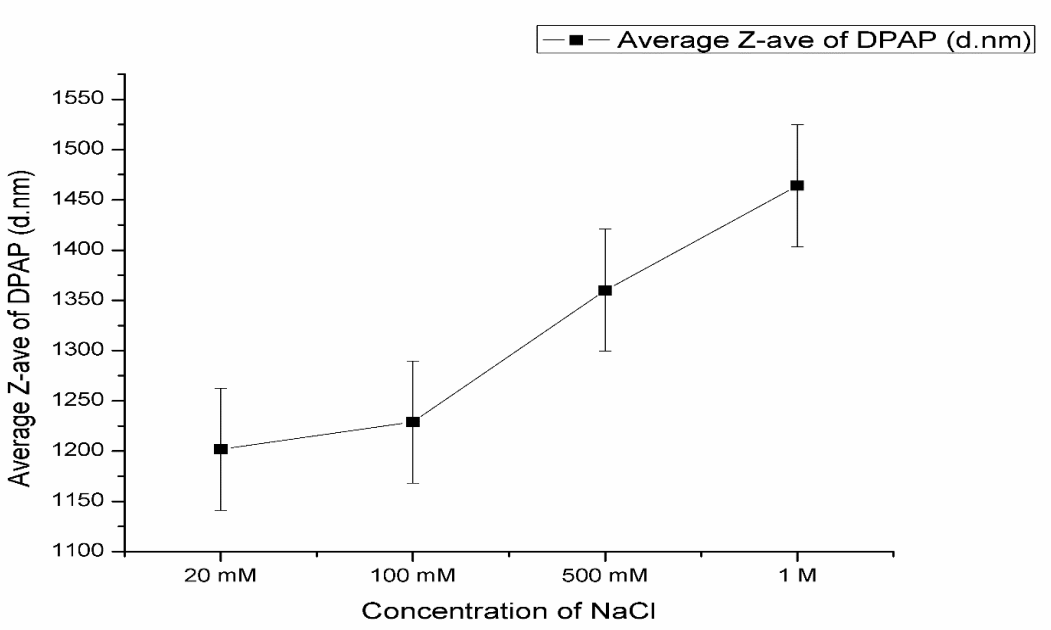

Figure 4.18: Hydrodynamic size stability of DPAP formulation under varying ionic strengths of 20 mM, 100 mM, 500 mM, and 1 M NaCl

DPAP formulation is a pH stimuli-dependent system that receives or releases protons in response to surrounding pH changes. DPAP solubility can be altered by modifying its surface charge characteristics as a result of its polyelectrolytic property. Figure 4.19 shows that DPAP zeta potential is not significantly affected by ionic strength variation between 20 mM and 1 M NaCl. This demonstrates that the characteristic surface charge stability and ionization of DPAP micro-particles were not significantly affected by the presence of Na^+ and Cl^- ions as the zeta potential was maintained in a narrow range from +8.5mV to +10.1mV. The net electropositive zeta potential is due to the Na^+ shielding conformation. The slight fluctuation in the surface charge can be explained by the increasing Na^+ concentration, creating a densed monolayer shielding effect. Further increase in the ionic strength results in Na+ saturation, resulting in some weak cooperative bindings and complex dissociation. This explains the decreasing zeta potential at 1 M NaCl ionic strength. The experimental results strongly support that the surface of DPAP particulate system is positively charged due to the intercalation of cationic PEI as the outer layer of DPAP formulation, potentially resulting in effective electrostatic interaction with desired cell membranes, improved internalization, higher transfection efficiency and cellular uptake of active ingredients for better intracellular therapeutic indices.

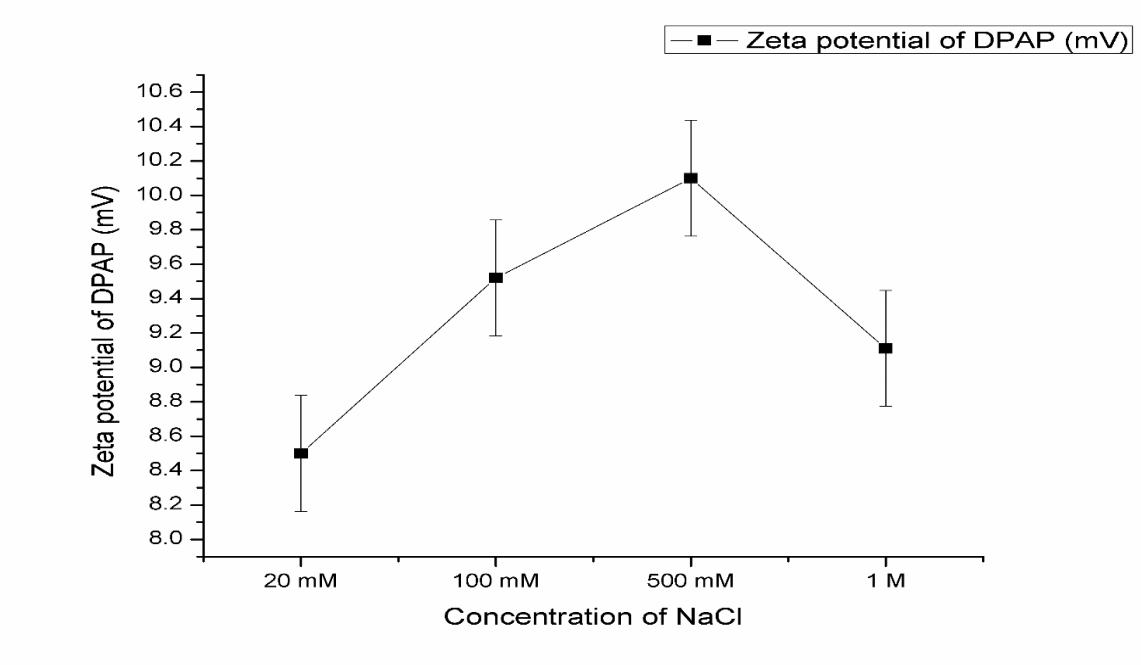

Figure 4.19: Effect of ionic strength on the surface charge stability of DPAP formulation. Different ionic strengths were established using 20 mM, 100 mM, 500 mM, and 1 M NaCl

4.8.2 Effect of ionic strength on BSA drug and aptamer release

UV-visible spectrophotometric analysis was used to determine the release characteristics of DPAP under varying ionic strength conditions of 20 mM, 500 mM, and 1000 mM NaCl. The concentrations of BSA and aptamer were measured at wavelengths of A260nm and A280nm respectively. Table 4.3 shows the relative amounts of free DNA aptamer and BSA released under different NaCl concentrations. The maximum concentration of free DNA aptamer released into solution was 0.9372 µg/ml under 20 mM NaCl ionic strength. Similar concentrations of free aptamer were detected in solution for 500 mM and 1 M NaCl ionic strengths. Under low ionic strength conditions, more aptamer and BSA molecules are released into solution, and this is a result of the electrostatic attractive pull from the positively charged medium. Na^+ acts as a chaotropic agent which interferes molecular interactions including Van der Waals forces, hydrogen bonding, and hydrophobic and electrostatic interactions. As a result, the conformational structure of DPAP is disrupted to induce release of encapsulated molecules. A low ionic strength is sufficient enough to affect the degradation rate and surface charge stability of DPAP

micro-particles. Under this condition, weak electrostatic forces are established between PEI particles and aptamer molecules, facilitating their release into the surrounding medium. With increasing NaCl ionic strength concentration, Na^+ shielding intensifies, creating a cationic membrane that restricts the release of more aptamer molecules into solution. Also, excess Na^+ ions generated under high ionic strength conditions interact with the anionic aptamer molecules, thus lowering the concentration of free aptamer molecules released.

The concentration of free BSA molecules released into solution under varying ionic strength conditions was negligible relative to the concentration of encapsulated BSA. This demonstrates the efficacy of the double-shielding effect provided by the multi-layered co-polymeric DPAP formulation as the BSA molecules are entrapped within the innermost PLGA core of the DPAP system, and are therefore not readily affected by increasing ionic strength. The low concentrations of BSA measured in solution could be the result of loosely entrapped BSA molecules on the PLGA polymeric surface which passively diffused into solution. The data is particularly important to support the potential resistive features of DPAP towards variations in physiological ionic conditions.

Table 4.3: Release analysis of BSA drug and thrombin-specific aptamer under varying NaCl concentrations

NaCl concentration (mM)	**Concentration of DNA aptamer at A260nm (µg/ml)**	**Standard deviation**	**Concentration of BSA protein at A280nm (µg/ml)**	**Standard deviation**
20	0.9372	0.0033	0.1900	0.0058
500	0.6633	0.0033	0.2100	0.0006
1000	0.6006	0.0019	0.1900	3.4000E-17

4.9 DLS ANALYSIS OF DPAP PARTICULATE SYSTEM USING DIFFERENT HOMOGENIZATION TECHNIQUES

DLS analysis was used to determine the average D[4,3] hydrodynamic size, size distribution, zeta potential and stability of each layered compartments of the DPAP formulation. The w/o/w double emulsion was utilized to generate DPAP formulation homogenised by either magnetic stirring or ultra-sonication. Figure 4.20 shows that the w/o/w double emulsion technique produced DPAP particles in the micron range irrespective of the homogenization technique. Ultra-sonication generated a smaller DP average particles size of 1041 nm. This indicates the efficiency of ultra-sonication in particle size reduction and dispersion. This becomes important as the number of individual DPAP particles increases and the average diameter of the DPAP particles decreases, resulting in decreasing inter-particulate distance and increasing surface area of particles for improved biosorption. Ultrasonic exposure enhances agitation of particles due to cavitation and results in uniform particle dispersion whilst magnetic stirring provides good mixing but poor particle dispersion (Chitra et al., 2014). The D[4,3] hydrodynamic size of DPAP particles generated produced using ultra-sonication was smaller (615.6 nm) compared to that generated with homogenization (685.6 nm). Although the size variation is not significantly high, there was a demonstration that ultra-sonication is more effective at dispersing small particles, forming emulsion and reducing particle size over a shorter processing period. This insignificant size variation also shows the efficacy of magnetic stirring in generating uniform DPAP particles, albeit with a longer processing time using the kinetic energy produced through a rotating magnetic field.

The effect of ultra-sonication and magnetic homogenization on the zeta potential of DPAP formulation is shown in Figure 4.21. The use of different homogenization techniques did not induce any significant effect on the surface charge of DPAP. The DP formulation remained electronegative, -8.92 mV and -9.77 mV, for both ultra-sonication and magnetic stirring, due to the encapsulation of electronegative BSA molecules within the neutral PLGA polymeric core. DPA formulation was electronegative with approximately -8.8 mV for both ultra-sonication and magnetic stirring. Therefore, the degree of effective aptamer coupling onto DP may not be significantly dependent on homogenisation mechanism. The final DPAP particulate system showed a positive zeta potential of around +9.0 mV

due to the introduction of cationic PEI polymeric particles intercalated into anionic aptamer molecules to form the outermost layer of the DPAP to facilitate interactions with targeted cell membranes.

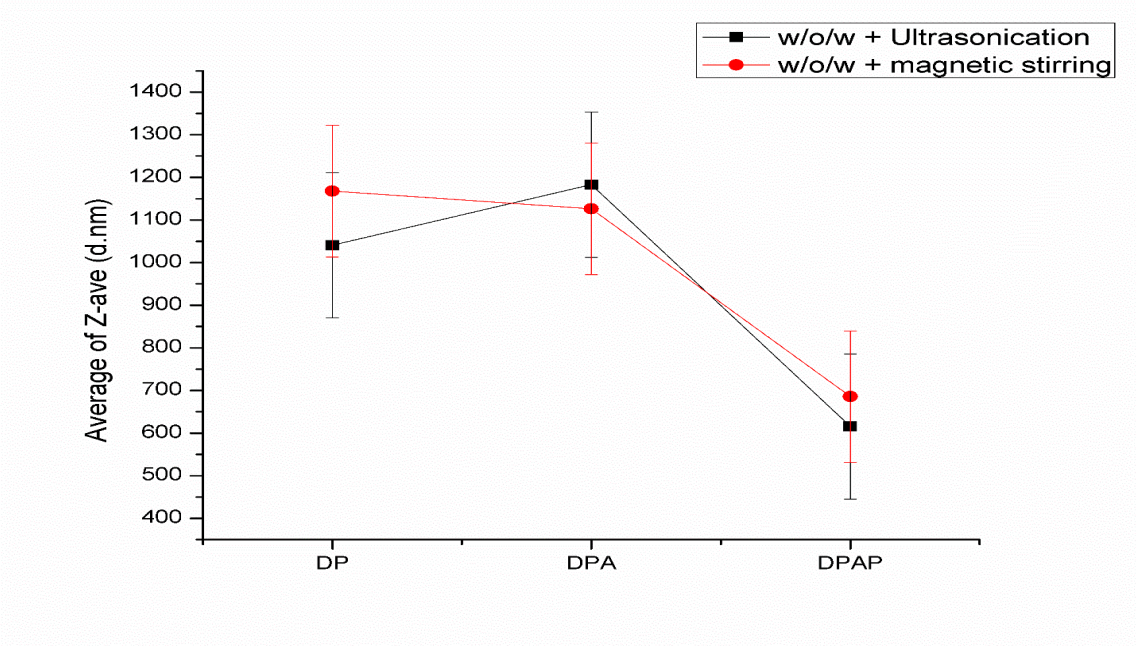

Figure 4.20: The average D[4,3] hydrodynamic size of different layered compartments of DPAP formulation: DP, DPA, DPAP under different homogenization approaches

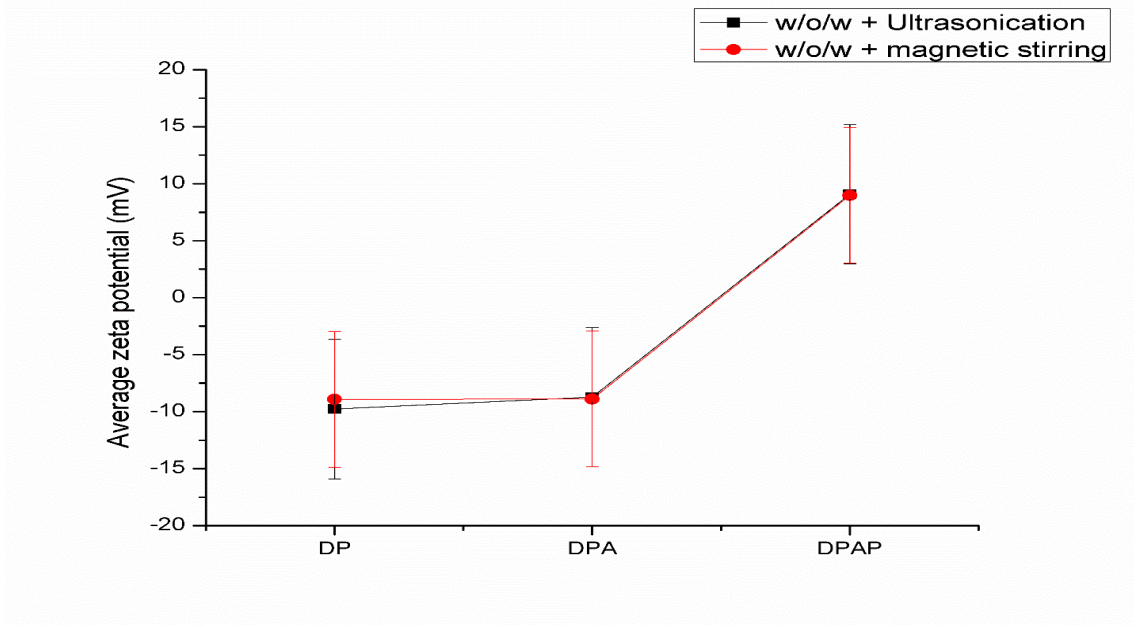

Figure 4.21: The average zeta potential of different layered compartments of DPAP formulation: DP, DPA, DPAP under different homogenization approaches

4.10 ENCAPSULATION EFFICIENCY AND LOADING CAPACITY OF DPAP FORMULATION

The encapsulation efficiency, drug-loading capacity and *in vitro* drug release characteristics of DPAP particulate formulation were investigated using UV spectrophotometric analysis. The experimental results showed that BSA was encapsulated into PLGA particles with an encapsulation efficiency of 89.4±3.6% and a loading capacity of 0.179±0.007 mg BSA protein per mg PLGA. The DPAP formulation also demonstrated effective conjugation of thrombin-specific DNA aptamer in the range of 65% to 75%. This result is in keeping with reported encapsulation efficiencies for other functional polymeric formulations (M. Alibolandi et al., 2015; Aravind, Jeyamohan, et al., 2012; Nguyen et al., 2008). The study by Nguyen et al. (2008) generated POE-PEI microspheres via a modified double emulsion (w/o/w) approach and obtained an encapsulation efficiency of 60-70% of entrapped DNA plasmid molecules. In comparison to POE-PEI microspheres developed by Nyugen et al (2008) using double emulsion (w/o/w) method, DPAP formulation obtained a higher encapsulation efficiency. This demonstrates that w/o/w double emulsion along with ultra-sonication technology promotes better encapsulation as a result of enhanced surface interaction and particulate composition of the co-polymeric system and active molecules. M. Alibolandi et al. (2015) developed EpCAM aptamer conjugated PEG-PLGA nanoparticles via EDC/NHS coupling and pH gradient. They also demonstrated a comparable encapsulation efficiency of 91.25±4.27% of entrapped doxorubicin drug to target breast adenocarcinoma. The DPAP formulation showed a higher encapsulation efficiency than result reported by Aravind, Jeyamohan, et al. (2012). They synthesized AS1411 aptamer-Paclitaxel-PLGA-lecithin-PEG nanoparticles and obtained an encapsulation efficiency of 60.76±3.4% using a nanoprecipitation synthesis technique. The result indicates that DPAP formulation is capable of shielding a significant load of DNA aptamer molecules from endonuclease degradation and rapid renal filtration thus retaining a sufficient quantity for targeted therapeutic activity. The effective

encapsulation can be attributed to strong electrostatic interactions between PEI and DNA aptamer molecules to form PEI-DNA complexes.

DPAP formulation demonstrated high encapsulation efficiencies for both BSA and thrombin-specific DNA aptamer under *in vitro* physiological conditions using isotonic PBS buffer with ionic strength and osmolarity similar to mammalian systems at pH 7.4. This is important to deliver sufficient amounts of intact aptamer molecules to bind onto their specific surface biomarkers or receptors at desired target sites to trigger endocytosis, leading to cellular uptake of drugs. Well-encapsulated aptamers can be protected from endonuclease attack and kidney filtration to maintain their functionality in the mammalian system. The high BSA efficiency of DPAP formulation demonstrates its ability to prevent drug leakage to non-specific cells and carry sufficient drug load enough to elicit therapeutic effects at specific sites. The encapsulation efficiency of a polymeric formulation is highly influenced by physicochemical factors including pH, ionic strength, temperature, mechanical impacts and changes in size or shape (Stevanovic & Uskokovic, 2009). The data for DPAP zeta potential showed the effects of protonation and deprotonation on the surface charge and size of DPAP, which are key drivers of polymer hydrolysis and degradations. Thus DPAP was synthesized to allow for high encapsulation efficiency whilst enabling controlled polymer degradation under isotonic PBS buffer conditions at pH 7.4 to mimics the human circulatory system. Double emulsion with solvent evaporation integrated with short periods of sonication was used for DPAP synthesis in order to reduce mechanical impacts and produce reduced particle size with spherical shape for high drug encapsulation. The ratio of BSA:PLGA used was 1:10 as this ratio has been demonstrated to produce high encapsulation efficiencies (Freitas, 2005).

4.10.1 Encapsulation efficiency and loading capacity of the particulate formulations

The encapsulation efficiency and loading capacity of the different DPAP formulations were determined to investigate the dependency of polymer composition and molecular weight on payload. As seen in Table 4.4, DPAP formulation with 65:35 PLA/PGA and PEI at ~25,000 Da MW possessed the highest BSA encapsulation efficiency and loading capacity of 85.46% and 0.1709 mg BSA per mg PLGA respectively. This can be attributed to increased affinity or interaction between hydrophobic moieties on BSA and PLGA

particles at higher lactide to glycolide ratio, resulting in a stronger drug incorporation. In contrast, the PLGA 50:50 with a lower lactide ratio and molecular weight possesses a higher degree of hydrophilicity and lesser affinity towards BSA hydrophobic molecules, making it more susceptible to water uptake for rapid degradation. The reduced polymer drug interaction explains the lower encapsulation efficiency. The PEGylated formulations showed similar drug encapsulation performances. BSA-PLGA-PEI-PEG-aptamer formulation demonstrated a drug encapsulation efficiency of 84.04% and drug loading capacity of 0.1681 mg BSA per mg PLGA; BSA-PLGA-PEI-PEG formulation showed an encapsulation efficiency of 83.66% and loading capacity of 0.1673 mg BSA/mg PLGA; and BSA-PLGA-PEG-aptamer formulation has an encapsulation efficiency of 85.66% and 0.1713 mg BSA per mg PLGA. This results indicate that PEGylation did not significantly enhance or affect drug encapsulation efficiency. However, the presence of PEG polymeric layer provided a stronger shielding effect to the encapsulated drug molecules, resulting in a slower overall degradation rate with reduced drug leakage and initial burst release. Also, PEGylation can enhance DPAP osmotic pressure and slow down the rate of hydration of the formulation for hydrolytic degradation.

The aptamer encapsulation efficiency of DPAP formulations with different polymeric compositions (PLGA 65:35, PLGA 50:50, PEI ~800 Da, PEI ~25,000 Da) was in the tight range of 75.02%-78.93%, with no significant impact on aptamer binding. This is because the binding affinity between aptamer molecules and DPAP formulation is largely dependent on strong electrostatic interactions between positively charged PEI and anionic aptamer molecules. In comparison to BSA-PLGA-PEG-Aptamer formulation, BSA-PLGA-PEI-PEG-aptamer formulation possessed a higher aptamer encapsulation efficiency of 80.99%. This can be explained by the presence of cationic PEI which electrostatically interacts with negatively charged DNA aptamer molecules, condensing the anionic molecules to generate a stable PEI-DNA complex. Also, the outermost PEG layer provides addition protection to the encapsulated payloads, resulting in a higher encapsulation efficiency. The low encapsulation efficiency of 61.83% for BSA-PLGA-PEG-Aptamer formulation is in keeping with that of Patil and Panyam (2009). However, the insertion of PEI polymeric layer into the formulation effectively improved the encapsulation efficiency. Aptamer-conjugated PLGA formulation was shown to have

~100% encapsulation efficiency. In the absence of BSA drug molecules, the PLGA polymeric particles completely adsorbed the aptamer molecules without reaching saturation point. The high encapsulation efficiencies of all formulations in Table 4.4 also demonstrate the effectiveness of w/o/w double emulsion-evaporation and homogenization technique in producing particulate delivery systems with high loading capacity.

Table 4.4: Average encapsulation efficiency and loading capacity of the different particulate formulations

Formulation	**Drug encapsulation efficiency (%)**	**Loading capacity (mg BSA/mg PLGA)**	**Aptamer encapsulation efficiency (%)**
DPAP (PLGA 50:50, PEI MW~800)	83.66±1.52	0.1632±0.0031	75.96±0.45
DPAP (PLGA 65:35, PEI MW~25,000)	85.46±1.51	0.1709±0.0030	75.02±0.31
DPAP (PLGA 65:35, PEI MW~800)	80.26±0.78	0.1605±0.0016	78.93±0.80
BSA-PLGA-PEI-PEG-aptamer	84.04±0.92	0.1681±0.0018	80.99±0.65
BSA-PLGA-PEI-PEG	83.66±0.33	0.1673±0.0007	
BSA-PLGA-PEG-aptamer	85.66±0.96	0.1713±0.0019	61.83±0.42
PLGA-aptamer			~ 100

4.10.2 Effect of homogenisation on encapsulation efficiency and loading capacity of DPAP

Formulation variables including homogenization speed, mixing time, temperature and pH were investigated during the synthesis of DPAP formulation to evaluate their impacts on the physiochemical and functional characteristics of DPAP. Two different homogenization strategies (ultra-sonication at 70% amplitude, 0.7 s pulse cycle for 2 min, and magnetic stirring at 500 rpm, room temperature for 5 min) were employed and the DPAP particles generated were characterized based on encapsulation efficiency and loading capacity. Table 1 shows that the encapsulation efficiency (92.8±1.6%) and loading capacity (0.1869±0.002 mg BSA per mg PLGA) of DPAP formulated with ultra-sonication as the dispersion method were higher as compared to DPAP micro-particles generated using magnetic stirring. These results are comparable to other reported studies including polyelectrolyte coated curcumin LbL nanoparticles produced using sonication with 80-90% encapsulation efficiency (Zheng et al., 2010); and microencapsulation of wheat germ oil with 70-89% encapsulation efficiency using ultrasonic homogenization (Yazicioglu et al., 2015). Ultra-sonication appears to be more effective than magnetic stirring and provides a more uniform unimodal distribution. This can be attributed to the provision of higher mechanical energy and intermolecular kinetic force that enhances the interparticle-surface interactions during emulsification over a short period time. This results in more entrapped BSA drug molecules within the PLGA polymeric particles. The magnetic stirring presented insufficient dispersion of the polymeric organic phase even at 500 rpm, and this causes a lower and unidirectional turbulent flow which can lead to drug diffusion from the organic phase.

DPAP formulation produced using magnetic stirring possessed a good encapsulation efficiency of > 80%, and this is noticeably higher compared to some reported functional polymeric nano/micro drug carriers such as Cyclosporin A-encapsulated chitosan nanoparticles with encapsulation efficiency of 73% (De Campos et al., 2001), and aptamer mediated-paclitaxel loaded PEG-PLGA nanospheres with 44.7% encapsulation efficiency (Jianwei Guo et al., 2011). Table 1 shows that variations in the dispersion technique had no impact on the aptamer encapsulation efficiency of DPAP, revealing that the quantity

of coupled aptamer molecules onto the PLGA polymeric layer is highly dependent on the efficacy of EDC/NHS coupling. The aptamer encapsulation efficiency of 75-76% was considered effective compared to reported values in the literature (Aravind, Jeyamohan, et al., 2012; Jianwei Guo et al., 2011; Sayari et al., 2014) indicating effective coupling of aptamer molecules via chemical activation of carboxylic functional groups of PLGA and amine groups of aptamer molecules. The rapid bond formation kinetics and strong covalent bonds between the EDC/NHS-activated PLGA particles and aptamer molecules resulted improved efficiency of aptamer coupling. The high electrostatic attractive forces associated with interactions between anionic DNA aptamer molecules and cationic PEI polymeric particles also play a crucial role in enhancing the aptamer encapsulation efficiency of DPAP formulation.

Table 4.5: Average loading capacity and encapsulation efficiency of DPAP formulation homogenised with ultrasonication and magnetic stirring

Formulation	**Encapsulation efficiency in loading BSA drug molecules (%)**	**Loading capacity (mg BSA/mg PLGA)**	**Encapsulation efficiency in loading aptamer molecules (%)**
DPAP generated via w/o/w double emulsion and ultra-sonication	92.8±1.6	0.1869±0.002	75
DPAP generated via w/o/w double emulsion and magnetic stirring	84.09±1.5	0.1615±0.006	76

4.10.3 Determination of loading capacity and encapsulation efficiency of DPAP-MGO_1 AND DPAP-MgO_2 particulate systems

Table 4.6 shows loading capacity and encapsulation efficiency comparisons between DPAP-MgO_1 and DPAP-MgO_2 formulations. MgO_1 nanoparticles encapsulated within the PLGA polymeric core with a loading capacity of 0.008 mg per mg PLGA and an encapsulation efficiency of 60.14% whilst MgO_2 nanoparticles registered a loading capacity of 0.031 mg per mg PLGA and an encapsulation efficiency of 93.69%. The significantly higher encapsulation efficiency of biosynthesised MgO nanoparticles (MgO_2) may be due to enhanced bio-complexation of MgO_2 nanoparticles into biodegradable PLGA polymeric particles potentially facilitated by residual bioactive compounds such as flavonoids accompanying the plant-leaf extract. The encapsulation efficiencies are either highly comparable or higher than others reported in the literature for functional polymeric delivery devices. For example, paclitaxel-loaded PLGA particles (N. Sharma et al., 2016) and paclitaxel-loaded aptamer-coupled PEG-PLGA nanocarriers (Jianwei Guo et al., 2011) showed an encapsulation efficiency of 44.7%; AS1411 aptamer-linked paclitaxel-carried PLGA-lecithin-PEG nanoparticles showed an encapsulation efficiency of 60.76% (Aravind, Jeyamohan, et al., 2012); and EpCAM aptamer-conjugated PEG-PLGA formulation showed 91.25% encapsulation efficiency (M. Alibolandi et al., 2015). DPAP-MgO_2 particulate system also demonstrated a more efficient coupling of aptamer molecules at an efficiency of 60.3%. The aptamer loading efficiency is in the same range of some reported findings. DNA-conjugated POE-PEI formulation showed approximately 65% (Nguyen et al., 2008); and AS1411-linked drug-polymeric formulations showed 60.76% (Aravind, Varghese, et al., 2012) and 44.7% (Jianwei Guo et al., 2011) aptamer encapsulation efficiencies.

The DLS data demonstrates the potential of DPAP formulation in protecting loaded aptamer molecules via intercalation between the aptamer molecules and cationic PEI to form a stable PEI-Aptamer polyplex. As a result, the aptamer and its functionality as the targeting ligand may be is preserved and protected from rapid glomerular filtration, nuclease-catalysed degradation and phagocytosis. The co-polymeric characteristic of DPAP particulate system allows a controlled and sustained release of encapsulated drug

molecules over a desired period due to the hydrolytic degradation mechanisms of both PEI and PLGA polymeric layers under changing pH conditions during targeted cellular events.

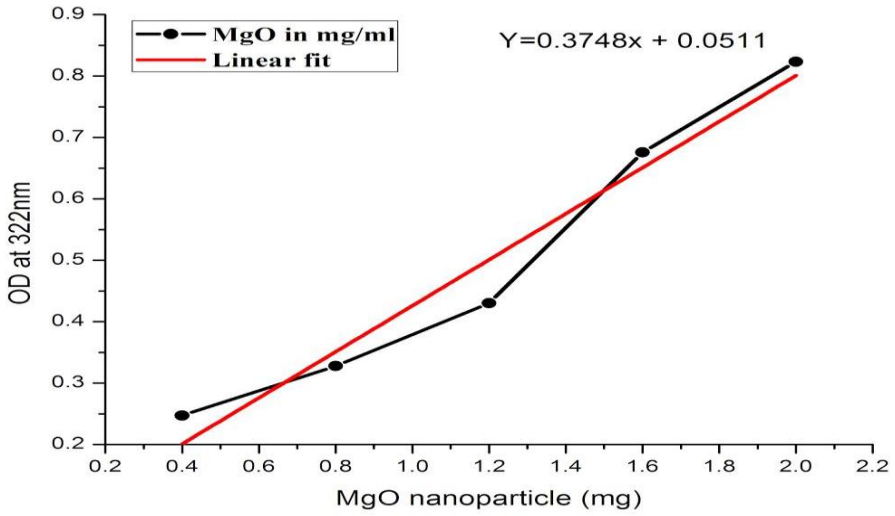

Figure 4.22: The calibration curve of a series of different MgO concentrations at 322 nm

Table 4.6: The average loading capacity and encapsulation efficiency of DPAP formulation carrying different kind of MgO nanoparticles.

Type of particulate delivery system	**Loading capacity (mg MgO/ mg PLGA)**	**Encapsulation efficiency in entrapping MgO (%)**	**Encapsulation efficiency in entrapping aptamer molecules (%)**
DPAP-MgO_1	0.00802	60.14	50.22
DPAP-MgO_2	0.03100	93.69	60.30

4.11 DRUG RELEASE PROFILE OF DPAP FORMULATION

The *in vitro* drug release characteristics of DPAP formulation was studied in PBS buffer at pH 7.4, temperature 37°C, and 120 rpm shaking. The result in Figure 4.23 shows the release kinetics of DPAP particulate formulation is in three phases. There was no initial burst release after first 24 h, indicating the multifunctional DPAP formulation is capable of retaining high drug dosage by preventing free diffusion or escape of drug molecules. This represents an effective initial pharmacokinetic behaviour. The incorporation of PLGA and PEI into various sections of the molecular architecture of DPAP particulate formulation provided a slow initial drug release characteristics, resulting from initial degradative hydrolysis of intercalated PEI under physiological buffer conditions. The first release phase (day 1 to day 11) was attributed to the release of BSA molecules poorly entrapped or near the surface of the microsphere. The continuing slow release phase was due to chemo-molecular diffusion of drug through the boundary layers of the DPAP polymeric matrix and DPAP-buffer interface into the physiological medium. The third release phase, starting from Day 38, demonstrated a higher kinetic rate of drug release due to enhanced degradative hydrolysis of DPAP microspheres, releasing more of the encapsulated drug from its microenvironment in the PLGA core into the physiological medium. The pharmacokinetics of DPAP microparticles is characterised to have a delayed and slow release profile with a controlled and small amount of BSA released each day. The tightly controlled release profile is due to the intercalation of PEI polymeric particles, acting as an additional shield and retaining drug molecules more efficiently within the DPAP particulate system as well as preventing the diffusion of water into the PLGA core. Consequently, the degradative hydrolysis rate of PLGA is reduced, leading to slow and controlled drug release characteristics.

Compared to other research studies, the encapsulation efficiency and loading capacity of DPAP particulate delivery system show better payloads with a drug loading efficiency of 89±3.6%. Some previously reported encapsulation efficiencies include POE-PEI microparticles (65%-75%) (Nguyen et al., 2008), AS1411-PEG-PLGA nanoparticles (44.7±3.9%) (J. Guo et al., 2011), MUC1-chitosan nanoparticles (7.1%) (Sayari et al., 2014), and AS1411 aptamer-Paclitaxel-PLGA-lecithin-PEG nanoparticulate system (60.76±3.4%) (Aravind, Jeyamohan, et al., 2012). This finding demonstrates the capacity

of of DPAP formulation to harbor and transport optimal drug dosages critical for effective therapeutic treatment to targeted sites. The outermost surface of DPAP formulation is positively charged in order to minimize electrostatic repulsions with negatively charged membrane surface of targeted cell for enhanced transfection and cellular uptake (Lakhin et al., 2013; McKeague & DeRosa, 2012). The drug release profile of DPAP showed a controlled release characteristics over a period of time. This indicates that DPAP formulation can engineered as delivery vehicles to provide extended shielding of encapsulated active ingredients using double layered PLGA and PEI system. All these findings show promise for DPAP as a targeted drug delivery carrier, and represent a major contribution to research efforts towards developing new and improved strategies for targeted drug delivery. These *in vitro* investigations are critical in setting the essential parameters required for the synthesis of DPAP particulate system with effective hydrodynamic size and surface charge characteristics as well as physiological conditions essential to optimize the potentials of DPAP as a targeted drug carrier. This is critical in preparation for the next phase of research in terms of *in vivo* validation of DPAP in cells and animals.

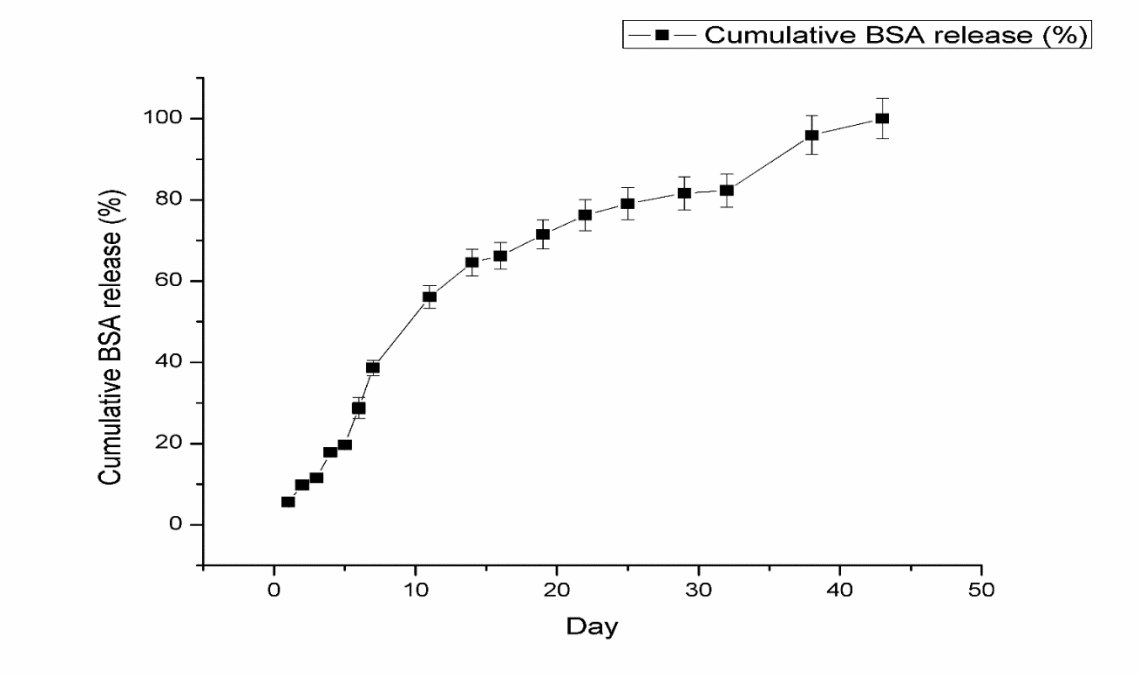

Figure 4.23: Cumulative release of BSA protein drug from DPAP formulation in PBS buffer at pH 7.4 and temperature 37ºC. Drug release was periodically

monitored via UV absorbance analysis every 24 h from Day 1-8, 72 h from Day 9-38, and 120 h after Day 38

4.11.1 Drug release profiles of standard DPAP formulation under varying ionic strengths

BSA drug release behaviors of DPAP particulate formulation under varying ionic conditions were investigated *in vitro* at pH 7.4, 37ºC and 120 rpm shaking in a PBS buffer over an incubation period of 26 days. NaCl was used to vary the ionic strength of the buffer system due to its high capability to salt out the particulate polymers based on the lyotropic series (Asare-Addo et al., 2013; Mitchell et al., 1993). It has been reported previously that the release rate of drug molecules from polymeric particles is dependent on the interactions between the polymeric particles, drug molecules, and the surrounding medium (Saša et al., 2006). Hence, ionic strength of the release media can significantly affect the ion pairing between the polymeric carrier and the entrapped drug molecules. The drug release profiles in Figure 4.24 show that increasing ionic strength resulted in a significant effect on the release profile of drug molecules from the DPAP formulation. The cumulative drug release profiles were largely based on the electrostatic pull of Na^+ ions which alters the electrostatics forces and surface charges of DPAP to increase drug release rates. This also shows that the low ionic strength level (100 mM NaCl) is capable of providing sufficient ionic displacement potential to release hydrophobic BSA molecules from the formulation. The DPAP formulation achieved 50% release rate at Day 11 in 100 mM NaCl PBS media, but achieved 50% release rate in Day 9 of 1 M NaCl PBS media, proving the degradation rate of DPAP is highly dependent on ionic stimulation.

Na^+ ions act as counter ions and interact with BSA molecules to form a complex via electrostatic pulling of encapsulated protein molecules, altering the association/disassociation of BSA-PLGA and BSA drug release from the DPAP micro-particles. As seen in Figure 4.24, there an increase in BSA release rate with increasing ionic strength. The higher ionic strength level triggered a higher drug release rate. Loosely bound BSA molecules near the surface of the PLGA polymeric particles are pulled more rapidly into the surrounding media. The presence of excess Na^+ ions increases the rates of solvent penetration, hydration, swelling, chain disentanglement and matrix erosion of

DPAP formulation to facilitate drug release. In addition, the presence of excess Na^+ ions enables protonation of amino or imine functional groups of PEI, causing swelling of DPAP and matrix degradation due to increased amount of fixed positive charges which resulted in strong electrostatic repulsion between PEI polymeric chains. This then exposes the inner BSA-PLGA particles to further degradation. The drug release profiles obtained at varying ionic strengths is important to predict and address potential effects of patients' salinity levels on drug pharmacokinetics.

The experimental data also showed that there was no initial burst after first 24 h, representing effective encapsulation of high payload drug molecules to avoid leakage or premature diffusion. The release rate of drug molecules increased with time due to increasing electrostatic stimulation and hydrolytic degradation of DPAP to induce polymer swelling rates. DPAP formulation displayed a controlled drug pharmacokinetic profile as the amount of drug molecules released per unit time intervals is small and sustained. This shows the effectiveness of the multi-layer co-polymeric architecture of DPAP to provide multiple shielding effects and prevent water diffusion into the PLGA innermost core in order to obtain a prolonged release characteristics.

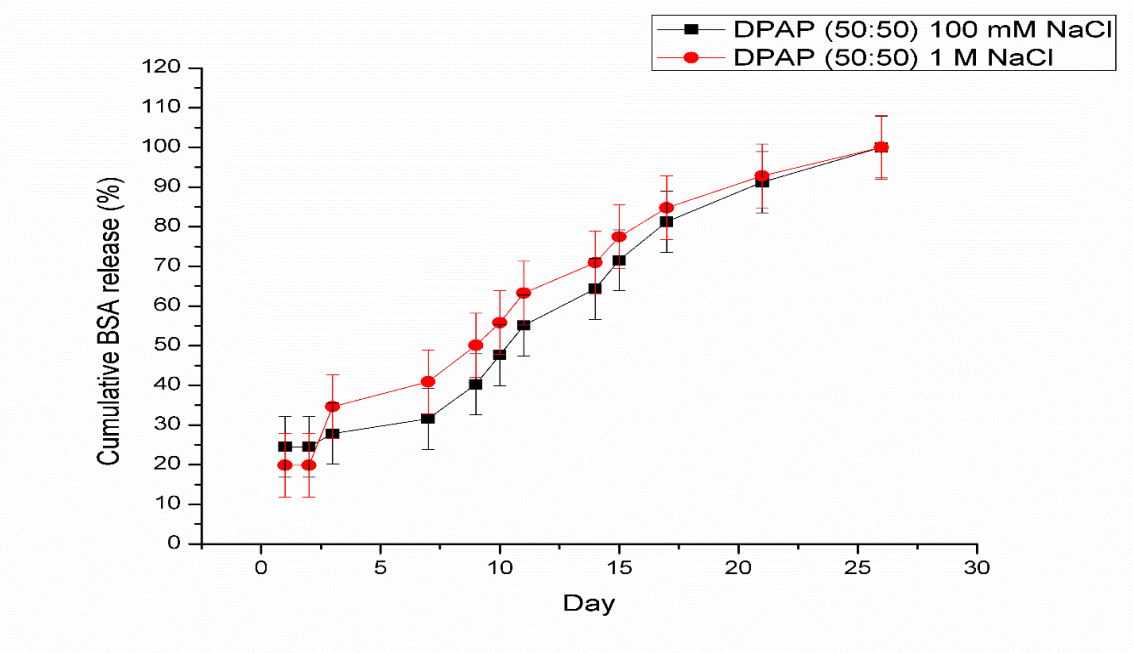

Figure 4.24: DPAP drug release profiles under varying ionic strengths of 100 mM and 1 M NaCl concentrations at pH 7.4 and 37ºC in PBS buffer. Drug release was

monitored at specific intervals for 1st hour and 5th hour, every 24 h from Day 1-3, every 48 h from Day 4-17, and every 96 h from Day 18-26

4.11.2 The drug release profiles of different multi-layered formulations

Figure 4.25 shows the effects of lactide/glycolide (PLA/PGA) ratio, molecular weight, and PEGylation on the drug release profiles of different DPAP formulations. The molecular weight of the polymeric matrix affects the hydrolytic potential and biomolecular diffusivity within the formulation under physiological conditions as well as biophysical interactions with active drug and aptamer molecules. It has previously been reported that the interactions between drug molecules and PLGA polymer particles can be altered by varying the molecular weight and PLA/PGA ratio of PLGA in order to optimize drug release characteristics (Zeng et al., 2011). The overall release of drug molecules from DPAP (PLGA 65:35, PEI MW~25,000) formulation was significantly higher as compared to DPAP (PLGA 50:50, PEI MW~800) and DPAP (PLGA 65:35, PEI MW~800) formulations. This can be attributed to the higher molecular weight of the DPAP (PLGA 65:35, PEI MW~25,000) formulation which contains more hydrated polymeric chains within a larger hydrodynamic volume (Asare-Addo et al., 2013; Sai Cheong Wan et al., 1995). This enhances polymer swelling and hydrolysis to increase drug release rate. Drug release rate from DPAP (PLGA 50:50) formulation was higher than DPAP (PLGA 65:35) formulation with the same PEI molecular weight. This finding is consistent with the experimental results of Zeng et al. (2011). They reported that increasing the PLA content of PLGA largely reduces drug release rate. This is attributed to the high hydrophobicity of PLA monomers which results in poor water absorption and thus, PLA monomers take a longer time to be hydrolyzed completely in the organic solvent. Also, high lactide content with hydrophobicity reacts better with hydrophobic groups of BSA, negatively impacting on BSA release from PLGA polymer matrix (Pereira et al., 2015). PGA is highly hydrophilic with crystalline structure which is responsible for its rapid degradation. In contrast, PLA possesses different mechanical, chemical and physical characteristics due to the extra pendant methyl side group on its α-carbon which lowers its degradation rate (Gentile et al., 2014). Nair and Laurencin (2007) reported that PLGA (50:50) has a faster degradation rate of 1-2 months than PLGA (85:15) with a slow degradation rate of 5-6 months due to high PLA. Consequently, DPAP (PLGA 50:50) formulation with equal

ratio of PLA/PGA showed better overall release rate than DPAP (PLGA 65:35) at the same PEI molecular weight of ~800 MW. All the 3 formulations, regardless of PLA/PGA ratio or PEI molecular weight, provided a sustained drug release characteristics over the experimental duration.

From the drug release profiles, the BSA-PLGA-PEG aptamer formulation experienced an initial burst of 35.29% after 24 h, demonstrating an ineffective shielding effect of PEG as compared to PEI as the outermost polymeric layer. DPAP formulation without PEGylation possesses better drug shielding capacity. Drug release from BSA-PLGA-PEI-PEG formulation within the first 20 days was poor, indicating that a combination of multiple bio-polymers in different layered compartments of the formulation increases structural complexity, excipient composition, and inter-particulate interactions which brings significant impacts to the drug release rate and degradation kinetics of the delivery system. Also, the presence of additional PEG layer lowered water penetration into the inner polymeric layer, thereby preventing hydrolysis and slowing drug release. Drug diffusion and matrix degradation rate are proportional to the surface-to-volume-ratio of the polymeric carrier.

In comparison to the BSA-PLGA-PEI-PEG formulation, the aptamer-conjugated PLGA-PEI-PEG formulation showed a higher release rate by achieving 50% drug release at Day 14. This suggests that strong electrostatic interactions between negatively charged aptamer molecules and positively charged PEI molecules play a significant role in reducing the overall particle size of PLGA-PEI-PEG-aptamer, resulting in improved better drug release rate. Also, the intercalation of aptamer molecules with PEI polymeric particles tends to weaken the interactions between PEI and PEG polymeric layer to increase BSA release from the innermost PLGA core. As seen in Figure 4.25, PLGA-PEI-PEG-aptamer formulation experienced a second burst release after Day 15 potentially due to the matrix erosion of the innermost PLGA core to release more entrapped BSA molecules. PLGA degrades via heterogeneous or bulk erosion with ester hydrolysis. Initially, water penetrates and causes PLGA hydration which breaks the hydrogen bonding, van der Waals forces, and covalent bonds, resulting in reduced molecular weight. Next, it undergoes autocatalyzed degradation of its carboxylic ends, causing the cleavage of

covalent backbone and mass loss. Finally, all the PLGA fragments are broken down and soluble in aqueous solution. The drug release profiles of both BSA-PLGA-PEI-PEG-Aptamer and BSA-PLGA-PEG-Aptamer presented a sustained release pattern, revealing the coupling of aptamer molecules does not affect the release of encapsulated molecules but enhances cell targeting and cellular transfection for better therapeutic effects.

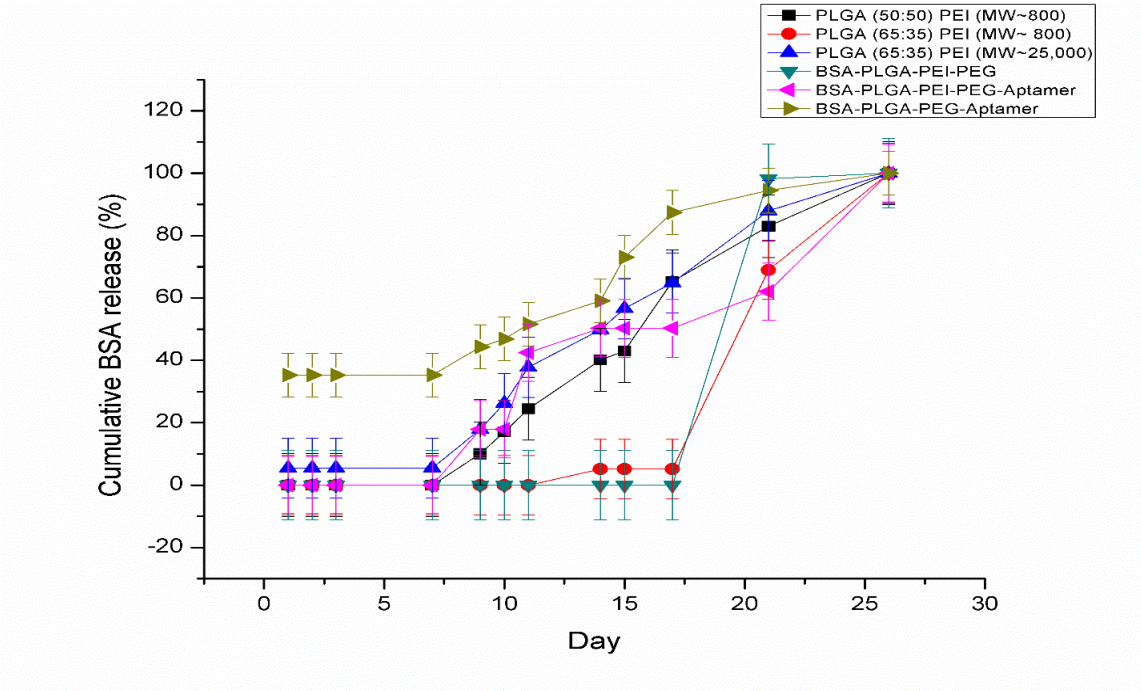

Figure 4.25: BSA drug release characteristics of DPAP formulations generated from different molecular weight PLGA and PEI polymers with or without PEGylation: a) DPAP (PLGA 50:50, PEI MW~800), b) DPAP (PLGA 65:35, PEI MW~800) c) DPAP (PLGA 65:35, PEI MW~25,000) d) BSA-PLGA-PEI-PEG, e) BSA-PLGA-PEI-PEG-Aptamer, f) BSA-PLGA-PEG-Aptamer formulation. Release experiment was performed at pH 7.4 and 37ºC in PBS buffering system. Drug release was monitored at specific intervals between the 1st hour and 5th hour, every 24 h from Day 1-3, every 48 h from Day 4-17, and every 96 h from Day 18-26

4.11.3 *In vitro* BSA release profile of DPAP formulation under varying temperature conditions

The *in vitro* drug release profile of DPAP under varying temperature conditions was investigated by incubating DPAP micro-particles at pH 7.4 and 120 rpm shaking in PBS buffer for 12 days. Figure 4.26 shows the drug release profiles. There was no initial burst release of BSA drug molecules from DPAP after 24 h of incubation for all 3 temperature

conditions, indicating that DPAP formulation possesses significant hydrolytic thermal stability to protect drug payload from escaping via initial stage diffusion. This is a desired initial pharmacokinetic property of an effective drug carrier or biological agent to deliver sufficient dosage of drugs to targeted sites. The double drug shielding effect facilitated by co-polymeric PLGA and PEI layers in separate structural compartments of DPAP formulation contributed to slowing initial drug release patterns of DPAP even at 41°C. From Figure 4.26, DPAP at 25 and 37 °C demonstrated a controlled and sustained drug release profiles throughout the incubation period. DPAP incubation at 41°C no initial lag due increased rate of diffusivity induced thermally. These profiles show that the release characteristics of entrapped BSA molecules depend on the incubation conditions, DPAP polymeric degradation in response to incubation conditions, and the biomolecular features of encapsulated drug. These factors are critical to understanding the kinetics of polymeric hydrolysis and initial burst characteristics. Moreover, the structural composition and the presence of internal pores within the polymeric formulation can affect the diffusion rate of drug molecules from the innermost compartment.

DPAP incubations at 25°C and 37°C displayed similar drug release trend, indicating a sustained release performance over the temperature range 25-37°C. However, the release profile of DPAP at 37°C reached a plateau phase earlier due to the effect of temperature in increasing the rate of diffusivity of drug molecules over the incubation period. The BSA release profile at 41°C displayed a clear 3-phase pattern. The elevated temperature induced an accelerated release of entrapped BSA drug molecules due to the provision of kinetic energy that increased the surface-area-to-volume-ratio of DPAP and the rate of molecular diffusivity. The elevated temperature provides the DPAP micro-particles and surrounding molecules with a greater kinetic energy, enhancing the rate of DPAP hydrolysis and drug release over a short period. BSA release profile at 41°C established an earlier plateau than the profiles at 25°C and 37°C. At 41°C, there was no initial burst release observed after Day 4 but a rapid release of BSA drug molecules was determined afterwards. Under the elevated temperature of 41°C, which is above DPAP glass transition temperature (T_g) of 38.93°C, there is an enhanced mobility of encapsulated BSA molecules which results in an accelerated release into the surrounding medium via erosion, mass loss and diffusion routes (Shameem et al., 1999).

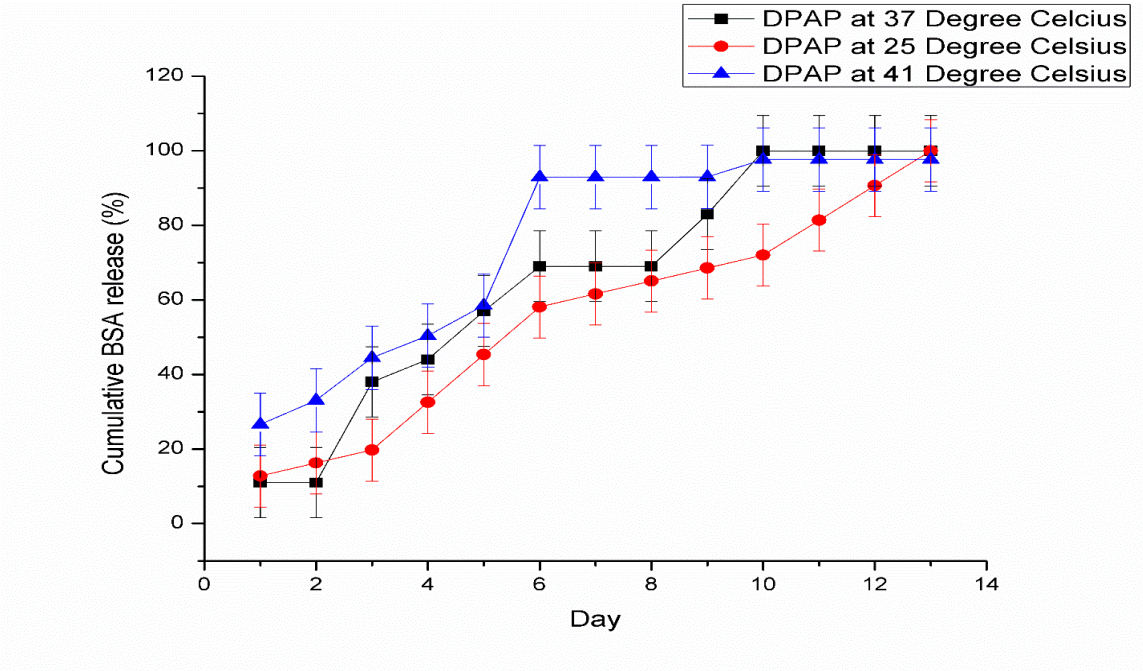

Figure 4.26: Cumulative BSA release from the DPAP micro-particles into the PBS physiological medium at pH 7.4 under varying temperature conditions: 25, 37, and 41°C

4.11.4 *In vitro* BSA release profile of DPAP formulation under various pH level

Figure 4.27 shows the BSA release profiles from DPAP at pH 5, 6 and 7. A controlled BSA release profile with 3-phase release kinetic characteristics at both pH 6 and 7 was observed. The drug release profile of DPAP formulation at pH 5 reached a plateau phase after a longer period of incubation compared to pH 6 and 7. Incubation at pH 6 reached a plateau phase in the shortest time. This indicates that pH ~5.5, which is approximately the pH condition in the acidic compartment of endosomes of targeted malignant cells, may be able to trigger DPAP formulation to release a larger dosage of encapsulated BSA drug molecules. On the other hand, the drug release profiles of DPAP at pH 6 and 7, demonstrate the efficacy of DPAP particulate system in carrying and preventing drug leakage under moderate pH conditions of interstitial fluids and blood plasma. There is no or negligible initial burst release for all the pH levels tested.

The release of encapsulated BSA drug molecules from DPAP micro-particles at pH 5, 6, and 7 is due to hydrolytic degradation of intercalated PEI which causes loosely entrapped BSA molecules to escape easily into the physiological medium. Subsequently, the gradual

increase in the concentration of released BSA over the incubation period is due to the unique hydrolytic characteristics of the innermost PLGA core to drive further DPAP degradation and trigger the release of more encapsulated BSA. The PLGA polymeric layer undergoes degradation due to the presence of surface pores which enhance hydration and subsequently hydrolysis. The phenomena of protonation and deprotonation due to the presence of excess H^+ or OH^- ions can significantly alter the drug release characteristics. For instance, protonation or deprotonation of the conjugated aptamer molecules can affect its affinity binding performance (Gates, 2009) the degradation rate of DPAP. At pH 6, nearly 50% of PEI nitrogen atoms undergo protonation, breaking the linkages between the PEI polymeric layer and the aptamer molecules, resulting in a higher DPAP degradation rate (Choosakoonkriang et al., 2003; Utsuno & Uludag, 2010). In contrast, approximately 10 to 20% of nitrogen atoms are protonated at pH 7, resulting in a more controlled release of encapsulated BSA drug molecules.

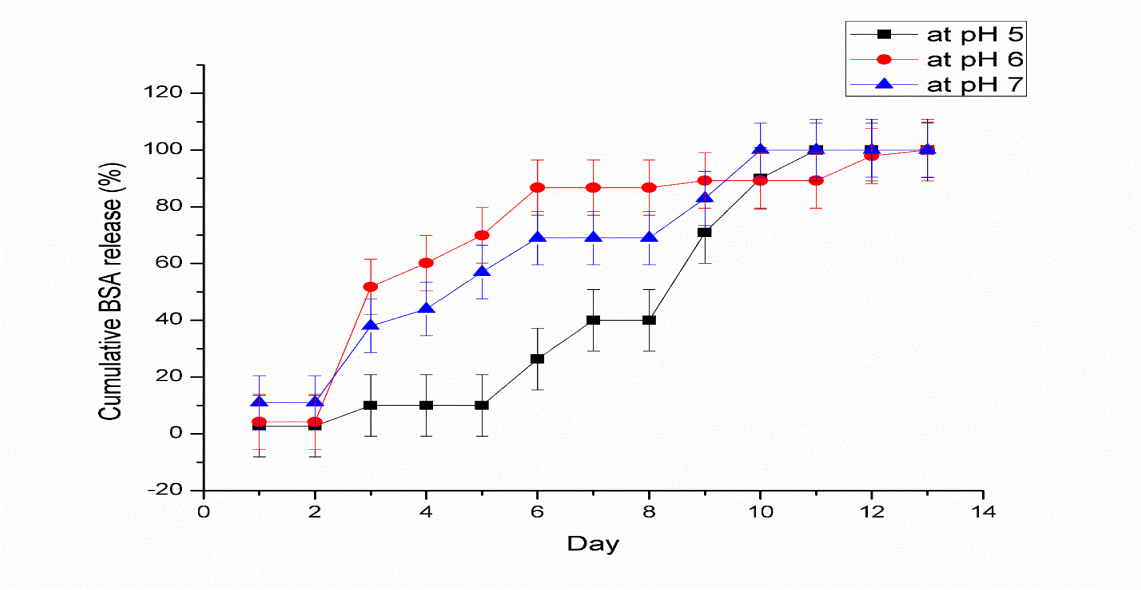

Figure 4.27: Cumulative BSA release from the DPAP micro-particles into the PBS physiological medium at temperature 37°C and pH levels: 5, 6, and 7

4.12 THE MTS CYTOTOXICITY ANALYSIS OF DPAP FORMULATION

The cytotoxic effect of DPAP formulation on cell viability was investigated by MTS cytotoxicity assay using V79B cells. V79B cells were treated with six different

concentrations of DPAP formulation in the range of 0.156 µl/ml to 5 µl/ml. IC_{50} is a measure of the concentration of DPAP formulation needed to inhibit V79B cell growth by half. Results demonstrated no detection of IC_{50} for all DPAP dosage levels, and the highest dosage of 5 µl/ml showed a cell viability of > 70% as shown in Table 4.7. Hence, the DPAP formulation did not cause any prohibitive cytotoxic effect in all 6 concentrations based on the cell viability studies under *in vitro* condition.

Table 4.7: Cell Viability Data in Triplicate Obtained for Varying Loadings of DPAP Particles

Concentration (µl/ml)	Viability 1 (%	Viability 2 (%)	Viability 3 (%)	Mean	SD
0.00	100.00	100.00	100.00	100.00	0.00
0.16	84.67	88.17	112.19	95.00	15.00
0.31	79.74	86.22	91.73	85.90	6.00
0.62	80.55	67.19	79.96	75.90	7.50
1.25	77.44	79.78	76.98	78.10	1.50
2.50	71.44	78.40	70.54	73.50	4.30
5.00	81.87	70.53	74.99	75.80	5.70

4.13 THERMOGRAVIMETRIC ANALYSIS OF DP AND DPAP MICRO-PARTICLES

Both thermogravimetric analysis and differential scanning calorimetric analysis were used to study the thermal stability of DP and DPAP micro-particles. Figure 4.28 a) shows the mass loss data for both lyophilized DP and DPAP particles, and 4.28 b) show the exothermic peaks of DP and DPAP formulations. The exothermic peak analysis is used to determine the manner of oxidation, decomposition and crystallization. Typically, sharp melting peaks occur over a narrow range of temperature when crystallization occurs (Hatakeyama & Quinn, 1999). Figure 4.28 (b) demonstrates that the decompositions of both DP and DPAP micro-particles have a steep declining slope of heat flow at the early stage. From the TGA and DSC data, the primary heat-stimulated event is the particulate

decomposition, occurring at ~225ºC. Both formulations entered a melting phase from 300ºC to 480ºC, as shown in Figure 4.28 (a). These findings are in keeping with those reported in the literature. Saliba et al. (2008) reported that PLGA polymeric particles showed complete mass loss of 100% over the temperature range 247ºC to 378ºC, indicating that the observed mass loss of DP and DPAP micro-particles could be the result of PLGA degradation (Saliba et al., 2008). Another study reported PLGA decomposition happening in the temperature range 280ºC to 360ºC (Yu et al., 2015).

TGA/DSC curves for both DP and DPAP micro-particles are similar, showing identical PLGA core polymer chain mobility. The strong attractive forces between the polymeric particles and the aptamer / BSA molecules are critical to thermal stability. The melting temperature of BSA is reported to be in the range 56-69ºC, and its melting phase can be observed with an endothermic peak (Michnik, 2003). However, this peak was not present in the TGA/DSC curves for both DP and DPAP formulations around this temperature range, suggesting that BSA was protected by the PLGA core.

Figure 4.28 (a) shows similarity in mass loss for both DP (black line) and DPAP (red line) over the temperature range 300-460ºC, with approximately 83.70% (7.7 mg) and 77.25% (7.11 mg) mass loss for DP and DPAP respectively. However, the total mass loss for DPAP is lower than DP, demonstrating a slightly better thermal stability. It has previously been reported that PEI TGA analysis showed a mass loss in the temperature range 310-410ºC (Y.-P. Huang et al., 2013). Hence, it is believed that PEI complexation is capable of improving the decomposition temperature of DPAP and enhance its thermal stability and biomolecular shielding efficacy.

Glass transition temperature, T_g is an important parameter to determine the supersaturation threshold of a polymeric dispersion where it remains in a glassy stage under this T_g and melts into viscous liquid phase above this temperature. The T_g values of DP and DPAP micro-particles were determined as 39.33ºC and 38.93ºC respectively. High T_g values are desirable for efficient storage and physical stability at room temperature, easier handling, and better drug dissolution (Jadhav et al., 2009). T_g values of DP and DPAP are similar with a negligible difference of 1ºC. The slight difference could be due to the polyplex nature of DPAP (Kalogeras, 2011).

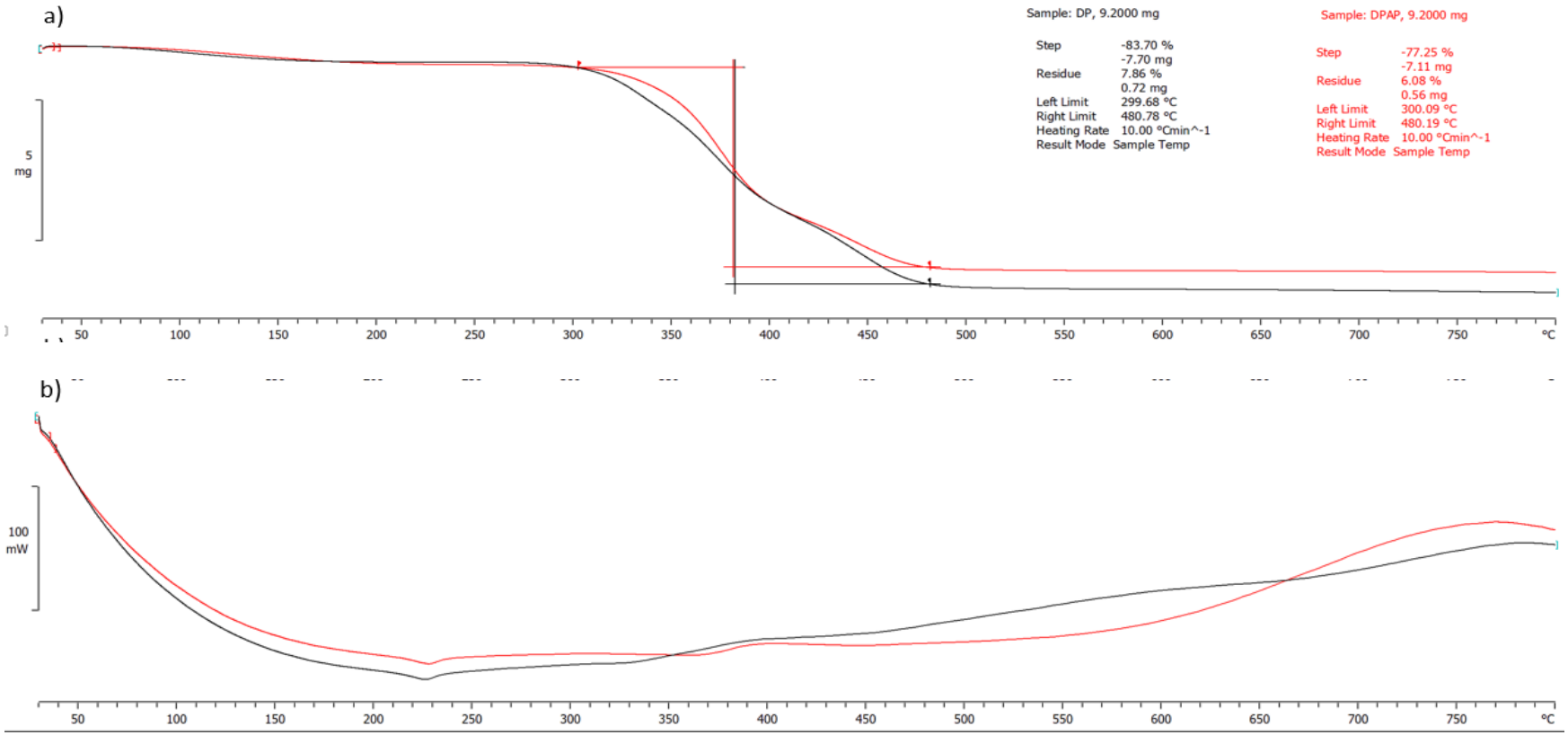

Figure 4.28: TGA and DSC analysis of DP and DPAP formulations: a) Mass loss analysis of DP and DPAP micro-particles, b) Differential enthalpy data for DP and DPAP formulations

4.14 CHARACTERISTICS OF BSA DRUG ABSORPTION ONTO PLGA COMPARTMENT

BSA drug binding characteristics onto PLGA particles were investigated to ensure optimal encapsulation of drug molecules into the inner polymeric compartment of DPAP formulation. Spectrophotometric analysis was carried out at different time intervals to determine the concentration of free drug molecules in solution until all the available sites on the PLGA particulate is completely occupied. Table 4.8 shows decreasing concentration of free BSA molecules in solution over the incubation duration, demonstrating adsorptive mass transfer of BSA molecules onto the PLGA particulate pore volume with increasing experimental time. The adsorptive binding between BSA molecules and PLGA particles is facilitated by electrostatic interactions between negatively charged BSA molecules and positively charged particle pore surfaces of PLGA. The mass transfer is also governed by instantaneous drug concentration differences between the liquid and solid phases. Hence, the rate of adsorptive binding decreases as BSA molecules are bound onto the solid phase. The drug encapsulation process was gently homogenized to provide extra kinetic energy for enhanced molecular interaction between BSA and PLGA. A loading capacity of 17.25 mg BSA protein/100 mg PLGA particles and an encapsulation efficiency of ~87% were achieved at the end of the incubation process.

Table 4.8: Time-dependent adsorption of BSA drug molecules onto PLGA particles at pH 7.4 and room temperature over a 30 min incubation period

Time (min)	A 280 nm absorbance value	Amount of free BSA drug molecules (mg)
0^{th}	1.018	0.081
10^{th}	0.896	0.071
30^{th}	0.7506	0.060

4.15 CHARACTERISATION OF APTAMER BINDING ONTO DP PARTICLES

Spectrophotometric analysis at 260 nm was conducted during aptamer coupling onto DP surface via EDC/NHS activation chemistry in order to investigate the rate of aptamer binding. Figure 4.29 shows the concentration of free DNA aptamer molecules remaining in solution during incubation. The decreasing concentration of aptamer molecules with time demonstrates aptamer binding onto the DP particulate phase to form the DPA compartment. The initial introduction of EDC to DP enabled the activation of carboxyl functional groups with generation of hydroxyl groups upon NHS activation. The aptamer molecules effectively binds onto the NHS-activated DP-COOH formulation by forming covalent bonds between the amine groups at the 3' end of the aptamer molecules and the activated carboxyl functional groups of the DP particles to produce aptamer-conjugated DP (DPA) formulation.

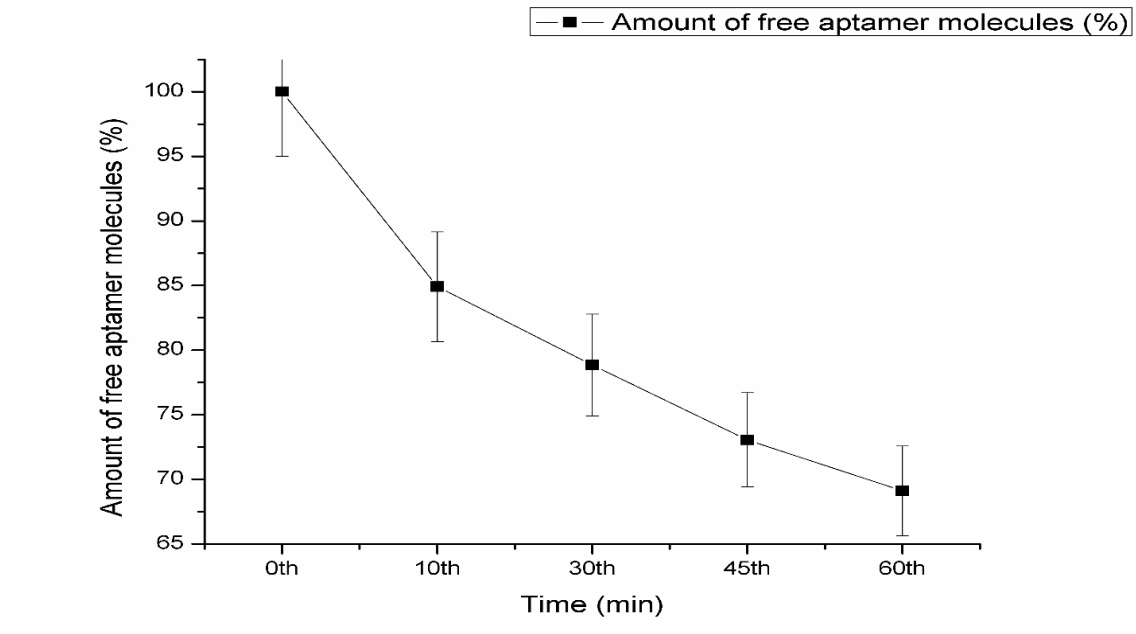

Figure 4.29: Binding analysis of aptamer molecules onto PLGA particles at pH 7.4 and room temperature for 1 h incubation period

4.16 THROMBIN BINDING ANALYSIS OF PA AND DPA FORMULATIONS

The thrombin targeting abilities of PA (PLGA coupled aptamer via EDC/NHS activation chemistry) and DPA (BSA encapsulated PLGA coupled with aptamer molecules via EDC/NHS activation chemistry) formulations were investigated to assess the potential for thrombin recognition and binding by the immobilised aptameric formulation. Free aptamer molecules were used as a positive control to compare the binding characteristics of DPA and PA. 0.05% w/v thrombin molecules were introduced to 1% w/v each of DPA, PA, and aptamer at pH 7.4. At 0^{th} min time intervals, 100% free thrombin molecules were presented in all 3 solutions. Figure 4.30 clearly reveals that the lowest concentration of free thrombin molecules was detected in DPA solution followed by PA solution and lastly aptamer solution with the highest thrombin concentration. Also, the amount of free thrombin molecules determined in DPA solution was the least at every time intervals (0^{th}, 10^{th}, 20^{th}, 30^{th} min) as compared to PA and aptamer solution whilst aptamer solution contained the highest concentration of free thrombin molecules at every time intervals. In addition, the experimental results demonstrated that the amount of free thrombin molecules in the solution decreased gradually over the 30 min incubation time, showing strong attractive forces were built between thrombin molecules with these 3 different formulations. This can be explained with the presence of thrombin-specific aptamer molecules coupled onto the surface of formulation which acted as targeting ligand that recognizes and binds onto desired thrombin molecules in the solution. Aptamer molecules work by folding into specific 3-D conformational structure in order to have the right fit with their cognate targets. Figure 4.30 indicates that DPA formulation had the highest targeting ability and binding affinity towards the free thrombin molecules as compared to PA formulation and aptamer solution as a high amount of thrombin molecules had been attracted and bond onto the aptameric layer of DPA formulation. This also proves that DPA formulation carrying encapsulated drug molecules is capable of protecting the functionality of conjugated aptamer molecules or even enhances the targeting capability of aptameric ligands as compared to the binding strength of PA formulation (without encapsulated drug molecules). However, both DPA and PA formulations are capable of targeting and binding specifically towards thrombin molecules. In addition, both DPA and PA displayed similar trend of binding kinetics as compared to the original aptamer

molecules, presenting that the binding properties of aptamer are not affected after the coupling process onto formulations. The aptamer solution had the lowest binding kinetic over the same incubation period, showing that polymeric formulations have the potentials of improving the performance of targeting ligands due to their desired surface charges.

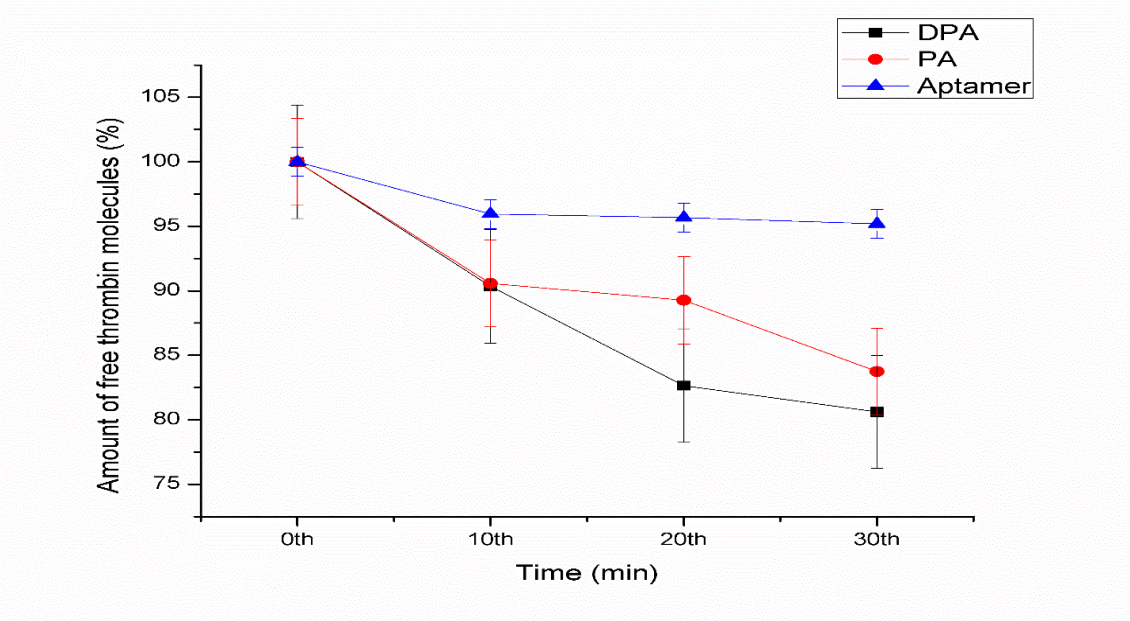

Figure 4.30: Analysis of thrombin targeting capabilities of 1) DPA formulation, 2) PA formulation, and 3) thrombin-specific DNA aptamer molecules at pH 7.4 and 30 min incubation period

4.16.1 Effect of PEGylation on thrombin binding

The effect of PEGylation on the targeting capability and binding strength of formulations was investigated. 3 different PEGylated formulations were studied: DP-PEI-PEG (without aptamer molecules), DP-PEI-PEG-Apt, and DP-PEG-Apt (without PEI polymeric layer). DP-PEI-PEG-Apt formulation is the PEGylated DPAP formulation synthesized to compare the binding characteristics of original DPAP formulation. Figure 4.31 shows the targeting capability and thrombin binding kinetics of DPAP were reduced significantly due after PEG introduction as the outermost layer. This was observed for both DP-PEI-PEG and DP-PEI-PEG-Apt formulations. There are numerous reported PEGylated polymeric carriers with the purpose of increasing the overall molecular weight of the formulations in order to prolong the circulation half-lives of the encapsulated targeting ligands and drug molecules and improve bio-accumulation in solid tumors (Zeng et al.,

2011). However, some reported PEG co-polymeric formulations are associated with limitations such as low encapsulation efficiency. These include AS1411-specific aptamer conjugated PEG-PLGA formulation (Jianwei Guo et al., 2011); AS1411-PLGA-Lecithin-PEG nanoparticles (Aravind, Jeyamohan, et al., 2012); and S2.2 aptamer conjugated PLGA-PEG particles (Z. Liu et al., 2015). The present work further demonstrates some potential limitations of PEGylation on the targeting performance and binding strength of DPAP formulations. DPAP formulation without PEGylation as seen in Figure 4.30 possesses effective thrombin targeting power and binding kinetics.

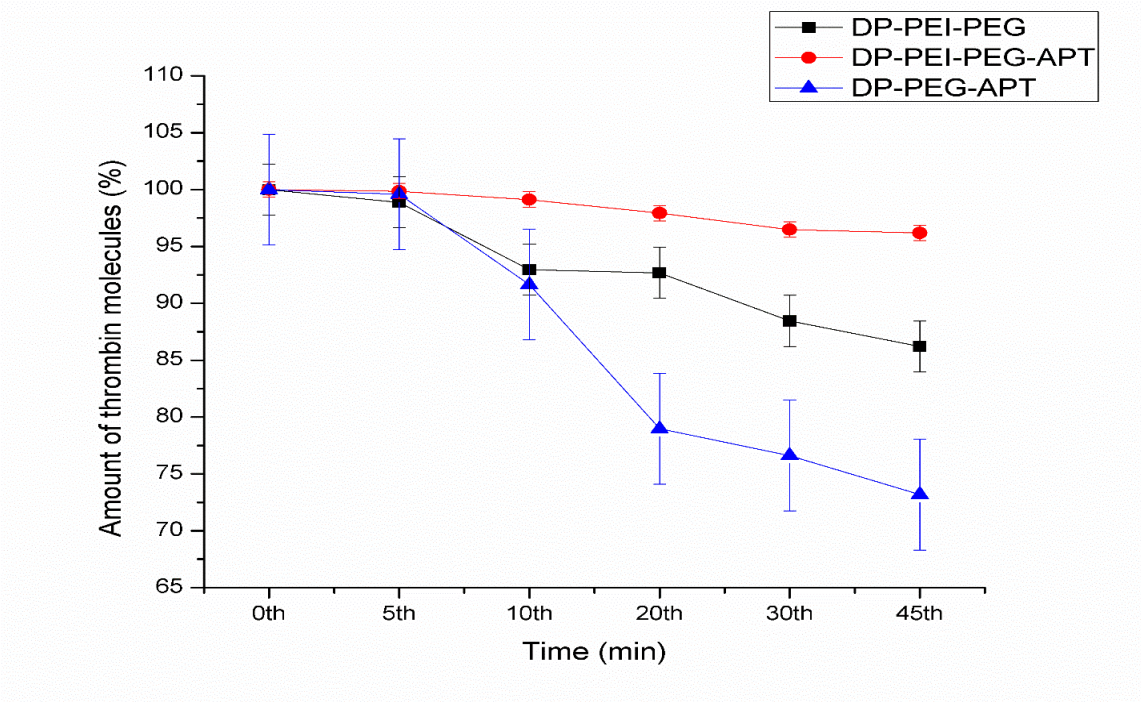

Figure 4.31: Analysis of thrombin targeting capabilities of the PEGylated formulations; a) DP-PEI-PEG, b) DP-PEI-PEG-Apt, and c) DP-PEG-Apt at pH 7.4 and 45 min incubation period

4.16.2 The selective binding capability and BSA release rate of DPAP formulation in the presence of different proteins

The selective binding of DPAP system towards targeted thrombin molecules was investigated by evaluating the release rate of BSA molecules from DPAP. The concentration of drug the protein increased gradually from 1.635 µg/mL to 1.876 µg/mL after 30 min in the presence of thrombin target protein as shown in Figure 4.32. DPAP

incubation without any protein was used as the control. The initial BSA concentration at 0.1603 µg/mL increased to 0.3587 µg/mL after 30 min. This is attributed to the escape of loosely entrapped BSA molecules near to the surface of DPAP formulation and possibly the hydrolytic degradation of outermost PEI polymeric layer over the incubation time. The conjugated aptamer molecules remained intact with no protein binding. This indicates that the presence of thrombin molecules in the PBS buffer medium induces the release of encapsulated BSA drug molecules from DPAP, resulting in increasing overall protein concentration in the medium. The thrombin-specific aptamer molecules intercalated into the PEI layer of the DPAP architecture act as targeting ligand to bind onto the thrombin molecules present in the incubating medium, a process that distorts the electrostatic equilibrium stability of DPAP and facilitate structural alterations and hydrolysis. Consequently, DPAP undergoes degradation which leads to the diffusion of entrapped BSA protein molecules from the innermost PLGA core into the surrounding medium.

Figure 4.32 further illustrates that there was a lower release of encapsulated BSA drug molecules from DPAP incubated in the presence of thrombin, lysozyme, and BSA proteins. The result demonstrated an effective targeting capability of DPAP formulation in the presence of BSA, lysozyme and targeted thrombin molecules. Thrombin-specific aptamer molecules coupled onto the DPAP formulation are able to distinguish between different types of proteins, indicating that DPAP formulation is highly specific towards its targeted thrombin molecules, leading to increased overall BSA concentration in the medium. Hence, DPAP formulation experienced structural changes and a slower degradation rate due to the lesser amount of thrombin molecules available in the medium compared to the scenario with thrombin alone. Also, the shielding effects of other protein molecules present in the medium can affect the rate of aptamer-thrombin interactions.

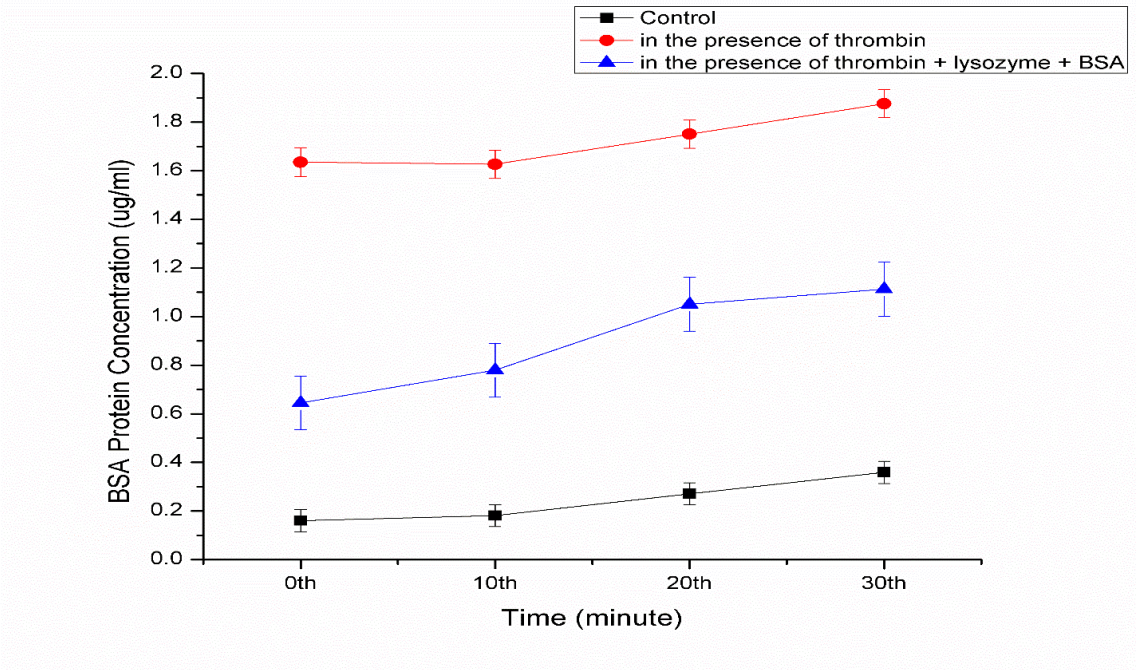

Figure 4.32: Selective binding and drug release kinetics of DPAP performed under the following conditions: 1) thrombin molecules only; 2) thrombin, lysozyme and BSA molecules; 3) control

4.16.3 BSA release from DPAP in the presence of free and immobilized thrombin molecules

The *in vitro* studies aimed to study the drug release kinetics of BSA drug molecules from the DPAP formulation in the presence of silica capsules surface-immobilised with thrombin as targeted cell surface receptors under physiological conditions. Figure 4.33(b) shows that the rate of release BSA drug released from DPAP was most significant in the presence of thrombin-conjugated silica capsules. The concentration of released BSA drug increased from 4.396 µg/mL to 7.127 µg/mL in the presence of thrombin immobilised silica capsules, strongly demonstrating that the efficacy of DPAP in effectively targeting thrombin surface receptors due to the efficacy of embedded thrombin-specific DNA aptamer molecules in navigating and directing DPAP formulation towards is the thrombin-immobilised silica capsules. Upon DPAP binding onto the thrombin surface receptors via aptamer-thrombin interactions, DPAP undergoes ionic equilibrium destabilisation and conformational changes of its layered structures, resulting in the diffusion of encapsulated BSA molecules. As a result, the BSA-PLGA polymeric layers

(DP formulation) are exposed to the external environment, resulting in DP particles degradation via heterogeneous or bulk erosion with ester hydrolysis. First, water molecules penetrate and cause PLGA hydration which breaks the hydrogen bonding, van der Waals forces, and covalent bonds. This results in a reduced molecular weight. Next, the PLGA undergoes autocatalyzed degradation of its carboxylic ends, causing the cleavage of the covalent backbone and mass loss. Finally, all the PLGA fragments are solubilise in aqueous solution in order to release the encapsulated BSA molecules.

Figure 4.33(b) also shows that encapsulated BSA molecules were well-protected within the DPAP framework in the presence of silica capsules. This validates that the presence of surface-immobilised thrombin significantly affects the hydrolytic stability of DPAP upon interaction, explaining why the silica capsules alone could not distort the intra-particulate architecture of DPAP and release the drug molecules. A small quantity of BSA drug was released after 20 min in the presence of free thrombin, potentially due to the degradation of DPAP outermost layer after extended an incubation period, facilitating the binding of significant quantities of thrombin molecules to cause DPAP destabilization and drive the escape of BSA drug molecules weakly bound or near to the surface.

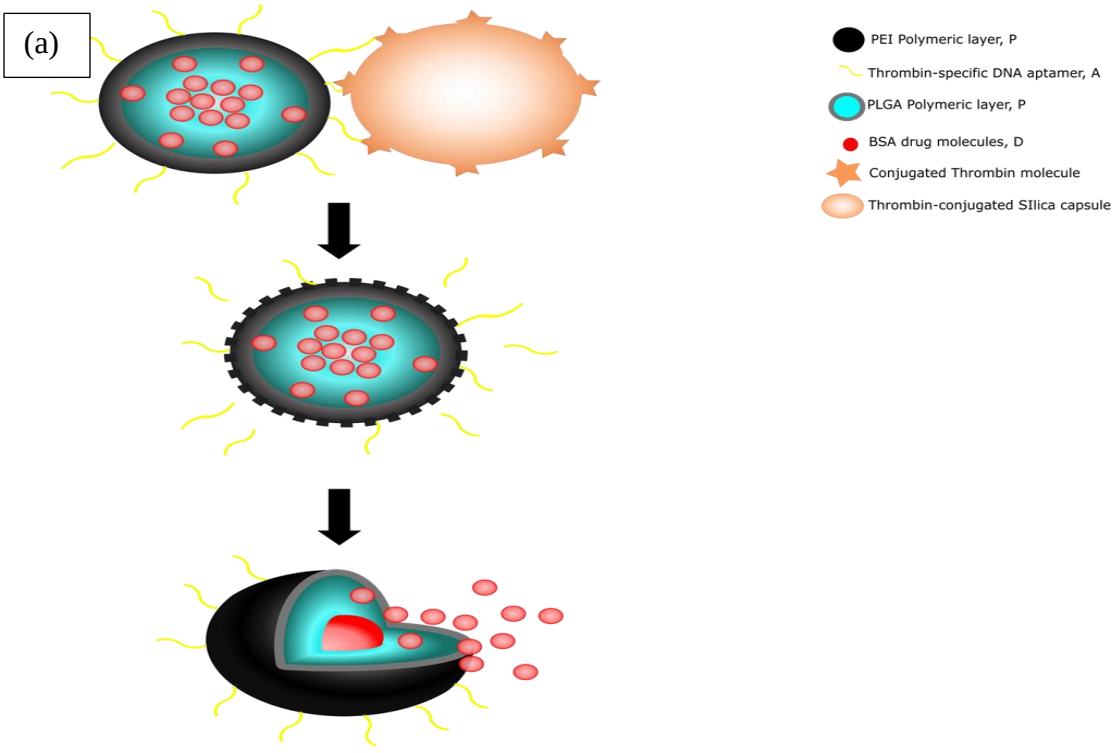

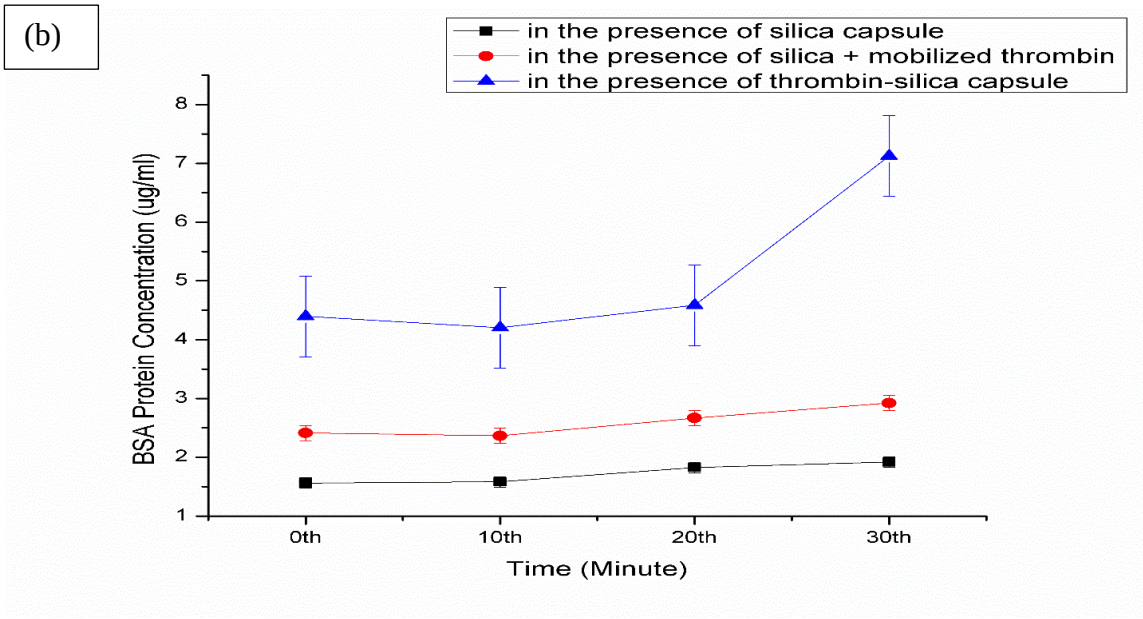

Figure 4.33: (a) A step-by-step schematic 3D illustration of DPAP targeting of thrombin-conjugated silica capsules, resulting in DPAP degradation and release of encapsulated BSA drug. (b) Drug release kinetics of BSA drug molecules from DPAP particulate system in the presence of 1) free thrombin molecules, 2) thrombin-immobilised silica capsules, and 3) silica capsules

4.17 THE AVERAGE HYDRODYNAMIC SIZE, AND ZETA POTENTIAL OF FORMULATIONS AT pH 7

The zeta potential and average D[4,3] hydrodynamic size of DPAP formulations (different PLGA ratios and PEI molecular weights) and PEGylated formulations were investigated

at pH 7. As displayed in Table 4.9, DPAP formulation with PLGA 65:35 showed a significantly smaller average D[4,3] hydrodynamic size than PLGA 50:50 due to the presence of a higher hydrophobic lactide concentration, reducing the potential for aggregation. DPAP (with PLGA 50:50) showed a larger average size of 1004 nm than DPAP (65:35) with 792.5 nm at the same PEI composition and molecular weight. For DPAP formulations with a constant PLGA (65:35) composition, those with a higher PEI molecular weight (25,000 Da) possessed a larger hydrodynamic size. This is due to increasing PEI polymeric chains and branches with increasing molecular weight. The average D[4,3] hydrodynamic size of DP-PEI-PEG-Aptamer formulation was the lowest followed by DP-PEG-Aptamer and DP-PEI-PEG. The small size of DP-PEI-PEG-Aptamer formulation is probably due to the strong electrostatic interactions between negatively charged aptamer molecules and cationic PEI particles, resulting in a more intense condensation of DNA aptamer molecules within the PEI polymeric layer to form a small size complex. All the formulations generated were microformulation, making them superior drug vehicles for non-parental route. The diameter size of these formulation was lower than 5 µm which provides them with micron aerodynamic features that favour the respiratory administration and deposition of drug molecules via the nasal cavity (Trows & Scherließ, 2016). In addition, formulations with micron size can significantly enhance the accumulation time of active pharmaceutical molecules at the targeted site via adherence and aggregation process of micro-particles (Nidhi et al., 2016). It has been reported that microformulations with hydrodynamic size ranging from 200 nm to 5 µm is highly suitable for intranasal immunisation (Caetano et al., 2016). Also, micro-particles are easily distributed systemically through lymphatic uptake followed by uniform distribution in the body system via interstitial fluids (N. Singh et al., 2009).

The net surface charge of both DPAP (PLGA 50:50, PEI MW~800) and DPAP (PLGA 65:35, PEI MW~800) formulations were negative as a result of high concentrations of negatively charged aptamer molecules intercalated within short chains of branched PEI polymeric particles. The net charge of DPAP (PLGA 65:35, PEI MW~25,000) increased to +0.0274 mV due to the incorporation of more cationic PEI molecules. This positive surface zeta potential is important to build a stable DNA/PEI polyplex and to trigger PEI proton sponge effect for enhanced endosomal release of encapsulated payload into the

cytoplasm and towards the nucleus. Table 4.9 clearly illustrates that both DP-PEI-PEG and DP-PEG-Aptamer formulations were negatively charged, showing these PEGylated formulations are prone to cell membrane electrostatic resistance that may affect endocytosis. Consequently, cellular uptake, transfection efficiency and aptamer targeting capability can be significantly affected, resulting in low therapeutic effects. DPAP formulation incorporating cationic PEI particles as the outermost layer is considered as an effective targeted delivery system for improved transfection efficiency via proton sponge effect. DP-PEI-PEG-Aptamer formulation possessed a less electronegative surface charge of -0.043 mV, hence may result in reduced cell membrane repulsion.

Table 4.9: The average D[4,3] hydrodynamic size, and zeta potential of various formulations

Formulation	**Z-average (d.nm)**	**Zeta potential (mV)**
DPAP(50:50)(MW ~800)	1004.0	-0.052
DPAP (65:35)(MW~800)	792.5	-4.250
DPAP (65:35)(MW~25,000)	984.0	+0.027
DP-PEI-PEG	1162.0	-4.500
DP-PEI-PEG-Aptamer	652.7	-0.043
DP-PEG-Aptamer	1062.0	-1.390

4.17.1 Hydrodynamic charge and size analysis of thrombin-conjugated formulation complexes

Dynamic light scattering analysis was used to investigate the average D[4,3] hydrodynamic size, and zeta potential of polyplexes generated from DPA, PA and aptamer binding onto thrombin. This is important to probe the effect of thrombin binding on biophysical characteristics of the formulations and ascertain thrombin binding efficacies. From Table 4.10, the average D[4,3] hydrodynamic size of DPA decreased from 1040 nm

to ~ 739.2 nm after thrombin binding, representing effective binding of thrombin molecules onto the aptamer formulations due to strong electrostatic interactions between positively charged thrombin molecules and negatively charged aptamer molecules at the physiological pH. The binding process results in a partial condensation of DPA due to inter-molecular bridging and intercalation of DPA particulates with aptamer linkages to form polyplexes with reduced hydrodynamic sizes. PA-T polyplex possesses a smaller average D[4,3] hydrodynamic size of 104.7 nm compared to 235.6 nm for the aptamer-T complex. The larger average diameter of aptamer-T complex demonstrates biophysical electrostatic complexation, resulting in molecular destabilization and inter-molecular agglomeration.

Table 4.10: The average D[4,3] hydrodynamic size and zeta potential analysis of thrombin bound DPA (DPA-T), thrombin bound PA (PA-T) formulation, and thrombin bound aptamer (Aptamer-T) complex

Formulation	**Average Z- Average (d.nm)**	**Average Zeta potential (mV)**
Before thrombin binding		
DPA	1040.00±76.20	-7.48±1.65
PA	92.38±22.09	-7.47±0.55
Aptamer	184.90±66.04	-9.2±1.31
After thrombin binding		
DPA-T	739.20±81.10	-7.36±0.18
PA-T	104.70±26.47	-8.27±1.43
Aptamer-T	235.60±99.46	-10.5±0.77

4.17.2 Effect of PEGylation on the hydrodynamic size and charge stability of DP and DPAP formulations

The effect of PEGylation on DPAP formulation was studied by analysing various formulations with and without PEGylation: 1) DPAP; 2) PEGylated DPAP; 3) DP-PEG-Aptamer; and 4) DP-PEI-PEG-Aptamer formulation via DLS analysis in terms of particle size and surface zeta potential. PEGylation is often utilized to improve various drug delivery formulations (Aravind, Jeyamohan, et al., 2012; Jianwei Guo et al., 2011; Z. Liu et al., 2015) in order to increase the overall molecular weight as well as enhancing the circulation half-life and bioaccumulation of encapsulated payloads. DLS analytical findings showed that DPAP formulation possessed a smaller average D[4,3] hydrodynamic size of 866.4 nm and highest electro-positivity of +9.85 mV as compared to DPAP-PEG and DP-PEG-Aptamer formulations in Table 4.11. The is due to the strong electrostatic attraction forces exist between negatively charged aptamer molecules and positively charged PEI particles which greatly shorten the inter-particles distance, forming a smaller particle size. DPAP microsphere is highly positively charged due to the cationic nature of the intercalated PEI polymeric particles in the outermost layer of DPAP formulation. The average diameter size of DP-PEI-PEG-Aptamer formulation was largely reduced to 775.7 nm which could be explained with the intensive electrostatic interactions between PEI and aptamer molecules to form a more stable polyplex. PEGylation causes an increment in the D[4,3] hydrodynamic size and electronegativity of DPAP formulation due to the insertion of PEG polymeric layer. Table 4.11 notably displays that all the three PEGylated formulations (DPAP-PEG, DP-PEG-Aptamer, DP-PEI-PEG-Aptamer formulations) showed electronegative surface charge due to the presence of more PEG and aptamer molecules. This feature is undesirable as PEGylated formulations could enhance cellular barriers and cell membrane impermeability between formulations and targeted cells due to the strong inter-electrostatic repulsions. Consequently, the targeting capability, endocytosis and cellular transfection efficiency can be significantly impacted, leading to low therapeutic indices. This finding clearly demonstrates that DPAP formulation without PEGylation is an ideal targeted delivery vehicle owning to its high electro-positivity, improved cellular uptake and proton sponge effects with the incorporation of PEI as the outermost layer.

Table 4.11: The average particle size and zeta potential of DPAP, PEGylated DPAP, DP-PEG-Aptamer, and DP-PEI-PEG-Aptamer formulation

Formulation	Average Z-Ave (d.nm)	PdI	Average Zeta Potential (mV)
DPAP	866.4	0.593	+9.85
DPAP-PEG	1076	0.551	-2.25
DP-PEG-Aptamer	1074	0.673	-1.79
DP-PEI-PEG-Aptamer	775.7	0.533	-0.04

4.17.3 Zeta potential and hydrodynamic size analysis of DPAP-MgO formulations

The average D[4,3] hydrodynamic particle size, zeta potential and polydispersity index (PDI) of DPAP, DPAP-MgO_1, and DPAP-MgO_2 are presented in Table 4.12 and Figure 4.34. This study investigated the effects on the biophysical characteristics of DPAP particulate system after MgO nanoparticles encapsulation. The average D[4,3] hydrodynamic size of DPAP micro-particles was 615.6 nm compared to the average size of DPAP-MgO_1 (766.6 nm) and DPAP-MgO_2 (641.3 nm). The slight increase in the hydrodynamic size shows the successful incorporation of the MgO nanoparticles into the DPAP architecture. The average hydrodynamic size of MgO_1 and MgO_2 nanoparticles synthesis was approximately 43.8 nm with hexagonal shape as shown in Table 4.13 and Figure 4.35 respectively. Hexagonal MgO nanoparticles have been reported to provide enhanced physiological features due to their edge effects (Jeevanandam et al., 2017a, 2017c). DPAP-MgO_1 showed a slightly larger average D[4,3] hydrodynamic diameter than DPAP-MgO_2, and this may be due to the presence of residual plant-based biochemicals or biomolecules that also interact with PLGA to increase the strength of electrostatic interactions, resulting in in a smaller average diameter. DPAP-MgO formulations in the micron size range are effective in enhancing the resident time of encapsulated drug molecules at localized desired sites via microparticulate adherence and

aggregation mechanisms (Nidhi et al., 2016). In addition, DPAP-MgO micro-particles possess the ideal size for respiratory or nasal administrative route and intranasal immunization (T. A. Ahmed & Aljaeid, 2016; Caetano et al., 2016; Trows & Scherließ, 2016). The average hydrodynamic diameter of both DPAP-MgO_1 and DPAP-MgO_2, being smaller than 2µm, presents an effective surface area for endocytosis and phagocytosis. As a result, the delivery of drug is enhanced with increased amount of internalized drug molecules into the desired cells (Pacheco, 2013). A number of reported micro-particulate delivery systems have demonstrated their efficacies in shielding payloads from challenges such as short circulating half-life, enzymatic attacks, low cellular permeability, and systemic clearance (M. Alibolandi et al., 2015; Balashanmugam et al., 2014).

Table 4.12: The average D[4,3] hydrodynamic size, PdI and zeta potential of DPAP-MgO_1 and DPAP-MgO_2 formulation at pH 7

Formulation	**Z-average (d.nm)**	**PdI**	**Zeta potential (mV)**
MgO_1-PLGA-Apt-PEI	766.6±182.12	0.572±0.051	+5.280±0.499
MgO_2-PLGA-Apt-PEI	641.3±72.14	0.624±0.027	-0.025±0.010
DPAP	615.6±23.99	0.665±0.063	+9.070±0.453

Table 4.13: Biophysical and morphological characterization of MgO_1 and MgO_2 nanoparticles

Drug sample	**Generation Method**	**Shape**	**Average Z-ave (d.nm)**	**PdI**	**Zeta potential (mV)**
MgO_1	Chemically synthesized	Hexagon	43.8±0.519	0.615±0.018	-7.21±0.211

MgO_2	Green synthesized	Hexagon	43.82±0.361	0.454±0.023	-3.39±0.784

(Jeevanandam et al., 2017a, 2017c)

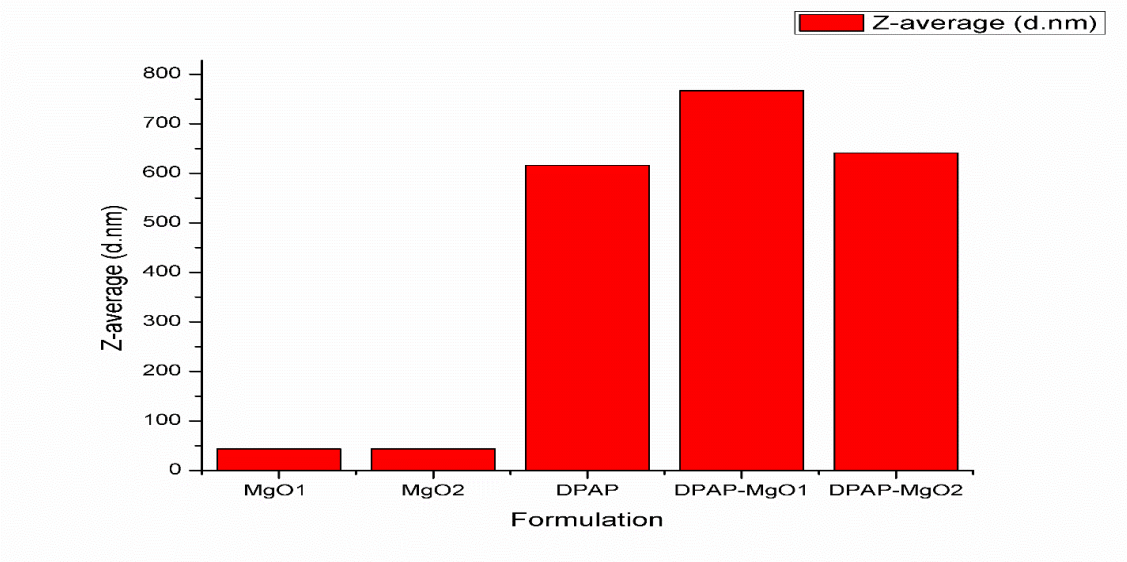

Figure 4.34: DLS data showing the average D[4,3] hydrodynamic size of DPAP carrying MgO_1/MgO_2 nanoparticles in comparison to that of the original MgO_1/MgO_2 nanoparticles and DPAP formulation with no drug molecule

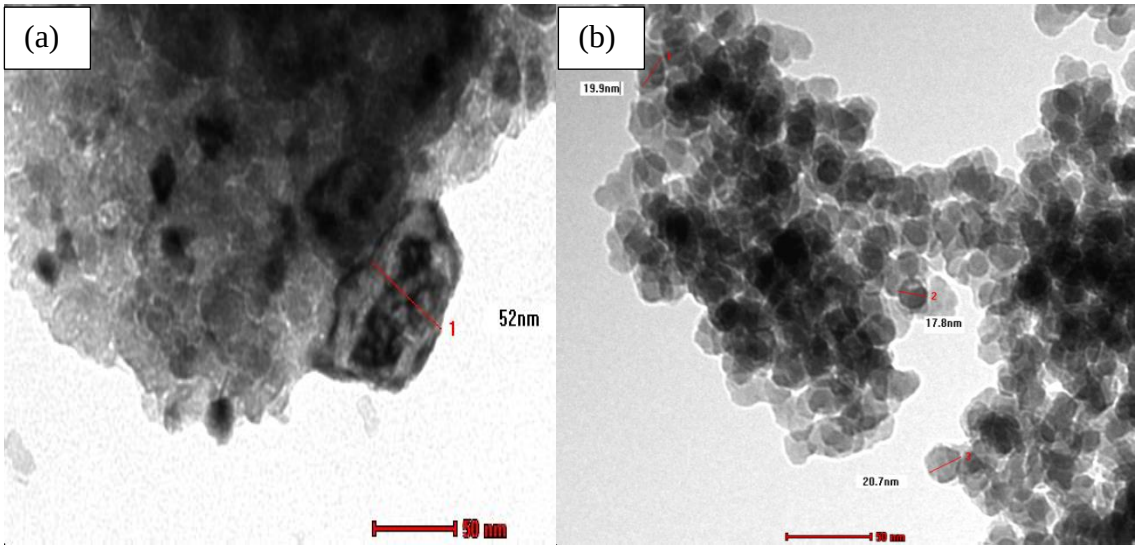

Figure 4.35: TEM Analysis of (a) MgO_1 and (b) MgO_2 nanoparticles with hexagonal shape

Figure 4.36(a) shows the particle size distribution of DPAP-MgO_1 micro-particles with 766.6 nm average D[4,3] hydrodynamic size. Peak 1 (from left) has 469.5 nm diameter, 84.4% intensity and 234.0 nm standard deviation; and peak 2 has 5560 nm diameter, 15.6% intensity and 805.3 nm standard deviation. Figure 4.36(b) shows 3 different peaks for DPAP-MgO_2 formulation. Peak 1 (from left) has 94.18 nm diameter, 11.3% intensity and 20.33 nm standard deviation; peak 2 has 646.6 nm diameter, 85.7% intensity and 183.6 nm standard deviation; peak 3 has 5560 nm diameter, and 2.9% intensity. The higher peak of DPAP-MgO_1 (peak 1) and the highest peak of DPAP-MgO_2 (peak 2) show intensities that constitute the characteristics of the individual particles. The presence of peak 2 in DPAP-MgO_1 size distribution is due to particulate aggregation formed via inter-particles collision amongst DPAP micro-particles during the solvent evaporation step of the synthesis process. The peak 1 in the size distribution of DPAP-MgO_2 formulation could be due to electrokinetic leaching of plant-based biomolecules accompanying the green synthesized MgO nanoparticles whilst peak 3 could be due to aggregation as explained earlier. Polydispersity (PdI) is a measure of the degree of uniformity of particulate distribution. The size distributions in Figure 4.36 (a) and (b) present PdI values of 0.399 for DPAP-MgO_1, and 0.531 for DPAP-MgO_2, showing the particles distribution is moderately polydispersed.

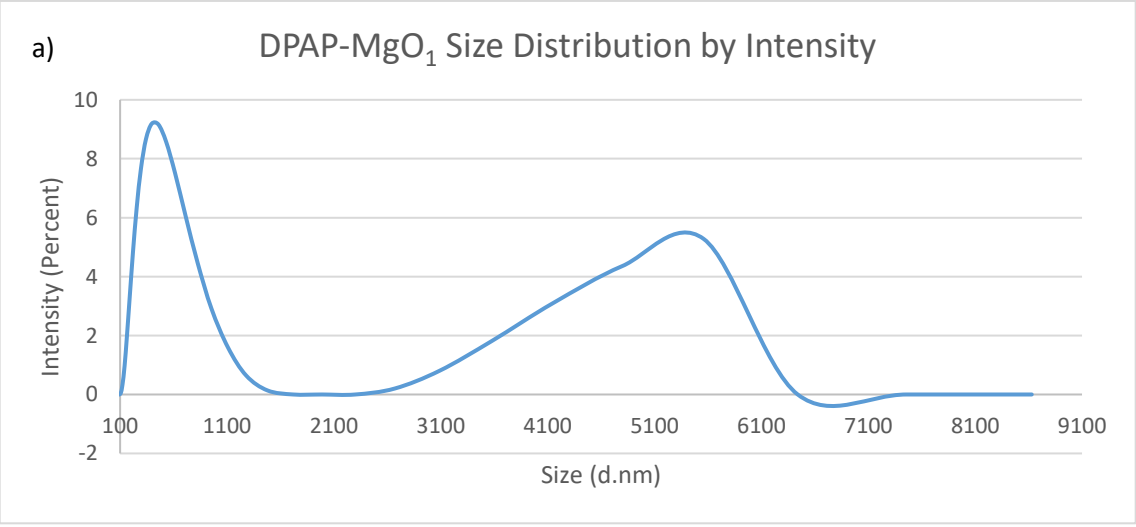

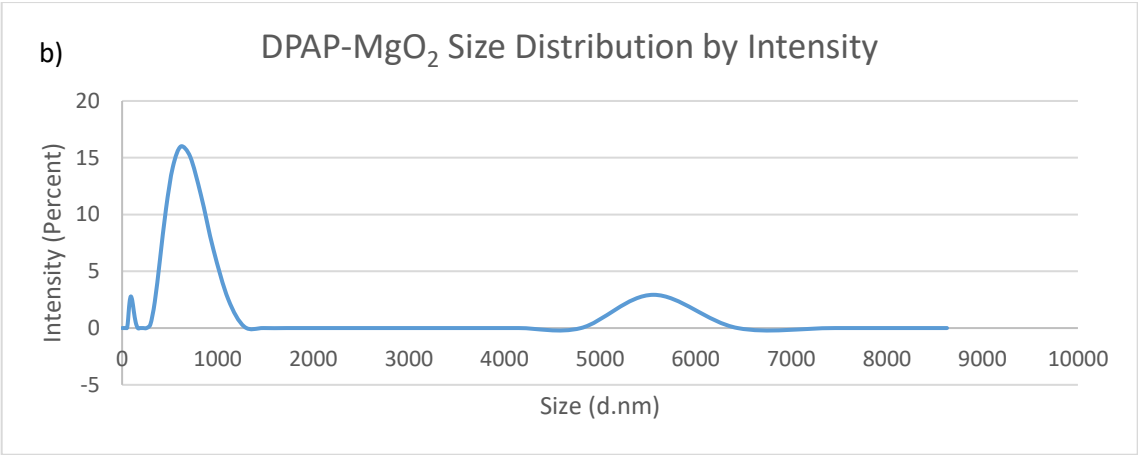

Figure 4.36: Particle size distribution data for (a) DPAP-MgO1 and (b) DPAP-MgO_2 formulations

The DLS data in Figure 4.37 shows the zeta potentials of DPAP-MgO_1, DPAP-MgO_2 and DPAP particulate systems as well as the original MgO_1 and MgO_2 nanoparticles. Both MgO_1 and MgO_2 nanoparticles were electronegative with a surface charge of -7.21 mV and -3.39 mV respectively. This is due to the anionic oxide deposits on the surface of MgO nanoparticles. The zeta potential of PLGA is more electropositive, facilitating electrostatic interactions with the negatively charged MgO nanoparticles and enhanced encapsulation within the core of DPAP. The zeta potential of DPAP formulation without MgO nanoparticles was +9.07 mV. After MgO nanoparticles introduction into DPAP architecture, the resulting DPAP-MgO system became slightly electronegative: +5.28 mV for DPAP-MgO_1 and 0 mV for DPAP-MgO_2. The net positive surface charge is induced by molecular intercalation between aptamer molecules and highly electropositive and hydrophilic PEI particles. Besides co-shielding and protecting the integrity of the encapsulated MgO_1 and MgO_2 nanodrug molecules, PEI intercalation with DNA aptamer molecules protects the functionality and bioactivity of the aptamer from nuclease attacks, systemic clearance, and cell membrane repulsion from targeted cells. The zeta potential of DPAP-MgO_2 formulation was neutral. It is ideal to achieve DPAP formulation with an overall zeta potential of positive, neutral or slightly negative in order to significantly minimize the strong electrostatic repulsive forces between the anionic payloads (MgO nanoparticles and aptamer molecules) and the negatively charged surface membrane of targeted cells in order to promote cell penetration, cellular uptake, and cell transfection.

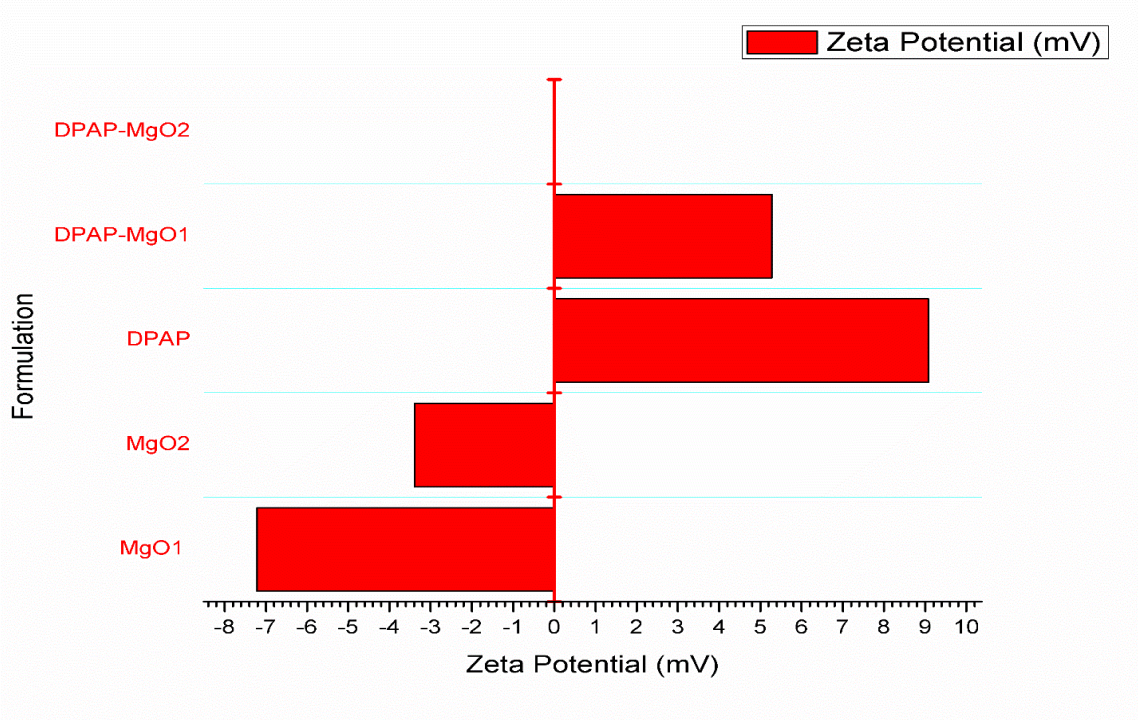

Figure 4.37: The average zeta potential (mV) of DPAP encapsulating MgO_1/MgO_2 nanoparticles compared to the original MgO_1/ MgO_2 nanoparticles and DPAP with no drug component

4.18 DNS ASSAYING OF DPAP-MGO PARTICLES

DNS assay is a colorimetric quantification method based on DNS reaction with reducing sugars or molecules containing free carbonyl group. Aldehyde and ketone functional groups present in the reducing sugars undergo oxidation to form carboxyl group. Consequently, DNS is reduced to 3-amino, 5-ntrosalicyclic acid, which absorbs light at wavelength 540 nm to produce a dark brown colored-compound. It is commonly applied to determine the amount of carbohydrate present in biological samples. In this work, 400 µl/ml of DPAP-MgO_1 and DPAP-MgO_2 microparticles were incubated with 3T3 L1 cells in the presence of DNS reagent 25 h. A mixture of 3T3 L1 cells and DNS reagent (without DPAP-MgO formulations) was used as the control. The concentration of glucose present in the DMEM medium was analyzed after every 5 h to investigate glucose uptake by 3T3 L1 cells and insulin resistance reversal.

The experimental data presented in Table 4.14. Figure 4.38 and Figure 4.39 demonstrate the potential of both DPAP-MgO_1 and DPAP-MgO_2 formulations to lower the concentration of reducing sugars. The optical density (OD) decreased over the incubation duration for both formulations. The color intensity is directly proportional to the concentration of reducing sugars available in the sample solution. This data also shows that DPAP formulation carrying either MgO_1 or MgO_2 nano-drug particles is capable of enhancing the targeting capability and transfection efficiency towards targeted 3T3 L1 cells to reverse insulin resistance. The presence of thrombin in the incubation medium is anticipated to induce affinity molecular attachments to the 3T3 L1 cell membrane, creating artificial receptors that improve DPAP interactions with the target cells. Table 4.14 shows a significant reduction in the concentrations of DPAP-MgO_1 and DPAP-MgO_2 supernatant samples after 25 h compared to the control samples, indicating that the DPAP formulations are capable of directing MgO nanoparticles to inhibit the oxidation of reducing sugars via improved transfection efficiency into 3T3 L1 cells.

It can be noted from Figure 4.39 that the DPAP-MgO particulate system binds with the 3T3-L1 cells due to the presence of thrombin which creates artificial receptors. The binding via thrombin based artificial receptors leads to the controlled release of MgO nanoparticles into the 3T3-L1 cells. The MgO nanoparticles enter the cells and dissociates into Mg^{2+} and O^{2-} ions where magnesium ions activate certain intracellular enzymes such as poly (ADP-Ribose) synthetase (X. Luo et al., 2017). The oxygen ion leads to the formation of intracellular reactive oxygen species and causes cell death. This promotes insulin reversal, resulting in a gradual increase in extracellular glucose uptake. The enhanced reversal of insulin resistance allows more glucose to enter into the cells which reduced the extracellular glucose compared to the control. This demonstrates that DPAP-MgO particulate system increases extracellular glucose uptake by reversing insulin resistance. Figure 4.40 shows the mechanism of DPAP-MgO particulate system in increasing glucose uptake in a diabetic cell model.

The targeted binding and release of DPAP-MgO nanoformulation can be attributed to engineered biophysical characteristics of DPAP formulation to facilitate effective cell transfection and delivery of intact drug molecules to targeted 3T3 cells via aptamer

navigation. The data from the DNS assay shows that both MgO_1 and MgO_2 nano-drugs offer similar therapeutic efficacy in inhibiting the oxidation of reducing sugars, indicating their huge potentials in controlling diabetes, hyperlipaemia, and obesity.

Table 4.14: Summary of DNS assay data for both DPAP-MgO_1 and DPAP-MGO_2 formulations using 3T3 L1 cell lines at different time intervals

Sample	0^{th} hr		5^{th} hr		10^{th} hr		15^{th} hr		20^{th} hr		25^{th} hr	
	OD	Concentration (µg)	OD	Concentration (µg)	OD	Concentration (µg)	OD	Concentration (µg)	OD	Concentration (µg)	OD	Concentration (µg)
Control	1.790	3.500	1.720	3.300	1.680	3.200	1.560	3.000	1.470	2.800	0.340	0.700
Control	1.760	3.400	1.700	3.250	1.690	3.250	1.590	3.050	1.500	2.900	0.270	0.550
DPAP-MgO_1	1.440	2.750	1.400	2.700	1.360	2.600	1.300	2.500	1.280	2.450	0.006	0.030
DPAP-MgO_1	1.400	2.700	1.390	2.650	1.350	2.600	1.280	2.450	1.260	2.400	0.006	0.030
DPAP-MgO_2	1.380	2.650	1.360	2.600	1.340	2.550	1.300	2.500	1.270	2.450	0.007	0.040
DPAP-MgO_2	1.390	2.700	1.340	2.550	1.320	2.500	1.310	2.500	1.290	2.500	0.008	0.040

Figure 4.38: DNS color intensity changes observed for DPAP-MgO_1 and DPAP-MgO_2 supernatants over a 25 h-incubation with 3T3 L1 cells. a-g) Comprised 2 sets of Controls, 2 sets of DPAP-MgO_1, 2 sets of DPAP-MgO_2. a) Control set without DNS added; b) Color intensity change at 0^{th} h; c) Color intensity change at 5^{th} h; d) Color intensity change at 10^{th} h; e) Color intensity change at 15^{th} h; f) Color intensity change at 20^{th} h; g) Color intensity change at 25^{th} h

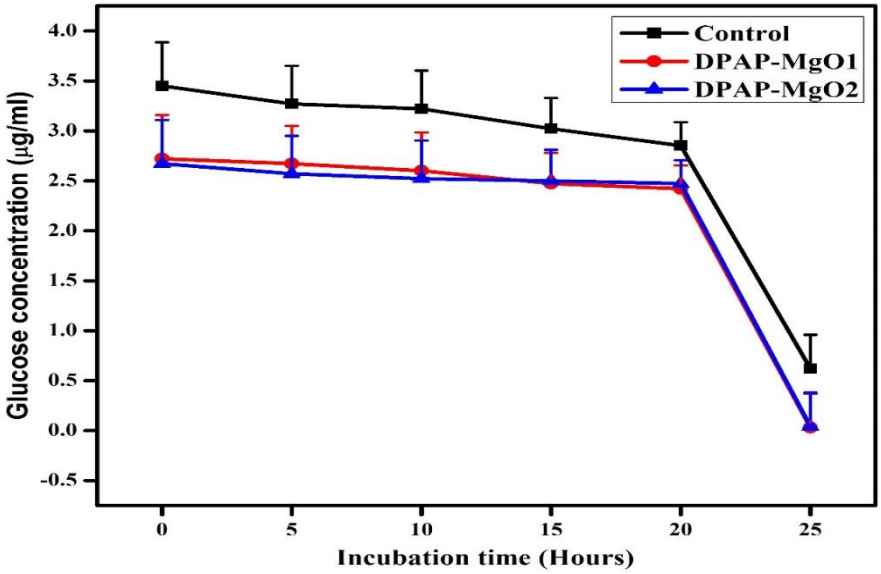

Figure 4.39: DNS glucose concentration (µg/ml) determined for DPAP-MgO_1 and DPAP-MgO_2 samples over a 25 h-incubation with 3T3 L1 cells

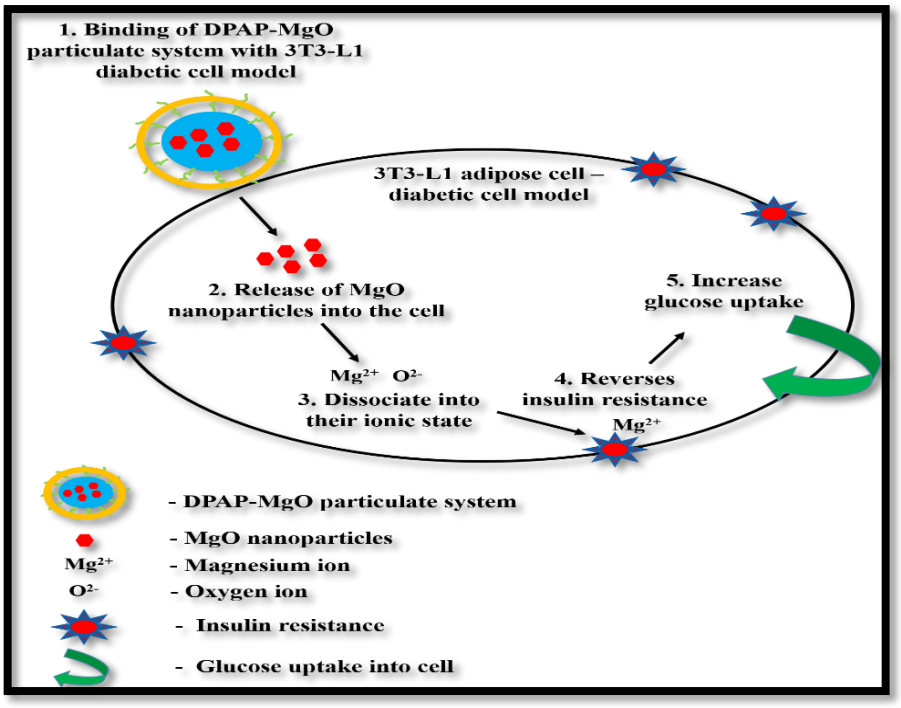

Figure 4.40: Proposed mechanism for the DPAP-MgO targeted delivery and insulin resistance reversal in 3T3-L1 adipose cell lines

CHAPTER 5

CONCLUSION AND FUTURE WORKS

Aptamer-mediated targeted drug delivery systems have emerged as a new era of advanced pharmaceutical drug delivery due to the superior clinical features of aptamers as targeting elements. Regardless of numerous reported therapeutic potentials of aptamers, the practical applications of aptamers are inhibited by various chemical and biophysical challenges. This has then driven extensive research interests into the application of biodegradable polymers as delivery carriers to optimise the performance of aptamer-navigated pharmaceutical delivery. However, to date, no single aptamer-polymeric formulation has been reported to completely address the existing limitations of aptamer-based pharmaceutical delivery. Current reported formulations still remain unresolved with various research gaps including poor targeting capability, endonuclease-mediated attacks, cell membrane impermeability, rapid renal filtration, aptamer polarity, and low transfection efficiency. Therefore, this research project seeks to design, synthesize and conduct a preliminary evaluation of a novel DPAP targeted delivery system that can overcome the aforementioned drawbacks of conventional aptameric formulations to offer better encapsulation efficiency, biophysical characteristics, pharmacokinetics, and therapeutic indices for a more controlled release profile by answering to several research

questions. Firstly, can a suitably targeted delivery formulation be generated with desired biophysical characteristics to improve drug efficiency and therapeutic index? Secondly, can such an aptamer-navigated co-polymeric particulate system provide a better targeting capability and more controlled drug release kinetics? Lastly, can DPAP formulation enhance the transfection efficiency and drug dosage at the targeted site?

A pH-sensitive, biodegradable, and cationic targeted drug delivery vehicle called DPAP polymeric particulate system was successfully generated via a w/o/w double emulsion integrated with ultra-sonication technique, with favourable biophysical characteristics and physicochemical stability which help to enhance drug efficiencies and therapeutic indices for a more controlled drug delivery kinetics to cover the scope of objective 1. DLS analysis was carried out to indicate the D[4,3] average particle size, particle size distribution and zeta potential of DPAP whilst UV-Visible spectrophotometry was used to determine the encapsulation efficiencies of BSA and aptamer at 280 nm and 260 nm wavelength, respectively. The morphological characteristics of DPAP were investigated using both SEM and TEM. The *in vitro* drug release profile of DPAP was investigated in a physiological PBS buffer system at pH 7.4, temperature 37°C and speed 120 rpm for 43 days. In addition, MTS cytotoxicity assay was conducted to determine the cytotoxic effects of DPAP formulation. The synthesized DPAP formulation was demonstrated to be a biodegradable and pH-stimulus formulation with a positively charged surface, resulting in improved encapsulation efficiencies of payloads. Biophysical characterization of the DPAP system showed a spherical shaped particulate formulation with a unimodal particle size distribution of average micron size ~0.685 μm and a positively charged surface. The DPAP formulation showed a high encapsulation efficiency of 89.4±3.6%, a loading capacity of 17.89±0.72 mg BSA protein/100 mg PLGA polymeric particles, 65-75% aptamer encapsulation efficiency, low cytotoxicity and a controlled drug release characteristics in 43 days with no initial burst release after first 24 h. The findings from this body of work show promise in the generation of suitable targeted drug delivery formulation with desired biophysical and controlled release profile.

A stage-by-stage analysis of the DPAP architecture was also performed in order to optimise the biophysical characteristics and probe the degradation and drug release profile

of DPAP particles. This answered the research question 1: ‘Can a suitable targeted delivery formulation be generated with desired biophysical characteristics to improve drug efficiency and therapeutic index?' The biophysical characterization of each surface layer configuration of DPAP formulation was examined during synthesis. *In vitro* drug release characterization of DPAP under various pH was investigated at 37°C, and 120 rpm for 12 days. The thermal stability of DPAP was analysed via TGA analysis from 30°C to 800°C at a constant heating rate of 10°C per min and 25.0 mL/min nitrogen gas as the inert medium. Layer-by-layer, DLS analysis validated that the negatively charged aptamer molecules were successfully conjugated onto positively charged DP particles whilst PEI particles were used to intercalate the negatively charged DPA particles surface to effectively produce DPAP formulation with tailored positive surface charge and D[4,3] average hydrodynamic size. DLS data of each DPAP layered compartment demonstrates DPAP is pH – dependent but not temperature dependent, indicating its modifiable endosomal degradation kinetics to release encapsulated drugs in a controlled delivery mechanism. Besides that, *in vitro* release data shows controlled and sustained drug release profiles under varying pH conditions and thus, pH is an influential parameter in maintaining specific drug release characteristics. In addition, thermogravimetric analysis indicates that DPAP formulation decomposes at ~300ºC, demonstrating thermal stability of the polymer composite for effective storage in temperate environments. DPAP micro-particles also reveal stability under varying physiological temperatures. Physicochemical and thermal characterisations, cytotoxicity analysis and *in vitro* release test of the DPAP particulate formulation demonstrate a great potential as a multifunctional polymeric vehicle for targeting and delivering sufficient drug dosage to specific cell with a sustained and controlled drug release profile.

In addition, the degradation kinetics of the DPAP aptameric formulation was well-investigated under varying physicochemical conditions. The experimental results of this study clearly reveals the good aptameric targeting capability, strong binding affinity and controlled release of DPAP formulation towards its targeted thrombin molecules and 3T3 L1 cells which addressed the objective 2 of this project. The *in vitro* release profile of DPAP formulation was compared to different DPAP formulations made up of varying molecular compositions, and other PEGylated formulations. This study was conducted at

pH 7.4 under variable ionic strengths at 37°C and over 26 days. Besides that, the effect of different pH, temperature and ionic strength on the drug release manner of DPAP was conducted over a 12-day incubation period in a PBS buffer. This is to have a better understanding of the drug release pattern and aptamer binding properties of DPAP under human physiological environments. The analysis of thrombin targeting capability and binding characteristics of DPAP was carried out in comparison to DPA, PA, thrombin-specific aptamer, and various PEGylated formulations at pH 7.4 over a 30-min incubation period. The selective binding kinetics of DPAP was also studied in the presence of different proteins and immobilized thrombin molecules over a 20-min incubation period at 200 rpm. The experimental data indicates that DPAP formulation is capable of specifically delivering encapsulated drug molecules via a more sustained and controlled release pattern towards its targeted cellular site in order to provide site-directed cyto-toxicity to malignant cells. In this work, DPAP microsphere demonstrated high stability at human physiological conditions of ~pH 7 and temperature of 37°C with a controlled and sustained pharmaceutical release behaviour. Moreover, DPAP formulation is sensitive to the slightly acidic environment of ~pH 6, revealing its desired characteristics of releasing encapsulated drug molecules more rapidly in organelles such as endosomes to enhance intracellular drug accumulation. The drug release rate of DPAP particulate system was demonstrated to be ionic strength-dependent with controlled pharmacokinetics. The ionic strength of the binding medium affected the degradation and release rates of DPAP micro-particles. A strong binding strength and shielding effect of DPAP towards encapsulated BSA molecules was observed under increasing ionic strength, for enhanced targeting and intracellular uptake at malignant sites. Experimental results also showed drug release rate increased with increasing buffer ionic strength whereby DPAP particulate system obtained the highest drug release of 50% at Day 9 under 1 M NaCl ionic strength. The binding analysis of drug and DNA aptamer molecules showed that both BSA and aptamer molecules were successfully encapsulated within DPAP formulation via strong electrostatic forces. In addition, DPAP particulate system was proved with strong targeting capability as it was highly specific towards the thrombin protein molecules in the presence of a mixture of various proteins. This is due to the coupling of thrombin-targeting DNA aptamer molecules as one of the individual

compartment of DPAP formulation. This also proved why the thrombin binding kinetics and targeting capacity of the different formulations increased in the presence of thrombin-specific aptamer molecules. Also, the experimental work which mimicked the mammalian cell with targeted surface receptors using thrombin conjugated silica capsules notably shows the targeting performance of DPAP formulation in binding onto the targeted receptors and triggering the release of encapsulated BSA molecules at the target sites.

DPAP micro-particles with different PLA/PGA ratios and PEI molecular weights, and PEGylated formulations were successfully generated using a w/o/w double emulsion-evaporation and homogenization technique. With regard to the second research question of whether such an aptamer-navigated co-polymeric particulate system provides a better targeting capability and more controlled drug release kinetics, it was demonstrated that physicochemical characteristics such as polymer composition, molecular weight and PEGylation can significantly impact the hydrodynamic size, surface charge, drug release profile, encapsulation efficiency, targeting capability and the binding affinity of DPAP particulate formulation. PEGylated micro-particles (DP-PEI-PEG; DP-PEI-PEG-Apt; DP-PEG-Apt), and DPAP with different molecular compositions (PLGA (50:50)-aptamer-PEI (800 Da); PLGA (65:35)-aptamer-PEI (25,000 Da); and PLGA (65:35)-aptamer-PEI (800 Da) were synthesized using w/o/w double emulsion technique. DPAP formulation using PLGA 65:35 and PEI molecular weight of ~800 MW demonstrated an encapsulation efficiency of 78.93% and a loading capacity of 0.1605 mg BSA per mg PLGA whilst DPAP (PLGA 65:35, PEI MW~25,000) formulation showed a high release rate with a biphasic release profile. Experimental data depicted a lower targeting power and reduced drug release rate for PEGylated DPAP formulations. It was also shown that DPAP drug release rate was higher for formulations using PLGA 50:50 and high molecular weight PEI. PEGylated formulations did not show good thrombin-specificity. Hence, DPAP formulation without PEGylation is an ideal targeted drug delivery vehicle due to its positively charged surface, improved cellular uptake and proton sponge effect within targeted cells. Overall, DPAP formulation with PLGA 65:35 and large PEI molecular weight showed higher encapsulation efficiency, and a controlled drug release profile. This research finding presents critical insights into the physicochemical

characteristics of different DPAP formulations, providing a rigorous basis for polymer selection, configuration and impacts on drug release behaviour and therapeutic indices. The effects of different homogenization methods in producing DPAP formulation with ideal biophysical properties were studied in this work. Experimental findings showed that both ultra-sonicator and magnetic stirrer are desired homogenizers for synthesis of DPAP microsphere with ideal particle sizes, surface charges and encapsulation efficiency. Therefore, DPAP formulation possesses superior features in order to provide better encapsulation efficiency, targeting ability and a more controlled drug release profile.

The DPAP particulate system was shown to improve the *in vitro* cell transfection efficiency and therapeutic dosage of carried MgO nano-drugs into the targeted 3T3 L1 cells which give significant clinical contributions to diabetic treatments. In this work, DPAP formulation was developed to carry, navigate and deliver entrapped MgO nanoparticles to examine its *in vitro* encapsulation efficiency, targeting capability and cellular transfection efficiency towards targeted diabetic 3T3- L1 cells in order to resolve the research objective 3. Two types of MgO nanoparticles (chemically synthesised MgO_1 and green synthesised MgO_2) were used to compare their therapeutic effects in this study. DNS assay was conducted by incubating DPAP-MgO_1 and DPAP-MgO_2 sample with 3T3 L1 cells over a 25 h-incubating time. The medium was tested with DNS assay at every designated time interval to determine the insulin resistance reversal ability of both formulations. The third research question of 'Can DPAP formulations enhance the transfection efficiency and drug dosage at the targeted site?' was answered with the following research outcomes: The *in vitro* experimental results demonstrated that both DPAP-MgO_1 and DPAP-MgO_2 particulate systems possess overall positive surface charges of +5.28 mV and +9.07 mV respectively. This is highly desirable in order to enhance the electrostatic interactions and endocytosis of MgO nanodrugs at the targeted cells which are negatively charged. The encapsulation efficiency and loading capacity of DPAP-MgO_2 formulation were 0.031 mg BSA protein per mg PLGA and 93.69% which was significantly higher than those of DPAP-MgO_1 formulation. This evidently showed that DPAP formulations are more capable of loading green-synthesised MgO_2 nanoparticles due to their biodegradable properties. In addition, the DNS assay data significantly indicated the clinical efficacies of both DPAP-MgO_1 and DPAP-MgO_2

particulate systems in navigating adequate therapeutic concentrations of MgO nanoparticles to the targeted 3T3 L1 cells as well as enhancing the cellular transfection efficiency. As a result, insulin resistance of 3T3 L1 cells was greatly reversed, showing their positive contributions in treating diabetes as well as great potencies in biomedical applications.

The findings from this work hold a great promise in advancing the targeted drug delivery research with the generation of a novel design concept of a targeted delivery system called DPAP. DPAP is capable of enhancing encapsulation efficiencies of both drug and aptamer molecules due to its multifunctional and co-polymeric structures which provide extra protective shielding effects. This can therefore resolve the challenges associated with rapid renal filtration and endonuclease-mediated degradation. The positively charged surface of DPAP allows increased particles-cells interactions for better binding, endocytosis and cellular uptakes due to the stable formation of polyplex between PEI and intercalated aptamer molecules. This shows great potentials in protecting the aptamer from the harsh physiological conditions whilst reducing the electrostatic repulsion between aptamer and the targeted cell membrane to deliver sufficient active drug ingredients to the targeted site. In addition, the co-polymeric nature of DPAP made up of both PLGA and PEI prevents the initial bust release of drug molecules and promotes a more sustained and controlled drug release profile. This is certainly important to ensure the amount of drug release at every interval is similar and in desired quantities in order to provide optimal drug concentration at the targeted malignant cells over a favourable period for effective therapeutic responses. Therefore, the research findings from this project will promote significant scientific merits and contributions to improve the pharmaceutical delivery and therapy.

FUTURE WORKS

Aptamer-conjugated DPAP biopolymer system represent a new and smart drug carrier capable of delivering adequate amounts of drug molecules sufficient to elicit effective *in vivo* therapies at target sites in a controlled and sustained drug release pattern. The high encapsulation efficiency, strong binding strength, and high decomposition temperature of

DPAP demonstrate an effective polymeric vehicle that provides strong protection and shielding characteristics to its payload from harsh physiological environment as well as prevent drug leakage and initial burst release. Notwithstanding, further *in vivo* studies are essential in cells and mouse models to completely characterise the capabilities of DPAP formulation for enhanced targeting and delivering of drug molecules to specific sites in mammalian systems. This can be conducted by molecularly engineering DPAP particulate structure to host multiple drugs and aptamers in unique sections of the system architecture to simultaneously target multiple disease sites.

REFERENCES

Ahmad, M. A., Mustafa, F., Ali, L. M., & Rizvi, T. A. (2014). Virus detection and quantification using electrical parameters. *Scientific Reports, 4*, 6831. doi:10.1038/srep06831

Ahmed, D., & Saeed, M. (2013). Temperature Effect on Swelling Properties of Commercial Polyacrylic Acid Hydrogel Beads. *International Journal of Advanced Biological and Biomedical Research, 1*(12), 1614-1627. Retrieved from http://www.ijabbr.com/article_7942_4eab21330deb04e601345c6ca47e4b83.pdf

Ahmed, T. A., & Aljaeid, B. M. (2016). Preparation, characterization, and potential application of chitosan, chitosan derivatives, and chitosan metal nanoparticles in pharmaceutical drug delivery. *Drug Des Devel Ther, 10*, 483-507. doi:10.2147/dddt.s99651

Alibolandi, M., Ramezani, M., Abnous, K., & Hadizadeh, F. (2016). AS1411 Aptamer-Decorated Biodegradable Polyethylene Glycol–Poly(lactic-co-glycolic acid) Nanopolymersomes for the Targeted Delivery of Gemcitabine to Non–Small Cell Lung Cancer In Vitro. *Journal of Pharmaceutical Sciences, 105*(5), 1741-1750. doi:http://dx.doi.org/10.1016/j.xphs.2016.02.021

Alibolandi, M., Ramezani, M., Sadeghi, F., Abnous, K., & Hadizadeh, F. (2015). Epithelial cell adhesion molecule aptamer conjugated PEG–PLGA nanopolymersomes for targeted delivery of doxorubicin to human breast adenocarcinoma cell line in vitro. *International Journal of Pharmaceutics, 479*(1), 241-251. doi:http://dx.doi.org/10.1016/j.ijpharm.2014.12.035

Aravind, A., Jeyamohan, P., Nair, R., Veeranarayanan, S., Nagaoka, Y., Yoshida, Y., . . . Kumar, D. S. (2012). AS1411 aptamer tagged PLGA-lecithin-PEG nanoparticles for tumor cell targeting and drug delivery. *Biotechnology and Bioengineering, 109*(11), 2920-2931. doi:10.1002/bit.24558

Aravind, A., Nair, R., Raveendran, S., Veeranarayanan, S., Nagaoka, Y., Fukuda, T., . . . Sakthi Kumar, D. (2013). Aptamer conjugated paclitaxel and magnetic fluid loaded fluorescently tagged PLGA nanoparticles for targeted cancer therapy.

Journal of Magnetism and Magnetic Materials, 344, 116-123. doi:http://dx.doi.org/10.1016/j.jmmm.2013.05.036

Aravind, A., Varghese, S. H., Veeranarayanan, S., Mathew, A., Nagaoka, Y., Iwai, S., . . . Kumar, D. S. (2012). Aptamer-labeled PLGA nanoparticles for targeting cancer cells. *Cancer Nanotechnology, 3*(1-6), 1-12. doi:10.1007/s12645-011-0024-6

Asare-Addo, K., Conway, B. R., Larhrib, H., Levina, M., Rajabi-Siahboomi, A. R., Tetteh, J., . . . Nokhodchi, A. (2013). The effect of pH and ionic strength of dissolution media on in-vitro release of two model drugs of different solubilities from HPMC matrices. *Colloids and Surfaces B: Biointerfaces, 111*, 384-391. doi:https://doi.org/10.1016/j.colsurfb.2013.06.034

Athulya Aravind, P. J., Remya Nair, Srivani Veeranarayanan,, & Yutaka Nagaoka, Y. Y., Toru Maekawa, D. Sakthi Kumar. (2012). AS1411 Aptamer Tagged PLGA-Lecithin-PEG Nanoparticles for Tumor Cell Targeting and Drug Delivery. *109*(11). doi:10.1002/bit.24558/abstract

Ayala-Breton, C., Russell, L. O., Russell, S. J., & Peng, K. W. (2014). Faster replication and higher expression levels of viral glycoproteins give the vesicular stomatitis virus/measles virus hybrid VSV-FH a growth advantage over measles virus. *J Virol, 88*(15), 8332-8339. doi:10.1128/jvi.03823-13

Baird, G. S. (2010). Where are all the aptamers? . *American Journal of Clinical Pathology, 134*, 529-531. doi:10.1309/AJCPFU4CG2WGJJKS

Bakand, S., Hayes A, Winder C. (2009). Development of in vitro methods for toxicity testing of workplace air contaminants. *International Journal of Occupational, 1*, 26-33.

Balamurugan, S., Obubuafo, A., Soper, S. A., & Spivak, D. A. (2008). Surface immobilization methods for aptamer diagnostic applications. *Anal Bioanal Chem, 390*(4), 1009-1021. doi:10.1007/s00216-007-1587-2

Balashanmugam, M. V., Nagarethinam, S., Jagani, H., Josyula, V. R., Alrohaimi, A., & Udupa, N. (2014). Preparation and characterization of novel PBAE/PLGA polymer blend microparticles for DNA vaccine delivery. *The Scientific World Journal, 2014*, 385135. doi:10.1155/2014/385135

Barbosa, L., Ortore MG, Spinozzi F, Mariani P, Bernstorff S, Ltri R (2010). The importance of protein-protein interactions on the pH-induced conformational changes of bovine serum albumin: a small-angle X-Ray scattering study. *Biophysical Journal, 98*, 147-157.

Bartlett, D. L., Liu, Z., Sathaiah, M., Ravindranathan, R., Guo, Z., He, Y., Guo, Z. S. . (2013). Oncolytic viruses as therapeutic cancer vaccines. *Molecular Cancer, 12*, 103. doi:http://doi.org/10.1186/1476-4598-12-103

Benjaminsen, R., Mattebjerg MA, Henriksen JR, Moghimi SM, Andresen TL. (2013). The possible 'proton sponge' effect of polyethylenimine (PEI) does not include change in lysosomal pH. *The American Society of Gene & Cell Therapy, 21*, 149-157.

Bhutia, S. K., Das, S. K., Azab, B., Menezes, M. E., Dent, P., Wang, X.-Y., . . . Fisher, P. B. (2013). Targeting breast cancer-initiating/stem cells with melanoma differentiation-associated gene-7/interleukin-24. *International Journal of Cancer, 133*(11), 2726-2736. doi:10.1002/ijc.28289

Caetano, L., Almeida, A., & Gonçalves, L. (2016). Effect of Experimental Parameters on Alginate/Chitosan Microparticles for BCG Encapsulation. *Marine Drugs, 14*(5), 90. Retrieved from http://www.mdpi.com/1660-3397/14/5/90

Cao, X., Li H, Yue Y, Wu Y. (2013). pH-induced conformational changes of BSA in fluorescent AuNCs@BSA and its effects on NCs emission. *Vibrational Spectroscopy, 65*, 186-192.

Cerruti, M., Jaworski, J., Raorane, D., Zueger, C., Varadarajan, J., Carraro, C., . . . Majumdar, A. (2009). Polymer-Oligopeptide Composite Coating for Selective Detection of Explosives in Water. *Analytical Chemistry, 81*(11), 4192-4199. doi:10.1021/ac8019174

Chen, X., Zhu, X., Li, L., Xian, G., Wang, W., Ma, D., & Xie, L. (2013). Investigation on novel chitosan nanoparticle–aptamer complexes targeting TGF-β receptor II. *International Journal of Pharmaceutics, 456*(2), 499-507. doi:http://dx.doi.org/10.1016/j.ijpharm.2013.08.028

Cheng, J., Teply, B. A., Sherifi, I., Sung, J., Luther, G., Gu, F. X., . . . Farokhzad, O. C. (2007a). Formulation of Functionalized PLGA-PEG Nanoparticles for In Vivo Targeted Drug Delivery. *Biomaterials, 28*(5), 869-876. doi:10.1016/j.biomaterials.2006.09.047

Cheng, J., Teply, B. A., Sherifi, I., Sung, J., Luther, G., Gu, F. X., . . . Farokhzad, O. C. (2007b). Formulation of functionalized PLGA–PEG nanoparticles for in vivo targeted drug delivery. *Biomaterials, 28*(5), 869-876. doi:http://dx.doi.org/10.1016/j.biomaterials.2006.09.047

Chiocca, E. A., Rabkin, S. D. . (2014). Oncolytic viruses and their application to cancer immunotherapy. *Cancer Immunology Research, 2*(4), 295-300. doi:10.1158/2326-6066.CIR-14-0015

Chitra, P., Muthusamy, A., Jayaprakash, R., & Ranjith Kumar, E. (2014). Effect of ultrasonication on particle size and magnetic properties of polyaniline NiCoFe2O4 nanocomposites. *Journal of Magnetism and Magnetic Materials, 366*, 55-63. doi:http://dx.doi.org/10.1016/j.jmmm.2014.04.024

Choosakoonkriang, S., Lobo, B. A., Koe, G. S., Koe, J. G., & Middaugh, C. R. (2003). Biophysical characterization of PEI/DNA complexes. *J Pharm Sci, 92*(8), 1710-1722. doi:10.1002/jps.10437

Chu, T. C., Twu, K. Y., Ellington, A. D., & Levy, M. (2006). Aptamer mediated siRNA delivery. *Nucleic Acids Research, 34*(10), e73. doi:10.1093/nar/gkl388

Cripe, T. P., Wang, P.-Y., Marcato, P., Mahller, Y. Y., Lee, P. W. . (2009). Targeting cancer-initiating cells with oncolytic viruses. *Molecular Therapy: The Journal of the American Society of Gene Therapy, 17*(10), 1677-1682. doi:http://doi.org/10.1038/mt.2009.193

Davaran, S., Rezaei, A., Alimohammadi, S., Khandaghi, A., Nejati-Koshki, K., Nasrabadi, H., & Akbarzadeh, A. (2014). Synthesis and physicochemical characterization of biodegradable star-shaped Poly Lactide-Co-Glycolide-β-Cyclodextrin copolymer nanoparticles containing albumin. . *Advances in Nanoparticles, 3*, 4-22. doi:10.4236/anp.2014.31003

De Bruyker, D., Recht, M. I., Bhagat, A. A., Torres, F. E., Bell, A. G., & Bruce, R. H. (2011). Rapid mixing of sub-microlitre drops by magnetic micro-stirring. *Lab Chip, 11*(19), 3313-3319. doi:10.1039/c1lc20354a

De Campos, A. M., Sánchez, A., & Alonso, M. a. J. (2001). Chitosan nanoparticles: a new vehicle for the improvement of the delivery of drugs to the ocular surface. Application to cyclosporin A. *International Journal of Pharmaceutics, 224*(1–2), 159-168. doi:https://doi.org/10.1016/S0378-5173(01)00760-8

De, S., & Robinson, D. H. (2004). Particle size and temperature effect on the physical stability of PLGA nanospheres and microspheres containing Bodipy. *AAPS PharmSciTech, 5*(4), 18-24. doi:10.1208/pt050453

Deng, J.-S., Li, L., Tian, Y., Ginsburg, E., Widman, M., & Myers, A. (2003). In Vitro Characterization of Polyorthoester Microparticles Containing Bupivacaine. *Pharmaceutical Development and Technology, 8*(1), 31-38. doi:10.1081/PDT-120017521

Derbyshire, N., White, S. J., Bunka, D. H. J., Song, L., Stead, S., Tarbin, J., . . . Stockley, P. G. (2012). Toggled RNA Aptamers Against Aminoglycosides Allowing Facile Detection of Antibiotics Using Gold Nanoparticle Assays. *Analytical Chemistry, 84*(15), 6595-6602. doi:10.1021/ac300815c

Dhar, S., Gu, F. X., Langer, R., Farokhzad, O. C., & Lippard, S. J. (2008). Targeted delivery of cisplatin to prostate cancer cells by aptamer functionalized Pt(IV) prodrug-PLGA–PEG nanoparticles. *Proceedings of the National Academy of Sciences of the United States of America, 105*(45), 17356-17361. doi:10.1073/pnas.0809154105

Du, L., Cheng, J., Chi, Q., Qie, J., Liu, Y., & Mei, X. (2006). Biodegradable PLGA microspheres as a sustained release system for a new luteinizing hormone-releasing hormone (LHRH) antagonist. *Chemical and Pharmaceutical Bulletin, 54*(9), 1259-1265. doi:10.1248/cpb.54.1259

Eager, R. M., Nemunaitis, J. . (2011). Clinical development directions in oncolytic viral therapy. *Cancer Gene Therapy, 18*(5), 305-317. doi:http://dx.doi.org.dbgw.lis.curtin.edu.au/10.1038/cgt.2011.7

Erdmann, V. A., Markiewicz, W. T., & Barciszewski, J. (2014). *Chemical biology of nucleic acids*

Farokhzad, O. C., Cheng, J., Teply, B. A., Sherifi, I., Jon, S., Kantoff, P. W., . . . Langer, R. (2006). Targeted nanoparticle-aptamer bioconjugates for cancer chemotherapy in vivo. *Proceedings of the National Academy of Sciences of the United States of America, 103*(16), 6315-6320. doi:10.1073/pnas.0601755103

Ferguson, M. S., Lemoine, N. R., & Wang, Y. (2012). Systemic delivery of oncolytic viruses: hopes and hurdles. *Advances in Virology, 2012*, 14. doi:10.1155/2012/805629

Ferlay, J., Soerjomataram, I., Dikshit, R., Eser, S., Mathers, C., Rebelo, M., . . . Bray, F. (2015). Cancer incidence and mortality worldwide: Sources, methods and major patterns in GLOBOCAN 2012. *International Journal of Cancer, 136*(5), E359-E386. doi:10.1002/ijc.29210

Ferlay, J., Soerjomataram, I., Ervik, M., Dikshit, R., Eser, S., Mathers, C., Rebelo, M., Parkin, D.M., Forman, D., Bray, F. . (2013). GLOBOCAN 2012 v1.0, Cancer incidence and mortality worldwide: IARC CancerBase No. 11 [Internet]. [http://globocan.iarc.fr, accessed on day/month/year.].

Fields, R. J., Cheng, C. J., Quijano, E., Weller, C., Kristofik, N., Duong, N., . . . Saltzman, W. M. (2012). Surface modified poly(β amino ester)-containing nanoparticles for plasmid DNA delivery. *Journal of controlled release : official journal of the Controlled Release Society, 164*(1), 41-48. doi:10.1016/j.jconrel.2012.09.020

Fisher, P., Palomino, P., Milbrandt, T., Hilt, J., & Puleo, D. (2014). Improved small molecule drug release from in situ forming poly(lactic-co-glycolic acid) scaffolds

incorporating poly(β-amino ester) and hydroxyapatite microparticles. *Journal of Biomaterials Science, 25*, 1174-1193. doi:10.1080/09205063.2014.923368

Freitas, S., Merkle H, Bruno G. (2005). Microencapsulation by solvent extraction/evaporation: reviewing the state of the art of microsphere preparation process technology. *Journal of Controlled Release, 102*, 313-332.

Gao, Y., Yu, X., Xue, B., Zhou, F., Wang, X., Yang, D., . . . Zhu, H. (2014). Inhibition of Hepatitis C Virus Infection by DNA Aptamer against NS2 Protein. *PLoS ONE, 9*(2), e90333. doi:10.1371/journal.pone.0090333

Gates, K. (2009). An overview of chemical processes that damage cellular DNA: spontaneous hydrolysis, alkylation, and reactions with radicals. *Chemical Research in Toxicology, 22*, 1727-1760.

Gedi, V., & Kim, Y.-P. (2014). Detection and characterization of cancer cells and pathogenic bacteria using aptamer-based nano-conjugates. *Sensors (Basel, Switzerland), 14*(10), 18302-18327. doi:10.3390/s141018302

Gentile, P., Chiono, V., Carmagnola, I., & Hatton, P. V. (2014). An overview of poly(lactic-co-glycolic) acid (PLGA)-based biomaterials for bone tissue engineering. *Int J Mol Sci, 15*(3), 3640-3659. doi:10.3390/ijms15033640

Giacca, M., & Zacchigna, S. (2012). Virus-mediated gene delivery for human gene therapy. *Journal of Controlled Release, 161*(2), 377-388. doi:http://dx.doi.org/10.1016/j.jconrel.2012.04.008

Gong, P., Shi, B., Zheng, M., Wang, B., Zhang, P., Hu, D., . . . Cai, L. (2012). PEI protected aptamer molecular probes for contrast-enhanced in vivo cancer imaging. *Biomaterials, 33*(31), 7810-7817. doi:http://dx.doi.org/10.1016/j.biomaterials.2012.07.011

Grumezescu, A. (2016a). *Engineering of Nanobiomaterials: Applications of Nanobiomaterials*: Elsevier Science.

Grumezescu, A. (2016b). *Surface Chemistry of Nanobiomaterials: Applications of Nanobiomaterials*: Elsevier Science.

Gu, F., Zhang, L., Teply, B. A., Mann, N., Wang, A., Radovic-Moreno, A. F., . . . Farokhzad, O. C. (2008). Precise engineering of targeted nanoparticles by using self-assembled biointegrated block copolymers. *Proceedings of the National Academy of Sciences, 105*(7), 2586-2591. doi:10.1073/pnas.0711714105

Guo, J., Gao, X., Su, L., Xia, H., Gu, G., Pang, Z., . . . Chen, H. (2011). Aptamer-functionalized PEG-PLGA nanoparticles for enhanced anti-glioma drug delivery. *Biomaterials, 32*(31), 8010-8020. doi:10.1016/j.biomaterials.2011.07.004

Guo, J., Gao, X., Su, L., Xia, H., Gu, G., Pang, Z., . . . Chen, H. (2011). Aptamer-functionalized PEG–PLGA nanoparticles for enhanced anti-glioma drug delivery. *Biomaterials, 32*(31), 8010-8020. doi:http://dx.doi.org/10.1016/j.biomaterials.2011.07.004

Guo, Z. S., Thorne, S. H., & Bartlett, D. L. (2008). Oncolytic virotherapy: Molecular targets in tumor-selective replication and carrier cell-mediated delivery of oncolytic viruses. *Biochimica et Biophysica Acta (BBA) - Reviews on Cancer, 1785*(2), 217-231. doi:http://dx.doi.org/10.1016/j.bbcan.2008.02.001

Hatakeyama, T., & Quinn, F. X. (1999). *Thermal Analysis: Fundamentals and Applications to Polymer Science*: Wiley.

Hawaii, R. I. o. (2011). A Single-Center Trial of Intravitreous Injections of Macugen (Pegaptanib Sodium) Given at Least 7 Days Before Vitrectomy Secondary To

Tractional Retinal Detachment in Proliferative Diabetic Retinopathy. Retrieved from https://clinicaltrials.gov/ct2/show/NCT01487070?term=aptamer+PEG&rank=2

Hawaii, R. I. O. (2011). *A Single-Center Trial of Intravitreous Injections of Macugen (Pegaptanib Sodium) Given at Least 7 Days Before Vitrectomy Secondary To Tractional Retinal Detachment in Proliferative Diabetic Retinopathy*. Bethesda (MD): National Library of Medicine. Retrieved from https://clinicaltrials.gov/ct2/show/NCT01487070?term=aptamer+PEG&rank=2

Huang, Y.-P., Lin, I. J., Chen, C.-C., Hsu, Y.-C., Chang, C.-C., & Lee, M.-J. (2013). Delivery of small interfering RNAs in human cervical cancer cells by polyethylenimine-functionalized carbon nanotubes. *Nanoscale Res Lett, 8*(1), 267. doi:10.1186/1556-276X-8-267

Huang, Y. F., Shangguan, D., Liu, H., Philips, J. A., Zhang, X., Chen, Y., & Tan, W. (2009). Molecular assembly of an aptamer-drug conjugate for targeted drug delivery to tumor cells. *ChemBioChem, 10*(5), 862-868. doi:10.1002/cbic.200800805

Huang, Y. F., Shangguan, D., Liu, H., Phillips, J. A., Zhang, X., Chen, Y., & Tan, W. (2009). Molecular assembly of an aptamer-drug conjugate for targeted drug delivery to tumor cells. *ChemBioChem, 10*(5), 862-868. doi:10.1002/cbic.200800805

Jadhav, N., VinodL, G., KarthikJ, N., & Hanmantrao, K. (2009). Glass Transition Temperature: Basics and Application in Pharmaceutical Sector. *Asian Journal of Pharmaceutics, 3*(2), 82. doi:10.4103/0973-8398.55043

Jeevanandam, J., Chan, Y. S., & Danquah, M. K. (2017a). Biosynthesis and characterization of MgO nanoparticles from plant extracts via induced molecular nucleation. *New Journal of Chemistry, 41*(7), 2800-2814. doi:10.1039/C6NJ03176E

Jeevanandam, J., Chan, Y. S., & Danquah, M. K. (2017b). Calcination-Dependent Morphology Transformation of Sol-Gel- Synthesized MgO Nanoparticles. *Chemistry select, 2*(32), 10393 - 10404.

Jeevanandam, J., Chan, Y. S., & Danquah, M. K. (2017c). Calcination-Dependent Morphology Transformation of Sol-Gel- Synthesized MgO Nanoparticles. *ChemistrySelect, 2*(32), 10393-10404. doi:10.1002/slct.201701911

Jun, J., Nguyen H, Paik S, Chun H, Kang B, Ko S. (2011). Preparation of size-controlled bovine serum albumin (BSA) nanoparticles by a modified desolvation method. *Food Chemistry, 127*, 1892-1898.

Kaida, Y., Fukami, K., Matsui, T., Higashimoto, Y., Nishino, Y., Obara, N., . . . Yamagishi, S.-i. (2013). DNA Aptamer Raised Against AGEs Blocks the Progression of Experimental Diabetic Nephropathy. *Diabetes, 62*(9), 3241-3250. doi:10.2337/db12-1608

Kalogeras, I. M. (2011). A novel approach for analyzing glass-transition temperature vs. composition patterns: application to pharmaceutical compound+polymer systems. *Eur J Pharm Sci, 42*(5), 470-483. doi:10.1016/j.ejps.2011.02.003

Khan, K. H. (2013). DNA vaccines: roles against diseases. *Germs, 3*(1), 26-35. doi:10.11599/germs.2013.1034

Kim, J., Nam, H. Y., Kim, T.-i., Kim, P.-H., Ryu, J., Yun, C.-O., & Kim, S. W. (2011). Active targeting of RGD-conjugated bioreducible polymer for delivery of

oncolytic adenovirus expressing shRNA against IL-8 mRNA. *Biomaterials, 32*(22), 5158-5166. doi:http://dx.doi.org/10.1016/j.biomaterials.2011.03.084

Kim, P.-H., Kim, J., Kim, T.-i., Nam, H. Y., Yockman, J. W., Kim, M., . . . Yun, C.-O. (2011). Bioreducible polymer-conjugated oncolytic adenovirus for hepatoma-specific therapy via systemic administration. *Biomaterials, 32*(35), 9328-9342. doi:http://dx.doi.org/10.1016/j.biomaterials.2011.08.066

Kim, S. Y. (2011). *Particle microstructure and polymer dynamics in concentrated polymer solutions.*, University of Illinois at Urbana-Champaign.

Kumari, A., Yadav, S. K., & Yadav, S. C. (2010). Biodegradable polymeric nanoparticles based drug delivery systems. Colloids and Surfaces B. *Biointerfaces, 7*(1-18).

Kurosaki, T., Higuchi, N., Kawakami, S., Higuchi, Y., Nakamura, T., Kitahara, T., . . . Sasaki, H. (2012). Self-assemble gene delivery system for molecular targeting using nucleic acid aptamer. *Gene, 491*(2), 205-209. doi:http://dx.doi.org/10.1016/j.gene.2011.09.021

Lakhin, A. V., Tarantul, V. Z., & Gening, L. V. (2013). Aptamers: problems, solutions and prospects. *Acta Naturae, 5*(4), 34-43. Retrieved from http://www.ncbi.nlm.nih.gov/pmc/articles/PMC3890987/

Lanao, R., Jonker A, Wolker J, Jansen J, van Hest J, Leeuwenburgh S. (2013). Physicochemical properties and applications of Poly(lactic-co-glycolic acid) for use in bone regeneration. *Tissue Engineering, 19*, 380-390.

Ledford, H. (2015). Cancer-fighting viruses win approval. *Nature, 526*(7575), 622-623. doi:10.1038/526622a

Li, L., Xiang, D., Shigdar, S., Yang, W., Li, Q., Lin, J., . . . Duan, W. (2014). Epithelial cell adhesion molecule aptamer functionalized PLGA-lecithin-curcumin-PEG nanoparticles for targeted drug delivery to human colorectal adenocarcinoma cells. *International Journal of Nanomedicine, 9*, 1083-1096. doi:10.2147/IJN.S59779

Li, Y., Lee, J., Lal, J., An, L., & Huang, Q. (2008). Effects of pH on the interactions and conformation of bovine serum albumin: comparison between chemical force microscopy and small-angle neutron scattering. *Journal of Chemical Physics, 112*, 3797-3806.

Liechty, W. B., Kryscio, D. R., Slaughter, B. V., & Peppas, N. A. (2010). Polymers for drug delivery systems. *Annual Review of Chemical and Biomolecular Engineering, 1*(1), 149-173. doi:10.1146/annurev-chembioeng-073009-100847

Lincoff, A. M., Mehran, R., Povsic, T. J., Zelenkofske, S. L., Huang, Z., Armstrong, P. W., . . . Alexander, J. H. (2016). Effect of the REG1 anticoagulation system versus bivalirudin on outcomes after percutaneous coronary intervention (REGULATE-PCI): a randomised clinical trial. *Lancet, 387*(10016), 349-356. doi:10.1016/s0140-6736(15)00515-2

Liu, J., Chen, H., Zheng, G., Xiang, L., Yu, X., Tang, Q., . . . Jia, L. (2016). Functionalized PLGA–PEG nanoparticles conjugated with aptamer for targeting circulating tumor cells for drug delivery. *Nanomedicine: Nanotechnology, Biology and Medicine, 12*(2), 508-509. doi:http://dx.doi.org/10.1016/j.nano.2015.12.176

Liu, Y., Li, K., Liu, B., & Feng, S. S. (2010). A strategy for precision engineering of nanoparticles of biodegradable copolymers for quantitative control of targeted drug delivery. *Biomaterials, 31*(35), 9145-9155. doi:10.1016/j.biomaterials.2010.08.053

Liu, Z., Zhao, H., He, L., Yao, Y., Zhou, Y., Wu, J., . . . Ding, J. (2015). Aptamer density dependent cellular uptake of lipid-capped polymer nanoparticles for polyvalent targeted delivery of vinorelbine to cancer cells. *RSC Advances, 5*(22), 16931-16939. doi:10.1039/C4RA16371K

Lu, Y. C., Chen, Y. J., Yu, Y. R., Lai, Y. H., Cheng, J. C., Li, Y. F., Shen, C. H., Tai, C. K. . (2012). Replicating retroviral vectors for oncolytic virotherapy of experimental hepatocellular carcinoma. *Oncology Reports, 28*, 21-26. doi:10.3892/or.2012.1789

Luo, J., Luo, Y., Sun, J., Zhou, Y., Zhang, Y., Yang, X. . (2015). Adeno-associated virus-mediated cancer gene therapy: Current status. *Cancer Letters, 356*(2), 347-356. doi:http://dx.doi.org.dbgw.lis.curtin.edu.au/10.1016/j.canlet.2014.10.045

Luo, X., Ryu, K. W., Kim, D.-S., Nandu, T., Medina, C. J., Gupte, R., . . . Gupta, R. K. (2017). PARP-1 controls the adipogenic transcriptional program by PARylating C/EBPβ and modulating its transcriptional activity. *Molecular cell, 65*(2), 260-271.

Ma, J., Wang C, Wei Y. (2016). Polyethyleneimine-facilitated high-capacity boronate affinity membrane and its application for the adsorption and enrichment of cis-diol-containing molecules. *RSC Advances, 6*, 43648-43655.

Majid, I., Nayik, G. A., & Nanda, V. (2015). Ultrasonication and food technology: A review. *Cogent Food & Agriculture, 1*(1), 1071022. doi:10.1080/23311932.2015.1071022

Makadia, H. K., & Siegel, S. J. (2011). Poly Lactic-co-Glycolic Acid (PLGA) as biodegradable controlled drug delivery carrier. *Polymers, 3*(3), 1377. Retrieved from http://www.mdpi.com/2073-4360/3/3/1377

McKeague, M., & DeRosa, M. C. (2012). Challenges and opportunities for small molecule aptamer development. *Journal of Nucleic Acids, 2012*, 748913. doi:10.1155/2012/748913

Mendonsa, S. D., & Bowser, M. T. (2004). In Vitro Selection of High-Affinity DNA Ligands for Human IgE Using Capillary Electrophoresis. *Analytical Chemistry, 76*(18), 5387-5392. doi:10.1021/ac049857v

Michnik, A. (2003). Thermal stability of bovine serum albumin DSC study. *Journal of Thermal Analysis and Calorimetry, 71*(2), 509-519. doi:10.1023/A:1022851809481

Min, K., Jo, H., Song, K., Cho, M., Chun, Y.-S., Jon, S., . . . Ban, C. (2011). Dual-aptamer-based delivery vehicle of doxorubicin to both PSMA (+) and PSMA (−) prostate cancers. *Biomaterials, 32*(8), 2124-2132. doi:http://dx.doi.org/10.1016/j.biomaterials.2010.11.035

Mitchell, K., Ford, J. L., Armstrong, D. J., Elliott, P. N. C., Rostron, C., & Hogan, J. E. (1993). The influence of concentration on the release of drugs from gels and matrices containing Methocel®. *International Journal of Pharmaceutics, 100*(1), 155-163. doi:http://dx.doi.org/10.1016/0378-5173(93)90086-U

Mondal, M. H., & Mukherjee, M. (2008). Effect of Annealing Induced Polymer Substrate Attachment on Swelling Dynamics of Ultrathin Polymer Films. *Macromolecules, 41*(22), 8753-8758. doi:10.1021/ma801622h

Nair, L. S., & Laurencin, C. T. (2007). Biodegradable polymers as biomaterials. *Progress in Polymer Science, 32*(8), 762-798. doi:http://dx.doi.org/10.1016/j.progpolymsci.2007.05.017

Nguyen, D. N., Raghavan, S. S., Tashima, L. M., Lin, E. C., Fredette, S. J., Langer, R. S., & Wang, C. (2008). Enhancement of poly(orthoester) microspheres for DNA vaccine delivery by blending with poly(ethylenimine). *Biomaterials, 29*(18), 2783-2793. doi:http://dx.doi.org/10.1016/j.biomaterials.2008.03.011

Ni, X., Castanares, M., Mukherjee, A., & Lupold, S. (2011). Nucleic acid aptamers: clinical applications and promising new horizons. *Current Medicinal Chemistry, 18*, 4206-4214.

Nidhi, Rashid, M., Kaur, V., Hallan, S. S., Sharma, S., & Mishra, N. (2016). Microparticles as controlled drug delivery carrier for the treatment of ulcerative colitis: A brief review. *Saudi Pharmaceutical Journal, 24*(4), 458-472. doi:https://doi.org/10.1016/j.jsps.2014.10.001

Nie, Y., Schaffert, D., Rödl, W., Ogris, M., Wagner, E., & Günther, M. (2011). Dual-targeted polyplexes: One step towards a synthetic virus for cancer gene therapy. *Journal of Controlled Release, 152*(1), 127-134. doi:http://dx.doi.org/10.1016/j.jconrel.2011.02.028

Nikitczuk, K. P., Schloss, R. S., Yarmush, M. L., & Lattime, E. C. (2013). PLGA-polymer encapsulation tumor antigen and CpG DNA administered into the tumor microenvironment elicits a systemic antigen-Specific IFN-$_{\gamma}$ response and rnhances survival. . *Journal of Cancer Therapy., 4*(280-290). doi:http://dx.doi.org/10.4236/jct.2013.41035

Novotny, J., Handschumacher, M., Haber, E., Bruccoleri, R. E., Carlson, W. B., Fanning, D. W., . . . Rose, G. D. (1986). Antigenic determinants in proteins coincide with surface regions accessible to large probes (antibody domains). *Proc Natl Acad Sci U S A, 83*. doi:10.1073/pnas.83.2.226

Nurmenniemi, S., Koivula, M. K., Nyberg, P., Tervahartiala, T., Sorsa, T., Mattila, P. S., . . . Risteli, J. (2012). Type I and III collagen degradation products in serum predict patient survival in head and neck squamous cell carcinoma. *Oral Oncol, 48*(2), 136-140. doi:10.1016/j.oraloncology.2011.09.002

Oh, S. S., Lee, B. F., Leibfarth, F. A., Eisenstein, M., Robb, M. J., Lynd, N. A., . . . Soh, H. T. (2014). Synthetic Aptamer-Polymer Hybrid Constructs for Programmed Drug Delivery into Specific Target Cells. *Journal of the American Chemical Society, 136*(42), 15010-15015. doi:10.1021/ja5079464

Orava, E. W., Cicmil, N., & Gariepy, J. (2010). Delivering cargoes into cancer cells using DNA aptamers targeting internalized surface portals. *Biochim Biophys Acta, 1798*(12), 2190-2200. doi:10.1016/j.bbamem.2010.02.004

Orava, E. W., Cicmil, N., & Gariépy, J. (2010). Delivering cargoes into cancer cells using DNA aptamers targeting internalized surface portals. *Biochimica et Biophysica Acta (BBA) - Biomembranes, 1798*(12), 2190-2200. doi:http://dx.doi.org/10.1016/j.bbamem.2010.02.004

Pacheco, P., White D, Sulchek T. (2013). Effects of microparticle size and Fc density on macrophage phagocytosis. *PLoS ONE, 8*(4), e60989. doi:10.1371/journal.pone.0060989

Patil, Y., & Panyam, J. (2009). Polymeric nanoparticles for siRNA delivery and gene silencing. *Int J Pharm, 367*(1-2), 195-203. doi:10.1016/j.ijpharm.2008.09.039

Pereira, M. C., Hill, L. E., Zambiazi, R. C., Mertens-Talcott, S., Talcott, S., & Gomes, C. L. (2015). Nanoencapsulation of hydrophobic phytochemicals using poly (dl-lactide-co-glycolide) (PLGA) for antioxidant and antimicrobial delivery

applications: Guabiroba fruit (Campomanesia xanthocarpa O. Berg) study. *LWT - Food Science and Technology, 63*(1), 100-107. doi:http://dx.doi.org/10.1016/j.lwt.2015.03.062

Peyvandi, F., Garagiola, I. Seregni, S. (2013). Future of coagulation factor replacement therapy. *Journal of Thrombosis and Haemostasis, 11*, 84-98. doi:10.1111/jth.12270

Putnam, D. (2006). Polymers for gene delivery across length scales. *Nature Materials, 5*(6), 439-451.

Radom, F., Jurek, P. M., Mazurek, M. P., Otlewski, J., & Jeleń, F. (2013). Aptamers: Molecules of great potential. *Biotechnology Advances, 31*(8), 1260-1274. doi:http://dx.doi.org/10.1016/j.biotechadv.2013.04.007

Rege, K., & Medintz, I. L. (2009). *Methods in Bioengineering: Nanoscale Bioengineering and Nanomedicine*: Artech House.

Rinker, S., Ke, Y., Liu, Y., Chhabra, R., & Yan, H. (2008). Self-assembled DNA nanostructures for distance dependent multivalent ligand-protein binding. *Nature nanotechnology, 3*(7), 418-422. doi:10.1038/nnano.2008.164

Russell, S. J., & Peng, K.-W. (2007). Viruses as anticancer drugs. *Trends in Pharmacological Sciences, 28*(7), 326-333. doi:http://dx.doi.org/10.1016/j.tips.2007.05.005

Sai Cheong Wan, L., Wan Sia Heng, P., & Fun Wong, L. (1995). Matrix swelling: A simple model describing extent of swelling of HPMC matrices. *International Journal of Pharmaceutics, 116*(2), 159-168. doi:http://dx.doi.org/10.1016/0378-5173(94)00285-D

Salgin, S., Salgin U, Bahadir S. (2012). Zeta potentials and isoelectric points of biomolecules: The effects of ion types and ionic strengths. *International Journal of Electrochemical Science, 7*, 12404-12414.

Saliba, J. B., Faraco, A. A. G., Yoshida, M. I., Vasconcelos, W. L. d., Silva-Cunha, A. d., & Mansur, H. S. (2008). Development and characterization of an intraocular biodegradable polymer system containing cyclosporine-A for the treatment of posterior uveitis. *Materials Research, 11*, 207-211. Retrieved from http://www.scielo.br/scielo.php?script=sci_arttext&pid=S1516-14392008000200016&nrm=iso

Sang, Y., Xie, K., Mu, Y., Lei, Y., Zhang, B., Xiong, S., . . . Qi, N. (2015). Salt ions and related parameters affect PEI-DNA particle size and transfection efficiency in Chinese hamster ovary cells. *Cytotechnology, 67*(1), 67-74. doi:10.1007/s10616-013-9658-z

Santosh, B., & Yadava, P. K. (2014). Nucleic acid aptamers: Research tools in disease diagnostics and therapeutics. *BioMed Research International, 2014*, 540451. doi:10.1155/2014/540451

Saranath, D., Khanna, A. . (2014). Current status of cancer burden: Global and Indian scenario. *Biomedical Research Journal, 1*(1), 1-5.

Saranya, S., & Radha, K. V. (2014). Review of nanobiopolymers for controlled drug delivery. *Polymer-Plastics Technology and Engineering, 53*(15), 1636-1646. doi:10.1080/03602559.2014.915035

Saša, B., Odon, P., Stane, S., & Julijana, K. (2006). Analysis of surface properties of cellulose ethers and drug release from their matrix tablets. *European Journal of*

Pharmaceutical Sciences, *27*(4), 375-383. doi:http://dx.doi.org/10.1016/j.ejps.2005.11.009

Sayari, E., Dinarvand, M., Amini, M., Azhdarzadeh, M., Mollarazi, E., Ghasemi, Z., & Atyabi, F. (2014). MUC1 aptamer conjugated to chitosan nanoparticles, an efficient targeted carrier designed for anticancer SN38 delivery. *International Journal of Pharmaceutics*, *473*(1–2), 304-315. doi:http://dx.doi.org/10.1016/j.ijpharm.2014.05.041

Shaikh, A. J. (2012). Molecular targeting agents in cancer therapy: Science and society. *Asian Pacific Journal of Cancer Prevention*, *13*, 1705-1708. doi:http://dx.doi.org/10.7314/APJCP.2012.13.4.1705

Shameem, M., Lee, H., & DeLuca, P. P. (1999). A short-term (accelerated release) approach to evaluate peptide release from PLGA depot formulations. *AAPS PharmSci*, *1*(3), 1-6. doi:10.1208/ps010307

Sharma, J. D., Kalit, M., Nirmolia, T., Saikia, S. P., Sharma, A., Barman, D. . (2014). Cancer: Scenario and relationship of different geographical areas of the globe with special reference to north east-India. *Asian Pacific Journal of Cancer Prevention*, *15*(8), 3721-3729. doi:http://dx.doi.org/10.7314/APJCP.2014.15.8.3721

Sharma, N., Madan, P., & Lin, S. (2016). Effect of process and formulation variables on the preparation of parenteral paclitaxel-loaded biodegradable polymeric nanoparticles: A co-surfactant study. *Asian Journal of Pharmaceutical Sciences*, *11*(3), 404-416. doi:https://doi.org/10.1016/j.ajps.2015.09.004

Si-shen, F., Chong, S., & Rompas, J. (2014). *Chemotherapeutic Engineering: Collected Papers of Si-Shen Feng—A Tribute to Shu Chien on His 82nd Birthday*: Pan Stanford Publishing.

Siegel, R. L., Miller, K. D., & Jemal, A. (2015). Cancer statistics, 2015. *CA: A Cancer Journal for Clinicians*, *65*(1), 5-29. doi:10.3322/caac.21254

Simmons, S. C., Jamsa, H., Silva, D., Cortez, C. M., McKenzie, E. A., Bitu, C. C., . . . Missailidis, S. (2014). Anti-heparanase aptamers as potential diagnostic and therapeutic agents for oral cancer. *PLoS ONE*, *9*(10), e96846. doi:10.1371/journal.pone.0096846

Singh, N., Manshian, B., Jenkins, G. J., Griffiths, S. M., Williams, P. M., & Maffeis, T. G. (2009). NanoGenotoxicology: the DNA damaging potential of engineered nanomaterials. *Biomaterials*, *30*. doi:10.1016/j.biomaterials.2009.04.009

Singh, P. K., Doley, J., Kumar, G. R., Sahoo, A. P., & Tiwari, A. K. (2012). Oncolytic viruses & their specific targeting to tumour cells. *The Indian Journal of Medical Research*, *136*(4), 571-584. Retrieved from http://www.ncbi.nlm.nih.gov/pmc/articles/PMC3516024/

Smith, T. T., Roth, J. C., Friedman, G. K., & Gillespie, G. Y. (2014). Oncolytic viral therapy: targeting cancer stem cells. *Oncolytic Virotherapy*, *3*, 21-33. doi:10.2147/OV.S52749

Smith, T. T., Roth, J. C., Friedman, G. K., & Gillespie, G. Y. . (2013). Oncolytic viral therapy: Targeting cancer stem cells. *Dove Medical Press*, *3*, 21-33. doi:http://dx.doi.org/10.2147/OV.S52749

Society, A. C. (2015). Cancer facts & figures 2015.

Song, K.-M., Lee, S., & Ban, C. (2012). Aptamers and their biological applications. *Sensors (Basel, Switzerland)*, *12*(1), 612-631. doi:10.3390/s120100612

Steel, J. C., Di Pasquale, G., Ramlogan, C. A., Patel, V., Chiorini, J. A., Morris, J. C. . (2013). Oral vaccination with adeno-associated virus vectors expressing the Neu oncogene inhibits the growth of murine breast cancer. *Molecular Therapy, 21*(3), 680-687. doi:http://doi.org/10.1038/mt.2012.260

Stevanovic, M., Radulovic A, Jordovic B, & D., U. (2008). Poly(DL-lactide-co-glycolide) nanospheres for the sustained release of folic acid. *Journal of Biomedical Nanotechnology, 4*, 1-10.

Stevanovic, M., & Uskokovic, D. (2009). Poly(lactide-co-glycolide)-based micro and nanoparticles for the controlled drug delivery of vitamins. *Current Nanoscience, 5*, 1-14. doi:10.2174/157341309787314566

Subramanian, N., Kanwar, J., Athalya, P., Janakiraman, N., Khetan, V., Kanwar, R., . . . Krishnakumar, S. (2015). EpCAM aptamer mediated cancer cell specific delivery of EpCAM siRNA using polymeric nanocomplex. *Journal of Biomedical Science, 22*(1), 4. Retrieved from http://www.jbiomedsci.com/content/22/1/4

Sun, H., Zhu, X., Lu, P. Y., Rosato, R. R., Tan, W., & Zu, Y. (2014). Oligonucleotide aptamers: new tools for targeted cancer therapy. *Molecular Therapy, 3*, e182. doi:10.1038/mtna.2014.32

Sundaram, P., Kurniawan, H., Byrne, M. E., & Wower, J. (2013). Therapeutic RNA aptamers in clinical trials. *European Journal of Pharmaceutical Sciences, 48*(1–2), 259-271. doi:http://dx.doi.org/10.1016/j.ejps.2012.10.014

Svyatchenko, V. A., Tarasova, M. V., Netesov, S. V., Chumakov, P. M. . (2012). Oncolytic adenoviruses in anticancer therapy: Current status and prospects. *Molecular Biology, 46*(4), 496-507. doi:http://dx.doi.org.dbgw.lis.curtin.edu.au/10.1134/S0026893312040103

Tan, K. X., Danquah, M. K., Sidhu, A., Lau, S. Y., & Ongkudon, C. M. (2017). Biophysical characterization of layer-by-layer synthesis of aptamer-drug microparticles for enhanced cell targeting. *Biotechnology Progress*.

Tan, M., & Danquah, M. K. (2012). Drug and protein encapsulation by emulsification: Technology enhancement using foam formulations. *Chemical Engineering & Technology, 35*(4), 618-626. doi:10.1002/ceat.201100358

Therapeutics, B. (2013). A Phase 2 Study to Determine the Safety and Efficacy of BIND-014 (Docetaxel Nanoparticles for Injectable Suspension), Administered to Patients With Metastatic Castration-Resistant Prostate Cancer. Retrieved from https://clinicaltrials.gov/ct2/show/NCT01812746?term=BIND-014&rank=1

Therapeutics, B. (2013). *A Phase 2 Study to Determine the Safety and Efficacy of Bind-014 (Docetaxel Nanoparticles for Injectable Suspension), Administered to Patients with Metastatic Castration-Resistant Prostate Cancer*. . USA: National Library of Medicine Retrieved from https://clinicaltrials.gov/ct2/show/NCT01812746?term=BIND-014&rank=1.

Therapeutics, B. (2014). A Study of BIND-014 (Docetaxel Nanoparticles for Injectable Suspension) as Second-line Therapy for Patients With KRAS Positive or Squamous Cell Non-Small Cell Lung Cancer. Retrieved from https://clinicaltrials.gov/ct2/show/NCT02283320?term=BIND-014&rank=4

Thorne D, Dalrymple A, Dillon D, Duke M, Meredith C. A comparative assessment of cigarette smoke aerosols using an in vitro air-liquid interface cytotoxicity test. Inhal Toxicol. 2015:1-12. doi:10.3109/08958378.2015.1080773.

Tiwari, A., & Tiwari, A. (2013). *Bioengineered Nanomaterials*: Taylor & Francis.

Tripathi, S., Garcia A, Makhatadze G. (2015). Alterations of nonconserved residues affect protein stability and folding dynamics through charge-charge interactions. *The Journal of Physical Chemistry B, 119*(41), 13103-13112.

Trows, S., & Scherließ, R. (2016). Carrier-based dry powder formulation for nasal delivery of vaccines utilizing BSA as model drug. *Powder Technology, 292*, 223-231. doi:https://doi.org/10.1016/j.powtec.2016.01.042

Tuerk, C., Gold, L. . (1990). Systematic evolution of ligands by exponential enrichment: RNA ligands to bacteriophage T4 DNA polymerase. *Science, 249*(4968), 505-510.

Upadhyay, N., Vyas, M., Behera, A. K., Shah, M., Meshram, D. B. . (2013). Aptamers: a novel approach for bio-imaging, bio-sensing and targeted drug delivery systems. *Intelligent Transportation Systems Journal*, *1*(2), 21-27.

Utsuno, K., & Uludag, H. (2010). Thermodynamics of polyethylenimine-DNA binding and DNA condensation. *Biophys J, 99*(1), 201-207. doi:10.1016/j.bpj.2010.04.016

Vähä-Koskela, M., J.V., Heikkilä, J.,E., Hinkkanen, A. E. . (2007). Oncolytic viruses in cancer therapy. *Cancer Letters, 254*(2), 178-216. doi:http://dx.doi.org.dbgw.lis.curtin.edu.au/10.1016/j.canlet.2007.02.002

Vater, A., & Klussmann, S. (2015). Turning mirror-image oligonucleotides into drugs: the evolution of Spiegelmer® therapeutics. *Drug Discovery Today, 20*(1), 147-155. doi:http://dx.doi.org/10.1016/j.drudis.2014.09.004

Vavalle, J. P., & Cohen, M. G. (2012). The REG1 anticoagulation system: a novel actively controlled factor IX inhibitor using RNA aptamer technology for treatment of acute coronary syndrome. *Future Cardiol, 8*(3), 371-382. doi:10.2217/fca.12.5

Verheije, M. H., & Rottier, P. J. M. (2012). Retargeting of Viruses to Generate Oncolytic Agents. *Advances in Virology, 2012*, 15. doi:10.1155/2012/798526

Vilar, G., Tulla-Puche, J., & Albericio, F. (2012). Polymers and drug delivery systems. *Curr Drug Deliv, 9*(4), 367-394.

Vilar, G., Tulla-Puche, J., Alericio, F. . (2012). Polymers and drugs delivery systems. *Current Drug Delivery, 9*, 367-394.

Vlerken, L. D., Z., Little, S., Seiden, M., Amiji, M. . (2008). Biodistribution and pharmacokinetic analysis of paclitaxel and ceramide administered in multifunctional polymer-blend nanoparticles in drug resistant breast cancer model. *Molecular Pharmaceutics, 5*, 516-526. doi:10.1021/mp800030k

Wang, C., Ge, Q., Ting, D., Nguyen, D., Shen, H. R., Chen, J., . . . Putnam, D. (2004). Molecularly engineered poly(ortho ester) microspheres for enhanced delivery of DNA vaccines. *Nat Mater, 3*(3), 190-196. doi:10.1038/nmat1075

Watt, S., Sheil M, Beck J, Prosselkov P, Otting G, Dixon N. (2007). Effect of protein stabilization on charge state distribution in positive- and negative-ion electrospray ionization mass spectra. *Journal of the American Society for Mass Spectrometry, 18*, 1605-1611.

Wengerter, B., Katakowski JA, Rosenberg JM, Park CG, Almo SC, Palliser D, Levy M. (2014). Aptamer-targeted antigen delivery. *Molecular Therapy, 22*(7), 1375-1387. doi:10.1038/mt.2014.51

Witt, M., Walter, J.-G., & Stahl, F. (2015). Aptamer microarrays—Current status and future prospects. *Microarrays, 4*(2), 115. Retrieved from http://www.mdpi.com/2076-3905/4/2/115

Woller, N., Gürlevik, E., Ureche, C.-I., Schumacher, A., Kühnel, F. . (2014). Oncolytic Viruses as Anticancer Vaccines. *Frontiers in Oncology, 4*, 188. doi:http://doi.org/10.3389/fonc.2014.00188

Wu, Z., Tang, L.-J., Zhang, X.-B., Jiang, J.-H., Tan, W. . (2011). Aptamer-modified nanodrug delivery systems. *ACS Nano, 5*(10), 7696-7699. doi:10.1021/nn2037384

Yang, L., Zhang, X., Ye, M., Jiang, J., Yang, R., Fu, T., . . . Tan, W. (2011). Aptamer-conjugated nanomaterials and their applications. *Adv Drug Deliv Rev, 63*(14-15), 1361-1370. doi:10.1016/j.addr.2011.10.002

Yazicioglu, B., Sahin, S., & Sumnu, G. (2015). Microencapsulation of wheat germ oil. *J Food Sci Technol, 52*(6), 3590-3597. doi:10.1007/s13197-014-1428-1

Ye, M., Hu, J., Peng, M., Liu, J., Liu, J., Liu, H., . . . Tan, W. (2012). Generating aptamers by cell-SELEX for applications in molecular medicine. *International Journal of Molecular Sciences, 13*(3), 3341-3353. doi:10.3390/ijms13033341

Yu, Y., Kong, L., Li, L., Li, N., & Yan, P. (2015). Antitumor Activity of Doxorubicin-Loaded Carbon Nanotubes Incorporated Poly(Lactic-Co-Glycolic Acid) Electrospun Composite Nanofibers. *Nanoscale Res Lett, 10*(1), 1044. doi:10.1186/s11671-015-1044-7

Zeng, L., An, L., & Wu, X. (2011). Modeling Drug-Carrier Interaction in the Drug Release from Nanocarriers. *Journal of Drug Delivery, 2011*, 15. doi:10.1155/2011/370308

Zhang, J., Chen, R., Fang, X., Chen, F., Wang, Y., & Chen, M. (2014). Nucleolin targeting AS1411 aptamer modified pH-sensitive micelles for enhanced delivery and antitumor efficacy of paclitaxel. *Nano Research, 8*, 201-218. doi:10.1007/s12274-014-0619-4

Zhang, X., Xu, J., Lawler, J., Terwilliger, E., & Parangi, S. (2007). Adeno-associated virus–mediated antiangiogenic gene therapy with thrombospondin-1 type 1 repeats and endostatin. *Clinical Cancer Research, 13*(13), 3968-3976. doi:10.1158/1078-0432.ccr-07-0245

Zheng, Z., Zhang, X., Carbo, D., Clark, C., Nathan, C.-A., & Lvov, Y. (2010). Sonication assisted synthesis of polyelectrolyte coated curcumin nanoparticles. *Langmuir : the ACS journal of surfaces and colloids, 26*(11), 7679-7681. doi:10.1021/la101246a

Zhu, J., Huang, H., Dong, S., Ge, L., & Zhang, Y. (2014). Progress in aptamer-mediated drug delivery vehicles for cancer targeting and its implications in addressing chemotherapeutic challenges. *Theranostics, 4*(9), 931-944. doi:10.7150/thno.9663

Zhu, X., Li, L., Zou, L., Zhu, X., Xian, G., Li, H., . . . Xie, L. (2012). A Novel Aptamer Targeting TGF-β Receptor II Inhibits Transdifferentiation of Human Tenon's Fibroblasts into Myofibroblast. *Invest Ophthalmol Vis Sci, 53*(11), 6897-6903. doi:10.1167/iovs.12-10198

Zhu, X., Xu, D., Zhu, X., Li, L., Li, H., Guo, F., . . . Xie, L. (2015). Evaluation of Chitosan/Aptamer Targeting TGF-beta Receptor II Thermo-Sensitive Gel for Scarring in Rat Glaucoma Filtration Surgery. *Invest Ophthalmol Vis Sci, 56*(9), 5465-5476. doi:10.1167/iovs.15-16683

Zimmermann, B., Bilusic, I., Lorenz, C., & Schroeder, R. (2010). Genomic SELEX: A discovery tool for genomic aptamers. *Methods (San Diego, Calif.), 52*(2-2), 125-132. doi:10.1016/j.ymeth.2010.06.004

"Every reasonable effort has been made to acknowledge the owners of copyright material. I would be pleased to hear from any copyright owner who has been omitted or incorrectly acknowledged."

APPENDICES: Front pages of all published articles

ISI-INDEXED JOURNALS

AIChE

Biophysical Characterization of Layer-by-Layer Synthesis of Aptamer-Drug Microparticles for Enhanced Cell Targeting

Kei X. Tan

Dept. of Chemical Engineering, Curtin University, Sarawak, 98009, Malaysia

Michael K. Danquah

Dept. of Chemical Engineering, Curtin University, Sarawak, 98009, Malaysia

Amandeep Sidhu

Curtin Sarawak Research Institute, Curtin University, Sarawak, 98009, Malaysia

Faculty of Health Sciences, Curtin University, Perth, 6102, Australia

Sie Yon Lau

Dept. of Chemical Engineering, Curtin University, Sarawak, 98009, Malaysia

Clarence M. Ongkudon

Biotechnology Research Institute, Universiti Malaysia Sabah, Kota Kinabalu, Sabah 88400, Malaysia

DOI 10.1002/btpr.2524

Published online 00 Month 2017 in Wiley Online Library (wileyonlinelibrary.com)

Targeted delivery of drug molecules to specific cells in mammalian systems demonstrates a great potential to enhance the efficacy of current pharmaceutical therapies. Conventional strategies for pharmaceutical delivery are often associated with poor therapeutic indices and high systemic cytotoxicity, and this result in poor disease suppression, low surviving rates, and potential contraindication of drug formulation. The emergence of aptamers has elicited new research interests into enhanced targeted drug delivery due to their unique characteristics as targeting elements. Aptamers can be engineered to bind to their cognate cellular targets with high affinity and specificity, and this is important to navigate active drug molecules and deliver sufficient dosage to targeted malignant cells. However, the targeting performance of aptamers can be impacted by several factors including endonuclease-mediated degradation, rapid renal filtration, biochemical complexation, and cell membrane electrostatic repulsion. This has subsequently led to the development of smart aptamer-immobilized biopolymer systems as delivery vehicles for controlled

and sustained drug release to specific cells at effective therapeutic dosage and minimal systemic cytotoxicity. This article reports the synthesis and in vitro characterization of a novel multi-layer copolymeric targeted drug delivery system based on drug-loaded PLGA-Aptamer-PEI (DPAP) formulation with a stage-wise delivery mechanism. A thrombin-specific DNA aptamer was used to develop the DPAP system while Bovine Serum Albumin (BSA) was used as a biopharmaceutical drug in the synthesis process by ultrasonication. Biophysical characterization of the DPAP system showed a spherical shaped particulate formulation with a unimodal particle size distribution of average size 0.685 mm and a zeta potential of 10.82 mV. The DPAP formulation showed a high encapsulation efficiency of 89.463.6%, a loading capacity of 17.8960.72 mg BSA protein/ 100 mg PLGA polymeric particles, low cytotoxicity and a controlled drug release characteristics in 43 days. The results demonstrate a great promise in the development of DPAP formulation for enhanced in vivo cell targeting. Vc 2017 American Institute of Chemical Engineers Biotechnol. Prog., 000:000–000, 2017

European Journal of Pharmaceutical Sciences 96 (2017) 89–101

Contents lists ScienceD

European Journal of Pharmaceutical Sciences

journal www.elsevier.com/loc

Review

Towards targeted cancer therapy: Aptamer or oncolytic virus?

Kei X. Tan[a], Michael K. Danquah[a,b], Amandeep Sidhu[b,c], Clarence M. Ongkudon[d], Sie Yon Lau[a]

[a] Department of Chemical Engineering, Curtin University, Sarawak 98009, Malaysia
[b] Curtin Sarawak Research Institute, Curtin University, Sarawak 98009, Malaysia
[c] Faculty of Health Sciences, Curtin University, Perth 6102, Australia
[d] Biotechnology Research Institute, Universiti Malaysia Sabah, Kota Kinabalu, Sabah 88400, Malaysia

article info

Keywords:
Cancer
Targeted cancer therapy
Aptamers
Oncolytic virus
Cell targeting
Pharmaceutical delivery

Article history:
Received 26 January 2016
Received in revised form 11 August 2016
Accepted 31 August 2016
Available online 1 September 2016

abstract

Cancer is a leading cause of global mortality. Whilst anticancer awareness programs have increased significantly over the years, scientific research into the development of efficient and specific drugs to target cancerous cells for enhanced therapeutic effects has not received much clinical success. Chemotherapeutic agents are incapable of acting specifically on cancerous cells, thus causing low therapeutic effects accompanied by toxicity to surrounding normal tissues. The search for smart, highly specific and efficient cancer treatments and delivery systems continues to be a significant research endeavor.

Targeted cancer therapy is an evolving treatment approach with great promise in enhancing the efficacy of cancer therapies via the delivery of therapeutic agents specifically to and into desired tumor cells using viral or nonviral targeting elements. Viral oncotherapy is an advanced cancer therapy based on the use of oncolytic viruses (OV) as elements to specifically target, replicate and kill malignant cancer cells selectively without affecting surrounding healthy cells. Aptamers, on the other hand, are non-viral targeting elements that are single-stranded nucleic acids with high specificity, selectivity and binding affinity towards their cognate targets. Aptamers have emerged as a new class of bioaffinity targeting elements can be generated and molecularly engineered to selectively bind to diverse targets including proteins, cells and tissues. This article discusses, comparatively, the potentials and impacts of both viral and aptamer-mediated targeted cancer therapies in advancing conventional drug delivery systems through enhanced target specificity, therapeutic payload, bioavailability of the therapeutic agents at the target sites whilst minimizing systemic cytotoxicity. This article emphasizes on effective sitedirected targeting mechanisms and efficacy issues that impact on clinical applications.

Contents

∗ Corresponding author at: Department of Chemical Engineering, Curtin University, Malaysia. E-mail address: mkdanquah@curtin.edu.my (M.K. Danquah).

http://dx.doi.org/10.1016/j.ejps.2016.08.061 0928-0987/

Send Orders for Reprints to reprints@benthamscience.ae

Current Drug Targets, 2016, 17, 000-000 1

REVIEW ARTICLE

Aptamer-Mediated Polymeric Vehicles for Enhanced Cell-Targeted Drug Delivery

Kei X. Tan[1], Michael K. Danquah[1,*], Amandeep Sidhu[2,3], Lau Sie Yon[1] and Clarence M. Ongkudon[4]

[1]Department of Chemical Engineering, Curtin University, Sarawak 98009, Malaysia; [2]Curtin Sarawak Research Institute, Curtin University, Sarawak 98009, Malaysia; [3]Faculty of Health Sciences, Curtin University, Perth 6102, Australia; [4]Biotechnology Research Institute, Universiti Malaysia Sabah, Kota Kinabalu, Sabah, 88400, Malaysia

ARTICLE HISTORY

Received: September 17, 2015
Revised: October 01, 2015
Accepted: June 06, 2016

DOI:
10.2174/1389450117666616061712 0926

Abstract: The search for smart delivery systems for enhanced pre-clinical and clinical pharmaceutical delivery and cell targeting continues to be a major biomedical research endeavor owing to differences in the physicochemical characteristics and physiological effects of drug molecules, and this affects the delivery mechanisms to elicit maximum therapeutic effects. Targeted drug delivery is a smart evolution essential to address major challenges associated with conventional drug delivery systems. These challenges mostly result in poor pharmacokinetics due to the inability of the active pharmaceutical ingredients to specifically act on malignant cells thus, causing poor therapeutic index and toxicity to surrounding normal cells. Aptamers are oligonucleotides with engineered affinities to bind specifically to their cognate targets.

Aptamers have gained significant interests as effective targeting elements for enhanced therapeutic delivery as they can be generated to specifically bind to wide range of targets including proteins, peptides, ions, cells and tissues. Notwithstanding, effective delivery of aptamers as therapeutic vehicles is challenged by cell membrane electrostatic repulsion, endonuclease degradation, low pH cleavage, and binding conformation stability. The application of molecularly engineered biodegradable and biocompatible polymeric particles with tunable features such as surface area and chemistry, particulate size distribution and toxicity creates opportunities to develop smart aptamer-mediated delivery systems for controlled drug release. This article discusses opportunities for particulate aptamer-drug formulations to advance current drug delivery modalities by navigating active ingredients through cellular and biomolecular traffic to target sites for sustained and controlled release at effective therapeutic dosages while minimizing systemic cytotoxic effects. A proposal for a novel drug-polymer-aptamer-polymer (DPAP) design of aptamer-drug formulation with stage-wise delivery mechanism is presented to illustrate the potential efficacy of aptamer-polymer cargos for enhanced cell targeting and drug delivery.

Keywords: Aptamer, drug delivery, biodegradable polymer, encapsulation, cell targeting.

INTRODUCTION

Aptamers have gained significant interests in biotechnology, biomedicine and drug delivery for advanced cell targeting in disease diagnosis and treatment due to their high sensitivity, specificity and binding affinity towards their cognate targets [1]. Aptamers are short, single-stranded oligonucleotides such as single-stranded ribonucleic acid (ssRNA) or deoxyribonucleic acid (ssDNA) molecules that fold into specific 3-D structures with pico- to nano-molar range of dissociation constants [2]. Consequently, they

The Canadian Journal of Chemical Engineering

STAGE-WISE PROBING OF A MULTI-LAYERED APTAMERIC FORMULATION FOR DRUG DELIVERY

Journal:	*The Canadian Journal of Chemical Engineering*
Manuscript ID	CJCE-17-0890.R1
Wiley - Manuscript type:	Article
Date Submitted by the Author:	03-Nov-2017
Complete List of Authors:	TAN, KEI XIAN; Curtin University, Chemical Engineering UJAN, SAFINA; Curtin University, Chemical Engineering Danquah, Michael K; Curtin University, Chemical Engineering LAU, JOHN; Curtin University, Chemical Engineering SIDHU, AMANDEEP; Curtin University, Chemical Engineering; Curtin University, FACULTY OF HEALTH SCIENCE
Keywords:	Aptamer, Targeted drug delivery, Biodegradable polymer, Microparticles, Pharmaceutical

• The design and development of a multi-layer, co-polymeric DPAP formulation as an improved targeted drug delivery vehicle.

• Demonstrated promising results for better encapsulation efficiency of active ingredients,

in vivo cell targeting, higher cellular transfection, and controlled drug release profile.

• This smart targeted drug delivery system possesses high potentials in overcoming the limitations associated with the conventional pharmaceutical delivery strategies.

STAGE-WISE PROBING OF A MULTI-LAYERED APTAMERIC FORMULATION FOR DRUG DELIVERY

Kei Xian Tan[1], Safina Ujan[1], Michael Kobina Danquah[1]*, Sie Yon Lau[1], Amandeep Sidhu[2,3]

[1]Department of Chemical Engineering, Curtin University, Sarawak 98009, Malaysia
[2]Curtin Sarawak Research Institute, Curtin University, Sarawak 98009, Malaysia
[3]Faculty of Health Sciences, Curtin University, Perth 6102, Australia

*Corresponding author's contact: Professor Michael K. Danquah, Department of Chemical Engineering, Curtin University, Malaysia. Email: mkdanquah@curtin.edu.my; Phone: +60 85 443836

Abstract

Aptamer-mediated targeted delivery is a promising advanced therapeutic delivery strategy with the potential to provide site-directed cyto-toxicity to malignant cells. However, effective translation of preclinical aptamer-navigated targeted delivery data into clinical success has been challenged by several biophysical and biochemical factors including rapid renal clearance, endonuclease-induced degradation, and cell membrane electrostatic repulsion. Aptamer conjugated biopolymer systems represent new and smart drug carriers capable of delivering adequate amounts of drug molecules sufficient to elicit effective *in vivo* therapies at target sites in a controlled and sustained drug release pattern. In this work, a novel co-polymeric multi-layer BSA-loaded thrombin aptamer-conjugated PLGA-PEI (DPAP) formulation was synthesised using a w/o/w double emulsion, and characterized layer-by-layer *in vitro*. DLS analysis of the DPAP particles showed a positively charged DPAP particulate system with a D[4,3] average hydrodynamic size of ~0.866 µm and a zeta potential of +9.85 mV. The surface charge and D[4,3] average hydrodynamic size of DPAP layered compartments demonstrated pH – dependence but are not temperature dependent. The ionic strength of the binding medium affected the degradation and release rates of DPAP micro-particles. A strong binding strength and shielding effect of DPAP towards encapsulated BSA molecules was observed under increasing ionic strength. Thermogravimetric analysis showed that DPAP formulation decompose ~300ºC, demonstrating thermal stability of the polymer composite for effective storage in temperate environments. The data from this study is vital to engineer the interactions between DPAP polymeric system and cellular structures in order to enhance targeting events. Whilst the DPAP construct demonstrates a great potential for targeted delivery, more *in vivo* delivery work is essential to prove its pre-clinical targeting capability.

Keywords: Aptamer; Targeted drug delivery; Biodegradable polymer; Microparticles; Encapsulation; Pharmaceutical

Manuscript Details

Manuscript number	JDDST_2017_721
Title	Binding characterization of aptamer-drug layered microformulations and in vitro release assessment
Short title	Binding characterization and in vitro release of aptamer-drug layered microformulations
Article type	Research Paper

Abstract

Efficient delivery of adequate active ingredients to targeted malignant cells is critical owing biophysical and biochemical challenges associated with conventional pharmaceutical delivery systems. Targeted delivery system is a promising development to deliver sufficient amounts of drug molecules to target cells in a controlled release pattern fashion. This study focuses on the development of a multi-functional drug-loaded aptamer-conjugated PLGA-PEI (DPAP) delivery system via a layer-by-layer synthesis method using a w/o/w double emulsion approach. The binding characteristics, targeting capability, biophysical properties, encapsulation efficiency, and drug release profile of the DPAP system were investigated under varying conditions of ionic strength, polymer composition and molecular weight, and degree of PEGylation of the synthetic core. Experimental results showed increased drug release rate with increasing buffer ionic strength. DPAP system obtained the highest drug release of 50% at Day 9 under 1 M NaCl ionic strength. DPAP formulation using PLGA 65:35 and PEI molecular weight of ~800 MW demonstrated an encapsulation efficiency of 78.93% and a loading capacity of 0.1605 mg BSA per mg PLGA. DPAP (PLGA 65:35, PEI MW~25,000) formulation showed a high release rate with a biphasic release profile. Experimental data depicted a lower targeting power and reduced release rate for PEGylated DPAP formulations.

Keywords	Aptamer; Microparticles; Targeted drug delivery; Biodegradable polymer; Encapsulation

Corresponding Author	Michael Danquah
Corresponding Author's Institution	Curtin University
Order of Authors	KEI XIAN TAN, Michael Danquah, Lau Sie Yon, AMANDEEP SIDHU

Suggested reviewers	Daniel Anderson, Gareth Forde, JENNY HO, Chun Wang

Submission Files Included in this PDF

File Name [File Type]

Danquah MK Cover letter.docx [Cover Letter]

Danquah MK Graphical Abstract.tif [Graphical Abstract]

Danquah MK Main Text.docx [Manuscript File]

To view all the submission files, including those not included in the PDF, click on the manuscript title on your EVISE Homepage, then click 'Download zip file'.

Manuscript Details

Manuscript number BIOPHA_2018_56

Title Process evaluation and in vitro selectivity analysis of aptamer-drug polymeric formulation for targeted pharmaceutical delivery

Article type Research Paper

Abstract

Targeted drug delivery is a promising strategy to promote effective delivery or conventional and emerging pharmaceuticals. The emergence of aptamers as superior targeting ligands to direct active drug molecules specifically to desired malignant cells has created new opportunities to enhance disease therapies. The application of biodegradable polymers as delivery carriers to develop aptamer-navigated drug delivery system is a promising approach to effectively deliver desired drug dosages to target cells. This study reports the development of a layer-bylayer aptamer-mediated drug delivery system (DPAP) via a w/o/w double emulsion technique homogenized by ultrasonication or magnetic stirring. Experimental results showed no significant differences in the biophysical characteristics of DPAP nanoparticles generated using the two homogenization techniques. The DPAP formulation demonstrated a strong targeting performance and selectivity towards its target receptor molecules in the presence of non-targets. The DPAP formulation demonstrated a controlled and sustained drug release profile the conditions of pH 7 and temperature 37°C. Also, the drug release rate of DPAP formulation was successfully accelerated under an endosomal acidic condition of ~pH 5.5, indicating the potential to enhance drug delivery within the endosomal microenvironment. The findings from this work are useful to understanding polymer-aptamer-drug relationship and their impact on developing effective targeted delivery systems.

Keywords Targeted delivery; Pharmaceutical formulation; Aptamer; Encapsulation; Biopolymer; Microparticles

Manuscript region of origin Asia Pacific

Corresponding Author Michael Danquah

Corresponding Author's Institution Curtin University

Order of Authors KEI XIAN TAN, Michael Danquah, Lau Sie Yon, AMANDEEP S. SIDHU

Suggested reviewers Daniel Anderson, Sakthi Kumar, Gareth Forde

Submission Files Included in this PDF

File Name [File Type]

MK Danquah Cover Letter.docx [Cover Letter]

MK Danquah Graphical Abstract.pdf [Graphical Abstract]

MK Danquah Main Text.docx [Manuscript File]

To view all the submission files, including those not included in the PDF, click on the manuscript title on your EVISE Homepage, then click 'Download zip file'

Anal Bioanal Chem (2018) 410:297–306
DOI 10.1007/s00216-017-0599-9

REVIEW

Prospects in the use of aptamers for characterizing the structure and stability of bioactive proteins and peptides in food

Dominic Agyei[1] & Caleb Acquah[2,3] & Kei Xian Tan[2,3] & Hieng Kok Hii[3] & Subin R. C. K. Rajendran[4] & Chibuike C. Udenigwe[5] & Michael K. Danquah[2,3]

Received: 16 May 2017 /Revised: 1 August 2017 /Accepted: 22 August 2017 /Published online: 7 September 2017

Abstract
Food-derived bioactive proteins and peptides have gained acceptance among researchers, food manufacturers and consumers as health-enhancing functional food components that also serve as natural alternatives for disease prevention and/or management. Bioactivity in food proteins and peptides is determined by their conformations and binding characteristics, which in turn depend on their primary and secondary structures. To maintain their bioactivities, the molecular integrity of bioactive peptides must remain intact, and this warrants the study of peptide form and structure, ideally with robust, highly specific and sensitive techniques. Short singlestranded nucleic acids (i.e. aptamers) are known to have high affinity for cognate targets such as proteins and peptides. Aptamers can be produced cost-effectively and chemically derivatized to increase their stability and shelf life. Their improved binding characteristics and minimal modification of the target molecular signature suggests their suitability for real-time detection of conformational changes in both proteins and peptides. This review discusses the developmental progress of systematic evolution of ligands by exponential enrichment (SELEX), an iterative technology for generating cost-effective aptamers with low dissociation constants (K_d) for monitoring the form and structure ofbioactive proteinsand peptides. The review also presents case studies of this technique in monitoringthe structural stability ofbioactive peptide formulations to encourage applications in functional foods. The challenges and potential of aptamers in this research field are also discussed.

Keywords Aptamer, SELEX technology, Food proteins, Bioactive peptides, Structural stability

JPP JOURNAL OF Pharmacy and Pharmacology ROYAL PHARMACEUTICAL SOCIETY

Aptamer-Navigated Copolymeric Drug Carrier System for In Vitro Delivery of MgO Nanoparticles as Type 2 Diabetes Insulin Resistance Reversal Drug Candidate

Journal:	*Journal of Pharmacy and Pharmacology*
Manuscript ID	JPP-18-0480
Wiley - Manuscript type:	Research Paper
Date Submitted by the Author:	07-Jun-2018
Complete List of Authors:	TAN, KEI XIAN; Curtin University, Chemical Engineering JEEVANANDAM, JAISON; Curtin University, Chemical Engineering LAU, JOHN SIE YON; Curtin University, Chemical Engineering Danquah, Michael; Curtin University, Chemical Engineering
Keywords:	Biological Characterisation of Novel Molecules < Biomedicinal Chemistry, Drug Synthesis and Characterisation < Biomedicinal Chemistry, Controlled and Sustained Release Systems < Pharmaceutics and Drug Delivery
Abstract:	Magnesium Oxide (MgO) nanoparticles have been reported to play a significant role in lowering the production of lipid and serum glucose for diabetes treatment. The emergence of aptamers, which can be molecularly engineered and conjugated onto biopolymers harbouring specific drug to navigate specific cellular sites, has created new opportunities in the development of smart drug delivery systems. Objectives: In this work, a multi-functional aptamer-navigated particulate delivery system (DPAP) harbouring MgO (synthesised via chemical - MgO1 and green - MgO2 approaches) nanoparticles is generated to target 3T3-L1 diabetic cells. Methods: In vitro performance indicators including encapsulation efficiency, targeting capability, cellular transfection efficiency, and insulin reversal capacity were investigated. Results: The DLS analysis indicates DPAP-MgO1 formulation showed 766.6 nm hydrodynamic size and +5.28 mV zeta potential whilst DPAP-MgO2 formulation showed 641.3 nm hydrodynamic size and -0.025 mV zeta potential. DPAP-MgO2 offered better encapsulation efficiency and loading capacity of 93.69% 0.03 mg MgO/mg PLGA respectively. 3,5-Dinitrosalicylic acid (DNS) assessment showed that both DPAP-MgO1 and DPAP-MgO2 particulate systems enhanced in vitro cellular uptake and insulin resistance reversal ability of 3T3-L1 cells. Conclusion: These results demonstrate the promising potential of DPAP particulate system as an effective carrier for the delivery of MgO nanoparticles in diabetes treatment.

Aptamer-navigated copolymeric drug carrier system for *in vitro* delivery of MgO nanoparticles as type 2 diabetes insulin resistance reversal drug candidate

Kei X. Tan[1], Jaison Jeevanandam[1], Lau Sie Yon[1], Michael K. Danquah[1]*

[1]Department of Chemical Engineering, Curtin University, Sarawak 98009, Malaysia

*Corresponding author's contact: Professor Michael K. Danquah, Department of Chemical Engineering, Curtin University, Malaysia. Email: mkdanquah@curtin.edu.my; Phone: +60 85 443836

Abstract

Magnesium oxide (MgO) nanoparticles are used for a wide range of medical applications due to their proven clinical efficacy and unique biodegradable, anti-apoptotic, and anti-oxidative characteristics. MgO nanoparticles have been reported to play a significant role in lowering the production of lipid and serum glucose for diabetes treatment. The emergence of nucleic acid based targeting elements such as aptamers, which can be molecularly engineered to navigate specific cellular sites, has created new opportunities in the development of smart drug delivery systems. Aptameric ligands can be conjugated onto biodegradable polymers harbouring specific drug molecules for targeted and controlled delivery. In this work, a multi-functional aptamer navigated particulate delivery system (DPAP) harbouring MgO (synthesised via chemical - MgO_1 and green – MgO_2 approaches) nanoparticles is generated to target 3T3-L1 diabetic cells. *In vitro* performance indicators including encapsulation efficiency, targeting capability, cellular transfection efficiency, and insulin reversal capacity were investigated. The DLS analysis indicates DPAP-MgO_1 formulation showed 766.6 nm hydrodynamic size and +5.28 mV zeta potential whilst DPAP-MgO_2 formulation showed 641.3 nm hydrodynamic size and -0.025 mV zeta potential. DPAP-MgO_2 offered better encapsulation efficiency and loading capacity of 93.69% 0.03 mg MgO/mg PLGA respectively, 3,5-Dinitrosalicylic acid (DNS) assessment showed that both DPAP-MgO_1 and DPAP-MgO_2 particulate systems enhanced *in vitro* cellular uptake and insulin resistance reversal ability of 3T3-L1 cells. These results demonstrate the promising potential of DPAP particulate system as an effective polymeric carrier system for the delivery of MgO nanoparticles in diabetes treatment. However, extensive *in vivo* data is required to demonstrate complete preclinical efficacy.

CONFERENCE PAPER

Engineered Aptamer-Based Micro-Formulation for Targeted Delivery

Kei X. Tan[1], Safina Ujan[1], Michael K. Danquah[1*], Lau Sie Yon[1]

[1]Department of Chemical Engineering, Curtin University, Sarawak 98009, Malaysia

Presenter: Ms. Tan Kei Xian, PhD Candidate. Email: tan.kei.xian@postgrad.curtin.edu.my; Phone: +60 16 800 1229
*Corresponding author's contact: Professor Michael K. Danquah, Department of Chemical Engineering, Curtin University, Malaysia. Email: mkdanquah@curtin.edu.my; Phone: +60 85 443836

Abstract

Conventional pharmaceutical delivery is often challenged by low targeting capabilities of therapeutic drugs towards malignant or tumor cells. This leads to low therapeutic indices with high systemic cytotoxicity to surrounding healthy cells. Targeted drug delivery systems have gained considerable research attentions since the emergence of aptamers as a new generation of targeting ligands. Aptamers are capable of directing and delivering sufficient dosage of therapeutic drugs to targeted tumor cells for site-specific therapeutic effects. Nonetheless, their targeting capability is limited by factors such as endonuclease attack, electrostatic repulsion and cell membrane barrier. This has fostered the application of bio-polymeric particles with tunable properties to create smart aptamer-mediated polymeric delivery systems to provide a sustained and controlled drug release profile for enhanced therapeutic indices. This article reports on the synthesis and biophysical characterization of a novel multifunctional and multilayered co-polymeric targeted delivery system made up of aptamer-conjugated drug-loaded PLGA-PEI (DPAP) formulation. Experimental results showed DPAP system with an average D[4,3] hydrodynamic size of 0.954 µm and a surface charge of +8.023 mV. DPAP formulation demonstrated a good encapsulation efficiency of 83.86% and loading capacity of 16.767 mg BSA protein/100 mg PLGA polymeric particles as well as a controlled drug release pattern over a desired period at certain pH and temperature. These findings demonstrate the potential of the co-polymeric DPAP system for better loading capacity, *in vivo* cell targeting, cellular uptake and drug delivery.

Keywords: Targeted drug delivery; Biopolymer; Aptamer; Microparticles; Pharmaceutical

Peptide Applications in Biomedicine, Biotechnology and Bioengineering

2018, Pages 231–251

9 – Peptides for biopharmaceutical applications

Dominic Agyei[1], Kei-Xian Tan[2], Sharadwata Pan[3], Chibuike C. Udenigwe[4], Michael K. Danquah[2]

Show more

https://doi-org.dbgw.lis.curtin.edu.au/10.1016/B978-0-08-100736-5.00009-0

Abstract

In the pharmaceutical industry, organic-based small molecules have been the most widely used therapeutics, but peptides are increasingly becoming an important class of therapeutic agent for biopharmaceutical applications. This trend is enhanced by research advances that have provided cutting-edge techniques and strategies to overcome challenges often encountered with the use of peptides. By their nature, peptide pharmaceutics are plagued with high cost of production, poor solubility, and difficulty in administration. However, the use of techniques such as peptide engineering,

Chapter 5

c0025 # Risks and toxicity of nanoparticles and nanostructured materials

Kei X. Tan*, Ahmed Barhoum**, Sharadwata Pan†, Michael K. Danquah*
*Curtin University, Miri, Malaysia; **Vrije Universiteit Brussel (VUB), Brussels, Belgium; †Technical University of Munich, Freising, Germany

Q1

s0020 1 INTRODUCTION

p0110 Nanotechnology has been growing rapidly since the mid-20th century and gaining relevance and popularity for its assests in diverse domains, including biotechnology, medicines, food, agriculture, electronics, and basic science. NPs are small and ultrafine particles with a size range of 1–100 nm. Nanomaterials (NMs) have been considered as a new epoch in bioengineering due to their unique properties and functionalities. Despite rapid research proliferation of engineered NPs, their novel properties have garnered significant concerns regarding their cytotoxicity and safety for environment, animals, workers, and consumers. The potential risks and toxicities of most NMs remain to be resolved completely. Consequently, a continuous development and enforcement of standard regulations is essential for assessing their safety and efficacy, especially for human use and applications. An in-depth understanding of the nanotoxicity of NMs is important not only to minimize their potential toxic effects but also for the generation of more efficient and safe NPs applications.

p0115 Dramatic advances in the R&D, synthesis, and modifications of NPs in nanoscience and nanotechnology have led to a significant increase in the types of NMs with distinct variations in their synthesis approaches, physical

Colloidal formulation of aptamers for advanced therapeutic delivery

Kei X. Tan, Safina Ujan, Michael K. Danquah*

[1]Department of Chemical Engineering, Curtin University, Sarawak 98009, Malaysia

*Corresponding author's contact: Professor Michael K. Danquah, Department of Chemical Engineering, Curtin University, Malaysia. Email: mkdanquah@curtin.edu.my; Phone: +60 85 443836

Abstract

Advanced pharmaceutical delivery via the use of targeting elements is an emerging research area with the potential to enhance the delivery of drug molecules to targeted sites. Conventional therapeutic delivery systems are significantly challenged by inefficient delivery of sufficient active drug dosage to maximize therapeutic effects on specific malignant sites, and this results in systemic cytotoxicity, low therapeutic indices, and adverse side effects.

Aptamers are short and single-stranded RNA or DNA oligonucleotides with high binding affinity, sensitivity and specificity towards their targets. They are generated from Systematic Evolution of Ligands by Exponential Enrichment (SELEX) assay which allows the isolation of aptamers for a wide range of targets including viruses, bacteria, cancer cells, ions, proteins, and tissues. Aptamers represent a new generation of targeting elements and have become paragons of affinity bio-navigators to improve targeted drug delivery platforms by providing effective pharmacokinetics and pharmacodynamics. Aptamers have demonstrated to be promising therapeutic delivery agents and targeting elements by navigating active drug molecules specifically to and into target cells. Notwithstanding, the therapeutic efficacy of aptamers are challenged by weak endocytosis due to cell membrane repulsion, renal filtration, and endonuclease degradation.

Delivery of aptamers in formulation with molecularly engineered biopolymers presents opportunities to minimize physicochemical challenges for effective delivery and enhanced therapeutic efficacy by providing a more controlled and prolonged drug release profile. This chapter provides an overview of the role of aptameric formulations in biopolymer colloids to enhance pharmaceutical delivery through improved drug encapsulation efficiency, loading capacity, *in vivo* half-life, targeted cellular uptake, drug release kinetics, and therapeutic effects.

Keywords: Aptamer; Drug delivery; Biodegradable polymer; Encapsulation; Cell targeting